BULLETIN
OF THE CHEMICAL
SOCIETY
Belgrade

Editor:
MILOŠ MLADENOVIĆ

Digitized by Google

CONTENTS

THIXOTROPY OF STARCH GELS AND
ITS MATHEMATICAL CRITERION

by

LJUBOMIR M. ĐAKOVIĆ

In studying the aging process of starch gels by rheological methods the degree of thixotropy of the given system is without doubt an important factor. This has been confirmed by H. J. Cornell[1]. This is logical considering the nature of the changes occurring in starch gels during aging, i.e. changes in particle asymmetry [2, 3], solvation, aggregation of asymmetrical particles, orientation, etc. These factors also affect the rheological characteristics of such systems, especially the degree of thixotropy.

Starch gel thixotropy does not imply the conventional definition of thixotropy, i.e. the property of some systems to become solid when left at rest while by mechanical treatment (shaking, stirring, etc.) they become fluid again. In the present work we shall deal with thixotropy from a broader standpoint, as it is interpreted and dealt with in rheology, which considers thixotropy as the "property of the body by virtue of which the ratio of shearing stress to deformation rate is temporarily reduced by previous deformation[4]". However, precise explanation of the real behavior of thixotropic systems is not given by this definition either, so we shall give some additional explanations.

When a thixotropic system is subject to a shearing current, e.g. in a rotational viscosimeter, the asymmetrical particles are oriented in flow lines thus causing relative reduction of the shearing stress. The degree of orientation depends on the shearing force and particle asymmetry. Consequently, any increase in the shearing rate and particle asymmetry leads to increased orientation and further reduction of the shearing stress. However, the basic characteristic of the thixotropic behavior of material is that at reverse shearing, i.e. when the shearing rate begins to decrease from the maximum, the system shows less resistance than that at the same shearing rate while increasing (Fig. 1). Therefore, the previous deformation induced by higher shearing rates shows certain consecutive effect on the viscous resistance of the system. Hence, we may say that thixotropic systems show a certain "disorientation inertia" which may be attributed, for example, to mutual interaction of oriented micromolecules.
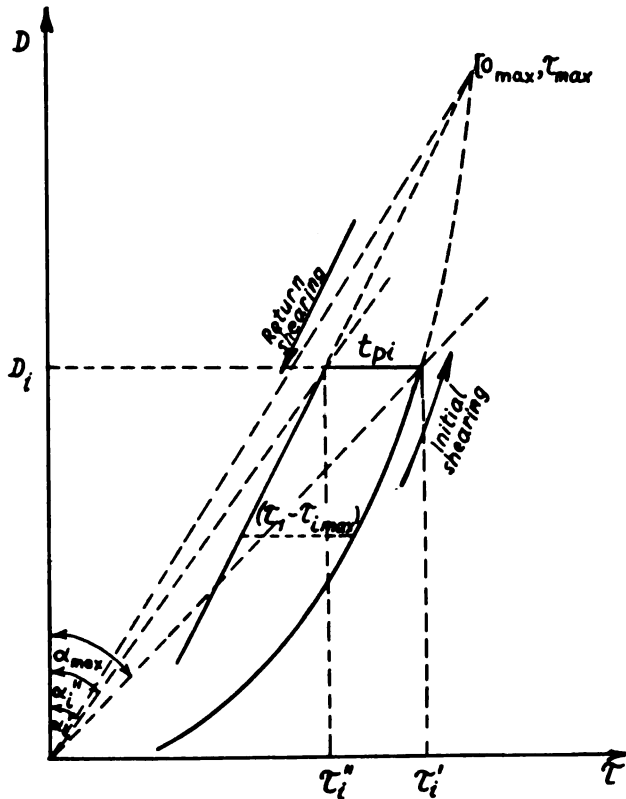
Fig. 1

General view of a thixotropic loop

Orientation of asymmetric particles in current lines also takes time, i.e. a certain tire is required for complete orientation. The time needed for unsolvated stiff asymmetric particles, which is a minimum, differs from that required for orientation of flexible linear solvated macromolecules. Certain effects of the concentration may also be expected in this case. Because of the linkages between linear macromolecules, orientation is gradual and slower at the same shearing rate, so that in such systems the duration of shearing at constant rate is also important.

In macromolecular concentrated systems such as starch gels, thixotropy is the result of destruction of the molecular lattice and partially also of molecular orientation. Since these two factors are associated with the form of the molecules (they appear in the presence of linear macromolecules) it may be concluded that amylose causes the thixotropic behavior of starch gels. However, no definite answer can be given as to whether amylopectin also contributes to the amount of thixotropy. Pure amylopectin does not cause thixotropy; nevertheless

it may be assumed that it contributes to the degree of thixotropy if amylose is also present. The effect of the linear component may be such as to involve the branched component into different forms of more inclined orientation (e.g. chain molecules of amylose may bind or incorporate spherical molecules of amylopection in prolongated aggregations or series).

The ageing process appears in rest conditions of the system, i.e. without the shearing force (in whose presence thixotropy is measured). However, the causes are the same for both phenomena, so it may be considered that changes in the degree of thixotropy of a given system are caused by the aging process.

PROBLEM STUDY

The terms degree of thixotropy and thixotropy of the system, used in the above explanation, imply the *area of the loop* which is formed between initial and reversal shearing in the coordinate system shearing rate (D) and shearing stress (τ). The larger the area of the loop the higher the thixotropy.

D and τ are given by Newton's equation of viscosity:

$$\frac{F}{A} = \eta \frac{dv}{dx}, \quad \text{or} \quad \tau = \eta \cdot D$$

where $F/A = \tau \left[\dfrac{\text{dyn}}{\text{cm}^2} \right]$, and $\dfrac{dv}{dx} = D\,[\text{cm}^{-1}]$

However, we encounter certain difficulties here, quite practical, because the size of the thixotropic loop depends on the maximum shearing rate of the instrument (constructional elements) and on the duration of the shearing process. Hence, these two conditions should also be coordinated so that they do not have any particular effect on the results.

Let us assume that a system is thixotropic to a certain degree and that there is a value for this system which may be termed the constant or the coefficient of thixotropy. For this value to be really constant for the given system, it should not depend on the construction and characteristics of the measuring instrument, or on other conditions, i.e. the measurements should be performed under conditions applicable to all cases.

If we first subject a thixotropic system to constant increase of the shearing rate and then to gradual decrease, and at the same time we are also able to change the duration of shearing at any desired rate, then for some thixotropic systems we may give the following criteria (Fig. 1).

1. At a given arbitrary shearing rate, D_i, there is some (minimum) shearing time, t_{Di}, after which there is no change in the resistance to shear.

2. With increasing shearing rate D_i, the t_{Di} of the system will change, i.e. $\Delta\tau$ ($\Delta\tau = \tau_i' - \tau_i''$), so that for some D_{max} and τ_{max}, $\Delta\tau_{max} = 0$, or mathematically:

$$\lim f(\Delta\tau_i) = 0$$

$$D_i \to D_{max}$$

This means that for $t_{D_i} = 0$, $\Delta\tau_i = 0$ and $\tau_i' = \tau_i'' = \tau_{max}$ (Fig. 1).

3. Values of τ_i'' coincide for a given shearing rate D_i, irrespective of whether they are obtained by shearing for t_{D_i} at initial shearing, or at reverse shearing. Therefore, the system will give the same values for τ_i'' up to any $D_i \leqslant D_{max}$, if $t \geqslant t_{D_i}$, although D_{max} has not been previously obtained.

4. Points for τ_i'' lie on a straight line.

Under these conditions the thixotropic criterion is the area between the intersection of two functions: the function $D = f(\tau)$ obtained at increasing shearing rate, and the straight line $D = a\tau + b$ obtained at reversel shearing, as is shown in Fig. 1.

Analysis of practical measurements shows that the experimental curves $D = f(\tau)$ may be represented by mathematical functions. Thus for example, a 10% gel of a starch and amylopectin admixture in a ratio 2 : 1 gives the relations: $D = 1 - 1.5\ R + 0.1\ R^2$ and $D = 6\ R - 60$, where R is proportional to the shearing stress. A 7% gel of 100% wheat starch gives $D = 0.8\ e^{0.08\ R}$ and at reverse shearing $D = 4\ R - 80$. An 8% gel of corn starch gives $D = -0.009 \cdot \tau + 0.00001 \cdot \tau^2$.

Therefore, considering the $D - \tau$ diagram, in which D is the shearing rate and τ the shearing stress, we can write in the general case the functions which close the thixotropic loop as follows:

$$D = a_0 + a_1\tau + a_2\tau^2 \tag{1a}$$

$$D = k_0 + k\tau \tag{1b}$$

The loop area S closed by these two functions is given by the difference between their integrals in the interval bounded by the points at which they intersect. Calculation gives

$$S = \frac{d^{3/2}}{6\ a_2^2} \tag{1}$$

where

$$d = (k - a_1)^2 - 4\ a_2\ (a_0 - k_0)$$

Expression (1) shows that to obtain S it is not necessary to know D_{max} or τ_{max} (the point at which $\tau_i = \tau_i'' = \tau_{max}$). Hence if the experimental values can be expressed mathematically, D_{max} need not be in the measuring range to get S. However, the measurements should be such as to provide long enough shearing at maximum shearing rate of the instrument for further prolongation of shearing not to cause any further changes in the shearing stress.

In the case of experimental curves the problem may be simplified if $a_0 = 0$, when equation (1a) becomes:

$$D = a_1 \tau + a_2 \tau^2 \tag{2a}$$

and equation (1)

$$S = \frac{[(k-a_1)^2 + 4 a_2 k_0]^{3/2}}{6 a_2^2} \tag{2}$$

The expression is still simpler if functions $D = f(\tau')$ and $D = f(\tau'')$ intersect at the coordinate origin. Then $k_0 = 0$, so we have

$$S = \frac{(k-a_1)^3}{6 a_2^2} = \frac{a_2}{6} \tau_{\max}^3 \tag{3}$$

OTHER CRITERIA OF THE DEGREE OF THIXOTROPY

If the experimental graphs deviate considerably from analytic dependence and the graph is plotted so that at the maximum velocity of the instrument $t_{D_{\max}}$, (i.e. $\Delta \tau$) is not close to zero, then the above equations cannot be used, neither can the total loop area be calculated graphically or measured with a planimeter.

For these reasons, and to simplify the calculation of the degree of thixotropy, it is necessary to have some other criterion which can be determined in a simpler and faster way, and is accurate enough to show different degrees of thixotropy.

1. If we observe the loop area it may be seen that it can be approximately calculated from the sum of the rhomboidal surfaces formed by the differences $(\tau_i' - \tau_i'')$:

$$S = \sum_1^n \frac{(\tau_i' - \tau_i'') + (\tau_{i+1}' - \tau_{i+1}'')}{2} (D_{i+1} - D_i) \tag{4a}$$

This expression cannot be used in the case of a truncated loop (to obtain the total loop area). However, if the difference $\Delta D_i = (D_{i+1} - D_i)$ is small enough, when $(\tau_i' - \tau_i'') \approx (\tau_{i+1}' - \tau_{i+1}'')$, (4a) may written

$$S \approx \sum_1^n (\tau_i' - \tau_i'') \Delta D_i \tag{4}$$

From equation (4) it may be seen that S is proportional to the sum of the distances $(\tau_i' - \tau_i'')$, so the following expression can be used:

$$K = \frac{1}{n} \sum_1^n (\tau_i' - \tau_i'') \tag{5}$$

where K is the criterion of thixotropy and where it is not necessary to measure over the whole loop area but only around the region in which

the difference $(\tau_i' - \tau_i'')$ is maximum (because now it is the mean difference).

3. To express the decrease of the shearing stress due to thixotropic destruction of the system, relative to the total shearing stress of the structured system, we may write:

$$K_{Td} = \frac{1}{n} \sum_1^n \frac{\tau_i' - \tau_i''}{\tau_i'}. \tag{6}$$

Since $\tau = \eta \cdot D$ (η is the apparent viscosity), or $\eta_i = \tau_i/D_i = \tan \alpha_i$,

then $K_{Td} = \frac{1}{n} \sum_1^n \frac{\tau_i' - D_i \tan \alpha_i''}{\tau_i'} = \frac{1}{n} \sum_1^n \left(1 - \frac{\eta_i''}{\eta_i'}\right) = \frac{1}{n} \sum_1^n \left(1 - \frac{\tan \alpha_i''}{\tan \alpha_i'}\right)$ (6a)

When $k_0 = 0$, then $\tau_i'' = D_i \tan \alpha_{max}$ (Figs. 1 and 3), and

$$K_{Td} = \frac{1}{n} \sum_1^n \left(1 - \frac{\eta_{max}}{\eta_i'}\right) = \frac{1}{n} \sum_1^n \left(1 - \frac{\tan \alpha_{max}}{\tan \alpha_i'}\right) \tag{6b}$$

Expression (6b) is applicable in the case of a truncated loop because in some cases (when $k_0 = 0$) tg α_{max} can be calculated without knowing D_{max} and τ_{max}, because $\tan \alpha_i'' = \tan \alpha_{max} = $ const.

4. To express the relative increase of the shearing stress with respect to the oriented system, due to thixotropic structuration of the system, the following expression may be used:

then $K_{Ts} = \frac{1}{n} \sum_1^n \left(\frac{\tau_i' - \tau_i''}{\tau_i''}\right)(1) = \frac{1}{n} \sum_1^n \left(\frac{\tan \alpha_i'}{\tan \alpha_i''} - 1\right) = \frac{1}{n} \sum_1^n \left(\frac{\eta_i'}{\eta_i''} - 1\right)$ (7)

or when $k_0 = 0$

$$K_{Ts} = \frac{1}{n} \sum_1^n \left(\frac{\tan \alpha_i'}{\tan \alpha_i''} - 1\right) = \frac{1}{n} \sum_1^n \left(\frac{\eta_i'}{\eta_i''} - 1\right) \tag{7a}$$

Expressions (6) and (7) give the same quantities, but they are calculated in relation to different states of the thixotropic system: oriented (destructed) and structurated (initial), so they may be termed as follows:

K_{Td} — coefficient of thixotropic destruction, calculated relative to a structurated state according to formula (6),

K_{Ts} — coefficient of thixotropic structuration, calculated relative to an oriented, i.e. destructed state, according to formula (7).

CHECK OF THE DERIVED EXPRESSIONS

To check the practical applicability of and to compare the above thixotropic criteria, expecially as to the possibility of applying the expressions to truncated loops in real systems, we compiled a table

of results calculated according to the formulae (1), (4), (5), (6) and (7) for corresponding thixotropic systems. Let us take the combinations:

I. $D = 6 - 1.5\ \tau + 0.1\ \tau^2$, with $D = 6\ \tau - 55$

Ia. Like combination I, but calculated for the truncated loop (Fig. 2).
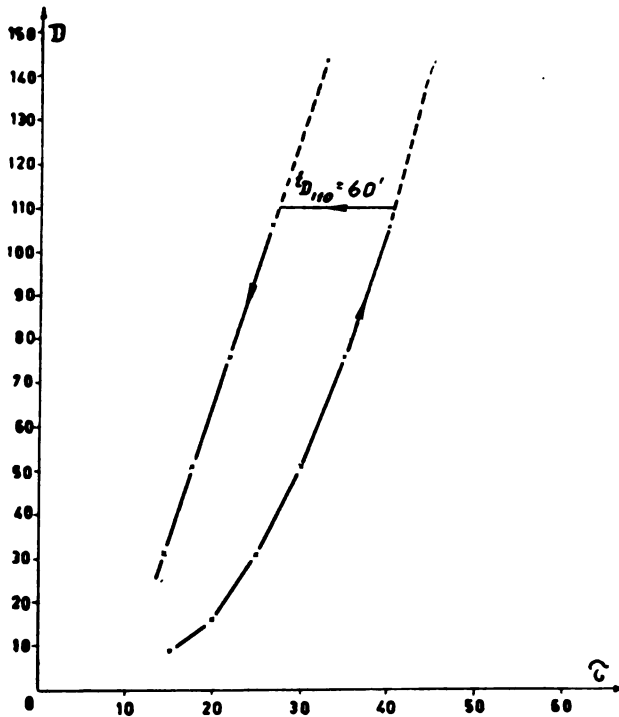
Fig. 2

Thixotropic loop formed by function $D = 6 - 1.5.\tau + 0.1 \cdot \tau^2$ (at initial shearing), and $D = 6 \cdot \tau - 55$ (at reverse shearing).

II. $D = 0.1\ \tau + 0.01\ \tau^2$ with a straight line of reverse shearing $D = 1.6\ \tau$, which assumes that the whole loop is contained inside the measuring range of the instrument (Fig. 3).

IIa. The same functions as II, but with a truncated loop (D_{max} of the thixotropic system is not in the measuring range of the instrument).

III. $D = 65 - \tau + 0.004\ \tau^2$, with the straight line $D = (3/2)\ \tau - 270$. This combination is characteristic for high values of τ'_i, contrary to cases I and II.

IIIa. The same curve — $D = 65 - \tau + 0.004\ \tau^2$ (as in case III), but with a larger loop area, i.e. with the straight line $D = 3/2\ \tau - 210$.

Thus in cases III and IIIa we have different values for τ''_i, and the same for τ'_i.
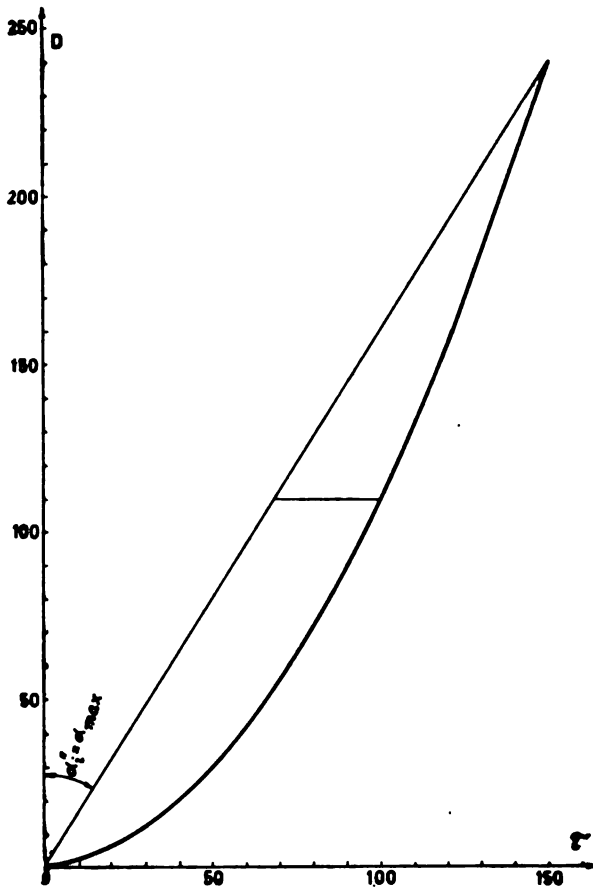
Fig. 3

Diagram of functions $D = 0.1 \cdot \tau + 0.01 \, \tau^2$, and $D = 1 \cdot 6 \cdot \tau$

TABLE 1

Check of results

Combination	Formula number				
	(1)	(4) for $\Delta D_l = 10$	(5)	(6) or (6a)	(7)
I	2.996	2.930	12.3	0.35	0.55
Ia	(1.215)	1.275	13.0	0.38	0.60
II	5.625	5.810	32.0	0.47	1.32
IIa	(3.399)	2.870	33.6	0.47	1.20
III	8.750	8.840	36	0.094	0.105
IIIa	26.210	25.920	76.0	0.187	0.233

CONCLUSIONS

From the values in Table 1, we may conclude the following:

1. Equation (4) holds for sufficiently small values of ΔD_i, while in the case of truncated loops, the area given by this formula is approximately 1/2 of the S given by formula (1), if the loop is truncated slightly beyond the maximum difference $(\tau'_i = \tau''_i)$.

2. Equation (5) holds for approximately the same range of D.

3. Equations (6) and (7) show well the differences due to different loop areas, but only if the shearing stresses τ'_i are approximately the same.

4. The results from formulae (6) and (6a) are in good agreement.

5. Formulae (4), (5), (6) and (7) can also be used for truncated loops, provided great deviations in $(\tau'_i - \tau''_i)$ are neglected in the calculation.

School of Technology
Institute of Chemistry
University of Novi Sad

REFERENCES

1. Cornell, H. J. "The Effect of Amylopectin on the Properties of Starch Gels" — *Die Stärke* (Stuttgart) 15 (2) : 43—50, 1963.

2. Holló, J., J. Szejtli, and G. S. Gantner. "Untersuchung der Retrogradation von Amylose" — *Die Stärke* (Stuttgart) 12 (3) : 73—77, 1960.

3. Holló, J., J. Szejtli, and G. S. Gantner. "Der Mechanismus der Retrogradation von Amylose" — *Die Stärke* (Stuttgart) 12 (4) : 106—108, 1960.

4. Fischer K. *Colloidal Dispersions* — New York: J. Wiley and Sons, 1959.

POLAROGRAPHIC DETERMINATION OF CADMIUM IN THE PRESENCE OF ANTIMONY*

by

SRETEN N. MLADENOVIĆ

The best known supporting electrolyte for quick and exact polarographic determination of cadmium is aqueous solution of ammonium cloride and ammonium hydroxide[1, 2]. From a preliminary study of the reactions of solutions of antimonic compounds it can be concluded that antimony precipitates with ammonium hydroxide in a hydroxide form whose excess does not dissolve. Therefore, antimony is not expected to be present in the solution in view of the fact that the solubility product of antimonic hydroxide $L_{Sb (OH)_3} = 4 \cdot 10^{-42}$.

Because of the reaction of antimonic ions with ammonium hydroxide and the small solubility product of antimonic hydroxide the accuracy of the method of polarographic determination of cadmium from ammoniac medium was not suspected. Another reason which explains the delay in discovery of interferences by antimony in polarographic determination of cadmium is the practice of recording from a solution containing some ferric hydroxide, which acts as a collector for antimony.

The results of polarographic determination of cadmium from ammoniac medium in the presence of antimony without ferric hydroxide were more or less higher depending on the concentration of antimony. Not only is there no explanation in the literature for such high results but also no literature report can be found that the results for cadmium in the presence of antimony are falsely high. Even in the latest polarographic spectra[3] there is no antimony wave in the supporting electrolyte $NH_4OH + NH_4Cl$. Analogous to our finding that in zinc in the presence of lead a high content of copper is obtained from ammoniac medium[4], we proved experimentally that high results for cadmium are caused by the presence of antimonic ions which do not precipitate and are reduced at approximately the same potential $[c_{Sb/Sb}^{3+} = -0.7 - -(-0.8) \ V]$ as cadmium.

We obtained these experimental data by polarographic determination of cadmium from amoniac medium in the presence of antimony.

By polarography of antimony in ammoniac medium we obtain a wave at almost the same potential at which cadmium ions are reduced.

The wave heights of cadmium with and without antimony are shown in Table 1.

TABLE 1

Supporting electrolyte: 1N NH$_4$OH + 1N NH$_4$Cl

Cadmium mg/50 ml	Antimony mg/50 ml	Ferric ammonium sulfate mg/50 ml	Wave height mm
1.00	—	—	20
2.00	—	—	43
3.00	—	—	64
4.00	—	—	85
1.00	1.00	—	22
1.00	2.00	—	21
1.00	3.00	—	34
1.00	4.00	—	68
2.00	1.00	—	42
—	1.00	—	0.0
—	2.00	—	0.0
—	3.00	—	25
—	4.00	—	54
1.00	3.0	20	21.5
2.00	3.0	20	42.0
3.00	3.0	20	64.0
4.00	3.0	20	86

From the polarogram it can be concluded that in determining 1 mg *Cd* without antimony and in the presence of 1 or 2 mg of antimony, there is no difference in the wave height; however, with increasing antimony concentration the difference increases, i.e. for the same quantity of cadmium *m*, the wave height increases.

In polarographic determination of 1 and 2 mg of antimony without cadmium practically no wave is obtained. With increasing antimony concentration the wave appears almost at the same potential as the cadmium wave. It can be concluded that the wave height does not increase linearly with antimony concentration (Table 1).

If cadmium is polarographically determined in the presence of antimony and ferric ions, the wave heights are the same as those of the same cadmium concentrations measured in solutions without antimony (Table 1). Ferric hydroxide in the electrolyte quantitatively collects antimony; this explains the absence of antimony waves on the polarograms, usually superposed with the cadmium waves causing high results for cadmium.

If ferric chloride or ferric ammonium sulfate is added to the ammoniac solution of antimony, the antimony wave disappears.

From these results it follows that precise polarographic determination of cadmium in the presence of antimony from ammoniac medium can be carried out in the presence of ferric hydroxide.

REFERENCES

1. Lingane, J. "Systematic Polarographic Metal Analysis; Characteristics of Arsenic, Antimony, Bismuth, Tin, Lead, Cadmium, Zinc, and Copper in Various Supporting Electrolytes" — *Industrial and Engineering Chemistry, Analytical Edition* (Washington) 15: 583—590, 1943.
2. Vǒrišková, M. — *Collection of Czechoslovak Chemical Communications* (Praha) 11: 580, 1939.
3. Kriukova, T. A., S. I. Siniakova, and T. V. Areféva. *Polarograficheskiĭ analiz* (Polarographic Analysis) — Moskva: Gosudarstvenoe nauchno-tekhnicheskoe izdatel'stvo khimicheskoi literatury, 1959.
4. Mladenović, S. "Polarografsko određivanje bakra pored olova" (Polarographic Determination of Copper in the Presence of Lead) — *Glasnik hemijskog društva* (Beograd) (In press).

CHEMICAL ASSAY OF DEOXYRIBONUCLEIC ACIDS IN ANIMAL TISSUES

by

MIODRAG D. CVETKOVIĆ and PREDRAG P. MILOŠEVIĆ

INTRODUCTION

Among the many methods for preparing polymeric nucleic acids, hydrolysis techniques have the following advantages: good yields, simplicity, and ease of application. On the other hand, they also have certain defects on certain critical points, primarily in the extraction of the acid soluble fraction, and also in the delipidation which follows it. These drawbacks lead to losses of nucleic acids. This problem was recently discussed by Hutchison et al.[1], Fleck and Munro[2], and Hallian and co-workers[3]. The use of warm acids also leads to nucleic acid losses, as recently discussed by Hutchison and co-workers[1] and by Lovtrupp and Roos[4, 5].

A simple and rapid technique for the assay of DNA has been proposed by A. S. Orlov and E. J. Orlova. The tissue is hydrolysed with NaOH solution, and then the proteins are precipitated with NaCl-saturated acetic acid, and the DNAs with cold absolute alcohol. Thereby, extraction of the acid soluble fraction, delipidation, and DNA extraction with warm acids are avoided. It was because of this that the method attracted our attention. The results obtained in our laboratories permit us to evaluate each stage of the method.

The aim of the present work was to study the Orlovs' method in more detail than is reported in their original publication, and also to try and improve the technique, to make it more convenient, more effective and more suited to the requirements of modern research. We have worked out a procedure, based on the Orlovs', which is very convenient for the assay of DNA in animal tissues. Our preliminary results were reported at the First Congress of Yugoslav Biochemists and at a meeting of the Association of Physiologists in Beograd[7, 8].

MATERIAL AND METHODS

The experimental animals were male white rats weighing 170 to 190g. Samples of tissue of the liver, spleen, kidneys, muscles, and heart were taken, homogenized, and treated in one of the following two

2*

ways: a) by the original technique of the Orlovs; by a modification of this technique, according to the following procedure:

About 500 mg of tissue is homogenized in a Potter-Elvehjem homogenizator in cold distilled water (0°C). To the homogenized tissue suspension N/1 KOH solution is added to a KOH concentration of N/3. The tubes are then kept at 37°C for one hour[2]. To 10 ml of the hydrolyzate refrigerated to 0°C is added 5 ml of 20% acetic acid saturated with NaCl. The mixture is then centrifuged 5 minutes at low speed. The precipitated proteins are washed in the base, and the supernatant is decanted into 60 ml alcohol at —25°C. The precipitate is redissolved by addition of the base. The reagent for precipitating the proteins is added once more and centrifuging carried out again. The supernatant is added to that of the previous centrifuging in the refrigerated alcohol. The tubes are kept 1 to 2 hours at —25°C, and then DNA isolated by centrifuging 5 min at low speed. When the DNA preparation no longer contains any phosphorous substances and gives no reaction with diphenyl amine, it is quantitatively dissolved in distilled water — 0.02—0.25 mg of DNA—P per ml of solution. DNAs are not completely soluble in water, but give a very homogeneous suspension (assay of deoxyribose and phosphorous in 8 parallel samples gave exactly the same values), which disperses completely in Burton's reagent[9]. To a 1 ml aliquot of the DNA solution TCA is added to a concentration of 5%, and then the mixture heated in a water bath at 60°C for 15 minutes. This treatment increases the optical density of the solution by about 27% when the DNAs are determined with diphenyl amine. After refrigeration, $HClO_4$ is added to a concentration of 0.5 N. The deoxyribose is determined by Burton's technique[9], and phosphorous, after mineralization according to Marinetti[10], is determined by Chen's technique[11] or by the method of Macheboeuf and Delsal[12]. Proteins are detected by the burette test and RNA by the orcinol reaction after Mejbaum[13].

RESULTS

Quantity of tissue

In the original technique of Orlov and Orlova the tissue-base ratio for hydrolysis was 50—100 mg of chopped up tissue to 1 ml N/1 NaOH (5 minutes in a boiling water-bath). We found that if the quantity of liver, spleen, kidney, muscle or heart tissue exceeds 50 mg, hydrolysis under these conditions is not complete. Furthermore, the precipitation of proteins in the next stage is not efficient and the DNA preparation in the cold alcohol still contains a certain amount of proteins. Table 1 indicates this contamination by the presence in the DNA preparations of substances which do not give a positive reaction with diphenyl amine. We suppose that most of the phosphorous which dominates the numbers for deoxyribose in incomplete hydrolysis was contained in phospho-proteins,

Quantity of tissue and the purity of the DNAs

100 mg (1) or 50 mg (2) of chopped up fresh tissue was hydrolyzed in 1 ml N/1 NaOH for 5 minutes in a boiling water-bath, with stirring. From the hydrolyzate the proteins were precipitated as described above and the DNAs separated in 95% ethyl alcohol at 0°C. After centrifuging and decanting, the precipitate was redissolved in distilled water. Deoxyribose (a) and phosphorous (b) were assayed by the techniques described above. The results are expressed in micrograms of DNA—P per 100 mg of fresh tissue. The table gives the mean values for 8 experiments. Statistical examination of the results shows significant differences between deoxyribose and phosphorous in group 1 (except in the case of muscle tissue).

TABLE 1

	Liver		Spleen		Kidneys		Muscles		Heart	
	a	b	a	b	a	b	a	b	a	b
1.	21.8	26.1	17.9	19.7	30.3	33.8	5.8	5.20	10.2	12.9
2.	22.1	22.1	18.1	18.0	30.8	32.1	5.21	5.19	10.5	10.8

Although the tissue-base ratio was reduced to 50 mg per ml, the DNAs isolated from the liver, spleen, kidneys and heart still contained small quantities of proteins, but the quantitity of phosphoric substances reacting with diphenyl amine was reduced below the limit of significance. Table 2 gives the results of assay of phosphorous and deoxyribose for a number of important striated muscles. The difference between the two methods of DNA assay are not significant. The orcinol reaction was negative.

Phosphorous/deoxyribose ratio in the DNAs prepared from striated muscles. Muscle tissue hydrolyzed 5 min in N/1 NaOH in a boiling water-bath. Proteins precipitated as described, DNAs precipitated in ethyl alcohol at —20°C. DNAs redissolved in distilled water. Quantity of deoxyribose (1) and phosphorous expressed as micrograms of DNA—P per 100 mg of fresh tissue.

TABLE 2

	Number of experiments	Extreme values	Mean	Standard deviation
1.	70	5.17—5.24	5.209	± 0.07492
2.	51	5.19—5.40	5.303	± 0.07928

Alkaline hydrolysis

The alkaline hydrolysis used by Orlov and Orlova seems to us too drastic. We would ascribe the presence of proteins in some of the DNA extractions to massive breakdown of proteins by the hydrolysis. That is why we compared their hydrolysis procedure with one taking one

hour at 37°C in N/3 NaOH. We consider that this latter technique has two advantages: a certain increase in yield, and absence of proteins from the preporations.

Alkaline hydrolysis and DNA yield. Hydrolysis performed by two methods: a) chopped up tissue (50 mg to 1 ml N/1 NaOH) hydrolyzed 5 min in a boiling water-bath; b) tissue homogenized in a Potter-El-vehjem apparatus in distilled water at 0°C, then hydrolyzed 1 hour at 37°C in 1 ml N/3 KOH. Remaining procedure as in preceding experiments. The results are expressed as micrograms of DNA—P per 100 mg of fresh tissue and are the mean values for 8 experiments.

TABLE 3

Hydrolysis	Liver	Spleen	Kidneys	Muscles	Heart
a	22.1	18.6	33.1	5.26	10.9
b	26.8	19.4	33.5	5.61	13.1

Separation of DNAs from a medium containing RNAs, low molecular weight nucleotides, acid soluble phosphorous and other phosphorous compounds: importance of the ethyl alcohol temperature.

We devoted special attention to the importance of the temperature of the ethyl alcohol used for the separation of the DNAs. Table 4 shows that a better yield is obtained at —25°C than at 0°C. Extraction at —10°C gives almost as good results as at —25°C. The time the DNAs stay in the cold alcohol makes no apparent difference above 1—2 hours (2—24 hours), but the yield progressively decreases the shorter the period under 1 hour.

Alcohol temperature and extraction efficiency. Tissue hydrolyzed 1 hour in N/3 KOH at 37°C. After precipitation of proteins, two extraction procedures were used: a) 1—2 hours in 95% ethyl alcohol at 0°C;

After centrifuging, the DNAs are redissolved in distilled water, and assayed as in the preceding experiments. The values in the table are micrograms of DNA—P per 100 mg of fresh tissue and represent the averages for a number of experiments.

TABLE 4

	Liver	Spleen	Kidneys	Muscles	Heart
a	22.6	19.0	33.5	5.34	11.3
b	27.1	19.6	36.5	5.63	13.4
Number of experiments	24	20	20	16	8

Conditions necessary for Dische's reaction[22] modified by Burton[9] using diphenyl amine as the reagent for DNA assay.

Usually solutions for DNA assay are obtained using bases (KOH or NaOH). Our experiments revealed a reduction in the otpical density

of the solutions due to the presence of the bases in them. We tried using various concentrations of KOH and NaOH (N/1—N/500) for dissolving the DNAs. The optical density was the more reduced (30—70% of that obtained in solutions without bases) the higher the base concentration. Care was taken to keep the pH of the medium constant throughout the experiments. Decrease of the base concentration below N/100 did not cause any further significant decrease of the optical density. On the other hand, the optical density showed a certain increase (15—20% over the base-free controls) with very low base concentrations (N/100—N/500), and also with acetic acid used in the corresponding concentrations instead of TCA.

For the above reasons, we used distilled water to disperse the DNA precipitate after separation in cold alcohol. A fine homogenous suspension is formed which readily dissolves in Burton's reagent. By increasing the TCA and $HClO_4$ concentrations we found that the maximum density is obtained at 5—10% TCA and 0.5 N $HClO_4$, which is in full agreement with Burton's data[9]. We were particularly interested in the effect of warm acids. We found that the extraction of DNA, prepared either by the original technique of Orlov and Orlova or by the modified technique, in 5% TCA at 90°C was not constant, and involved considerable losses of deoxyribose (or of intermediate products of the breakdown of DNAs which react with diphenyl amine). Table 5 shows the losses for liver and muscle tissue.

Extraction of DNA in warm TCA, and the resulting losses. Hydrolysis and the precipitation of proteins and DNAs as in the preceding experiments. The hydrolyzate was divided into two parts, (a) and (b). (a) — DNAs dissolved in distilled water. (b) — DNAs twice extracted 15 min in 5 ml 5% TCA at 90°C. DNA assay by Burton's method[9]. The results are expressed as micrograms of DNA-P per 100 mg of fresh tissue.

TABLE 5

Tissue		Number of experiments	Extreme values	Mean value	Standard deviation
Liver	a	11	25.9—27.0	26.427	± 0.408
	b		16.4—23.1	19.936	± 4.368
Muscles	a	27	5.48—5.57	5.538	± 0.036
	b		4.12—4.93	4.466	± 0.240

On the other hand, DNA samples heated at relatively low temperatures (in 5% TCA) gave a relatively higher optical density (Graph 1). Similarly, extraction of DNAs 15 min in 5% TCA at 50—60°C increased the optical density by 27%. Temperatures lower than 50—60°C for 15 to 30 min negligibly affected the optical density. Temperatures above 70°C caused a rapid fall to below the control values.

Treatment (referred to above) of the DNAs with warm TCA, and the optical density in the reaction with diphenyl amine.
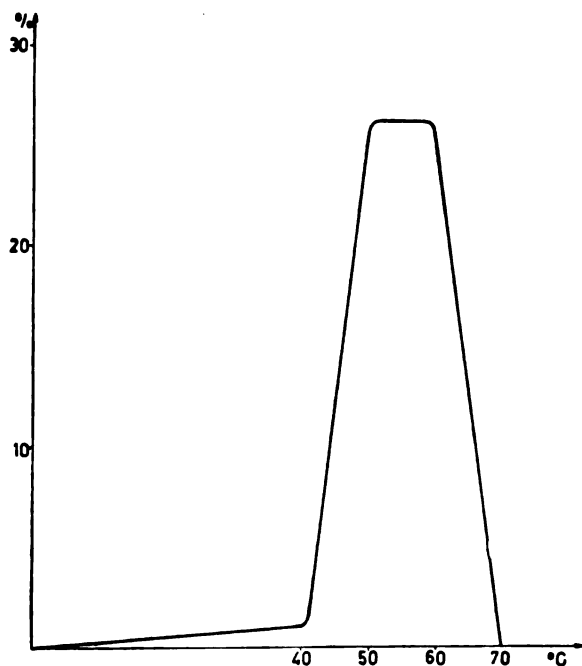
Fig. 1

Liver DNAs prepared as described above (b), and redissolved in 10 ml of distilled water. To each 1 ml aliquot of the solution TCA was added to a final concentration of 5%. Some of the tubes were heated 15 to 30 min at different temperatures between 30° and 100°C. Aliquots which were not heated before the addition of diphenyl amine were the controls. After refrigeration, $HClO_4$ was added (to the controls as well) to a final concentration of 0.5 N, and then Burton's reagent was added. The reading was made at 600 mμ.

The optical density of solutions prepared as above (with warm TCA) and incubated in Burton's reagent at 25—35°C was found to be very sensitive to light: after exposure to light for 10—15 min the color changed from blue to green. The absorption maximum remained at 600 m μ, but the optical density was decreased. The sensitivity to light seemed to be greater with DNAs prepared by the method we have described than with those obtained by the method of Schmidt and Thannhauser.

DISCUSSION

During moderate alkaline hydrolysis of the tissues the RNAs break down into acid soluble nucleotides, while the phosphoproteins

give a quantitative yield of phosphorous in inorganic form. The DNAs are also soluble in mineral acids, in the presence of which both the DNAs and the proteins precipitate. Schmidt and Thannhauser[14] hydrolyzed the tissue 15 hours in N/1 NaOH at 37°C. Under such conditions the proteins are denatured to such an extent that they become partially acid soluble[1, 2]. Orlov and Orlova used an even more drastic hydrolysis (boiling water-bath and N/1 NaOH). Thanks to the insolubility of the proteins in saturated NaCl solution (the DNAs remaining in solution), they were able to precipitate the proteins of the hydrolyzate using 20% acetic acid saturated with NaCl. However, it seems to us that the destruction of proteins in the course of such operations must be considerable — the proteins which get destroyed can no longer be precipitated by the simultaneous action of acetic acid and NaCl. This protein fraction then precipitates together with the DNAs in the cold alcohol, and separates together with them in centrifugation. Since we decided to avoid extracting the DNAs with warm acids, this represented a disadvantage of the procedure as a whole.

Scott et al.[16] recently proposed a more moderate hydrolysis: 1 hour at 22°C in N/1 NaOH, obtaining complete DNA extraction. Fleck and Munro[2] obtained complete extraction of tissue RNAs in the form of acid soluble nucleotide after 1 hour hydrolysis at 37°C in N/3 KOH. In this procedure the destruction of proteins is minimal, and they are precipitated almost quantitatively by mineral acids. Prolongation of the incubation considerably increases the extraction of proteins in acid soluble form, but does not affect the yield of nucleic acids. In our experiments using this technique we observed a significant decrease in the acid soluble protein yields, and the protein contamination of the DNAs was reduced in equal measure. Furthermore, with this relatively mild and brief hydrolysis, the DNA yield was increased·

In studying the mechanism of the diphenyl amine reaction Burton treated highly polymerized DNAs prepared from the calf thymus by the method of Hammarsten[17] and Key et al.[18] 30 and 60 min in 0.5 N $HClO_4$ at 70°C. Pretreating the DNAs in this way accelerates the development of the color in the diphenyl amine reaction, but at the same time causes a reduction in the optical density of the solution by 7% (30 min) and 14% (60 min) respectively. DNA preparations heated at 90°C in 5% TCA undergo similar changes. Burton also observed the liberation of 25% of phosphorous in inorganic form during the first phase of the reaction. He considers that the diphenyl amine reacts with the deoxyribose liberated from the purine bond, or with an intermediate product of the degradation of purine deoxyribonucleotides.

M. de Deken-Grenson and R. H. Deken[23] found that after preliminary heating of the DNAs of various tissues at 90°C, Dische's[22] diphenyl amine reaction gave values about 10% lower than for preparations heated to 70°C. S. Lovtrupp and K. Roos[4, 5] heated the highly polymerized DNAs obtained from salmon sperm at 70°C in 5% $HClO_4$. They found that the optimal time for getting the maximum optical density was 20 min at this temperature. Prolongation of the extraction

causes a fall in the absorption, which is the more rapid the higher the temperature. These authors also confirmed experimentally the above hypothesis that it is the purine deoxyribose of the depolymerized DNAs which reacts with the diphenyl amine.

With the technique of Orlov and Orlova, to get the maximum absorption for rat liver DNAs it was found necessary to treat the preparations 15 min in 5% TCA at 50—60°C. This is in accord with data recently confirmed a number of times: DNAs of different origin show differing resistance in warm acids[1].

From these facts it seems to us that: a) to get maximum absorption in the diphenyl amine reaction it is necessary to depolymerize the DNAs. The depolymerization by means of warm acids, or the breakdown of the DNAs under prolonged action of the acids (leading to a decrease in absorption), is performed under different conditions for different tissues, as is the case with the extraction itself. However, it seems to us that a temperature about 70°C (5% TCA, 0.5 N $HClO_4$, 15 min) is suitable for all tissue DNAs. This is the critical temperature above which considerable breakdown of DNAs takes place, with a consequent reduction in absorption.

We got a higher DNA yield by precipitating at —25°C than at 0°C. This is probably due to polymerization of the DNA molecules at the lower temperature. Mirsky and Pollister[19, 20], and Gulland et al.[21] have in fact established a rapid increase of the viscosity of DNA solutions kept in cold alcohol. The results of our research on certain physical properties of DNA in alcohol at 0°C and —25°C were published earlier. In this respect one detail which would seem to be relevant is that in separating the acid soluble fraction (in the control experiments) by washing in 10% TCA, and then separating the DNAs by the method described above with precipitation in alcohol at 0°C, we found that in order to get a good decantation it was necessary to centrifuge three times longer than in the experiments without separation of the acid soluble fraction. This may be ascribed to the fact that DNAs treated with acids are less resistent to bases. Because of this the molecular weight of the DNAs is reduced after extraction of the acid soluble fraction. Nevertheless, in case of separation in alcohol at —25°C we got a sedimentation comparable to that with DNAs prepared without preliminary extraction of the acid soluble fraction.

In order to check the efficiency of the procedure reported here, we have compared our results with those obtained by most of the more frequently used techniques. Table 6 shows that the DNA values obtained with our modification of the method of Orlov and Orlova are about the same as those obtained with the other principle methods for DNA assay at present in use[14, 24, 27, 6, 2, 29].

We also made some experiments using the method of Fleck and Munro (which is very convenient for preparation and assay of RNAs) for DNA assay[2]. The results were somewhat lower than those obtained by the modified method of Orlov and Orlova (Table 6, last column).

TABLE 6

Organ	Our results	Schmidt and Thannhauser	Schneider	Ogur and Rosen	Orlov and Orlova	Fleck and Munro
Liver	27.1	22.5 [14] 26.0	19.6 [24] 26.4	14.1 [27] 14.8	25.7	20.8 [28]
Spleen	82.7	54.5 [14]	140.0 [25]		165.7	85.6 [28]
Kidneys	36.3	33.5 [14]	41.8 [25]			31.9 [28]
Muscles	5.36	5.03 [29]	5.7 [26]			4.07 [28]

CONCLUSION

Our modification of the original method of Orlov and Orlova is thus as follows:

Carefully chopped up and (cold) homogenized fresh tissue is hydrolyzed 1 hour in N/3 KOH at 37°C. The most suitable ratio of tissue weight to volume of base is 50 mg to 1 ml. To 10 ml of the hydrolyzate cooled to 0°C 5 ml of NaCl saturated acetic acid is added (to precipitate the proteins). After centrifuging, the supernatant is decanted into 60 ml of absolute alcohol at —25°C .The precipitate is redissolved by addition of the base. The reagent is again added in order to precipitate the proteins. After another centrifuging the supernatant is combined with that already in the refrigerated alcohol. The tubes are kept at —25°C 1—2 hours. The DNAs (which precipitate in the cold alcohol) are isolated by centrifugation at low speed for 5 min. The precipitated DNAs are then made into a fine homogenous suspension in distilled water. To 1 ml aliquots of this suspension TCA is added to a final concentration of 5%, and then the mixture heated in a water-bath 15 min at 60°C (to increase the optical density). After cooling, $HClO_4$ is added to a final concentration of 0.5 N. Finally either deoxyribose (Burton) or phosphorous (Marinetti, Chen, Macheboeuf) is determined.

In comparison with other current method the yield obtained is completely satisfactory.

REFERENCES

1. Hutchison, W., E. Downie, and, H. Munro. — *Biochimica et Biophysica Acta* 55: 561—570, 1962.
2. Fleck, A., and H. Munro — *Biochimica et Biophysica Acta* 55: 571—583, 1962.
3. Hallinan, T., A. Fleck, and H. Munro. — *Biochimica et Biophysica Acta* 68: 131—133, 1963.
4. Lovtrupp, S., and K. Roos. — *Biochimica et Biophysica Acta* 53: 1—10, 1961.
5. Lovtrupp, S., and K. Roos.—*Biochimica et Biophysica Acta* 68: 425—433, 1963.
6. Orlov, A., and E. Orlova. — *Biokhimiia* 26: 934—839, 1961.
7. Milošević, P., M. Cvetković, and S. Kostić. "Uporedno ispitivanje metoda za preparisanje i doziranje DNK i RNK" (Comparison of Methods for the Preparation and Assay of DNA and RNA), in: I kongres medicinskih biohemičara, Zagreb, 7—11 juni 1963. (Ist Congress of Medical Biochemists, Zagreb, 7—11 June 1963).

8. Milošević, P., M. Cvetković, and S. Kostić. "Prilog proučavanju metoda za doziranje DNK" (Study of DNA Assay Methods), in: Sastanak Podružnice za Srbiju Jugoslovenskog društva fiziologa, Beograd, 11. XI 1963. (Meeting of the Serbian Branch of the Yugoslav Society of Physiologists, Beograd, 11 Nov. 1963).

9. Burton, K. — *Biochemical Journal* 62: 315—323, 1956.

10. Marinetti, G., J. Erbland, M. Albrecht, and E. Stotz. — *Biochimica et Biophysica Acta* 30: 543—548, 1958.

11. Chen, P., T. Toribara, and H. Werner. — *Annals of Chemistry* 28: 1756—1759, 1956.

17. Macheboeuf, M., and H. Delsal. — *Bulletin de Societé Chimique et Biologique* 25: 116—121, 1943.

13. Mejbaum, W. — *Zeitsshrift Physiologishe Chemie* 258: 117—123, 1939.

14. Schmidt, G., and S. Thannhauser. — *The Journal of Biological Chemistry* 161: 83—89, 1945.

15. Steudal, H., and E. Peiser. — *Zeitsshrift Physiologische Chemie* 120: 292—297, 1922.

16. Scott, J., A. Fraccastoro, and E. Taft. — *Journal of Histochemistry and Cytochemistry* 4: 1—4, 1956.

17. Hammarsten, E. — *The Biochemical Journal* 144: 383—390, 1924.

18. Kay, E., N. Simmons, and A. Dounce. — *Journal of the American Chemical Society* 1129: 1129—1136, 1947.

19. Mirsky, A., and H. Pollister. — *Proceedings of the National Academy of Science of the U. S.* 28: 344—350, 1942.

20. Mirsky, A., and H. Pollister. — *Biological Symposia* 10: 24—29, 1943.

21. Gulland, M., D. Jordan, and C. Threlfall. — *Journal of the Chemical Society* 1129: 1129—1145, 1947.

22. Dische, Z. — *Mikrochemie* 8: 4—9, 1930.

23. De Deken-Grenson, M., and R. De Deken. — *Biochimica et Biophysica Acta* 31: 195—207, 1959.

24. Schneider, W. — *The Journal of Biological Chemistry* 161: 293—303, 1945.

25. Schneider, W. — *The Journal of Biological Chemistry* 164: 747—752, 1946.

26. Schneider, W., and H. Klug. — *Cancer Research* 6: 691—699, 1946.

27. Ogur, M., and G. Rosen. — *Archives of Biochemistry* 25: 262—276, 1950.

28. Milošević, P., Unpublished results.

29. Mandel, P. — *Comptes Rendus des Seances de la Societé de Biologie* 143: 536—543, 1949.

EXPLANATION OF THE OPTIMUM CONDITIONS
FOR THE SEPARATION OF MATERIALS
BY FLUIDIZATION CHARGING

by

DEJAN M. BAJIĆ, SLOBODAN K. KONČAR-ĐURĐEVIĆ,
and VLADETA LJ. PAVASOVIĆ

INTRODUCTION

In the fluidization of mixtures of solid mineral materials by air, it has been observed that the material becomes charged on account of particle friction. In the fluidization layer there is a strong electric field which makes it possible to separate two or more components of the mixture on a metallic condenser electrode placed in the fluidization column[1,2]. Numerous investigations of this phenomenon have been performed for practical and scientific reasons[3,4,5]. The results have shown that there are many mixtures which can be separated into components by this method, and in a considerable number of cases the purity and amount of the separated components are very high.

In this paper we give the results of some measurements which indicate that the separation of material by fluidization charging follows some general regularities. The separation may be considered as due to the joint action of air, earth gravity and electric forces between the charged particles and the charged metal electrode. Therefore we condsidered it necessary to determine the mean value of the electric charge per particle of the separated material and its dependence on various factors, as for example: the position of the electrode in the column, the total weight of solids, the rate of air flow, the granulometric composition, the relative weight ratio, the nature of the material, the specific gravity of the separated material, the dielectric permeability of components etc. for a column at constant temperature and constant air humidity.

These measurements showed that the optimum values of the above factors for maximum separation can be interpreted in terms of the charge per particle of separated material and the strength of the electric field created in the column.

MEASUREMENT TECHNIQUE

Fluidization was carried out as described in previous papers[1,2,3,4,5] by means of an air pump, a column of silicagel for air drying, a rotameter for the measurement of air flow (up to 160 l/min),

a valve for controlling the air flow, an apparatus for measuring the temperature and humidity of the air, and the plexiglass column which was square in cross section.
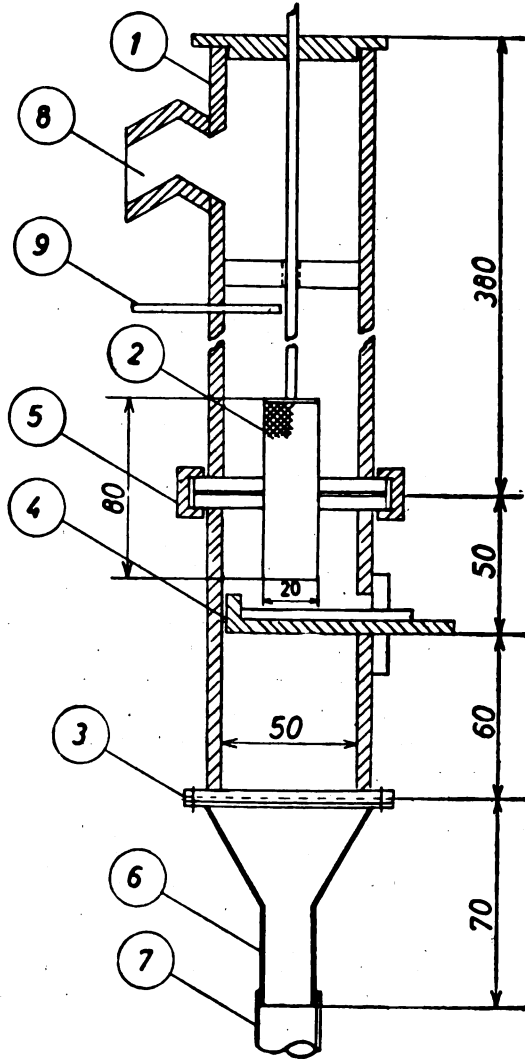
Fig. 1

1 — Plexiglass column;
2 — Metal electrode;
3 — Porous metal grid;
4 — Movable collecting drawer;
5 — Joiners;
6 — Metal cone;
7 — Rubber tube;
8 — Air outlet.

A diagram of the column is given in Fig. 1. It consists of plexiglass walls (1), and a metal electrode (2) of cylindrical net which was found to afford optimum separations on account of the intensity of the electric field in the vicinity of its thin wires. The column has also a porous metal grid for supporting the material (3), a movable collecting drawer (4), joiners of movable parts (5) which make possible the exchange of material in the column; a metal cone (6) which serves for the distribution of air; rubber tubes (7), an opening for the outlet of air and left over material (8), and a movable rod of plexiglass (9) to shake the deposited material from the electrode to the collecting drawer.
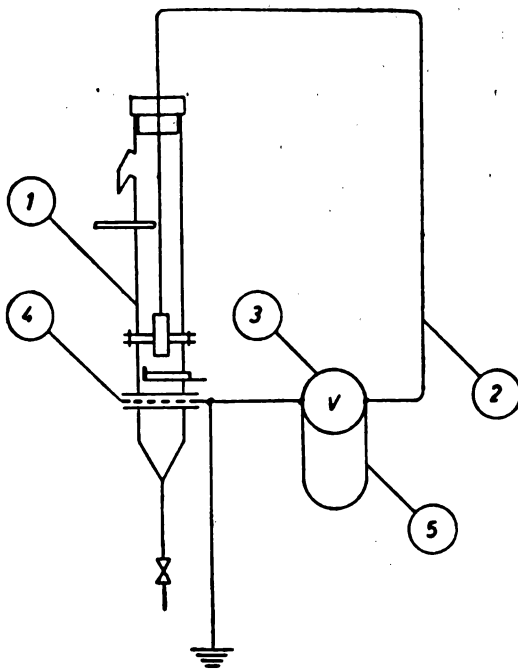
Fig. 2

1 — Column;
2 — Conducting wire;
3 — Electrostatic voltmeter;
4 — Metal grid;
5 — Metal wire.

A diagram of the electrical apparatus for the measurement of the electric charge per particle is shown in Fig. 2. It consists of a column (1), a conducting wire (2) which connects the electrode with one end of an electrostatic voltmeter (3), a metal grid (4) which is connected with the other end of the voltmeter; and a metal wire (5) which connects to the end of the apparatus during fluidization.

The whole column is set vertically and attached to a plate of insulation material; the electrostatic voltmeter is placed in its vicinity on a horizontal plate of insulation material. During fluidization relatively small charges (order of magnitude of 10^{-9}C) of high voltage (some thousands of volts) are generated. Therefore, the insulation of the conductor through which flow the currents of about 10^{-10}A (and less) and the insulation of the whole column should be examined carefully. The whole column and the voltmeter are surrounded by a wirenet which plays the role of a Faraday's cage, and operations are performed outside of this. In this way, stray and irregular capacitance losses are reduced to a minimum.

The measurement of the quantity of electricity was carried out in the following way[6]. During the air flow through the column, a mixture of solid ground dielectric material was fluidized. The investigated material was a mixture of two components, one being always quartz sand and the other was marble, KNO_3 and $Pb(NO_3)_2$ respectively in different experiments. On account of mutual friction in the fluidization bed the particles became charged with opposite polarity. It was found that sand was charged negatively and marble positively[3]. This phenomenon was in agreement with Cohen's rule[7] since the dielectric permeability of marble is greater than that of the sand. During fluidization the metal electrode dipped into the fluidized bed became negatively charged and attracted the positively charged marble particles. After cessation of the fluidization, the movable collecting drawer was placed below the electrode, and the separated material was shaken down onto the movable drawer. In this way, the amount of electricity with which the particles were charged was liberated at the electrode, and caused deflexion of the voltmeter needle according to the equation

$$Q = C \cdot U$$

where C is the known capacitance of the electrostatic voltmeter when the needle is deviated for a definite voltage, U, which is read from the scale.

From the total weight of separated material shaken from the electrode, from its specific gravity, and from the known volume (v') of particles (particles were assumed to be balls whose diameter was determined by granulation), the weight of one particle (g') was determined. Hence the number of separated particles was

$$n = g/g'$$

and the mean charge of each particle

$$Q' = Q/n$$

During the course of measurements the humidity and temperature of the material was kept constant. The material had been previously dried for several hours at 110°C, and the relative humidity of the air was about 20%. The temperature of the air and material was 20°C. To avoid the unfavorable effects of other substances, the investigated material contained only a small amount of impurities.

The specific gravities and dielectric permeabilities of the investigated materials are given in Table 1. During fluidization, sand was always charged negatively and the other component positively. The mixtures of sand + marble and sand + $Pb(NO_3)_2$ follow Cohen's rule, but the mixture of sand + KNO_3 deviates, since the dielectric permeability of potassium nitrate is smaller than that of sand. According to Cohen's rule of polarity the charges should have been the reverse. This is not the only known deviation from Cohen's rule [3, 7, 8].

TABLE 1

Chemical composition	Specific-gravity g/cm³	Relative dielectric permeability
Sand	2.56	4.8
Potassium nitrate	2.09	2.56
Marble	2.70	8.5
Lead nitrate	4.41	16.0

All experiments were carried out in the same fluidization column, one of the following experimental factors being altered each time:
— the distance between the electrode and the porous bottom of the column, h_0;
— the weight ratio of components in the mixture;
— the granulometric composition of the mixture according to DIN 1171 standards;
— the rate of air flow, q (l/min);
— the totalweight of the mixture in the column G (g);
— the fluidization time, t (sec);
— Measurements of the following were performed:
a) the weight of material separated on the electrode, g (g),
b) the total electric charge of material separated on the electrode Q (c),
c) the electric charge per particle of separated material Q' (c).

RESULTS

Using the amount of separated material as the measure for the functioning of the separation, we found, in the case of the marble + sand mixture, the following:

1. By changing the height of the electrode, h_0, which is dipped into the fluidization bed (other experimental conditions constant) we found that there is an optimal height, h_{opt}, which is 48 mm for the given column and electrode (Fig. 3).

2. By changing the weight ratio of components in the mixture we found that the optimal ratio is 1 part marble : 10 parts sand (Fig 4), and that a larger percent of the marble separates when there is less marble in the mixture.

3
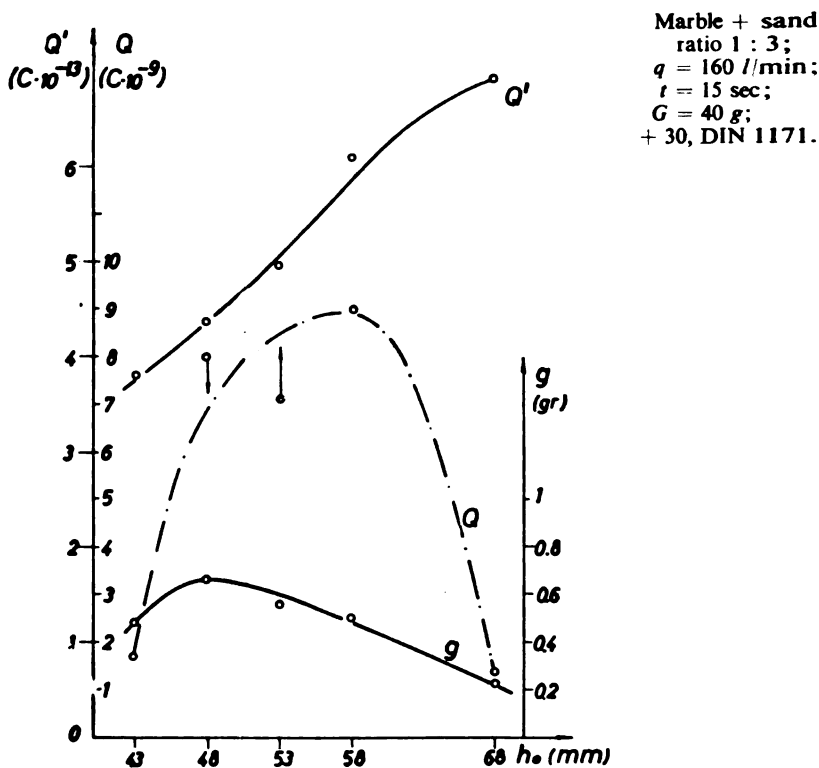
Fig. 3

3. By changing the granulometric composition we found that the best granulation is about + 50 (Fig. 5). Figure 5 also gives the particle weight for each granulometric composition.

4. By changing the rate of the air flow, q, we found that the optimal flow for this system is 140 l/min (Fig. 6).

5. As for the fluidization time, t, it has been found that there is an optimal time for every column and mixture under constant conditions. In our experiment the optimal time was about 15 sec (Fig. 7). In shorter fluidization periods the amount of separated material was too small, and in periods longer than 15 sec, the separation of material was not linearly proportional to the time, but much smaller as shown in Fig. 7.

6. By changing the total weight of the mixture, G, one can obtain its optimal value for a given column and a given mixture. In the investigated case it amounted to 80 g (Fig. 8). An optimal weight should exist since there is also an optimal height for the electrode in the fluidization bed. These two factors are interdependent.

Marble + sand;
+ 30, DIN 1171;
$q = 140$ l/min;
$t = 15$ sec;
$G = 40$ g;
$h_0 = 48$ mm

Fig. 4

Marble + sand;
ratio 1 : 3;
$q = 100$ l/min;
$t = 15$ sec;
$G = 40$ g;
$h_0 = 48$ mm.

Fig. 5

3•
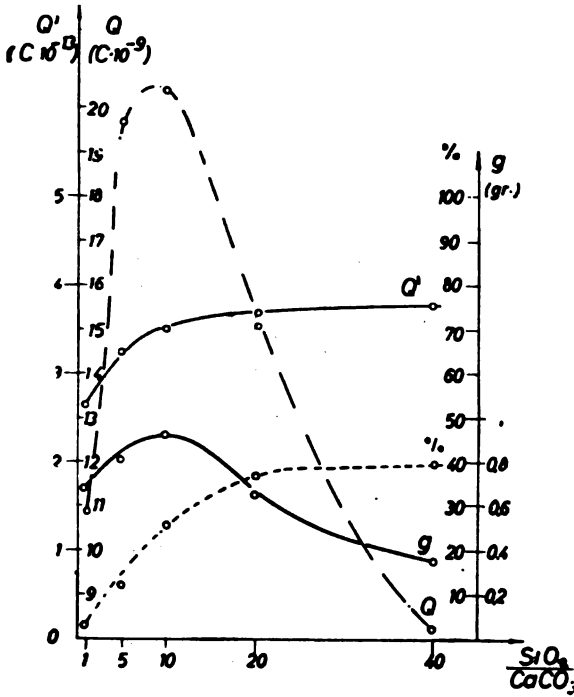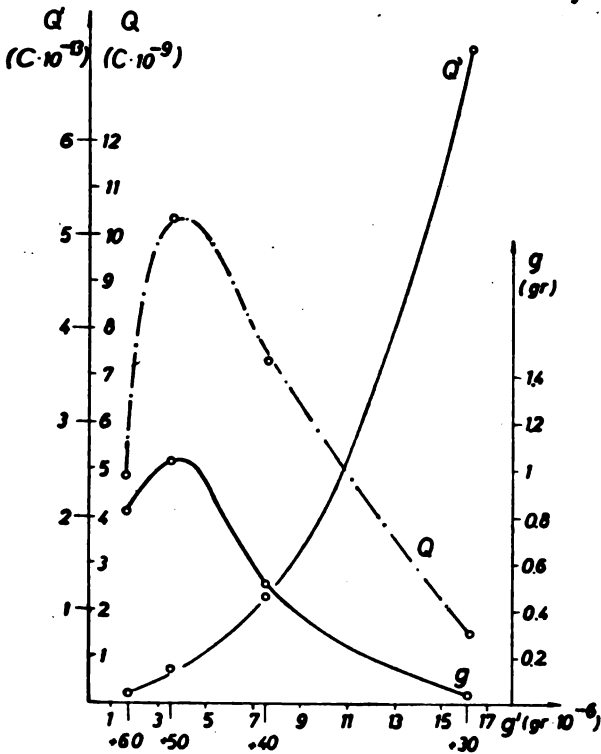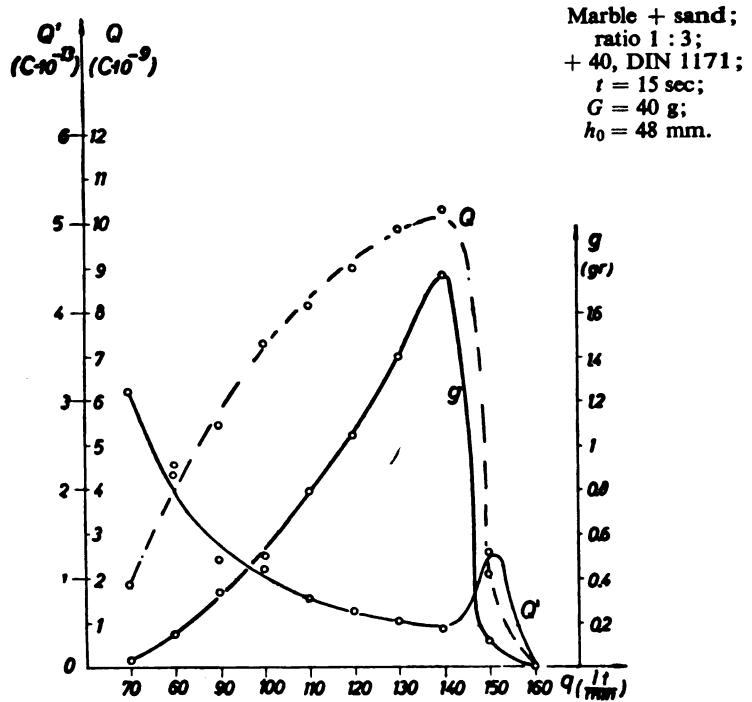
Fig. 6

It is of interest to compare the curves representing the weight of separated material (g) for the mixtures of marble and sand having different granulometric compositions ($+30$, $+40$, $+50$) in relation to the rate of air flow (other conditions constant) (Fig. 9). Figure 9 shows that a decrease of granule size decreases the air flow required for maximum separation. The optimal flow and the optimal granulation for the given mixture are easily determined and they are: $q_{opt} = 140$ l/min and optimal granulation $+40$. Under these conditions the separation of material from the mixture is maximal.

The existence of optimal values is of general significance. It has been found that they exist with other mixtures as well. Investigations were also performed with the following mixtures: sand potassium nitrate and sand $+$ lead nitrate. These mixtures were used in order to determine whether great differences in dielectric permeability or specific gravity exhibit any effect. It was found that they affect only the intensity of the separation, while its character remains the same.

The curves showing changes in the weight of separated material, g, for all three mixtures in relation to air flow are given in Fig. 10. The diagram shows that the optimal value for the air flow increases with the increasing specific gravity of the separated component. The optimal
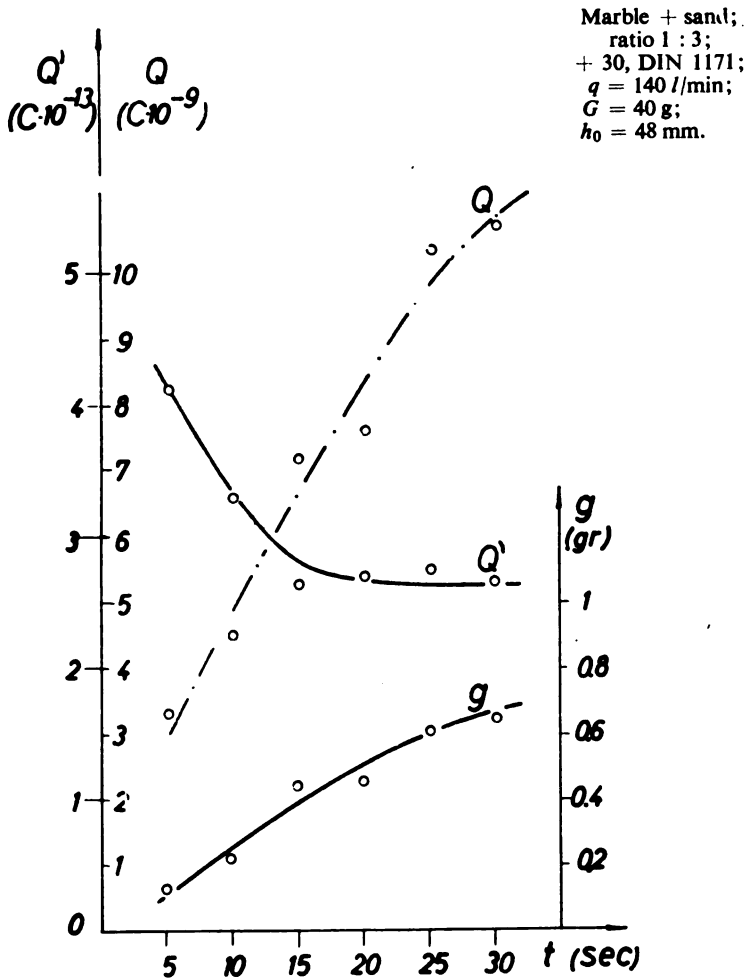
Fig. 7

flow for the mixture of sand + potassium nitrate is 120 l/min; for sand with marble it is also about 120 l/min; but for the mixture of sand + lead nitrate, which is about twice as heavy as the mentioned components, it is 140 l/min.

DISCUSSION

In addition to the described measurements we also measured the electric charge of the whole mixture, Q, and calculated the mean charge per particle Q'. The values are plotted on graphs against the corresponding factors (Fig. 3—10). Q is about 10^{-9}C, whereas Q' is about 10^{-13}C. Comparing the curves of g, Q, and Q' in the graphs, a close relation among the values is observed. Therefore, Q', which we can assume to

Marble + sand;
ratio 1 : 3;
+ 30, DIN 1171;
$q = 140 \, l/min$;
$t = 20 \, sec$;
$h_0 = 48 \, mm$

Fig. 8

Marble + sand;
ratio 1 : 3;
$t = 15 \, sec$;
$G = 40 \, g$;
$h_0 = 48 \, mm$.
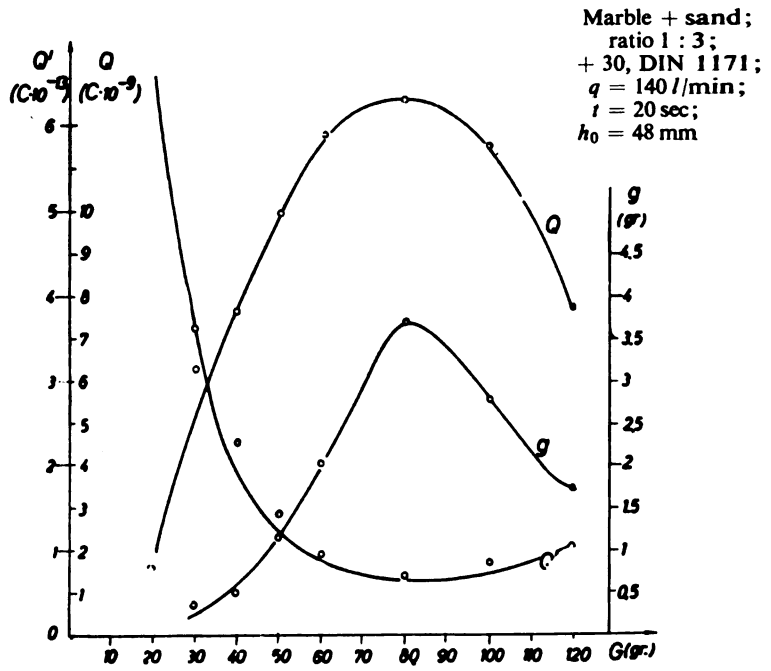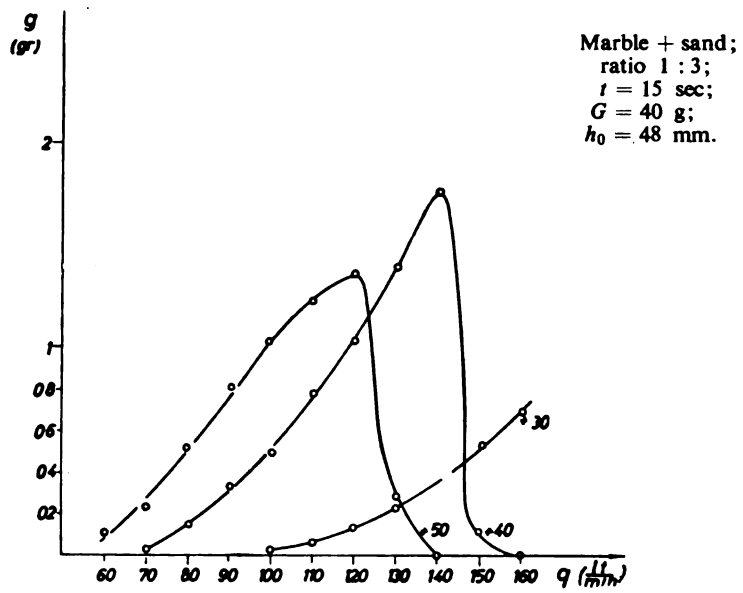
Fig. 9
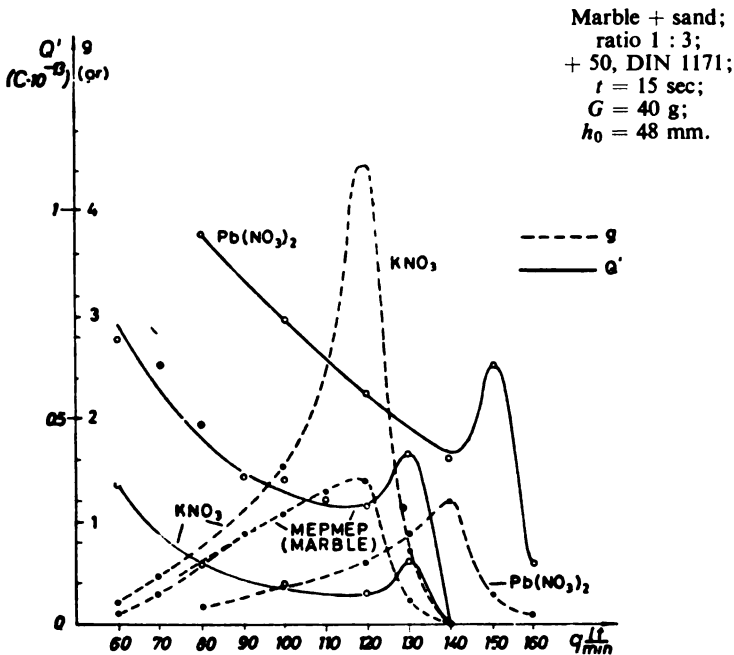
Fig. 10

be the cause of the attractive force between the electrode and a particle, was taken for the explanation of the results obtained (Figs. 3—10).

The fluidization layer in which the particles collide and get charged is formed at small flow rates (for materials of low specific gravity — about 80 l/min, and for materials of high specific gravity — about 120 l/min). An electric field is formed in the column. The probability that particles will be attracted by the electrode in a certain time period during fluidization is relatively small, since the air current must first bring them close to the electrode, and then the latter must attract them by its weak field and hold them up. This is only possible when the particles acquire a great charge. This is why the amount g is small in spite of a large electric charge per particle when the electrode is placed high (Fig. 3), or the air flow is small (Figs. 6 and 9), or the fluidization time is short (Fig. 7).

By increasing the rate of air flow the particles collide more forcefully and more frequently, and they are nearer to the electrode on account of the expansion of the layer. The electrode is more negatively charged due to the increase in the total charge of the fluidization layer. The electric field directed toward the electrode is stronger and therefore even the particles of smaller charge which are most numerous are brough close to the electrode and are more easily retained on it. These facts explain the existence of an optimal electrode height (Fig. 3), an optimal air flow (Figs. 6 and 9) and the most efficient fluidization time (Fig. 7).

When the flow rate is too great the material is carried away, the collisions take place less frequently, although they may be very strong and hence the charging is small. With very rapid air flow, deposited material is blown off the electrode, and only particles possessing slightly greater charge (appearance of maximum at curve Q, Fig. 6) are retained. However, on further increase of the flow rate there are no collisions any more and the whole material is carried away. The separation of material is no longer observed.

If the electrode is dipped too far into the fluidization layer the formation of many charged particles is prevented because the oppositely charged particles collide with the electrode and get neutralized. The whole mass of material is agitated so that the particles of small charge which had been deposited on the electrode are removed with the falling mass of material.

Larger particles, due to stronger collisions, possess a greater electric charge (Fig. 5). However, the amount of separated material (g) depends upon the attractive electric forces and upon the kinetic pressure of the air as well.

The weight ratio between the two components of the mixture is of the greatest importance for charging (Fig. 4). When the weight ratio of marble to sand is the smallest, the possibility of frequent collisions of marble particles with sand particles is the greatest, and hence, the quantity of electricity per marble particle is the greatest. However, the optimal separation of material takes place when the amount of material to be separated is slightly greater and the quantity of electricity per particle is smaller, under these conditions the statistical probability for (marble) particles to be in the vicinity of the electrode is greater. When the weight ratio of components is 1 : 1 the electric charge per particle is small, since the possibillity for particles of different kinds to collide is decreased, and thus the amount of material separated at the electrode is reduced.

The role of specific gravity is shown in Fig. 10. At a certain flow rate, as for example 100 l/min, the material whose particles are heavy is separated in a small amount but the electric charge per particle is great. For example: the particles of $Pb(NO_3)_2$ are twice as heavy as marble particles and therefore they are not brought as close to the electrode by the same air current. Only particles possessing a greater charge are deposited at the electrode. Particles of smaller specific gravity are closer to the electrode and they can be separated even though they have a smaller charge. This explains the phenomenon that, under given conditions, material of lower specific gravity is separated in greater amount (Fig. 10), whereas the electric charge per particle is greater with particles of higher specific gravity. Dielectric permeability is of significance for the polarity of the charged particles, but its effect on the amount of separated material was not observed. The role of dielectric permeability and crystal structure as well as the effects of other physical and chemical properties of the material require a further detailed study.

To determine the polarity of the separated component and to study the behavior of the electric field a generator of direct current of h'gh voltage was used. It served as a source of additional electric field. By connecting the electrode and the porous metal grid of the column with the corresponding poles of the generator, the strength of the electric field was reduced to zero. It was found that the separation of material is more rapid and much greater when the electrode is connected with the corresponding pole of the generator. If the electrode is connected with the opposite pole of the generator and the voltage of the latter is smaller than the potential of the fluidization layer between the electrode and the metal grid, the amount of the separated component is smaller than that deposited when the electrode is short-circuited to the grid. When the voltage of the generator is increased above that of the column the separation of the other component takes place. By charging the electrode in such a way it was established that the polarity of particles is not changed during fluidization and that it does not depend upon the electrode charge. For example, using a source of 2500 V between the electrode (negative pole) and the metal grid (positive pole) in the fluidization of a mixture of marble and sand, the amount of material separated on the electrode was 1.59 g and the mean value of the electric charge per particle was 0.56×10^{-13}C. Under the same experimental conditions but without the added field, only 0.5060 g of marble was separated and the mean value of the charge per particle was 1.14×10^{-13}C (Fig. 6). The amount of separated material was three times greater and the mean value of the electric charge per particle about half as large than when the fluidization was performed without the presence of the added field. This can be explained by the fact that the strong electric field attracts even the particles which are less charged. Thus it is clearly demonstrated that the electrical phenomena are very significant and that the electrical properties of the materials play an important role in the separation of material by fluidization charging.

CONCLUSIONS

A close relation between the amount of material separated on the electrode and the electric charge per particle has been established. Under unfavorable conditions (electrode placed too high above the fluidization layer, large weight ratio of components in the mixture, particles too large, small air flow, small total weight of mixture, and fluidization time too short) only particles which have acquired a great electric charge are deposited on the electrode. On account of the weak electric field and slight fluidization only these particles can be attracted to the electrode. Their number is small and hence the amount of separated material is small as well.

Under the optimal conditions for all the given factors, the electric charge per particle of the separated material is small but sufficient to cause, in an electric field created by fluidization, the greatest number of particles to be attracted to the electrode. If the electric field between the electrode and the fluidization layer is increased by means of an

added source of direct current of a voltage higher than the potential of the layer, the number of particles is increased and the electric charge per particle, needed to cause separation, is decreased.

It is evident that the maximal separation of material will be achieved when the optimal conditions for the formation of a strong electric field in the fluidization layer are fulfilled.

Institut for Chemistry, Technology
and Metallurgy
Beograd

School of Technology
Department of Chemical Engineering
Beograd

REFERENCES

1. Končar-Đurđević, S., L. Čapo, and D. Vuković. "Influence de certains facteurs de fluidisation sur l'électrisation de particules fluidisées". — *Chimie et industrie — Genie Chimique* (Paris) 86 (4): 110—115, 1961.

2. Končar-Đurđević, S. and D. Vuković. "Separation in Fluidized Systems by Means of Dielectric Charging of Materials" — *Nature* (London) 193 (4810): 58—59, 1962.

3. Končar-Đurđević, S., D. Bajić, B. Đorđević, and N. Šišković. *Razdvajanje mineralnih materija pon oč ι fluidiziranog naelektrisanja* (Separation of Mineral Materials by Fluidized Charges). — Beograd: Institut za hemijska, tehnološka i metalurška istraživanja, December, 1962.

4. Končar-Đurđević, S., D. Bajić, and B. Đorđević. "Proučavanje vrste naelektrisanja pri fluidizacionom naelektrisanju i objašnjenje oblika izdvojenog materijala" (Investigation of the Types of Electric Charging during Fluidization Charging and Explanation of the Type of Material Separated). — *Glasnik hemijskog društva* (Beograd) 28: 501, 1963.

5. Končar-Đurđević, S., D. Bajić, and B. Đorđević. "Optimalni uslovi izdvajanja materijala pri fluidizacionom naelektrisanju" (optimal Conditions for Material Separation during Fluidization Charging). — *Glasnik hemijskog društva* (Beograd) 28: 513, 1963.

6. Bajić, D., S. Končar-Đurđević, and V. Pavasović. "Determination of Quantity of Electricity in the Process of Deposition of Materials by Fluidizing Charges". — *Chemie et Industrie* (Paris) 90 (3): 165, 1963.

7. Ralston, O. C. *Electrostatic Separation of Mixed Granular Solids.* — New York: Elsevier Publishing Co., 1961, p. 31.

8. Olofinski, N. F. *Elektricheski metodi obogashcheniia* (Separation by Electric Charging) — Moskva: Metalurgizdat, 1953, p. 56.

•

INVESTIGATION OF CARBON DIFFUSION ON THE STEEL-MOLTEN GRAY IRON CONTACT SURFACE

by

BRANKO BOŽIĆ and DRAGICA MIHAJLOVIĆ

It is known that characteristics of the diffusion zone in surface enrichment of metals with foreign elements basically depend on: the composition and the activity of the medium used as the source of the foreign element, the temperature and the metal is kept in the active medium at high temperature, and the rate of subsequent cooling to room temperature. Because of its exceptional technical importance the influence of the above factors on the diffusion process of surface carbon enrichment of iron and its alloys has been a subject of numerous theoretical and experimental investigations. The study of carbon diffusion at high temperatures and the use of highly-active media[1-4] attract special attention. However, the works published so far indicate experimental difficulties, which give the results mostly only qualitative value. Calculation of the diffusion coefficient has either been impossible or it has been considered of unreliable accuracy.

The purpose of the present experiment was to investigate surface diffusion of carbon into steel at high temperatures using a specific active medium, molten gray iron.

EXPERIMENTAL DATA

Specimens were made of Č.1220 steel of the following chemical composition: C 0.12%, Si 0.28%, Mn 0.35%, P 0.024%, S 0.040%. The steel was in the normalized state. The specimens were cylindrical in form, 10 mm in diameter and 25 or 30 mm long. The dipping depth into the molten gray iron was constant (20 mm), so that the difference in height (h) did not affect the results.

The specimens were treated in molten gray iron of the following ranges of chemical composition: C 3.33—3.43%, Si 1.8—2.2%, Mn 0.60—0.80%, P 0.25—0.40% and S 0.09—0.12% and at temperatures of 1310°, 1270°, 1235° and 1185°C. The temperatures were measured with an optical pyrometer. These are in fact mean temperatures because during the experiment the temperature in the pouring ladles decreased by about 20°, i.e. it varied $\pm 10°$ from the values given.

Carbon enrichment of the specimen surface was performed in 700 kg pouring ladles by the following procedure: eight specimens were simultaneously dipped into molten gray iron of a given temperature. One by one they were taken out at different time intervals• — 15, 30, 45, 60, 75, 90, 105 and 120 seconds, and air-cooled. The specimens which stayed in the melt more than 100 seconds at 1310 and 1270° completely or almost completely melted, therefore the maximum experimental time was 90 seconds.

To determine the effect of the alloying elements, preliminary investigations were carried out on three types of alloyed steel under the experimental conditions given for carbon steel.

RESULTS

The changes in the specimens induced by treatment under the above conditions were observed by:
a) macroscopic examination
b) determination of changes in weight
c) investigation of the microstructure of the diffusion zone.

a) *Macroscopic examination*

Examination after treatment showed that there was intense melting of the specimens at the highest experimental temperature (1310°C). After 100 seconds the specimen completely melted. Changes in dimension and form were also visible at 1270 and 1235°C, although at the latter they occurred much later and were less intense. At 1185° the melting was not visible with the naked eye.
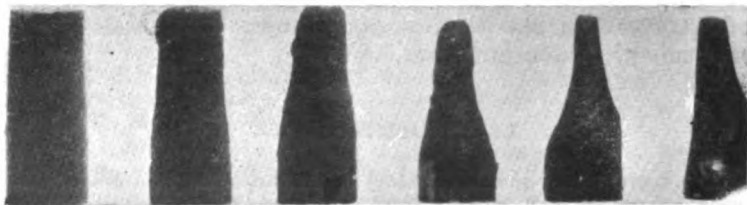
Fig. 1

Specimens of Č. 1220 dipped in molten iron at a temperature of 1310° for: 15, 30, 45, 60, 75 and 90 sec

The appearance of the specimens after treatment is shown in Figs. 1 through 4. The rough places observed at 1235° and 1185° are due to the iron which adhered to the specimen after removal from the crucible.

Figs 1 and 2 on a scale of 1:1; Figs 3 and 4 reduced 1.5:1.
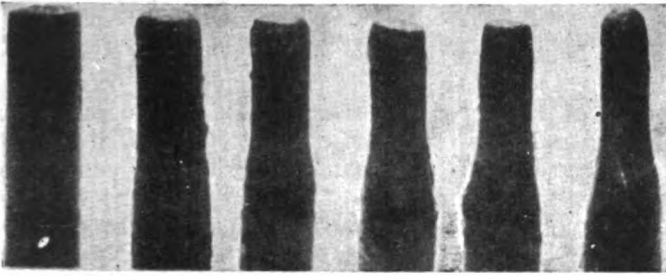
Fig. 2

Specimens of Č. 1220 dipped in molten gray iron at 1270° for: 15, 30, 45, 60, 75, and 90 sec
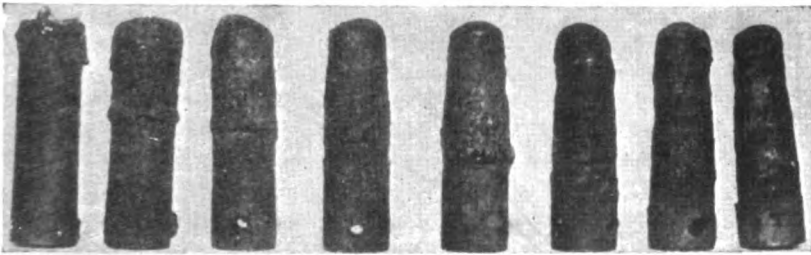
Fig. 3

Specimens of Č. 1220 dipped in molten gray iron at 1235° for: 15, 30, 45, 60, 75, 90. 105 and 120 sec
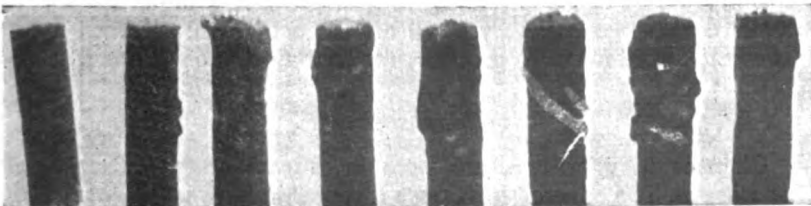
Fig. 4

Specimens of Č. 1120 dipped in molten gray iron at 75, 90 105 and 120 sec

b) *Determination of changes in weight.*

The specimens were weighed before (G_0) and after immersion (G_1). The weight loss $\Delta G\ (=G_0-G_1)$ is expressed in percentage of the initial weight of the dipped part. The purpose of the measurement was to obtain a quantitative melting-rate index. However, at lower temperatures the increased viscosity caused considerable adhesion of the iron. On taking the specimen out of the melt the iron solidified on the surface thus causing scattering and inaccuracy of the results of the measurement. As may be seen from Figs. 1 through 4 this phenomenon is practically negligible at 1310° and 1270°, which is also proved by the result of measurement. Therefore, only the results for these two temperatures, shown in Fig. 5, are taken for discussion.
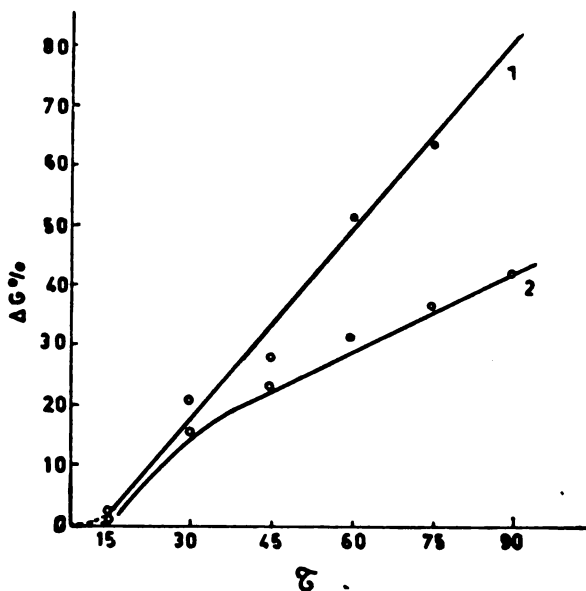
Fig. 5

Weight loss $\Delta G\%$ as a function of time (τ) in the melt (1)—1310° (2)—1270°

A considerable influence of the temperature on the melting rate was observed. Both the photographs and the graph show that for 15 seconds the changes are very small and then there is a sudden jump. Part of this time interval is probably for heating of the specimen.

c) *Microstructure*

Changes in microstructure were investigated on all four series of specimens. The adhered iron, even a very thin film, was a convenient edge protection in the preparation of metallographic specimens, thus a thin, carbon-enriched surface layer of steel was preserved for investigation.

A characteristic view of the microstructure in the area of the contact surface of the specimen dipped 60 seconds at 1270° is shown in Fig. 6. Indentical microstructural zones appear on all other specimens as well, differing only in the penetration depth in dependence on the temperature and time.

I   II   III
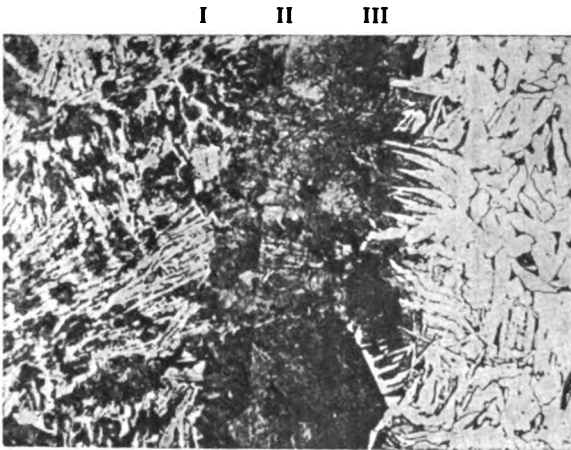
Fig. 6

Microstructure at the contact zone between steel and cast iron after 60 sec at t⁰ = 1270°; > 150

Zone I — represents the microstructure of the adhered iron which, due to sudden cooling and probable change in composition, solidified as white iron.

Zone II — from the appearance and distribution of this zone of all specimens, it is assumed to be the microstructure of a thin layer of iron right against the surface of the specimen. The structure is in part hypereutectoid, predominantly eutectoid, with very fine lamellar pearlite. The presence of this zone of iron, considerably depleted in carbon, implies a high diffusion rate on the contact interface. The question remains open as to whether diffusion in the melt, with respect to the reaction rate on the surface, is not sufficient to completely compensate the amount of carbon in the boundary layer of iron, or whether depletion takes place in a short time after withdrawing the specimen, when the diffusion process continues on the solid-solid contact interface. Zone II appears on all specimens on which iron remained on the surface.

Zone III — represents the microstructure of the carbon-enriched specimen surface layer, i.e. the diffusion zone. Right next the boundary of the specimen the structure is hypereutectoid, predominantly eutectoid. The depth of the diffusion layer measured to nearly the end of the eutectoidal area is 0.076—0.28 mm, depending on the temperature and time of treatment. The transition to basic iron structure is abrupt.
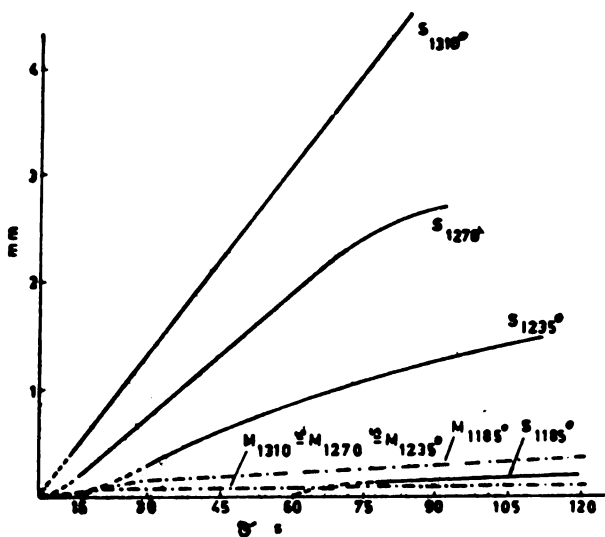
Fig. 7

Relation between the depth of the molten zone (S), the depth of the diffusion
zone (M) and the time in the melt (τ)
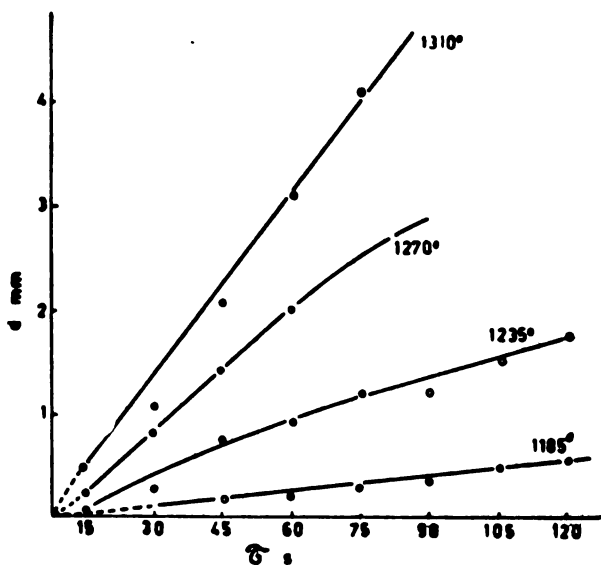
Fig. 8

Relation between the depth of the zone $d = (S + M)$ and the time in the melt (τ)

TABLE 1

Time (τ) s

depth of zone — mm

Temp. °C	15			30			45			60			75			90			105			120		
	M	S	M+S	M	S	M+S	M	S	M+S	M	S	M+S	M	S	M+S	M	S	M+S	M	S	M+S	M	S	M+S
1310	—	0.5	0.5	0.08	1.0	1.08	0.093	2.0	2.093	0.10	3.0	3.10	0.10	4.0	4.10	0.10	—	—	—	—	—	—	—	—
1270	0.093	0.11	0.203	—	0.83	0.83	0.08	1.39	1.47	0.10	1.94	2.04	0.086	2.22	2.306	0.10	—	—	—	—	—	—	—	—
1235	0.076	—	—	—	0.28	0.28	0.10	0.66	0.76	0.086	0.83	0.916	0.088	1.11	1.198	0.095	1.11	1.205	0.099	1.39	1.489	0.097	1.66	1.757
1185	—	—	—	0.133	—	0.133	0.153	—	0.153	0.20	—	0.20	0.20	0.11	0.31	0.26	0.16	0.42	0.28	0.22	0.50	0.28	0.28	0.56

4

Not only zone III but also the melted zone of the steel specimen represents the real depth of the diffusion zone (d). The depth of the melted zone (S) was calculated from the difference between the initial specimen diameter (D_0) and the diameter after treatment (D_1), i.e. $S = \dfrac{(D_0 - D_1)}{2}$. D_1 was measured on each specimen about 1 mm from the top. After etching, the adhered iron distinctly marked the boundary of the specimen. Measurement on specimens where no iron remained was difficult.

Results of measuring the depth of zone III (M) and the melting zone (S), and calculation of the total diffusion depth (d) are shown in Table 1 and Figs. 7 and 8. As could be expected the diffusion process depended on temperature and time, but the exceptionally high diffusion rate in the boundary layer was unexpected.

Figure 7 clearly shows that melting of the specimen surface layer at three higher temperatures is incomparably faster than the progress of diffusion into the specimen, while at the lowest temperature melting is negligible.

RESULTS OF ALLOYED-STEEL INVESTIGATIONS

Specimens of the following steel composition were investigated.
1. Č.4120 with 0.60% Cr
2. Č.5420   ,,   1.95% Cr and 1.95% Ni
3. Č.4720   ,,   1.15% Cr, 1% Mn, and 0.25% Mo.
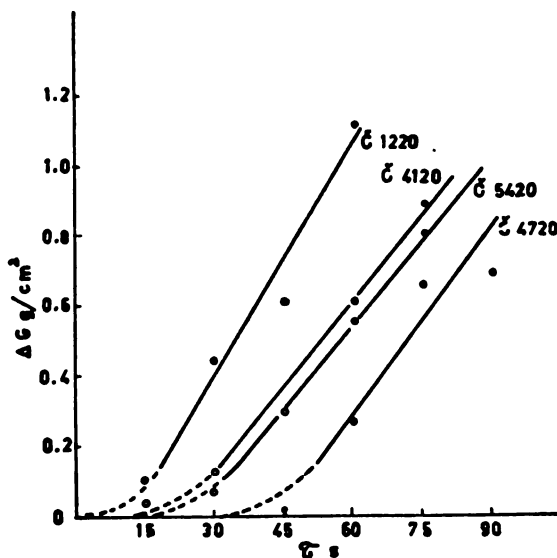
Fig. 9

Weight loss $\Delta G\%$ as a function of time (τ) at temperature 1310^0

The steels were in the normalized state. The specimens were cylindrical, dimensions $d=18$ mm and $h=25$ mm. The temperature of molten gray iron, the time the specimen was kept in the melt and the experimental procedure correspond to the conditions for carbon-steel investigations. The results of weight loss due to melting at 1310°C expressed in g/cm² of the immersed area are shown in Fig. 9.

From the results it follows that all three alloyed steels melt more slowly than carbon steel. The effect of the presence of the alloying element alone cannot be determined from this experiment because the diameter of the alloy specimen ($d = 18$) was larger than that of the carbon steel ($d = 10$). Masses of the dipped parts of the specimens are in the same ratio. Heating of the larger specimen is slower and cooling of the molten iron around the dipped specimen more rapid. By expressing the weight loss in grams per unit contact area, the effect of the difference in dimensions is reduced but it cannot be neglected.

The results for the alloyed steels show a regularity. It is known that the maximum effect of chromium on carbon concentration is in the enriched surface layer. Manganese and molybdenum exert effect in the same direction but it is less intense. Nickel reduces the concentration of carbon, while if nickel and chromium are simultaneously present, the effect of chromium is less intense.

Comparing the composition of the alloyed steels and the curves for the melting rate of these steels at 1310°C, one may conclude that the behavior correlates with that theoretically expected.

DISCUSSION OF RESULTS

The microphotographs in Figs. 1 through 4 and the graph in Fig. 5 show that at 1310° and 1270°C melting of steel specimens dipped into molten gray iron is fast. At 1235° melting is considerably slower, while at 1185° it is negligible.

In view of the high temperature and the highly active medium melting is to be expected. This phenomenon has also been observed by other authors[3, 4]. However, it is necessary to point out the very high and rather unexpected rate of the process, as manifested by the occurrence of melting shortly after the specimen has been dipped into the melt. Thus at 1310°, in 45 seconds the specimen loses about 28% of the initial weight of the dipped part. After 60 sec it loses 51% and after 100 sec the dipped part completely melts.

The quick start of melting implies that the carbon concentration in the boundary layer of the specimen suddenly and considerably increases. In case diffusion into depth in the contact surface-active medium interaction can be neglected, a high carbon concentration in the boundary layer would be obtained in a short time. However, diffusion of carbon atoms (ions) into the specimen takes place simultaneously with surface enrichment. Not only does this process produce a diffusion zone of variable composition, but it also limits the increase of the concentration in the boundary layer. Consequently, the carbon

4*

Fig. 10

Č. 1220 specimen
t⁰ — 1185⁰, time — 30 sec
× 150
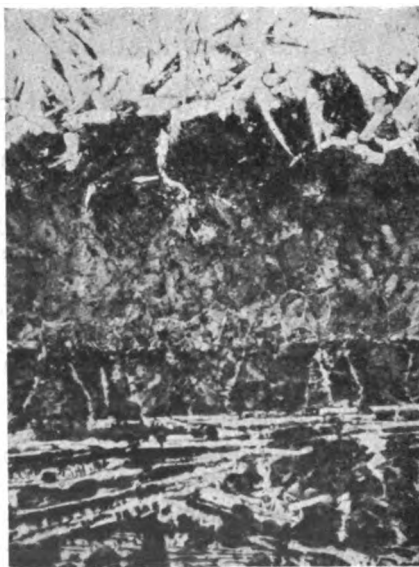
Fig. 11

Č. 1220 specimen
t⁰ — 1185⁰, time — 45 sec
× 150
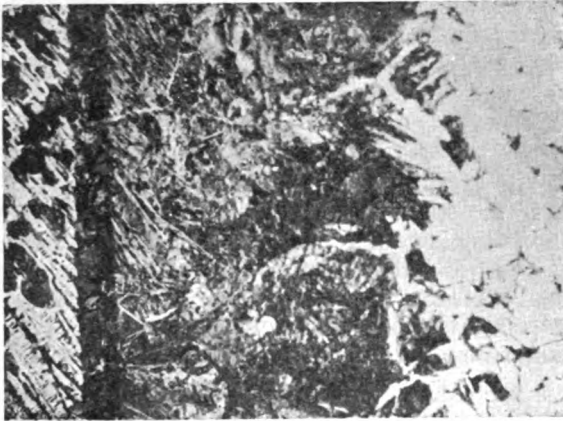
Fig. 12

Č. 1220 specimen
$t^0 - 1185^0$, time — 60 sec
$\times 150$

concentration in this layer depends on two in principle opposing processes, and it is determined by

$$\frac{dm_p}{d\tau} \quad \text{against} \quad \frac{dm_u}{d\tau}$$

where $dm_p/d\tau$ denotes the amount of carbon which in unit time per unit area is transferred from the active medium to the boundary layer
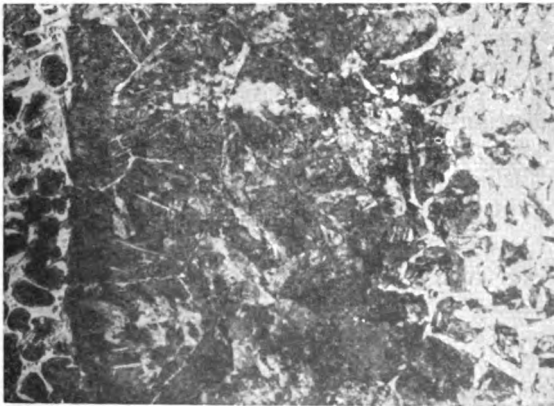
Fig. 13

Č. 1220 specimen
$t^0 - 1185^0$, time — 90 sec
$\times 150$

of the specimen, while $dm_u/d\tau$ denotes the amount which is simultaneously carried into the specimen.

Hence, for melting to occur at all it is necessary that

$$\frac{dm_p}{d\tau} > \frac{dm_u}{d\tau}.$$

In addition, if the specimens melt at 1235—1310°C, then according to the equilibrium diagram for the Fe—Fe$_3$C system (neglecting the presence of Si, Mn, P and S) the carbon concentration in the boundary layer must increase from 0.12% to 2.9—3.5%, depending on the temperature. As the results in the graph (Fig. 7) show that melting is very fast, one must also assume that carbon diffusion into depth is much slower.

From the microstructure of the diffusion layer for the three highest temperatures and the results of measuring the layer thickness (M), both represented by the $M_1 \cong M_2 \cong M_3$ curve plotted in Fig. 7, one sees that the depth of the layer (M) measured up to the boundary of the eutectoidal zone is 0.083—0.10 mm and it is approximately the same for 1310°, 1270° and 1235°C. Subsequent investigation showed that during specimen cooling diffusion continues for a short time on the solid-solid contact surface too. Therefore the observed variations in M cold be due to small differences in sample cooling rate. Taking this into account and comparing the $M_1 \cong M_2 \cong M_3$ curve with the S_1, S_2 and S_3 curves in Fig. 7, it may be concluded that in the diffusion process at 1310°, 1270° and 1235° the surface reaction absorption of carbon atoms (ions) and melting of the enriched zone is extremely fast as compared to the depthwi:e diffusion rate. Likewise, it is also assumed that an approximately constant, maximum concentration of carbon is maintained in the boundary layer. Hence, the amount by which the maximum carbon concentration reached is decreased due to depthwise diffusion is simultaneoulsy compensated by new atoms arriving from the active medium. According to A. A. Popov[5] this is an extreme case which arises from the very high activity of the surface reaction. The experiment at 1310°C corresponds best to this state; this is confirmed by the rectilinear shape of the S_1 curve. The S_2 and S_3 curves show a certain deceleration of the process with time, which may indicate decrease of the concentration gradient at the contact surface. However, it is more probable that the deceleration is due to the decrease in temperature during the experiment which is more critical for this temperature range than for 1310°C.

The results at high temperatures as used for iron carbonization in blast furnaces confirm one of the hypotheses of paper (3). Namely, from studying processes in blast furnaces the question arises as to whether carbonization is possible only after complete melting of the obtained metal, the melted alloy then washing off coke, or whether carbonization is so intense that enrichment and melting of the enriched surface layer proceed in parallel. Our results speak in favor of the latter hypothesis.

At 1185°C the process of surface carbon enrichment is completely different. In view of the proximity of the temperature of iron solidi-

fication, and the reduced rate of carbon diffusion into the melt, this would be expected. According to the results in Fig. 7, and taking into account the limiting accuracy of measurement, melting is in general questionable. Nor theoretically can this phenomenon be explained under the given experimental conditions. However, the depth of the diffusion layer (M) increases normally in dependence on time and temperature, as shown by curve M_4 and the microphotographs in Figs. 10, 11, 12 and 13.

Instead of qualitative description, the reaction at the steelmolten gray iron contact surface would be defined much better by calculating the diffusion coefficient at the interface and in the specimen. However, the results of this experiment do not allow reliable calculation of these coefficients. The rough value calculated from the change in depth of the diffusion zone with time at 1185°C using a graphical method[5] is $D=0.4 . 10^{-5}$ cm²/s. Although this value must be considered unreliable, in view of the accuracy of measurement and calculation, it should be pointed out that correlates with the diffusion coefficient of carbon in steel at 1250°C obtained by M. Paschke and A. Hautmann[2].

The calculated diffusion coefficient in the boundary layer at higher temperatures is very high and it needs to be confirmed by further investigations.

The results of the present work show that a high temperature and the use of molten gray iron gives high activity of the process at the specimen-melt contact interface. Comparing our results with those of other authors[2, 4], it may be concluded that the nature of the active medium is a decisive factor in diffusion acceleration, because the other parameters of the process are similar. Assuming that carbon in the melt is in ionic form, this conclusion is reasonable. However, to confirm this it is necessary to repeat the experiment under strictly controlled conditions, to make changes of the specimen cooling procedure and to determine the diffusion of all elements (C, Si, Mn, P and S) by chemical analysis of each layer in the zone of the contact interface. The effect of other elements in this experiment was intentionally neglected assuming, on the basis of literature data, that they have relatively little effect. However, the present results and the impossibility of ascribing the phenomena observed in all cases only to carbon diffusion require more detailed investigations of diffusion at the contact interface, and of the effect of the presence of alloying elements.

School of Technology
Institute for Iron and Steel and
Physical Metallurgy
    Beograd

REFERENCES

1. Holbrook, W. F., C. C. Furnas and T. L. Joseph. "Diffusion of S, Mn, P, Si and C through Molten Iron" — *Industrial Engineering* (Washington) 24: 993, 1932.

2. Paschke, M. and A. Hautmann. "Versuche über die Diffusion von Kohlenstoff, Silicium und Mangan in festen und flüssigen Eisen" — *Archiv fur Eisenhüttenwesen* (Düsseldorf) 9: 305—309, 1935.

3. — — — — —*Domennii protsess po eksperimental'nim dannim* (Melting Process According to Experimental Data) — Leningrad: Leningradskogo politekhnicheskogo instituta, 1949.

4. Vanin, V. S. and V. K. Tishov. "Tsementatsiia stali v zhidkhikh organicheskikh sredakh" (Steel Carbonization in Liquid Organic Media) — *Metallovedenie i termicheskaia obrabotka metallov* (Moskva) 4: 51—53, 1960.

5. Popov, A. A. *Teoreticheskie osnovi khimiko-termicheskoi obrabotki stali* (Theoretical Basis for Chemical-Thermal Treatment of Steel) — Sverdlovsk: Metallurgizdat, 1962.

BULLETIN
OF THE CHEMICAL
SOCIETY
Belgrade

Editor:
MILOŠ MLADENOVIĆ

CONTENTS

COMPLEX COMPOUNDS OF *l*-ASCORBIC ACID WITH METAL IONS

I. COMPLEXES OF U, Co, Ni, Mn, AND Zn IN ACID MEDIUM

by

DRAGAN S. VESELINOVIĆ and MILENKO ŠUŠIĆ

Formation of complexes of *l*-ascorbic acid* with metal ions was first described by Szent-Györdi et al.[1]. They showed that with ferric ion a violet complex is formed in alkaline solution. On the basis of polarographic analyses and data on complexes of ferric ion with other enol-containing compounds, J. Doskočil[2] concluded that the complex is composed of one ferric ion and two ascorbic acid anions whereby the ascorbic acid behaved as a dibasic acid. By analysing the isolated complex and by studying its oxidation, J. Anelli[3] found that the violet complex consists of one ferric ion and one dibasic anion of ascorbic acid.

The composition of complexes of ascorbic acid with UO_2^{++} ion has been studied by Gal[4], Gregorczyk[5,6] and Sobkowska and Minczewski[7]. All the authors agreed that in acid media, pH < 3, complex cation of the formula $[UO_2A]^+$ is obtained (A^+ — the anion of the monobasic acid). The dissociation constant of this complex at 25°C and at ionic strength of $\mu = 0.1$ was found to be $K = 2.2 \times 10^{-3}$ (from pH-metric measurements) and $K = 2.7 \times 10^{-3}$ (from spectra-photometric measurements)[4], whereas at 19—22°C $K = 1.3 \times 10^{-3}$ (from spectrophotometric measurements)[6]. The stability constant in 1 M $NaClO_4$ at 20°C was established to be $K = 2.5 \times 10^2$ from pH--metric data[7]. The composition of complexes at pH > 3 has been explained in different ways. According to Gal[8] at pH > 6 complex anion with two OH^- groups is formed; its existence was proved by the isolation of the complex salt $[UO_2A (OH)_2] NH_4$. The intermediary product was a neutral complex with one OH^- group. Sobkowska et al.[7] have found that in addition to the cation complex, two complexes are formed consisting of two and three anions of ascorbid acid. Stability constants of these complexes in 1 M $NaClO_4$ at 20°C were found

---

* In the subsequent text ascorbic acid - *l*-ascorbic acid,

to be $K_2 = 1.7 \times 10^{-4}$ and $K_3 = 1.3 \times 10^5$. From this it follows that the complex with two anions should be neutral and that with three anions negatively charged, i.e. anionic. The existence of anionic complex was proved by Korkisch et al.[9], who absorbed it on anionic-exchange resin. However, they did not determine its composition.

The formation of complexes of TiO^{++} ion with ascorbic acid was studied by Gregorczyk[5,6], Sommer [10,11] and Šušić[12] spectrophotometrically. The authors agreed with the formation of complex cation $[TiOA]^+$ in acid medium, pH < 3. The dissociation constant of this complex at 19—22°C was found to be $K = 9.58 \times 10^{-4}$ [6] and its stability constant $K = 70.5$ at ionic strength of $\mu = 0$[12]. In solutions with higher pH values, according to Gregorczyk, a complex with two ascorbic acid anions is formed ($K = 5.5 \times 10^{-3}$), while according to Sommer complexes containing two and three acid anions are formed. Analogously to uranium complexes, these complexes should be neutral or negatively charged. Šušić established the formation of anionic complex and this finding was also confirmed by Korkisch[9] who observed its absorption on anionic-exchange resin.

Sobkowska and Minczewski[13] found that vanadyl ions form three types of mononuclear complexes with ascorbic acid by successive incorporation of one, two and three acid ions depending on the pH of the solution. Stability constants of these complexes in 1 M $NaClO_4$ at 20°C were founed to be $K_1 = 1.5 \times 10^2$, $K_2 = 4.5 \times 10^2$ and $K_3 = 2.5 \times 10^4$.

By determining the adsorption distribution coefficients on cationic-exchange resin Schubert and Lindenbaum[14] established that in slightly alkaline media (pH = 7.2—7.3) cationic complexes of calcium and strontium, $[CaA]^+$ and $[SrA]^+$ are formed. Their stability constants at 25°C, for $\mu = 0.16$, were found to be $K_1 = 1.55$ (for Ca) and $K_2 = 2.24$ (for Sr).

Romanchuk[15] reported that solid magnesium ascorbate when dissolved possesses the properties of a complex salt. Its dissociation constant obtained from conductivity measurements was found to be $K = 2.8 \times 10^{-3}$.

Šušić et al.[16] found that ascorbic acid with WO_4^{2-} ions to gives two types of compounds: complex anion $(WO_3A_2)^{-2}$ and polyanion $HW_6O_{21}^{5-}$, under the influence of H^+ ion.

Finally, by means of polarographic, spectrophotometric and other investigations it has been shown that ascorbic acid forms complexes with a series of ions [17,18] but their compositions have not been determined.

It may be seen then that it has only been definitely established that UO_2^{++} and TiO^{++} ions form cationic complexes with one ion of ascorbic acid in acid media, pH < 3.

We investigated the formation of complexes of ascorbic acid with Co^{++}, Ni^{++}, Mn^{++}, Zn^{++}, and UO_2^{++}, in order to study ascorbic acid complex formation with bivalent ions other than the known UO_2^{++} and TiO^{++} complexes.

In general, complex formation of UO_2^{++} ion with ascorbic acid can be represented as a reaction of bivalent metal ion and weak acid:

$$m\ Me^{2+} + n\ HA\ [Me_m\ A_n]^{2m-n} + H^+ \qquad (1)$$
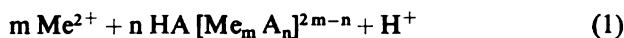
Me^{2+} denotes the bivalent metal ion and HA the molecule of weak monobasic, in this case ascorbic acid. Hydrogen ions liberated in this reaction together with the anion of the metal salt give a strong inorganic acid and this is convenient for investigation of the reaction by means of pH-metric measurements.

Our investigations were carried out by the method of continual variations[19,20] which Siddhanta[21,22,23,24] and others[25] have used in the study of acetate complexes of bivalent metals by measuring the change of pH. Since the formation of these complexes takes place according to eq. (1), this method could be applied to the study of the complexes of ascorbic acid and the metal ions.

The investigations were carried out with solutions of ascorbic acid and metal salts of equal molar concentrations. By mixing a ml of ascorbic acid solution with b ml of metal salt solution in such a way that always a + b = 10 ml, solutions having different molar ratios, n, were obtained; in these cases the molar ratio was equivalent to the ratio of ml of solution used: $n = a/b$. In addition, solutions were prepared by mixing: a ml of ascorbic acid and b ml of water; and b ml of metal salt solution and a ml of water. After equilibration at a definite temperature, the pH of each of the three types of solutions was measured. The increase of H^+ ion concentration which is proportional to the amount of the complex formed was calculated from the expression:

$$\Delta C_{H^+} = C_{H^+}^s - (C_{H^+}^{Ac} + C_{H^+}^M) \qquad (2)$$

where $C_{H^+}^s$ denotes the H^+ ion concentration in the solution mixture and $C_{H^+}^{Ac}$ and $C_{H^+}^M$ the concentrations of H^+ ions in solutions of ascorbic acid and metal salt respectively.

Graphic plots of ΔC_{H^+} against n give a curve with a maximum. The n value corresponding to the maximum denotes the ratio of components in the complex formed.

EXPERIMENTAL

Determinations were carried out with 0.500, 0.600 and 0.400 M ascorbic acid solutions and $Co(NO_3)_2$, 0.0500, 0.100 and 0.200 M ascorbic acid solutions and $UO_2(NO_3)_2$, and 0.200, 0.300 and 0.400 M ascorbic acid solutions and $Ni(NO_3)_2$, $Zn(NO_3)_2$ and $MnCl_2$. Solution mixtures were left to equilibrate for 6 hours at $25 \pm 0.02°C$. The pH values of the solutions are given in Tables 1, 2, and 3 and curves $\Delta C_{H^+} = F(n)$ in Figs. 1—5.

TABLE 1

Molar ratio	Solution mixture in ml			0.05M U-HA	0.2M Mn-HA	0.2M Zn-HA	0.2M Ni-HA	0.4M Co-HA
	HA	Me	H_2O	pH	pH	pH	pH	pH
	1.0	9.0	—	2.39	2.82	2.81	2.80	2.55
0.11	1.0	—	9.0	3.30	3.00	3.00	2.99	2.82
	—	9.0	1.0	2.77	6.50	6.08	6.15	5.70
	2.0	8.0	—	2.34	2.66	2.65	2.65	2.40
0.25	2.0	—	8.0	3.13	2.83	2.83	2.82	2.65
	—	8.0	2.0	2.80	6.52	6.13	6.22	5.70
	3.0	7.0	—	2.33	2.58	2.57	2.57	2.30
0.43	3.0	—	7.0	3.03	2.73	2.73	2.72	2.51
	—	7.0	3.0	2.85	6.40	6.19	6.25	5.71
	4.0	6.0	—	2.32	2.53	2.52	2.51	2.24
0.67	4.0	—	6.0	2.98	2.66	2.66	2.65	2.48
	—	6.0	4.0	2.90	6.51	6.23	6.35	5.70
	4.5	5.5	—	2.31	2.50	2.49	2.49	2.21
0.82	4.5	—	5.5	2.95	2.63	2.63	2.62	2.47
	—	5.5	4.5	2.92	6.55	6.28	6.40	5.70
	5.0	5.0	—	2.31	2.48	2.47	2.48	2.19
1.00	5.0	—	5.0	2.92	2.60	2.60	2.60	2.44
	—	5.0	5.0	2.95	6.58	6.30	6.45	5.72
	5.5	4.5	—	2.32	2.46	2.46	2.46	2.18
1.22	5.5	—	4.5	2.90	2.58	2.58	2.58	2.41
	—	4.5	5.5	2.98	6.62	6.35	6.50	5.72
	6.0	4.0	—	2.33	2.45	2.44	2.45	2.17
1.50	6.0	—	4.0	2.88	2.55	2.55	2.55	2.40
	—	4.0	6.0	3.01	6.63	6.36	6.58	5.72
	7.0	3.0	—	2.36	2.43	2.43	2.43	2.16
2.33	7.0	—	3.0	2.82	2.51	2.51	2.51	2.35
	—	3.0	7.0	3.10	6.60	6.48	6.70	7.74
	8.0	2.0	—	2.41	2.41	2.42	2.42	2.17
4.00	8.0	—	2.0	2.79	2.48	2.48	2.48	2.31
	—	2.0	8.0	3.21	6.65	6.56	6.85	5.74
	9.0	1.0	—	2.50	2.40	2.41	2.41	2.18
9.00	9.0	—	1.0	2.76	2.45	2.45	2.44	2.29
	—	1.0	9.0	3.40	6.69	6.70	6.95	5.74

TABLE 2

Molar ratio	HA	Me	H₂O	0.1M U-HA pH	0.3M Mn-HA pH	0.3M Zn-HA pH	0.3M Ni-HA pH	0.5M Co-HA pH
	1.0	9.0	—	2.19	2.68	2.64	2.64	2.44
0.11	1.0	—	9.0	3.16	2.90	2.90	2.90	2.79
	—	9.0	1.0	2.57	6.06	5.48	5.76	5.72
	2.0	8.0	—	2.13	2.53	2.49	2.49	2.30
0.25	2.0	—	8.0	2.99	2.73	2.73	2.73	2.80
	—	8.0	2.0	2.61	6.18	5.75	5.88	5.70
	3.0	7.0	—	2.08	2.46	2.42	2.41	2.22
0.43	3.0	—	7.0	2.89	2.63	2.63	2.63	2.51
	—	7.0	3.0	2.66	6.27	5.84	5.99	5.80
	4.0	6.0	—	2.07	2.41	2.38	2.37	2.17
0.67	4.0	—	6.0	2.81	2.56	2.56	2.57	2.43
	—	6.0	4.0	2.71	6.30	5.88	6.10	5.80
	4.5	5.5	—	2.07	2.38	2.36	2.34	2.16
0.82	4.5	—	5.5	2.79	2.53	2.53	2.53	2.42
	—	5.5	4.5	2.74	6.39	5.90	6.17	5.75
	5.0	5.0	—	2.06	2.36	2.34	2.32	2.15
1.0	5.0	—	5.0	2.76	2.51	2.51	2.51	2.40
	—	5.0	5.0	2.77	6.43	5.93	6.25	5.80
	5.5	4.5	—	2.07	2.35	2.33	2.31	2.14
1.2	5.5	—	4.5	2.74	2.49	2.49	2.49	2.35
	—	4.5	5.5	2.79	6.49	5.98	6.28	5.75
	6.0	4.0	—	2.08	2.34	2.32	2.30	2.12
1.5	6.0	—	4.0	2.71	2.47	2.47	2.47	2.31
	—	4.0	6.0	2.82	6.50	6.02	6.38	5.70
	7.0	3.0	—	2.10	2.32	2.31	2.29	2.12
2.3	7.0	—	3.0	2.67	2.44	2.44	2.43	2.28
	—	3.0	7.0	2.90	6.52	6.15	6.48	5.72
	8.0	2.0	—	2.16	2.31	2.31	—	2.13
4.1	8.0	—	2.0	2.64	2.40	2.40	—	2.25
	—	2.0	8.0	3.01	6.59	6.24	—	5.72
	9.0	1.0	—	2.26	2.31	2.30	2.28	2.16
9	9.0	—	1.0	2.61	2.38	2.38	2.37	2.22
	—	1.0	9.0	3.21	6.66	6.29	6.75	5.75

TABLE 3

Molar ratio	Solution mixture in ml			0.2M U-HA pH	0.4M Mn-HA pH	0.4M Zn-HA pH	0.4M Ni-HA pH	0.6M C$_0$-HA pH
	HA	Me	H$_2$O	pH	pH	pH	pH	pH
	1.0	9.0	—	1.78	2.56	2.51	2.52	2.35
0.11	1.0	—	9.0	2.98	2.82	2.82	2.81	2.73
	—	9.0	1.0	2.29	6.52	5.55	5.50	5.75
	2.0	8.0	—	1.74	2.42	2.35	2.39	2.22
0.25	2.0	—	8.0	2.83	2.65	2.65	2.64	2.57
	—	8.0	2.0	2.34	6.43	5.67	5.64	5.75
	3.0	7.0	—	1.70	2.33	2.28	2.31	2.15
0.43	3.0	—	7.0	2.73	2.56	2.56	2.55	2.45
	—	7.0	3.0	2.40	6.39	5.76	5.76	5.80
	4.0	6.0	—	1.69	2.28	2.24	2.26	2.11
0.67	4.0	—	6.0	2.66	2.49	2.49	2.48	2.38
	—	6.0	4.0	2.45	6.37	5.89	5.93	5.80
	4.5	5.5	—	1.69	2.26	2.22	2.24	2.08
0.82	4.5	—	5.5	2.63	2.45	2.45	2.45	2.36
	—	5.5	4.5	2.48	6.43	—	6.01	5.80
	5.0	5.0	—	1.69	2.24	2.20	2.22	2.07
1.0	5.0	—	5.0	2.60	2.43	2.43	2.42	2.34
	—	5.0	5.0	2.51	6.53	5.97	6.09	5.75
	5.5	4.5	—	1.71	2.23	2.20	2.21	2.06
1.2	5.5	—	4.5	2.58	2.40	2.40	2.39	2.29
	—	4.5	5.5	2.54	6.45	6.01	6.13	5.75
	6.0	4.0	—	1.73	2.22	2.19	2.21	2.05
1.5	6.0	—	4.0	2.56	2,37	2.37	2.37	2.28
	—	4.0	6.0	2.58	6.51	6.08	6.22	5.75
	7.0	3.0	—	1.76	2.21	2.18	2.20	2.05
2.3	7.0	—	3.0	2.53	2.33	2.33	2.33	2.23
	—	3.0	7.0	2.67	6.54	6.16	6.35	5.73
	8.0	2.0	—	1.83	2.20	2.18	2.19	2.06
4.1	8.0	—	2.0	2.49	2.30	2.30	2.29	2.21
	—	2.0	8.0	2.79	6.65	6.33	6.64	5.70
	9.0	1.0	—	1.96	2.21	2.20	2.20	2.08
9	9.0	—	1.0	2.48	2.26	2.26	2.26	2.17
	—	1.0	9.0	3.00	6.60	6.43	6.81	5.70
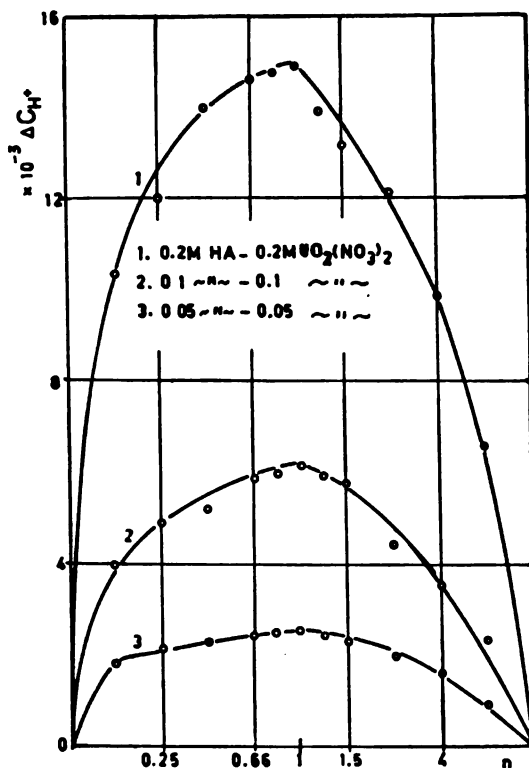
Fig. 1. Dependence of ΔC_H+ on n for $UO_2(NO_3)_2$ — HA system

From the curves in these figures it may be seen that in all cases the n values corresponding to the maximum is $n = 1$, indicating the formation of complexes of the type [MeA]+, according to eq.[1]. The result for uranium complex is consistent with published data.

All the curves shown in Figs. 1—5 are asymmetric with respect to the straight line passing through the maximum which is not allowed by Job's theory for complexes with component ratio 1 : 1. The existence of asymmetry, if it is not due to experimental errors, indicates the formation of other types of compounds apart from 1 : 1 complex. Therefore we studied the asymmetry of the curve obtained with 0.500 M ascorbic acid solution and 0.5 M $Co(NO_3)_2$ (Fig. 3, curve 2). By assuming that the experimental error in pH measuring amounts to 0.01 pH unit we calculated the error in ΔC_H+ determination for each point. Figure 6 shows curve 2 from Fig. 3 passing through points denoting the error (curve 1). The error in determining n is negligible. If the left branch of the curve is drawn on the right side, and the right branch on the left side (a — a' and b — b') the total course of the obtained curve does not fall within the limit of experimental accuracy. This means that the asymmetry of the curve is not caused by the errors of pH measurements. Likewise, various activity factors of H+ ions in solutions with various n, neglected in ΔC_H+ calculation, also have little influence on the asymmetry of the curve.
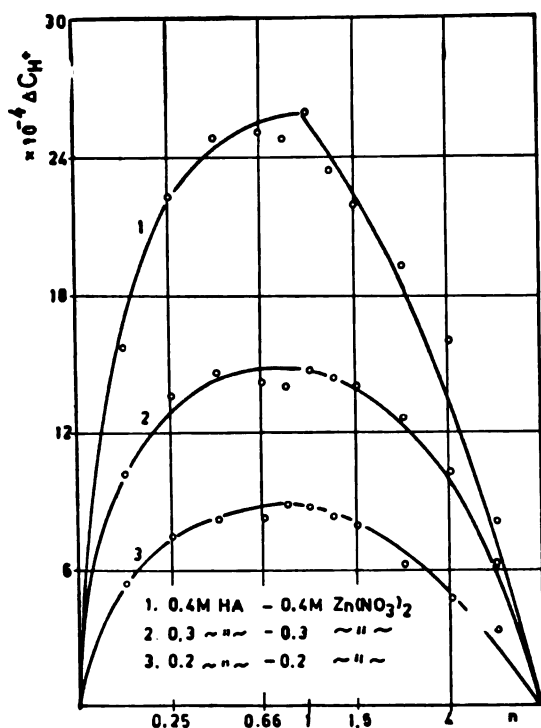
Fig. 2. Dependence of ΔC_{H^+} on n for $Zn(NO_3)_2$ — HA system
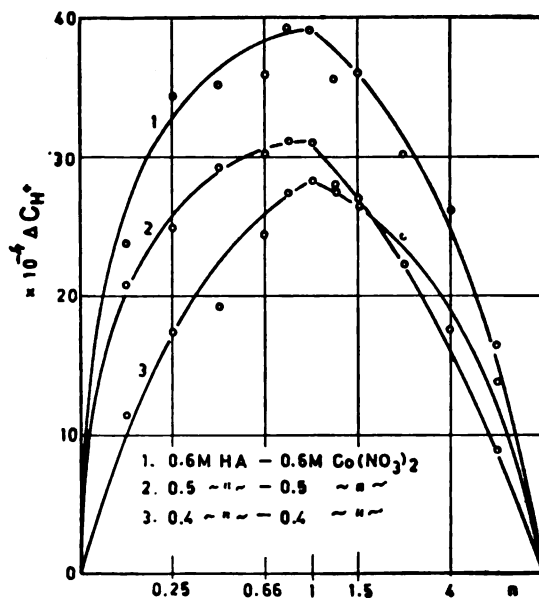
Fig. 3. Dependence of ΔC_{H^+} on n for $Co(NO_3)_2$ — HA system
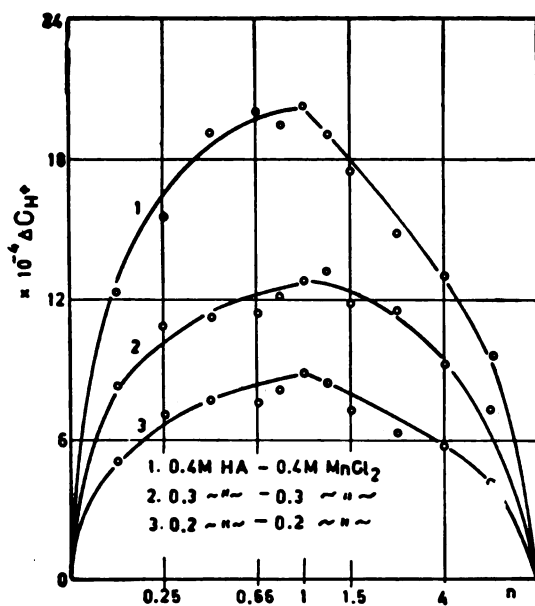
Fig. 4. Dependence of $\Delta C_{H}+$ on n for $MnCl_2$ — HA system
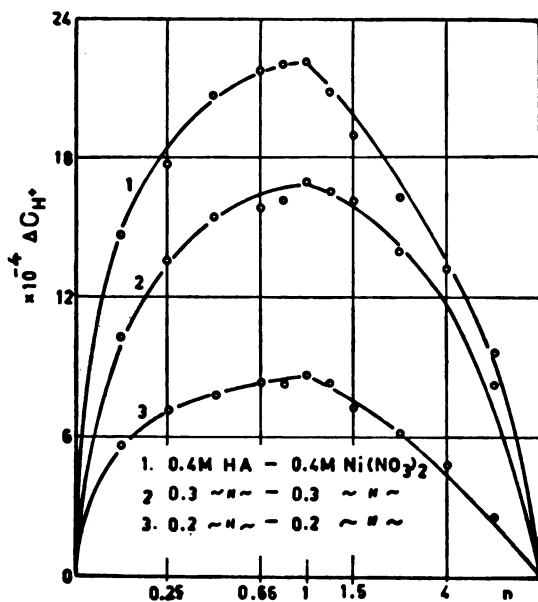
Fig. 5. Dependence of $\Delta C_{H}+$ on n for $Ni(NO_3)_2$ — HA system
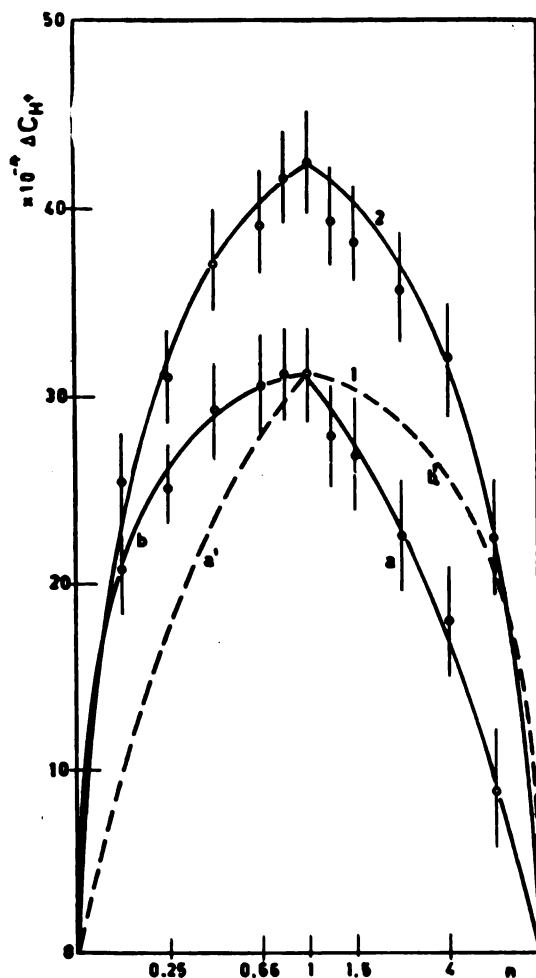
Fig. 6. Dependence of ΔC_H+ on n for 0.5 M $Co(NO_3)_2$ — 0.5 M HA system.
Curve 1: ΔC_H+ obtained from the measurements; curve 2: ΔC_H+ corrected.

The existence of asymmetry is caused by the unequal dissociation degree of ascorbic acid in the mixture solution and the pure acid solution due to their different pH values. As a result the H^+ ion concentration in ascorbic acid solution is not equal to the H^+ ion concentration formed by dissociation of the acid in mixture solution. The concentration of H^+ ions in this solution is determined by the expression:

$$C_{H+}^s = C_{A-}^s + C_k \qquad (3)$$

where C_{A-}^s denotes the ascorbic acid anion concentration and C_{k-} concentration of the complex, since H^+ ion concentration formed by hydrolysis of metal salts may be ignored (Table 2). In the pure acid solution we will have:

$$C_{H+}^{HA} = C_{A-}^{HA} \qquad (4)$$

Substraction of eq.[4] from eq.[3] gives:

$$C_k = C_{H+}^s - C_{H+}^{HA} + C_{A-}^{HA} - C_{A-}^s \qquad (5)$$

which only converts to eq. (2) only if $C_{A-}^{HA} = C_{A-}^s$. This equality of ascorbic acid anion concentrations, according to the dissociation constant:

$$k = \frac{[C_H] \times [C_{A-}]}{[C_{HA}]} \qquad (6)$$

will only be satisfied if $C_H^{s+} = C_{H+}^{HA}$ indicating that a comlex compound does not form. In the remaining cases it is necessary to determine the correction term $\delta = C_{A-}^{HA} - C_{A-}^s$ to make correction of eq. (1) and obtain the complex concentration according to eq. (5).

The correction term is determined from eqs. (6) and (5):

$$\delta = C_{A-}^{HA} - C_{A-}^s = \frac{\overset{\circ}{C}_{HA} + k}{C_{H+}^{HA} + k} - \frac{k(\overset{\circ}{C}_{HA} - C_k)}{C_{H+}^{HA} + k} \qquad (7)$$

where $\overset{\circ}{C}_{HA}$ denotes total ascorbic acid concentration equal in both solutions. Since, for the final values, C_k is always $\overset{\circ}{C}_{HA} - C_k < \overset{\circ}{C}_{HA}$ and $C_{H+}^s > C_{H+}^{HA}$, the right hand side of eq. (7) is always larger than zero, i.e. the correction term δ is always positive. Its highest value will be at the maximum of the curve. This indicates that the maximum obtained with noncorrected values for ΔC_{H+} is not sharp.

The correction term δ was determined with C_k, C_{H+}^s and C_{H+}^{HA} obtained by calculation of the dissociation constant of the complex and correction by the activity coefficient. After their calculation by eq. (7) the obtained values were corrected with the activity coefficient to relate to the measurement conditions. Curve 2 in Fig. 6 is obtained with corrected values for ΔC_{H+}. It shows that the symmetric curve was obtained within the accuracy of measurement. This indicates that the asymmetry of the curve for cobalt and other metal complexes is due to the differing dissociation degree of ascorbic acid both in pure solution and in the presence of metal salts, and it follows that there are only complexes of the $[MeA]^+$ type in the pH region ≈ 2—3.

The dissociation constant at the given ionic strength is calculated from data for $\overset{\circ}{C}_{HA}$, $\overset{\circ}{C}_{Me}$ and pH in mixture solutions with different n by the method of Siddhanta et al.[21, 22, 23, 24, 25]. In Figs. 7 and 8 graphic plots of pK (—log K) against $\sqrt{\mu}$ give a curve for each complex. Table 4 shows pK values for $\mu = 0$ obtained by extrapolating the obtained straight lines to $\sqrt{\mu} = 0$. The pK was determined with an error of ± 0.1.

TABLE 4

pK values for $\mu = 0$ *at* 25° C

Me	U	Co	Ni	Mn	Zn
pK	3.04	1.4	1.05	1.1	1.0
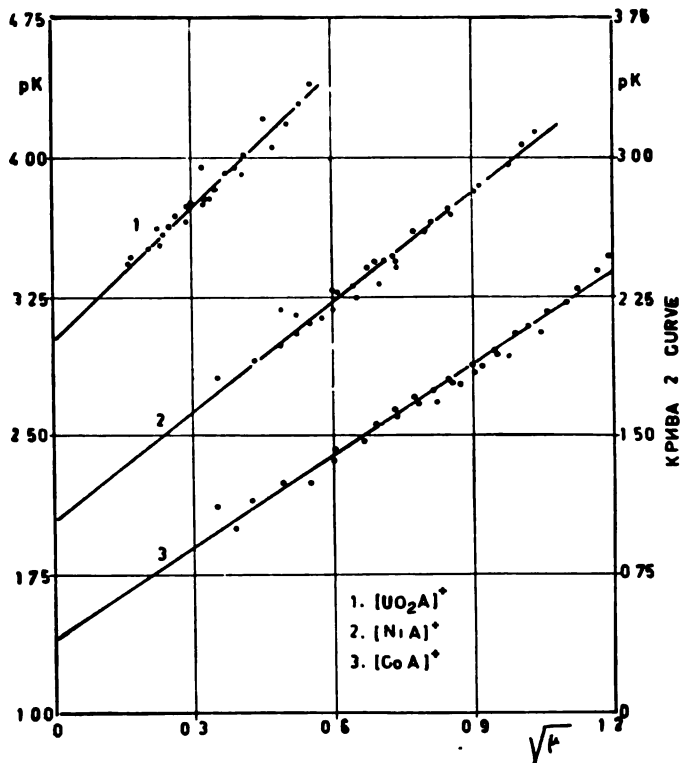
Fig. 7. Dependence of pK on $\sqrt{\mu}$.
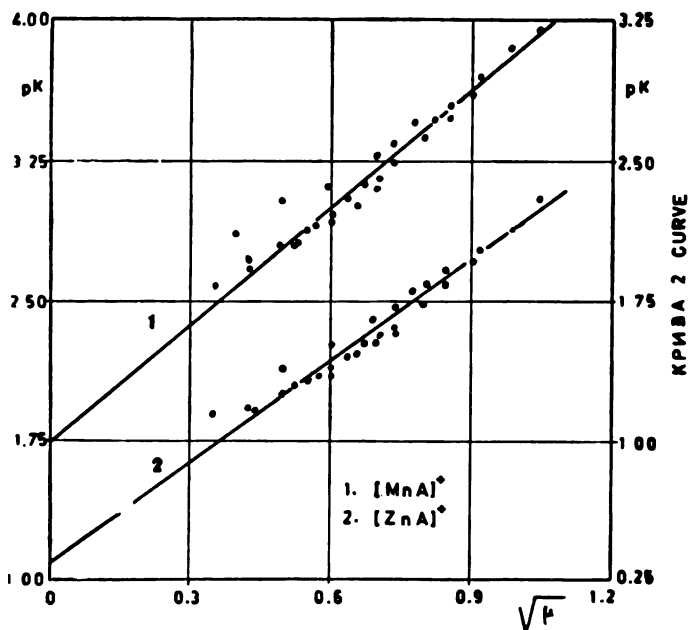
Fig. 8. Dependence of pK on $\sqrt{\mu}$.

DISCUSSION

Comparison of the obtained pK values with published data can only be made for uranium. According to Gal[4] pK = 2.6 and pK = 2.7 for $\mu = 0.1$. By converting the pK values from Table 4 to ionic strength 0.1 we obtain pK = 2.5 which is in agreement with the above data.

Comparison of the dissociation constants may be made according to Irving-Williams' series[26] on the basis of which stability constants of divalent cation complexes may be arranged serially as follows: Mn < Fe < Co < Ni < Cu > Zn. The stability constants of investigated complexes with ascorbic acid are arranged serially as follows: Ni < Mn < Co > Zn. This shows that Ni diverges from the rule, since it lies in front of manganese. The same was found for acetate complexes of these metals[25].

APPARATUSES AND REAGENTS

Beckman H-2 pH-meter and PHM 22 "Radiometer" were used. Temperature control was performed with the "VEB Prüfgeräte-Werk"--NB-type thermostat. All the reagents were p.a. The pH-meters were calibrated with a "Beckman" standard buffer solution and a saturated potassium bitartrate[27].

REFERENCES

1. Szent-Györgi, A., J. Banga, M. Gerendás, K. Laki, G. Papp, E. Porges, and F. B. Straub. "Autoxidation by Dehydrogenation and Biological Oxidations" — *Chemical Abstracts* (Columbus) 32 : 9105—9106, 1938.

2. Doskočil, J. "The Polarographic Reduction of Hydrogen Peroxide Cctalyzed by Iron Complexes of Catechol, Pyrogallol and Ascorbic Acid". In: *Proceedings of the I International Polarographic Congress in Prague* — Part I, 1951, p. 674.

3. Anelli, J. "Combination of Iron with Ascorbic Acid" — *Chemical Abstracts* (Columbus) 53 : 12915 i , 1959.

4. Gal. I. *Reakcija uranil jona sa l-askorbinskom kiselinom* (Reaction of Uranyl Ions with l-Ascorbic Acid). Doctoral Thesis — Beograd: Prirodno-Matematički Fakultet, 1956.

5. Gregorczyk, Z. "Oznaczanie liczb koordynacyjnych zwiazkow kompleksowych kwasu askorbinowego z jonami UO_2^{++} i TiO^{++}" (Determination of Coordinate Bonds in Complexes of Ascorbic Acid with UO_2^{++} and TiO^{++} tons) — *Acta Poloniae Pharmaceutica* 15 : 129, 1958.

6. Gregorczyk, Z. "Oznaczenie stalych nietrwalosci zwiazków kompleksowych kwasu askorbinowego z jonami TiO^{++} i UO_2^{++}" (Determination of Instability Constant of Complexes of Ascorbic Acid with TiO^{++} and UO_2^{++} Ions) — *Acta Poloniae Pharmaceutica* 15 : 333, 1958.

7. Sobkowska, A., and J. Minczewsky. "Potencjometryczne badenie ukladu jon uranylowy — kwas askorbinowy" (Potentiometric Determination of Stability Constant of Complex of Vanadyl Ion and Ascorbic Acid) — *Roczniki chimii* 35 (1) : 47, 1961.

8. Gal. I. "Izdvajanje kompleksa uran-askorbinska kiselina" (Isolation of Uranium-Ascorbic Acid Complex — Preliminary note) — *Bilten Instituta za nuklearne nauke "Boris Kidrič"* (Beograd—Vinča) 6 : 173—178, 1956.

9. Korkisch, J. A. Farag and F. Hecht. "Eine neue Methode zur Arreicherung des Urans mittels Jonenaustausches und deren Anwendungen zur Bestimmung des Urans in festen Proben" — *Mikrochimica Acta* (Wien) 3: 415, 1958.

10. Sommer, L. "Ueber die genaue spektrophotometrische Eisen (III) — und Titan (IV) — Bestimmung mit Polyphenolen und vervandten Verbindungen" — *Acta Chimica Academiae Scientiarum Hungaricae* (Budapest) 33 (1): 23, 1962.

11. Sommer, L. "Spektrophotometrische Titan (IV) — Bestimmung mit Ascorbinsäure" — *Collection of Czechoslovak Chemical Communications* (Prague) 28: 449, 1963.

12. Šušić, M. V. "Kompleksi titana sa askorbinskom kiselinom i njihove konstante stabilnosti" (Titanium Complexes with Ascorbic Acid and their Stability Constants) — *Bilten Instituta za nuklearne nauke "Boris Kidrič"* (Beograd—Vinča) 14 : (3): 125—128, 1963.

13. Sobkowska, A. and J. Minczewski. "Potencjometryczne oznaczenie stalych trwalośi kompleksów jonu wanadylowego z kwasem askorbinovym" (Potentiometric Study of the Uranyl Ion-Ascorbic Acid Reaction) — *Roczniki chimii* 36(1): 17, 1962.

14. Schubert J. and A. Lindenbaum. "Stability of Alkaline Earth-Organic Acid Complexes Measured by Ion Exchange" — *The Journal of the American Chemical Society* (Easton, Pa) 74: 3529, 1952.

15. Romanchul, P. S. "Stabiliziriushchee deistvie magniia na askorbinoviu kiselotu" (Stabilizing Effect of Magnesium on Ascrobic Acid) — *Dokladi Akademiii Nauk SSSR* (Moskva) 117: 665—669, 1957.

16. Šušić, M. V., D. S. Veselinović, and D. Ž. Sužnjević. "Ispitivanje reakcije natrijumvolframata sa l-askorbinskom kiselinom" (Investigations of the Reaction of Sodium Tungstate with Ascorbic Acid) — *Glasnik hemijskog društva* (Beograd) 29: 121—129 (1964).

17. Šušić, M. V. *Polarografija urana. Polarografsko odredivanje urana u rudama* (Polarography of Uranium. Polarographic Determination of Uranium in Minerals), Doctoral Thesis — Beograd: Prirodnomatematički fakultet, Univerzitet u Beogradu, 1955.

18. Stoliiarov, K. P. and I. A. Amantova. *Spektrofotometricheskoe issledovanie askorbinatnikh kompleksov elementov II i III grup periodicheskoi sistemi* (Spectrophotometric Investigation of Ascorbic Acid Complexes of the Elements of the Second and Third Groups of the Periodic System) — Leningrad: Vestnik Leningradskogo universiteta, 19(4), Seriia fiziki i khimii, No. 1: 132, 1964.

19. Job. P. "Etude spectrographique de la formation des complexes en solution et de leur stabilité" — *Comptes rendus hébdomadaires des séances de l'academie des sciences* (Paris) 180: 928, 1925.

20. Job, P. "Recherches sur la formation de complexes minéraux en solution et sur leur stabilité" — *Annales de Chimie* (Paris) 9: 113, 1928.

21. Banjerjee, S. N., A. K. Sen Gupta, and S. K. Siddhanta. "Some Aliphatio Monocarboxylate Complexes of Bivalent Metals in Aqueous Solution. I. Lead Monoacetate Complex" — *Journal of the Indian Chemical Society* (Calcutta) 35: 269, 1958.

22. Siddhanta, S. K. and S. N. Banjerjee. "Aliphatic Monocarboxylate Complexes of Bivalent Metals in Aqueous Solution. IV— Cobalt Monoacetate Complex" — *Journal of the Indian Chemical Society* (Calcutta) 35: 339, 1958.

23. Siddhanta, S. K. and S. N. Banjerjee. "Aliphatic Monocarboxylate Complexes of Bivalent Metals in Aqueous Solution. VI— Manganese Monoacetate Complex" — *Journal of the Indian Chemical Society* (Calcutta) 35: 349, 1958.

24. Siddhanta, S. K. and S. N. Banjeree. "Aliphatic Monocarboxylate Complexes of Bivalent Metals in Aqueous Solutions. VIII— Nickel Monoacetate Complex" — *Journal of the Indian Chemical Society* (Calcutta) 35: 419, 1958.

25. Rai, A. K. and R. C. Mehrotra. "Some Lower n-Alkanoate Complexes of Bivalent Metals in Aqueous Solutions. Copper Monoacetate and Zinc Monoacetate Complexes" — *Zeitschrift für physikalische Chemie* (Berlin) 29: 237, 1961.

26. Irving, H. and R. J. P. Williams. "The Stability of Transition-Metal Complexes" — *Journal of the Chemical Society* (London) 3192, 1953.

27. Lingane, J. J. "Saturated Potassium Hydrogen Tartrate Solution as a pH Standard" — *Analytical Chemistry* (Easton, Pa) 19: 810, 1947.

COMPLEX COMPOUNDS OF *l*-ASCORBIC ACID AND METAL IONS.
II — Ca, Pb, Cd AND Al COMPLEXES IN ACIDIC MEDIUM

by

DRAGAN S. VESELINOVIĆ and MILENKO V. ŠUSIĆ

Complex compounds of Ca^{++}, Pb^{++}, Cd^{++} and Al^{3+} ions and ascorbic acid were investigated under the same conditions as described n an earlier paper[1].

The results of determinations with 0.200, 0.300 and 0.400 M ascorbic acid solutions and $CaCl_2$, $CdCl_2$, $(Pb(No_3)_2$ and $Al(NO_3)_3$ are shown in Tables 1 and 2.

From the curves in Figs. 1 through 4, which show ΔC_{H+} as a function of n, it may be seen that Ca, Cd and Pb have maxima at $n = 1$. This implies that ascorbic acid forms cationic complexes of the $[MeA]^+$ — type with ions of these metals as with the other cations investigated so far. For aluminum, the value n = 2 was obtained. Hence, it follows that trivalent ion of aluminum forms a complex with two ions of ascorbic acid $[AlA_2]^+$. Conditions of symmetry used for 1 : 1 complexes cannot
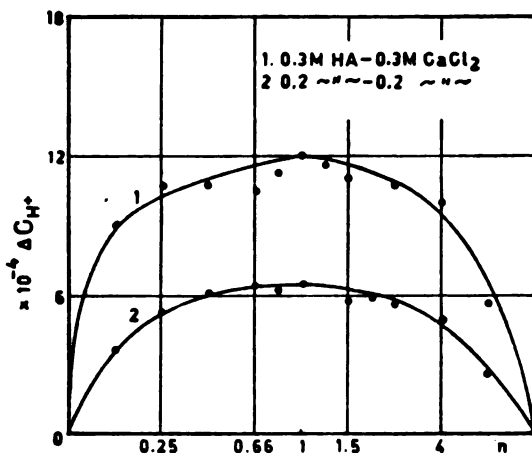
Fig. 1 — ΔC_{H+} against n for the $CaCl_2$ — HA system

2*

be employed in this case. Therefore, with regard to the shape of the curve, the possibility of forming a 1 : 1 complex of ascorbic acid and Al^{3+} ion is not excluded.
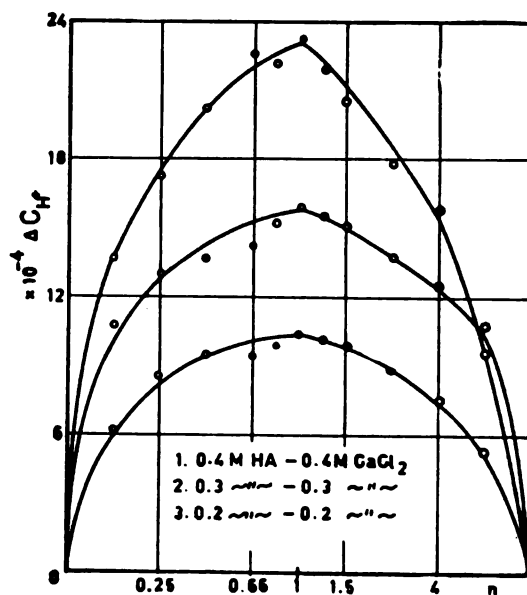
Fig. 2 — ΔC_{H+} against n for the $CdCl_2$ — HA system
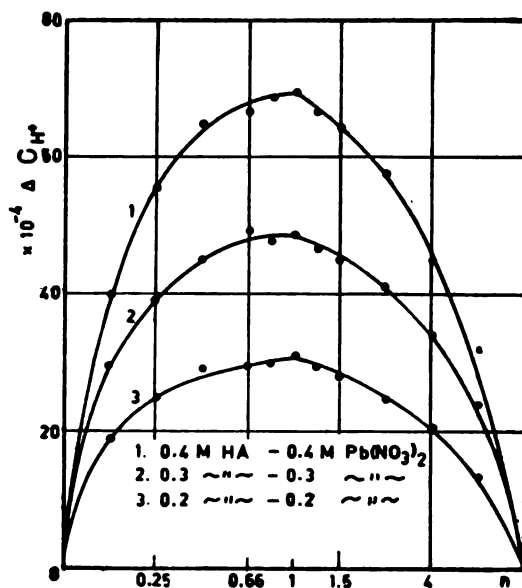
Fig. 3 — ΔC_{H+} against n for the $Pb(NO_3)_2$ — HA system

TABLE 1

| Molar ratio | Solution mixture in ml | | | 0.4M Cd-HA pH | 0.3M Cd-HA pH | 0.2M Cd-HA pH | 0.4M Pb-HA pH | 0.3M Pb-HA pH | 0.2M Pb-HA pH |
	HA	Me	H$_2$O						
	1.0	9.0	—	2.54	2.63	2.79	2.25	2.36	2.53
0.11	1.0	—	9.0	2.82	2.90	3.00	2.82	2.90	3.00
	—	9.0	1.0	5.65	5.38	6.30	3.88	3.82	4.47
	2.0	8.0	—	2.39	2.50	2.63	2.11	2.23	2.40
0.25	2.0	—	8.0	2.65	2.73	2.83	2.65	2.73	2.83
	—	8.0	2.0	5.82	5.50	6.30	3.93	3.89	4.55
	3.0	7.0	—	2.32	2.43	2.55	2.03	2.16	2.32
0.43	3.0	—	7.0	2.56	2.63	2.73	2.56	2.63	2.73
	—	7.0	3.0	5.98	5.64	6.30	4.00	3.98	4.59
	4.0	6.0	—	2.26	2.38	2.50	2.00	2.11	2.29
0.67	4.0	—	6.0	2.49	2.56	2.66	2.49	2.56	2.66
	—	6.0	4.0	6.13	5.73	6.40	4.11	4.04	4.66
	4.5	5.5	—	2.24	2.35	2.47	1.98	2.11	2.27
0.82	4.5	—	5.5	2.45	2.53	2.63	2.45	2.53	2.63
	—	5.5	4.5	6.21	5.77	6.37	2.15	2.10	4.72
	5.0	5.0	—	2.22	2.33	2.45	1.97	2.10	2.25
1.00	5.0	—	5.0	2.43	2.51	2.60	2.43	2.51	2.60
	—	5.0	5.0	6.28	5.91	6.46	4.21	4.15	4.75
	5.5	4.5	—	2.21	2.32	2.44	1.97	2.10	2.25
1.22	5.5	—	4.5	2.40	2.49	2.58	2.40	2.49	2.58
	—	4.5	5.5	6.35	5.98	6.43	4.27	4.22	4.86
	6.0	4.0	—	2.20	2.31	2.42	1.97	2.10	2.25
1.50	6.0	—	4.0	2.37	2.47	2.55	2.37	2.47	2.55
	—	4.0	6.0	6.41	5.98	6.47	4.35	4.28	4.90
	7.0	3.0	—	2.19	2.30	2.40	1.98	2.11	2.25
2.3	7.0	—	3.0	2.33	2.44	2.51	2.33	2.44	2.51
	—	3.0	7.0	6.61	6.10	6.50	4.52	4.46	5.00
	8.0	2.0	—	2.18	2.29	2.39	2.02	2.13	7.12
4	8.0	—	2.0	2.30	2.40	2.48	2.30	2.40	2.48
	—	2.0	8.0	6.73	6.33	6.58	4.73	4.65	5.16
	9.0	1.0	—	2.19	2.28	2.39	2.06	2.1-	2.31
9	9.0	—	1.0	2.26	2.38	2.45	2.26	2.38	2.45
	—	1.0	9.0	—	6.56	6.56	5.06	4.92	5.45

TABLE 2

Molar ratio	Solution mixture in ml			0.4M Al-HA	0.3M Al-HA	0.2M Al-HA	0.4M Ca-HA	0.2M Ca-HA
	HA	Me	H_2O	pH	pH	pH	pH	pH
	1.0	9.0	—	2.49	2.60	2.74	2.61	2.86
0.11	1.0	—	9.0	2.81	2.90	2.99	2.81	2.99
	—	9.0	1.0	2.84	3.00	3.11	6.70	6.35
	2.0	8.0	—	2.32	2.45	2.62	2.47	2.69
0.25	2.0	—	8.0	2.64	2.73	2.82	2.64	2.82
	—	8.0	2.0	2.90	3.05	3.15	6.90	6.55
	3.0	7.0	—	2.22	2.34	2.51	2.41	2.60
0.43	3.0	—	7,0	2.55	2.63	2.72	2.55	2.72
	—	7.0	3.0	2.95	3.10	3.19	6.93	6.68
	4.0	6.0	—	2.17	2.28	2.45	2.36	2.54
0.67	4.0	—	6.0	2.48	2.57	2.65	2.48	2.65
	—	6.0	4.0	3.01	3.16	3.23	6.95	6.75
	4.5	5.5	—	—	2.26	—	2.33	2.52
0.82	4.5	—	5.5	—	2.53	—	2.45	2.62
	—	5.5	4.5	—	3.19	—	7.00	—
	5.0	5.0	—	2.13	2.23	2.41	2.30	2.50
1.00	5.0	—	5.0	2.42	2.51	2.60	2.42	2.60
	—	5.0	5.0	3.08	3.21	3.28	7.00	6.75
	5.5	4.5	—	—	2.22	—	2.28	—
1.2	5.5	—	4.5	—	2.49	—	2.39	—
	—	4.5	5.5	—	3.24	—	7.02	—
	6.0	4.0	—	2.11	2.21	2.38	2.27	2.47
1.5	6.0	—	4.0	2.37	2.47	2.55	2.37	2.55
	—	4.0	6.0	3.16	3.28	3.35	7.02	6.73
	6.5	3.5	—	2.10	—	2.36	—	2.46
1.9	6.5	—	3.5	2.35	—	2.53	—	2.53
	—	3.5	6.5	3.20	—	3.39	—	6.68
	7.0	3.0	—	2.10	2.19	2.35	2.24	2.44
2.3	7.0	—	3.0	2.33	2.43	2.51	2.33	2.51
	—	3.0	7.0	3.23	3.35	3.42	7.01	6.70
	8.0	2.0	—	2.10	2.20	2.34	2.22	2.42
4	8.0	—	2.0	2.29	2.39	2.48	2.29	2.48
	—	2.0	8.0	3.34	3.46	3.52	7.01	6.70
	9.0	1.0	—	2.12	2.21	2.35	2.21	2.41
9	9.0	—	1.0	2.26	2.37	2.44	2.26	2.44
	—	1.0	9.0	3.51	3.61	3.67	7.00	6.70
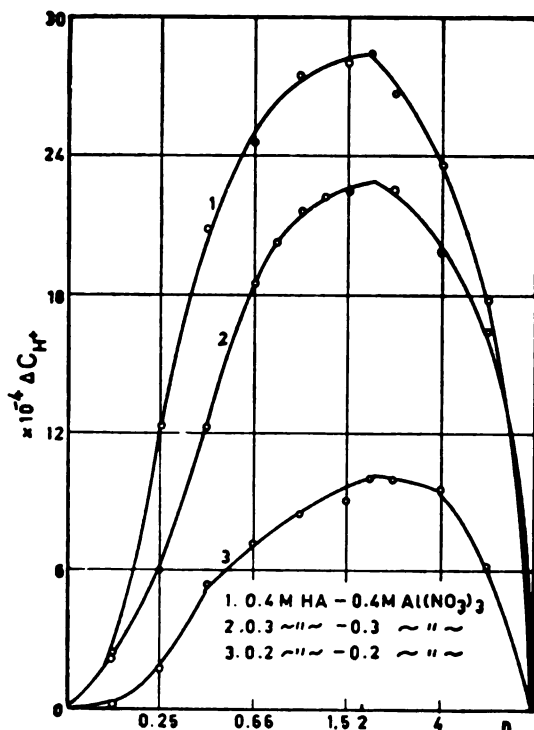
Fig. 4 — ΔC_{H+} against n for the $Al(NO_3)_3$ — HA system

The pK values for ionic strength $\mu = 0$ at 25°C, obtained by extrapolating the straight lines representing pK against $\sqrt{\mu}$ (Figs. 5 and 6), are shown in Table 3. However, to calculate the dissociation constant for the $[AlA^2]^+$ complex we have partially modified the procedure used for the 1 : 1 complex.

In the solution containing $Al(NO_3)_3$ and ascorbic acid there are the following equilibrium reactions:

$$[AlA]^+ \rightleftharpoons 2 A^- + Al^{3+} \tag{1}$$

$$HA \rightleftharpoons H^+ + A^- \tag{2}$$

with dissociation constants:

$$K = \frac{[C_{A^-}]^2 \times [C_{Al^{3+}}]}{[C_{AlA_2^+}]} \times \frac{[f_{A^-}]^2 \times [f_{Al^{3+}}]}{[f_{AlA_2^+}]} \tag{3}$$

$$k + \frac{[C_{H^+}] \times [C_{A^-}]}{[C_{HA}]} \times \frac{[f_{H^+}] \times [f_{A^-}[}{[f_{HA}]} \tag{4}$$

where C denotes the concentrations of the corresponding ions or molecules and f their activity coefficients.

The total content of ascorbic acid in the solution is:

$$C_{HA}^{\circ} = C_{HA} + C_{A^-} + 2\,C_{AlA_2^+} \tag{5}$$

and of metals

$$C_{Al^{3+}}^{\circ} = C_{Al^{3+}} + C_{AlA_2^+} \tag{6}$$

assuming that $Al(NO_3)_3$ in the solution is completely dissociated. C° values are the initial concentrations of metal salts and ascorbic acid.

The concentration of H^+ ions in the solution is expressed by:

$$C_{H^+} = 2\,C_{AlA_2^+} + C_{A^-} \tag{7}$$

which follows from eqs. 1 and 2. Knowing the C° and k values and measuring C_{H^+}, all the values needed for the deteimination of the dissociation constant of the complex (eq. 3), except for the activity coefficients, are calculated from equations 4 through 7.

1. [PbA]$^+$
2. [CaA]$^+$
3. [CdA]$^+$
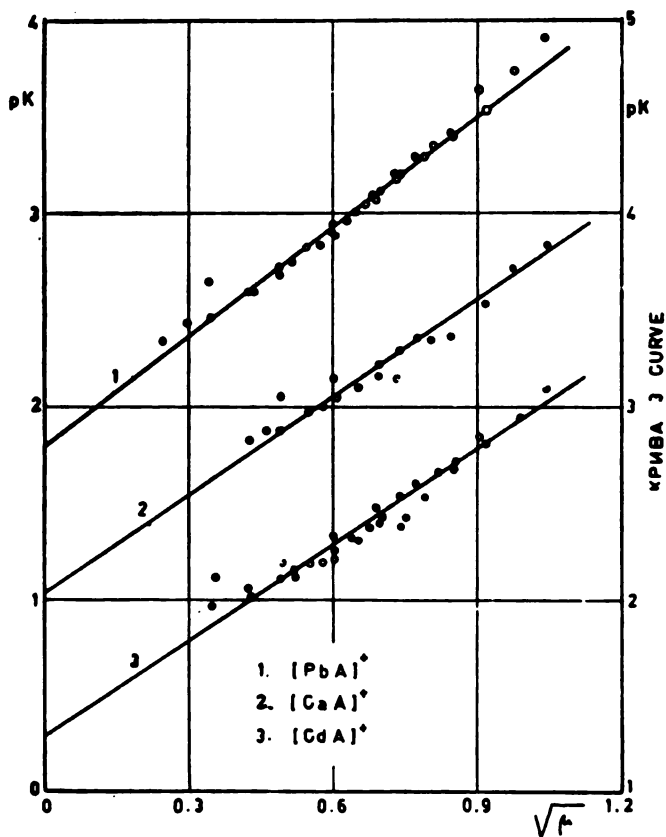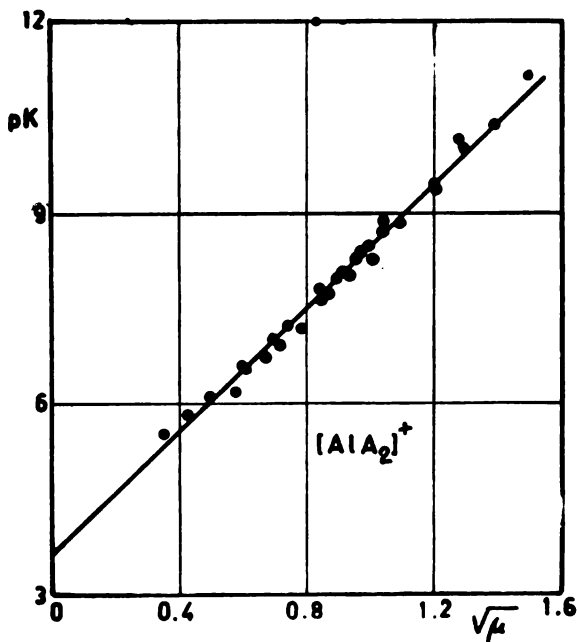
Fig. 5 — pK against $\sqrt{\mu}$

Fig. 6 — pK against $\sqrt{\mu}$

As the activity of H^+ ion is measured with a glass electrode, it is necessary to know f_{H+} if the H^+ ion concentration needed for further calculations is to be obtained from the activity. Therefore, concentrations of all ions in the solution are first calculated by the procedure described, assuming that their activity coefficients are equal units. From the values obtained we determine the ionic strength of the solution and from it the activity coefficients. After correction with the activity coefficients the ion concentrations in the solution, used to determine the complex dissociation constant for the given ionic strength of the solution, are calculated again. The pK value for ionic strength $\mu = 0$ is calculated from the curve representing pK against $\sqrt{\mu}$, by its extrapolation to $\sqrt{\mu} = 0$.

TABLE 3

pK values for $\mu = 0$ at 25° C

Me	Ca	Pb	Cd	Al
pK	1.05	1.8	1.3	3.7

From the data given in the literature, which are shown in our previous paper[1], it may be seen that for the cationic complex of calcium and ascorbic acid we obtained pK=0.19 at 25°C with ionic strength $\mu = 0.16$. Correcting pK in Table 3 to ionic strength $\mu = 0.16$ we obtain pK = 0.23.

The consistency of these values, ours being obtained at pH 2—3 and that in the literature at pH 7.2—7.3, denotes that in this pH region there is only a cationic complex of calcium, as distinct from the other cations dealt with in the literature so far.

School of Sciences
Institute of Physical Chemistry
Belgrade
Institute of Chemistry,
Technology and Metallurgy
Belgrade

REFERENCES

1. Veselinović, D. S. and M. V. Šušić. "Kompleksna jedinjenja l-askorbinske kiseline i jona metala. I — Kompleksi U, Co, Ni, Mn, i Zn u kiseloj sredini" (Complex Compounds of l-Ascorbic Acid and Metal Ions. I — U, Co, Ni, Mn, and Zn Complexes in Acidic Medium) — Glasnik Hemijskog društva (Beograd), in press.

POLAROGRAPHIC DETERMINATION OF VITAMIN K₃ (MENADIONE) IN MENADIONE-SODIUM-BISULPHITE PREPARATIONS

by

VILIM J. VAJGAND and FILIP S. UVODIĆ

Vitamin K_3 or menadione (so-called by some American authors) is 2-methyl-1, 4-naphthoquinone; it is the most active compound of the K-vitamin group. Since it is practically insoluble in water it can be administered only orally. However, in its bisulphite form it is water--soluble and as such it is used in therapy since it can be administered both orally and parenterally.

The method for the determination of menadione sodium bisulphite adopted by the United States Pharmacopeia, USP-XVI[1] consists in the conversion of this compound to menadione by means of sodium hydroxide followed by its extraction with chloroform and reduction with zinc and hydrochloric acid to 2-methyl-1, 4-naphtho-hydroquinone which is then determined by means of ceric sulphate. The British Pharmacopeia, BP-63[2] recommends titration with titanium chloride.

A number of papers dealing with the polarographic determination of menadione have been published so far but all these determinations were performed in organic solvents. Thus, Onrust and Wöstmann[3] carried out the determination of vitamin-K_3 content of food in a mixture of petroleum ether and isopropanol, whereas Jonkind, Buzza and Fox[4] investigated the K_3-content of multivitamin preparations.

A polarographic determination of menadione sodium bisulphite which is soluble only in aqueous solvents was first published by Varela[5] in 1951 but the details of the procedure were not recorded. In 1954, Kékedy and Hajdu[6] presented a method for its determination in injection preparations by comparing the wave height of the investigated sample with that of a standard solution in which vitamin K_3-content had been determined by some other method; thus their results were not given with respect to some official standard. In 1962, Burger[7] applied Kékedy-Hajdu's method to the determination of menadione sodium bisulphite in multivitamin preparations with an erroe of $\pm 5\%$.

We attempted to find a more convenient methord of the determination of menadione sodium bisulphtie and to express the results with respect to pure vitamin K_3 as a primary standard. By comparing the polarographic behavior of these two compounds (menadione and
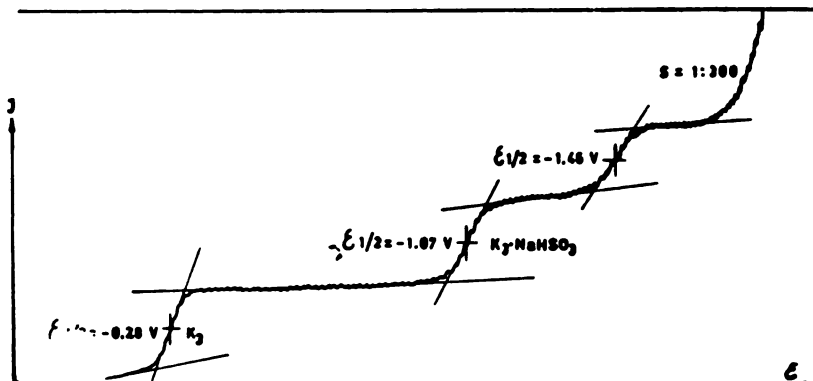
Fig. 1

menadione sodium bisulphite) we succeeded in finding a supporting electrolyte which permits a simultaneous observation of their waves (Fig. 1) and makes possible a direct determination of vitamin K_3 in bisulphite preparations.

EXPERIMENTAL

USP standard menadione and "Merck" menadione of 98.5% purity was used. The purity of the latter sample was verified by the standard USP method[1]., the titration being performed in an inert atmosphere[2]. Sodium bisulphite was always checked iodometrically for the content of SO_2. The solutions for polarographic determination were prepared in bidistilled water. Nitrogen from which oxygen was removed by passing through an alkaline solution of pyrogallol was added to the solutions. The gelatin concentration was always 0.01%. Britton-Robinson buffers were used whose values were checked with a "Radiometer" PHM-22 pH meter. All polarographic curves were recorded on a "Radiometer" PO3 polarograph.

Investigating the behavior of menadione in different solvents and in the presence of variable quantities of sodium bisulphite we found that the best results were obtained with a 20% alcoholic solution of Britton-Robinson buffer of pH 7. Gradual addition of a sodium bisulphite solution to an alcoholic solution of vitamin K_3 produced a decrease in its wave height to $e_{1/2} = -0.28$ V (SCE) and an increase of the wave of newly-formed menadione bisulphite to $E_{1/2} = -1.07$ V (SCE) (Fig. 2).

Vitamin K_3. $NaHSO_3$ at various pH values also gives the best defined wave in the same buffer at pH 7. Deformed waves were obtained at lower pH values, while at pH values above 8 there is a wave which corresponds to the reduction of free vitamin K_3 formed by decomposing bisulphite compounds in alkaline medium. It is seen from Fig. 2 that the wave height of menadione bisulphite is practically unaltered in the presence of 4—8 times larger qantities of sodium bisulphite than vitamin K_3, while on further addition of $NaHSO_3$ the curve shows a tendency to a slight decrease.

From the same figure it may be seen that on addition of more than one mole of $NaHSO_3$ the entire amount of K_3-vitamin is converted to its bisulphite compound; this fact permits the preparation of standard menadione bisulphite solution by precisely weighing vitamin K_3.

Standard solutions for the analysis of menadione sodium bisulphite samples were prepared in the following way: a weighed amount of vitamin K_3 was dissolved in ethanol and a solution of Britton-Robinson buffer pH 7 containing a sixfold excess of $NaHSO_3$ (with respect to vitamin K_3) was added until the final solution contained 20% of ethanol. Samples for analysis were prepared in the same way.

The results of all samples were read from calibration curve which covered concentrations range from 5.10^{-4} to 5.10^{-3} M/l.

TABLE 1

Determination of menadione in samples of raw materials of menadione sodium bisulphite

| | | POLAROGRAPHIC METHOD | | | USP METHOD | | | |
Sample	Taken mg K₃.NaHSO₃	Found mg K₃	% K₃ in K₃.NaHSO₃	Mean Value	Taken mg K₃.NaHSO₃	Found mg K₃	% K₃ in K₃.NaHSO₃	Meann Value
1	8.92	4.75	53.2		300.0	151.2	50.4	
	11.13	5.98	53.7	53.5	300.0	154.7	51.6	50.7
	13.76	7.40	53.7		300.0	150.3	50.1	
2	8.92	4.78	53.5		300.0	153.0	51.0	
	11.13	6.00	53.8	53.7	300.0	155.0	51.7	51.2
	13.76	7.40	53.7		300.0	153.0	51.0	
3	8.92	4.66	52.3		300.0	150.5	50.2	
	11.13	5.93	53.3	52.6	300.0	151.1	50.4	50.6
	13.76	7.17	52.1		300.0	153.4	51.1	

TABLE 2

Determination of menadione in menadione sodium bisulphite injections
Injections contain 10 mg of menadione sodium bisulphite/ml

| | | POLAROGRAPHIC METHOD | | | | USP METHOD | | | | |
Sample	Taken mg K₃.NaHSO₃	Found mg K₃	% K₃ in K₃.NaHSO₃	mg K₃/ml	Mean Value	Taken mg K₃.NaHSO₃	Found mg K₃	% K₃ in K₃.NaHSO₃	mg K₃/ml	Mean Value
1	2.94	1.53	52.1	5.21		50.0	25.3	50.6	5.06	
	3.92	2.06	52.5	5.25	5.24	50.0	25.3	50.6	5.06	5.06
	6.86	3.61	52.6	5.26		50.0	27.3	54.6	5.46	
2	2.94	1.57	53.4	5.34		50.0	25.8	51.6	5.16	
	3.92	2.04	52.0	5.20	5.25	50.0	26.5	53.0	5.30	5.31
	6.86	3.57	52.0	5.20						
3	2.94	1.51	51.3	5.13		50.0	27.0	54.0	5.40	5.35
	3.92	2.04	52.0	5.20	5.14					
	6.86	3.49	50.8	5.08						

Fig. 2

TABLE 3

Determination of menadione in menadione sodium bisulphite coated tablets
Coated tablets contain 10 mg menadione sodium bisulphite

POLAROGRAPHIC METHOD

Sample	Taken mg $K_3 \cdot NaHSO_3$	Found mg K_3	% K_3 in $K_3 \cdot NaHSO_3$	mg K_3 pro tablet	Mean Value
	1,96	1,05	53.5	5.35	
1	3.92	2.10	53.5	5.35	5.35
	7.84	4.20	53.5	5.35	
	1.96	1.05	53.5	5.35	
2	3.92	2.07	52.8	5.28	5.33
	7.84	4.20	53.5	5.35	
	1.96	1.05	53.5	5.35	
3	3.92	2.07	52.8	5.28	5.33
	7.84	4.20	53.5	5.35	

The results obtained in the polarographic determination of vitamin-K_3 content in menadione sodium bisulphite samples are shown together with results obtained by the USP-XVI method in Table 1.

Vitamin-K_3 content in injections labelled to contain 10 mg of menadione-sodium-bisulphite per ml was also determined polarographically.

The United States Pharmacopeia, USP-XVI, does not give any method for determining the bisulphite form of medione in coated tablets. We attemted to apply the method given for injection solutions but no satisfactory results were obtained. In fact, after the extraction of menadione-sodiumbisulphite from coated tablets with water and the addition of sodium hydroxide, the solution was very weak and the extraction with chloroform was not quantitative. However, we succeeded in determining menadione content in coated tablets polarographically, the concentrations of solutions obtained corresponded to those of the standard curve. The results obtained are given in Table 3.

From our results it follows that the results obtained in determining menadione--sodium-bisulphite by USP-XVI method are lower than expected; and this might be due to numerous extractions, decomposition of menadione by light and the oxidation of naphthohydroquinone (reduced vitamin-K_3) by air. Moreover, this method is long, requires large sample amounts and does not postulate the titration to be carried out in inert atmosphere.

The advantages of the described polarographic method lie in the possibility of direct determination of menadione in menadione-sodium-bisulphite samples, the results being expressed with respect to standards given in pharmacopeia; the duration of the analysis is shorter and a much smaller amount of sample is required.

School of Science
Department of Chemistry
University of Belgrade
Inspection Laboratory,
Galenika Beograd

REFERENCES

1. *"United States Pharmacopeia"*, 16th rev. — Easton, Pa.: Mack Publishing Company, 1960, p. 402.

2. *"British Pharmacopeia"* — London: General Medical Council, 1963, pp. 467—470.

3. Onrust, H. and B. Wöstmann. "Polarographic Determination of Vitamin K_3 (2-methyl-1,4naphthoquinone) in Prepared Food" — *Recueil des travaux chimiques des Pays-Bas* (Amsterdam) 69: 1207—1216, 1950.

4. Jongkind, J. C., E. Buzza, and S. H. Fox. "Assay of Menadione — A Polarographic Procedure" — *Journal of the American Pharmaceutical Association* (Easton, Pa) 46: 214—216, 1957.

5. Varela, G. "Sobre la determination polarografica de la vitamina K hidrosoluble" — *Anales de la real sociedad española de fisica y quimica* (Madrid) 47B: 885—888, 1951.

6. Kékedy, L. and E. Hajdu. "Contributii la dosarea polarografică a vitaminei K_3" — *Academia Republicii Populare Romine, Studii si cercetari de chimie* (Bólyai Univ. Cluj) 4: 145—160, 1956.

7. Burger, K. "Polivitamin készitmények analitikai ellenörzéséről. I — A K vitamin tartalom meghatározása polarográfiós eljárással" (Analytical Check of Polyvitamin Products. I — Polarographic Determination of Vitamin-K Content) — *Acta pharmaceutica Hungarica* (Budapest) 32(4): 180, 1962.

DETERMINATION OF MICRO AMOUNTS OF COPPER BY RING COLORIMETRY USING BIS (DIMETHYLGLYOXIMATO) — COPPER (II) COMPLEX*

by

TOMISLAV J. JANJIĆ, ZVONKO S. ČERVENJAK and
MILENKO B. ĆELAP

The determination of micro amounts of copper by the ring colorimetry method has been investigated by several authors.[1] In one of these studies copper was determined by means of rubeanic acid i.e. by the colorimetry of dark green rings of copper rubeanate. However, the presence of silver, mercury nickel and cobalt interfered with this determination and it was found that when solutions contain these elements the copper should first be separated out and then determined.

Copper has also been determined by means of a universal silver sulphide scale[2] but this method can only be used when the solution to be analyzed does not contain elements forming sulphides insoluble in hydrochloric acid.

Otherwise, the interfering elements must be separated out before determination. Thus, copper has been determined in the presence of lead, cadmium, iron, cobalt and zinc by means of the silver-sulphide scale when previously separated by paper chromatography[3,4].

The determination of copper has also been carried out by means of a cupric ferrocyanide scale[5]. However, this method is disturbed by the presence of ions which from insoluble ferrocyanides such as UO_2^{2+}, Mn^{2+}, $Ag_2''^{2+}$, Ag^{2+}, Zn^{2+}, Pb^{2+} and Ni^{2+}.

Some authors[6] have determined copper by carrying out the colorimetry of green-brown rings of copper-dithiocarbamate, when the solution to be analyzed contained also aluminium. Copper was first precipitated at the starting spot by means of alkali diethyl dithiocarbamates or tartrates and aluminium was washed out into the ring. The centre of the paper with precipitated copper was cut out and placed in the center of another paper and then, copper was washed in the ring with pyridine.

3

It will be seen that in all these methods it is necessary to separate the copper from elements giving similar reactions with the detecting agent; hence, these methods involve two chemical operations, both separation and determination of copper, and are therefore rather long. To avoid the separation of copper and to enable its determination in the presence of other elements we worked out a method in which copper is directly washed in the ring on a ring oven by means of n-butanol containing 2% of dimethyl glyoxime and saturated with 2N ammonia.* The other elements remained at the starting spot. The obtained brown colored rings of bis (dimethylglyoximato)-copper (III) complex** are very suitable for colorimetry, their colour being very stable over six months.

To check the reproducibility of this method we determined copper in a series of solutions of known copper concentrations. The results of six successive determinations are given in Table 1.

TABLE 1

Determination of Copper in Solution

Concentration of Copper Solution mg/ml	
Calculated	Found
0.90	0.90
0.90	0.87
0.45	0.48
0.45	0.45
0.30	0.30
0.30	0.30

The table shows that the values obtained were consistent with those calculated; the average error was 1.9%. The amount of copper required for one determination amounted to about 5 μg.

This method can be used for the determination of copper in the presence of following elements: molybdenum (1 : 500), mercury (1 : 300), bismuth (1 : 300), cadmium (1 : 200), platinum (1V) (1 :100), gold (1 : 100), silver (1 : 100), arsenic (1 : 100), antimony (1 : 50), tin (1 : 50), zinc (1 : 20), nickel (1 : 10), manganese (1 : 10) and iron (1 : 5). The results obtained in 4 successive determinations are given in Table 2.

The table shows that the mean error in determining copper in the presence of different metals is as follows: molybdenum 3.7%, mercury 4.6%, bismuth 3.1%, cadmium 4.5%, platinum 3.6%, gold 2.6%, silver 2.5%, arsenic 2.7%, antimony 3.0%, tin 3.3%, zinc 2.9%, nickel 2.6%, manganese 4.3% and iron 3.8%.

On the basis of these results it might be concluded that the average error in the determination of copper by ring colorimetry of bis(dimethylglyoximato)-copper (II) complex in the presence of these elements

---

* This solvent mixture was used by J. Anderson and M. Lederer[7] in chromatographic seperations of copper from a series of other elements.
** This complex was first obtained by L. Čugaev in 1905.

TABLE 2

Determination of Copper in the Presence of Other Elements

In the presence of	Concentration of copper solution mg/ml		In the presence of	Concentration of copper solution mg/ml	
	Calculated	Found		Calculated	Found
Molybdenum 1 : 500	0.30	0.32	Mercury 1 : 300	0.89	0.90
	0.30	0.31		0.89	0.95
	0.23	0.24		0.30	0.32
	0.23	0.23		0.30	0.32
Bismuth 1 : 300	0.87	0.85	Cadmium 1 : 200	0.88	0.85
	0.87	0.85		0.88	0.85
	0.44	0.45		0.90	0.85
	0.44	0.47		0.90	0.85
Platinum 1 : 100	0.90	0.86	Gold 1 : 100	0.90	0.90
	0.90	0.86		0.90	0.95
	0.46	0.45		0.43	0.45
	0.46	0.45		0.43	0.43
Silver 1 : 100	0.90	0.95	Arsenic 1 : 100	0.91	0.90
	0.90	0.90		0.91	0.95
	0.46	0.47		0.45	0.45
	0.46	0.45		0.45	0.47
Antimony 1 : 50	0.89	0.94	Tin 1 : 50	0.90	0.88
	0.89	0.90		0.90	0.85
	0.46	0.47		0.44	0.43
	0.46	0.45		0.44	0.45
Zinc 1 : 20	0.85	0.90	Nickel 1 : 10	0.90	0.85
	0.85	0.85		0.90	0.90
	0.88	0.85		0.45	0.45
	0.88	0.90		0.45	0.43
Manganese 1 : 10	0.93	0.90	Iron 1 : 5	0.88	0.85
	0.93	1.00		0.88	0.85
	0.46	0.45		0.46	0.42
	0.46	0.47		0.46	0.46

lies within the limits of errors obtained by methods previously described, the difference is in that the method is simple and more rapid since it is not necessary to separate copper before its determination.

We also attempted to determine copper in the presence of lead, cobalt and aluminium but found that these elements interfere with determination.

To illustrate the applicability of the described method to the determination of micro analysis of copper in different materials we applied it to the determination of copper in ores (pyrite, sphalerite, galena, iron oxide ores), washed anode slime and alloys. Finally, it was checked by determining copper in some materials of biological origin. The results were compared with those obtained by the iodometric method[9,10] for higher concentrations, or the spectrophotometric method[11,12] when the concentrations were small.

Examples of some of the results obtained are shown in Table 3; as it is seen, they are consistent with the results obtained iodometrically and spectrophotometrically.

TABLE 3

Copper Content in Ores, Alloys and Biological Material

No.	Sample	Percentage of copper*			Amounts of elements in whose presence the determination was performed %
		Ring colori- metry	Iodometry	spectro- photo- metry	
1.	Pyrite Concentrate	0.21	0.20		Mo — 0.017
2.	Sphalerite	0.96	0.93		As — 0.1 Mo — Traces
3.	Galena Concentrate	0.045	0.045		Sn — 0.8 As — 0.04 Bi — 0.082 Au — 0.0001 Sb — 0.056
4.	Oxide Iron Ore	1.02	1.05		Sn — 0.3 Mo — 0.001
5.	Oxide Iron Ore	0.82	0.88		Sb — 0.1 Mo — 0.001
6.	Washed Anode Slime	0.43	0.44		Ag — 33.4 Zn — 1.25 Fe — 0,23
7.	Gold-Copper Alloy	6.60	6.41		Au — Main Com- ponent
8.	Bismuth-Copper Alloy	1.28	1.35		Bi — Main Com- ponent
9.	Hen Stomach	0.00019		0.00021	Sn — Traces As — Traces
10.	Hay	0.00049		0.00050	Mo — Traces

* Mean values of two determinations

On the basis of this data it may be concluded that this method for the determination of micro-amounts of copper by ring colorimetry of bis (dimethylglyoximato)-copper (II) complex can be successfully used in the determination of copper content in different materials of inorganic and organic origin. The procedure requires only a few micro-grams of copper and thus can be applied to the analysis of samples containing only traces of copper. In spite of these small amounts the experimental error is less than 5%. The advantage of the method descri-bed is the simplicity of equipment required with respect to the very expensive apparata usually employed in the determination of micro--amounts of elements by other methods.

EXPERIMENTAL

Preparation of the standard cupric sulphate solution (0.9 mg/ml)

This solution was made from "Merck" p.a. $CuSO_4 — 5H_2O$ and was standardized electrogravimetrically. It was also used for the preparation of the dilute cupric sulphate solutions used for the preparation of the standard scale and for investigation.

Preparation of solutions of elements in the presence of which copper was determined.

For the preparation of these solutions the following "Merck" p.a. reagents were used: ammonium molybdenate, mercuric nitrate, bismuth, nitrate, cadmium sulphate, hydrogen hexachlorplatinate (1V), gold (elementary), silver nitrate, arsenic trioxide, antimony trioxide, stanous chloride, zinc sulphate, nickel sulphate, manganeous sulphate and ferric chloride.

Preparation of the solution for washing

In a 250 ml separatory funnel 50 ml of n-butanol and 50 ml of 2N ammonia were shaken for 10 minutes, the lower aqueous layer was thrown off and 1g of dimethyl glyoxime was dissolved in n-butanol saturated with 2N ammonia. The solution was kept in a flask with ground glass joint.

Preparation of the standard scale

For the preparation of the standard scale cupric sulphate (0.3 mg/ml) solution was used; rings were made with 1, 2, 4, 6, 8 and 10 drops respectively, of this solution. Capillary volume was 1.2 μl. Copper was washed on Schleicher and Schüll 589[2] filter paper with a 2% solution of dimethyl — glyoxime in n-butanol saturated with 2N ammonia. After being washed on the ring oven, the filter papers with obtained rings were dried in a current of warm air.

DECOMPOSITION OF SAMPLES AND THE PREPARATION OF THE SOLUTION FOR THE DETERMINATION OF COPPER

Pyrites, sphalerites, galena, oxide ores and biological materials

Samples were decomposed in the usual way. Copper was precipitated with the other elements of the second analytical group by means of hydrogen sulphide in the presence of mercuric chloride as collector. The obtained precipitate was heated and the residue was dissolved in hydrochloric acid with addition of some drops of nitric acid.

Anode slime

The solution obtained after the decomposition of the sample in usual way was treated with ammonia and yellow ammonium sulphide. The obtained precipitate was dissolved in aqua regia and diluted with water in a volumetric flask.

Alloys

Samples were dissolved in concentrated hydrochloric acid with addition of some drops of nitric acid and the obtained solution was then diluted with water.

School of Sciences
Institute of Chemistry
  Beograd
      and
Institute for Nuclear
  Raw Materials
    Beograd

REFERENCES

1. Weusz, H. "Anwendung des Ringsofens in die Tüpfelkolorimetrie" — *Mikochimica Acta* (6): 785—794, 1954.

2. Weisz, H., M. B. Ćelap and V. V. Almažan. "Ringofen-Tüpfelkolorimetriemit Hilfe einer Silbersulfid-Standardskala" — *Mikrochimica Acta* (1): 36—43, 1959.

3. Ćelap, M. B. and H. Weisz. "Anwendung der Ringofentüpfelkolorimetrie mit Hilfe einer Silbersulfil-Standardskala in der anorganischen Papierchromatographie" — *Mikrochimica Acta* (5—6): 706—712, 1960.

4. Ćelap, M. B. and T. J. Janjić. "Determination of Micro Amounts of Elements Using Ring Oven Method with Preliminary Chromatographic Separation" — *Mikrochimica Acta* (2): 313—315, 1963.

5. Ćelap, M. B. T. J. Janjić and M. Ristić. "Određivanje mikro-količina elemenata kolorimetrijom prstenova kupri-ferocijanida. II. Odredjivanje bakra, cinka, olova, nikla i ferocijanida" (Determination of Micro Amounts of Elements by Cupric Ferrocyanide Ring Colorimetry. II. Determination of copper, zinc, lead, nickel and ferrocyanides) — *Glasnik Hemijskog Društva* (Beograd) 27 (2—3): 99—102, 1962.

6. Malissa, H. and L. J. Ottenderfer. "Ringofen-Tüpfelkolorimetrischen Nachweis carbamatbilderner Metallionen neben Aluminium und anderen Metallen" — *Analitica Chimica Acta* 25: 461—462, 1961.

7. Anderson, J. R. A. and M. Lederer. "Quantitative Paper Chromatography III. The Separation and Gravimetric Determination of Copper — *Analitica Chimica Acta* 5: 396—400, 1951.

8. Tshugaeff, L. "Uber komplexe Verbindungen der α-Dioxime" — *Zeitschrift für Anorganischen Chemie* 46 (2): 144—169, 1905.

9. Kolthoff, J. M. and E. B. Sandell. "*Anorganska kvantitativna analiza*" (Inorganic Quantitative Analysis) — Zagreb: Školska knjiga, 1951, pp. 572—574.

10. Vogel, A. I. "*Quantitative Inorganic Analysis*" — London: Longmans Green and Co, 1951, pp. 344—345.

11. Snell, F. and C. Snell. "*Colorimetric Methods of Analysis*" London: D. Van Nostrand Comp. Inc., 1957, pp. 112—118.

12. Kolthoff, J. M. and E. B. Sandell. "*Anorganska kvantitativna analiza* (Inorganic Quantitative Analysis) — Zagreb: Školska knjiga, 1951, pp. 609—612.

NICKEL PLATING OF PASSIVATED STEEL SHEETS*

by

SRETEN N. MLADENOVIĆ and MILAN DIMOVSKI

Nickel electroplating of oxidized sheets of steel and aluminum has recently been investigated by several workers [1,2]. However, the properties of these galvanized coatings have not been thoroughly studied. It is known that the adherence of the metal coating to the basis metal is bad when the surface of the latter is covered with oxide.

In this investigation we have studied the properties of nickel coatings on passivated cold-rolled steel strips.

The adherence of nickel coatings to passivated steel surfaces decreases with increasing time of passivation (Table 1).

TABLE 1

Passivation bath: NaOH	400 g/l
Anodic current density:	7A/dm²
Temperature:	110°C
Nickel plating bath: $NiSO_4$	200 g/l
Na_2SO_4	100
NaCl	5
H_3BO_3	20
pH	5—5.3
Temperature:	25°C
Cathodic current density:	0.5A/dm²
Thickness of nickel coating:	4 μ

		Adherence	
Experiment No	Passivation time	Angle — 90°	Angle 180°
1	30	100	100
2	30	100	98
3	60	100	100
4	60	100	100
5	90	100	100
6	90	96	96
7	120	78	78
8	120	90	84
9	150	88	84
10	150	84	70

TABLE 2

Determination of porosity by means of potassium
ferrocyanide and sodium chloride solutions

Experiment No	Passivation time in sec.	Number of pores per dm^2
1	30	490
2	30	570
3	60	450
4	60	365
5	90	183
6	90	200
7	120	122
8	120	46
9	150	24
10	150	46

Four microns thick nickel coatings on steel strips passivated for 90 seconds adhere well and practically cannot be peeled. This behavior can be explained by the porosity of the oxide layer deposited on steel sheets. The porosity of the oxide layer on steel sheets which are passivated for 90 seconds at the most, is considerably high. This indicates that a great part of the basis metal is not covered with adherence-
-resistant (Table 2).

The porosity of coatings which are directly deposited on steel sheets is considerably greater than the porosity of nickel coatings on passivated steel surfaces (Table 3).

TABLE 3

Porosity of nickel coatings. Thickness of the layer 4 μ.

Kind of basis metal	Number of pores per dm^2
Steel sheet	150
Passivated steel sheet:	
Passivation time: 30 sec.	8
60 sec.	4
90 sec.	4

The considerably smaller porosity of nickel coatings on passivated steel sheets may be ascribed to the presence of an oxide layer between the basis metal and the nickel coating. The higher the porosity of the nickel coating, the greater is the corrosion of the basis metal (steel in this case) since favorable conditions for the formation of a galvanic cell with iron as the anode are thus created. On the basis of the porosity investigation, it was concluded that the resistance of the basis metal to the corrosion was increased when the basis metal was passivated before being subjected to nickel plating.

Nickel coatings on passivated steel sheets when dipped in 1% aqueous sodium sulphate solution are corroded more slowly than nickel coating deposited directly on clean steel sheets. This behavior cannot be explained simply by means of porosity but also by means of the corresponding potential values (Table 4).

TABLE 4

Potentials in 1% sodium sulphate solution

Steel sheet	Nickel sheet	Passivated steel sheet coated with nickel	Passivation time in sec			
			30	60	90	120
—0.197	—0.020	—0.094 (—0.003)	+0.049	0.073	0.122	0.218

Table 4 shows that the nickel coating behaves as a positive electrode with respect to the steel sheet. The potential of the nickel coating is more negative than the potential of the passivated steel sheet. In such a system, therefore, nickel behaves as an anode.

The anodic polarization of the nickel coating on passivated steel sheets results also in a change of the potential. In the course of time the potential of the nickel coating on passivated steel sheets becomes more and more positive (Table 5).

TABLE 5

Passivated steel sheets coated with nickel in 1% sodium sulphate solution

Potential measurement after standing in the above solution for (sec)	Potential V	Note
15	—0.0094	Passivation time
30	—0.081	90 sec.
45	—0.066	
60	—0.056	
75	—0.048	
90	—0.041	
105	—0.033	
120	—0.028	
135	—0.023	
150	—0.018	
165	—0.013	
180	—0.010	
195	—0.010	
210	—0.003	
225	—0.003	
240	—0.003	
255	—0.003	
270	—0.003	

In the cell:

Iron oxide (Na_2SO_4, H_2O) Ni

nickel behaves as a negative electrode which is anodically polarized and which is passivated in the presence of dissolved oxygen, whereby

the protective action of nickel coating is increased. In this case iron oxide acts as a layer of copper in the decorative nickel plating.

On account of its porosity and its more positive potential with respect to iron, in sodium sulphate solution, the layer of iron oxide alone has no protective action.

From the results obtained it may be concluded that in some cases iron oxide-nickel can be successfully applied for protection.

REFERENCES

1. Kadaner, L. I. and A. H. Masik. "Trudy 4-go soveshchaniĭa po elektrokimii (Proceedings of the Forth Conference on Electrochemistry) — Moskva: Izdatel'stvo Akademii nauk SSSR, 1959, p. 512.

2. Tavers, W. J. "Plating on Aluminum" — *Transactions of the Electrochemical Society* 75: 201, 1939.

COULOMETRIC DETERMINATION OF MANGANESE*

by

SRETEN N. MLADENOVIĆ and SLAVKA DELIBAŠIĆ

Neither the oxidation nor the reduction of manganous ions represent the sole process which takes place at platinum and other electrodes in aqueous solutions. Before and during the reduction of manganous ions, hydrogen ions are reduced at the cathode:

$$2\,H^+ + 2\,e \rightarrow H_2 \ldots e_o = \pm\,0.000\ V$$
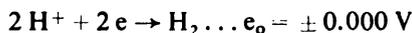
The oxidation products of manganous ions, namely manganic ion, manganese dioxide and permanganate can be reduced prior to manganous ions:

$$Mn^{3+} + e \rightarrow Mn^{2+} \ldots e_o = 1.51\ V$$

$$MnO_2 + 4\,H^+ + 2\,e \rightarrow Mn^{2+} + 2\,H_2O\ e_o = 1.24\ V$$

$$MnO_4^- + 8\,H^+ + 5\,e \rightarrow Mn^{2+} + 4\,H_2O\ e_o = 1.51\ V$$
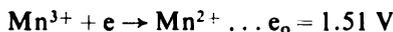
Oxygen, manganese dioxide, manganic ion and permanganate can be formed either individually or simultaneously at the anode, depending on the concentration of manganous ions, the concentration of sulphuric acid, the temperature of the solution and the current density.

It is impossible to recure in aqueous solutions conditions which would only give rise to the oxidation of manganous ions at the electrodes. It is not possible, therefore to carry out the coulometric titration of manganous ions neither at controlled potential nor at constant current strength.

The reaction which takes place at the platinum anode in slightly acid or neutral solution,

$$H_2O \rightarrow 2\,H^+ + 1/2\,O_2 + 2\,e \quad e_o = 1.23\ V$$

$$Mn^{2+} + 2\,H_2O \rightarrow MnO_2 + 4\,H^+ + 2e \quad e_o = 1.23\ V$$
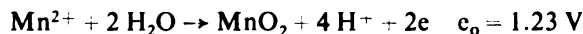
was used as the basis for the coulometric determination of manganous ions. The given equations show that the passage of the same amount of electricity which deposits manganese dioxide, gives rise to hydrogen

---

* Communicated at XXXIV International Congress of Industrial Chemistry Beograd, September 1963.

ions in an amount which is twice as great as that obtained by water oxidation. In the coulometric determination of manganous ions at constant current strength[1], during the time required for the quantitative separation of manganese dioxide, hydrogen ions are formed in the electrolyte in an amount which is greater than that obtained in water electrolysis. The increase of hydrogen ion concentration takes place in a definite proportion: during the exidation of 1 gram ion of manganous ions, the total hydrogen ion concentration increases for 4 gram equivalents.

In this indirect coulometric determination of manganous ions, the precipitation of manganese dioxide and the coulometric titration of hydrogen ions should be carried out with separate anode and cathode compartments. For better accuracy the electrolysis should be interrupted immediately after quantitative precipitation of manganese dioxide.

In our second procedure the time required for the quantitative separation of manganese dioxide may be exceeded; the separation should be carried out in two vessels connected with a bridge or a diaphram the current need not be constant. It is only important that the deposited manganese dioxide sticks fast (adheres well) to the anode.

During the electrolysis of aqueous solutions of manganous sulphate the following reactions take place at platinum electrodes: At the anode:

$$Mn^{2+} + 2 H_2O - 2 e \rightarrow MnO_2 + 4 H^+$$

$$2 H_2O - 4 e \rightarrow 4 H^+ + O_2$$

At the cathode:

$$6 H^+ + 6 e \rightarrow 3 H_2$$
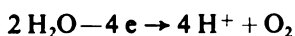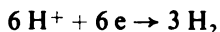
From these equations it may be seen that in cases when manganese dioxide is separated, the amount of hydrogen ions produced is greater than the amount of hydrogen evolved at the cathode; therefore, the acidity of the solution is increased. The increase of hydrogen ion concentration is equivalent to the amount of manganous ions.

The determination of manganous ions is not dependent on the time used for the separation of manganese dioxide since after quantitative precipitation of manganese dioxide only water is electrolyzed and the amount of acid remains unchanged.

In the indirect coulometric determination of manganous ions it is important that manganese dioxide is deposited in a form which adheres well to the anode. It was observed that at low current strength a well-adhering form of MnO_2 was deposited whereas at high current strength a deposit which stuck very poorly to the anode was obtained.

The dispersed particles of MnO_2 make the solution brown colored and in these brown colored solutions it is difficult to detect the end-point of the acid titration with methyl red. These facts can explain greater deviations of results in experiments in which manganese dioxide was precipitated at higher current strength (Table 2).

TABLE 1

Electrolyte for MnO₂ separation:
1 ml 0.1 M MnSO₄ + 1g Na₂SO₄ + 80 ml H₂O
Electrolyte for the coulometric titration of the acid:
Anolyte: Na₂SO₄ + H₂O
Catholyte: H₂SO₄ + Na₂SO₄ + H₂O + methyl red

Experiment No	MnO₂ — separation		Titration of the acid		Manganese		Error %
	Current strength (mA)	Time in min.	Current strength (mA)	Time in sec.	Taken mg	Found mg	
1	20	180	10	882	2.490	5.511	0.84
2	20	180	10	871	2.490	2.479	—0.44
3	20	120	10	876	2.497	2.495	—0.08
4	20	120	10	888	2.497	2.510	0.12
5	20	120	10	867	2.497	2.468	—1.16
6	20	60	10	878	2.497	2.499	0.08
7	20	60	10	868	2.497	2.471	—1.04
8	20	60	10	864	2.497	2.459	—1.52

TABLE 2

Electrolyte for MnO₂ separation:
1 ml 0.1 M MnSO₄ + 1 g Na₂SO₄ + 80 ml H₂O
Coulometric titration of the acid:
Anolyte: Na₂SO₄ + H₂O
Catholyte: H₂SI₄ + Na₂SO₄ + H₂O + methyl red

Experiment No	MnO₂ separation		Titration of the acid		Manganese		Error %
	Current strength (mA)	Time in min.	Current strength (mA)	Time in sec.	Taken mg	Found mg	
1	10	65	10	882	2.497	2.511	0.56
2	10	65	10	871	2.497	2.479	—0.72
3	10	65	10	876	2.497	2.493	—0.16
4	10	65	10	880	2.497	2.504	0.28
5	20	75	10	854	2.490	2.429	—2.50
6	20	75	10	866	2.490	2.465	—1.00
7	20	75	10	876	2.490	2.493	0.12
8	50	60	10	855	2.490	2.434	—2.24
9	50	60	10	874	2.490	2.488	—0.08
10	50	60	10	864	2.490	2.458	—1.24

In the determination of greater amounts of manganous ions a dispersed precipitate of MnO₂ is formed, and only a thin film of this precipitate adheres well to the anode. In this case, as in the separation of manganese dioxide at high current strength, the solution is brown

colored and an accurate determination of the titration end-point is almost impossible. Therefore, the errors in the determination of greater amounts of manganous ions are higher than in other experiments (Table 3).

TABLE 3

Electrolyte for MnO_2 separation:
1—4 ml 0.1 M $MnSO_4$ + lg Na_2SO_4 + 80 ml H_2O
Coulometric titration of the acid:
Anolyte: Na_2SO_4 + H_2O
Catholyte: H_2SO_4 + Na_2SO_4 + H_2O + methyl red

Experiment No	MnO_2 separation		Titration of the acid		Manganese		Error %
	Current strength (mA)	Time in min.	Current strength (mA)	Time in sec.	Taken mg	Found mg	
1	20	60	10	878	2.497	2.499	0.08
2	20	120	10	868	2.497	2.471	—1.04
3	20	120	10	888	2.497	2.510	0.12
4	20	65	10	1768	4.969	5.032	1.26
5	20	100	10	1759	4.969	5.006	0.74
6	20	90	10	1753	4.969	4.989	0.42
7	20	100	10	2661	7.459	7.572	1.51
8	20	100	10	2670	7.459	7.599	1.87
9	20	100	10	2700	7.459	7.684	3.01
10	20	100	10	3571	9.938	10.16	2.23
11	20	100	10	3550	9.938	10.10	1.63
12	20	100	10	3572	9.938	10.16	2.23

The accuracy of the indirect determination of manganous ions is increased when manganese dioxide is filtered off before the titration of the acid.

Sodium sulphate which is a constituent of the electrolyte used in the separation of manganese dioxide and the titration of the acid can affect the accuracy of manganous ions determination if it is contaminated with substances which, during electrolysis, can give rise to acid, or, when the electrolysis is carried out at high current densities when persulphate ions can be produced.

Data given in Tables 1, 2 and 3 show that optimal conditions for the indirect coulometric determination of manganous ions are the following:

Current strenth for the separation of MnO_2 — 10 mA
Time required for MnO_2 separation — 60 minutes
Amount of manganese — 1 to 3 mg.

The procedure involves two steps. In the first step manganese dioxide is deposited on the anode. In the second step, the catholyte is the electrolyte from the first step in which acid was produced in an amount equivalent to the deposited manganese dioxide. The electrolysis was carried out in a 150 ml glass vessel; the anode was a perforated platinum cylinder of 30 mm diameter and 50 mm height; the openings were of 1 mm diameter. The cathode was a spiral of platinum wire of 0.5 mm diameter whereas the diameter of the spiral was 6 mm.

The coulometric titration was carried out according to the previously published procedure.

The described indirect determination of manganous ions represents a further application of the method of indirect coulometric determinations founded by Tutundžić and Mladenović.

Institute of Physical Chemistry and
        Electrochemistry
    Faculty of Technology
        Beograd

REFERENCES

1. Mladenović, S. "Kulometrijsko odredjivanje mangano jona" (Coulometric Determination of Manganous Ion) – *Glasnik hemijskog društva* (Beograd): in press.
2. Tutundžić, P. S. and S. Mladenović. "Indirekte coulometrische Titration von Kathionen und Anionen" — *Analytica Chimica Acta* (Amsterdam): prepared for press.

STEREOCHEMISTRY OF THE NUCLEOPHILIC ADDITION OF ACETYLENE TO p-MENTHONE*

by

VUKIĆ M. MIĆOVIĆ, MILUTIN STEFANOVIĆ
and SLOBODAN A. MLADENOVIĆ

The addition of acetylene to p-menthone was first described by H. Ruppe et al[1,2]; recently it was reinvestigated by several authors[3,4,5]. H. Ruppe isolated only one reaction product 3-ethynyl-p-menthol, which he assumed to be a mixture of two stereoisomeric forms since the addition of acetylene to p-menthone, produces a new asymmettric C-atom in the 3-position. In fact, the isolated 3-ethynyl-p-menthol gave two acetates, one of which was crystalline and the other liquid. H. Ruppe carried out the ethynylation of p-menthone by passing acetylene into a boiling solution of p-menthone in the presence of sodium amide as condensing agent. All other authors [3,4,5] only varied the experimental conditions in order to obtain higher yields of 3-ethynyl-p-menthone and did not investigate the stereochemical relations of products obtained.

Extending our investigations on the ethynylation of alycyclic and heterocyclic ketones[6] we carried out the ethynylation of p-menthone. The reaction can give rise to two products:
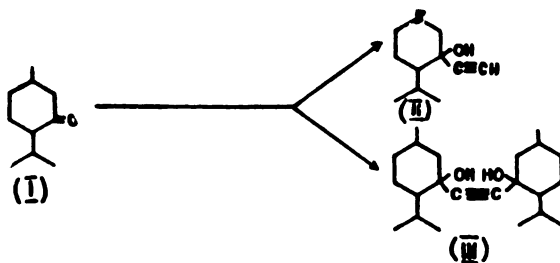
4

Although it was known that this reaction is stereospecific, the separation of isomeric 3-ethynyl-p-menthols (II) and bis(3-hydroxy--p-menthyl)-acetylene(III) was not effected and hence the configurations of isomeric forms were not determined. We have attacked this problem (the separation of stereoisomers and the determination of their configurations) since it offers the possibility of studing the stereochemical relations of acetylene glycols of similar type.

The ethynylation of (-)-menthone,* with only minor alterations, was carried out by the method of S. Chodroff and M. Dunkel[4]. Pure (-)-menthone, obtained by the oxidation of Merck's (-)-menthol, p.a. was used. In each experiment the purity of (-)menthone was checked chromatographically. Acetylene was passed into a toluene solution of (-)menthone containing potassium hydroxide, redistilled n-butanol and N,N-dimethylformamide; the molar ratio of components was (-)-menthone: toluene: Potassium hydroxide: n-butanol: N,N-dimethyl-formamide = 2 : 7.5 : 5 : 1 : 1. Following the method described in the experimental part we isolated two reaction products: 3-ethynyl--p-menthol(II) and bis(3-hydroxy-p-menthyl)-acetylene(III). The ratio of their yields depended upon the reaction temperature as given in Table 1.

TABLE 1

Experiment No	Temperature C°	Product II %	Product III %
1	—10	68.2	4.2
2	0	60.6	6.8
3	+20	45.3	19.2
4	+30	31.4	9.2
5	+110	22.2	5.3

Table 1 shows that the reaction is reversible and dependent on the reaction temperature, which is consistent with the reaction mechanism given by Gverdciteli and Barbajan[7,8]. According to these authors the intermediary products of the ethynylation reaction are the alcoholates of tertiary ethynyl carbinols and the glycolates of ditertiary acetylenic glycols. Similarly to all reversible reaction, the direction of this reaction is determined by the dissociation degree of the intermediary products. Since the dissociation constants of these products depend on their solubility in the reaction medium, and the solubility is proportional to the temperature of the reaction system, the weight ratio of the reaction products (II and III) depends on the reaction temperature.

The configurations of the reaction products were established in the following way.

_ _ ___ _ _ _

* Most experiments were performed simultaneously with DL and (-)-menthone. The ketonic component will be henceforth designated only as (-)-menthone.

3-Ethynyl-p-menthol(II) was identified by comparing its physical properties with those described in the literature and by interpreting its I.R. spectrum (v OH at 3350 cm^{-1}; $v — C = CH$ at 3280 cm^{-1}; no v C $= 0$ maxima). Its purity was checked by thin layer chromatography whereby a chrotogram containing two zones of proximate Rf-values was obtained showing that the isolated 3-ethyly-p-menthol was a mixture of two geometrical isomers. Qualitative estimation of spot intensities indicated an approximate ratio of isomer IIa (smaller Rf-value) to isomer IIb (greater Rf-value) to be 9 : 1*.

The obtained results show that the ethnylation of (-)-menthone is stereospecific since under given experimental conditions one of the two possible geometrical isomers is formed predominantly.

In compounds of this type the cyclohexane ring assumes the thermodynamically more stable convex ("Z") conformation and hence the isomers IIa and IIb should possess the following configurations and corresponding conformations:
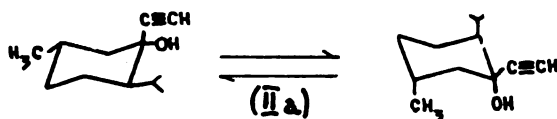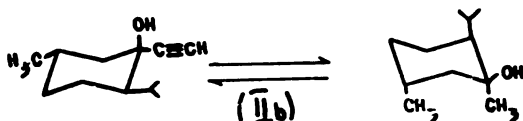
On account of the conversion of the cyclohexane ring each isomer is in equilibrium with its conformational isomer, in which the cyclohexane ring also assumes the convex ("Z") conformation but with the opposite orientation of substituents. Which conformational isomer will predominate in the reaction mixture depends mainly on the nature of the substituent itself.

From the chromatographic behavior of isomers IIa and IIb some conclusions about their configurations can be deduced. According to D. H. R. Barton[9] the geometrical isomer possessing equational polar groups is usually more strongly adsorbed than its corresponding axial isomer. Since the hydroxyl is more polar than the ethynyl group, the predominant isomer having a smaller R_1-value should possess the configuration IIa with the equatorial hydroxyl, methyl and isopropyl group respectively. The other isomer which travels further on the thin

---

* Separation of isomers by distillution was not successful even when a very efficient column was used.

** Designations a and e (for example eae) indicate the orientation of —CH$_3$, —C $\equiv$ CH and —CH(CH$_3$)$_2$ groups at C$_1$, C$_3$ and C$_4$.

4*

— layer chromatoplate should possess the configuration IIb with hydroxyl in the axial, and methyl and isopropyl group in the equatorial position.

The above data also permits some conclusions about the stereochemical course of menthone ethynylation to be drawn. The addition of nucleophillic acetilide anion to the (-)-menthone carbonyl group is determined by steric factors on one hand, and by the stability of the products obtained on the other. Although it is not possible to establish which of these two factors is more important in determining the stereochemical course of the reaction, it might be assumed that the axial addition of the acetilide anion predominates, whereby the isomer IIa is produced. The addition of the acetilide anion from the other side of the molecule gives rise to isomer IIb.

Similar results were obtained by J. N. Nazarov *et al*.[10,11] in the study of the stereochemistry of the nucleophillic addition of acetylene and hydrogen cyanide to 2-methylcyclohexanone. By means of spectral and chemical methods these authors established that predominantlly the isomer with an axially oriented entering substituent and equatorially oriented hydroxyl group, is produced, and the other isomer with oppositely oriented substituents is obtained in a much smaller quantity.

The obtained 3-ethynyl-p-menthol (II) mixture of isomers was used as the starting material for the synthesis of the γ-lactone of 3- -hydroxy-p-menthyl-propionic acid (V) according to the following reaction scheme:
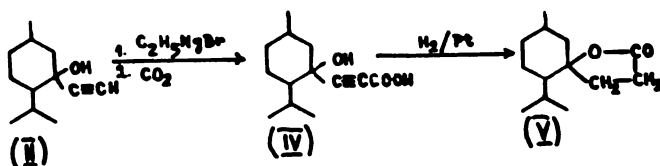
The carboxylation of 3-ethynyal-p-menthol (II) was carried out according to L. J. Haynes and E. R. H. Jones[12]. A benzene solution of 3-ethynyl- -p-menthol (II) was added dropwise to the benzene solution of ethyl magnezium bromide (1 mole) in the cold. When the reaction was over, the reaction mixture was transferred to an autoclave and treated with an excess of solid carbon dioxide. After the decomposition of the Grignard complex the usual way (3-hydroxy-p-methyl)-propiolic acid (IV) was isolated with a yield of 48%. Its structure was established by elementary analysis, infra-red spectrum (ν OH 3380 cm^{-1}; ν — C $\equiv$ C — disubstituted 2235 cm^{-1}; ν C = 0 (conjugated with acetylenic bond) 1715 cm^{-2}) and by analogy with already known reactions.

The hydrogenation of (3-hydroxy-p-menthyl)-propiolic acid (IV) in ethanol solution in the presence of Adam's catalyst resulted in the formation of the spirolactone (V) in a quantitative yield. The structure of the latter compound was deduced from its elementary micro-analysis and the infra-red spectrum (strong maxima for the lactone ν C = 0 at 1780 cm^{-1} and for the cyclohexane ring at 1455 cm^{-1}).

Since the starting substance for the synthesis of the γ-lactone of (3-hydroxy-p-menthyl)-propionic acid (V) was the mixture of isomeric 3-ethynyl-p-menthols, it was expected that the isolated spirolactone (V) would also be a mixture of geometrical isomers and this was proved by thinlayer chromatography.

The structure of the second reaction product obtained in the ethynylation of (-)-menthone, bis(3-hydroxy-p-menthyl)-acetylene (III) was also deduced from its elementary micro-analysis and the infra-red spectrum (IR exhibited only one maximum at 3380 cm^{-1} for v OH, whereas there was no maximum for $v — C \equiv C —$*. This glycol has already been synthetized by Ž. Jocić[13] by condensation of dibromo magnesium acetylene with (-)-menthone and the constants reported by Jocić are consistent with those we obtained for product III.

However we synthetized bis(3-hydroxy-p-menthyl)-acetylene (III) according to Inhofen and Weisermel[16] by condensing lithium derivate of 3-ethynyl-p-menthol (II) with s (-)-menthone. The infra-red spectrum obtained in this way was completely identical with the infra-red spectrum of bis(3-hydroxy-p-menthyl)-acetylene (III), obtained by direct ethynylation of (-)-menthone, whose structure was thus shown to be correct.

Since bis(3-hydroxy-p-menthyl)-acetylene (III) was synthetized by ethynylation of (-)-menthone in one step, in spite of the stereospecifity of the reaction product, was not homogenous but rather a mixture of geometrical isomers, a feature which had not previously been established for this or other acetylenic glycols. Consequently, neitheir had the stereochemistry of the acetylenic glycols of this type been studied until now.

From the models it may be concluded that bis(3-hydroxy-p-menthyl) acetylene (III) can exist in three stereoisomeric forms:

---
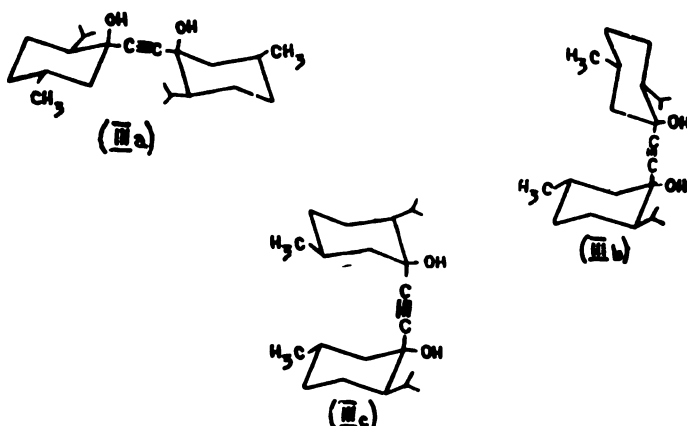
* The intensity of $v —C \equiv C—$ is the strongest in compounds in which it is terminal; the intensity decreases with movement of the $—C \equiv$ away from the end of the molecule[14]. In symmetrical compounds the acetylenic bond vibrates about the center of pseudo-symmetry and because of this is inactive in the infra-red[15].

a) isomer IIIa possessing both hydroxyl groups in axial position (with respect to the cyclohexane ring);

b) isomer IIIb possessing one axial and one equatorial hydroxyl and

c) isomer IIIc possessing both hydroxyl groups in equatorial position.

Each of these isomers, on account of the free rotation about —C—C ≡ C—C— system, can possess an endless number of conformations; however amongst these conformations some will be more stable than others and the models suggest some conclusions about the existence of these.

In order to establish how many isomeric glycols are formed in the ethynylation of (-)-menthone, we chromatographed bis(3-hydroxy-p-menthyl)-acetylene (III) on a column of silica gel and isolated three homogeneous crystalline isomers melting at 128°, 108° and 169°C with a weight ratio 4.5 : 4.5 : 1 (melting points and weigth ratio are given according to the order of elution*).

What is the configuration of the isolated isomers. Since the ethynylation of (-)-menthone yields approximately 90% of isomeric 3-ethynyl-p-menthol IIa (equatorial hydroxyl) and only 10% of isomer IIb (axial hydroxyl) it is likely that the isomer melting at 169°C which is isolated in the smallest amount possesses the configuration IIIa (both hydroxyl groups axial) whereas the other two configurations (IIIb and IIIc) belong to the isomers melting at 128°C and 108°C.

The configurations of isolated isomers of bis(3-hydroxy-p-menthyl)-acetylene were determined on the basis of hydrogenation and dehydration** reactions carried out according to the scheme on the p. 55.

Hydrogenation of all three isomers bis(3-hydroxy-p-menthyl-)-acetylene was carried out under the same strictly controlled conditions in ethanol solution in the presence of platinum as catalyst. It is known that the acetylenic glycols of this type can be catalytically hydrogenated to saturated glycols only at high pressures and at elevated temperatures[17]; since these conditions are likely to cause isomerization of configurations, the isomeric bis(3-hydroxy-p-menthyl)-acetylenes were selectively hydrogenated to their olefinic analogues.***

Under these conditions the isomer of m. p. 128°C was hydrogenated quickest, yielding a substance melting at 122°C whose elemen-

---

* Each of the isolated isomers showed depression of m.p. when in admixture with other isomers.

** Olefinic glycols obtained by selective hydrogenation of isomeric bis(3-hydroxy-p-menthyl)-acetylenes were dehydrated. It is likely that during the dehydrogenation, which was performed under very mild conditions, no isomerization took place, so that the results may also be used for the determination of the configuration of isomeric bis(3-hydroxy-p-menthyl)-acetylene II.

*** The most effective catalyst for the hydrogenation of the acetylenic to olefinic bond is Lindlar's catalyst[19]. However, since the acetylenic bond of ditertiary acetylenic glycols is sterically hindered, good results can be obtained in the presence of platinum as catalyst as well.
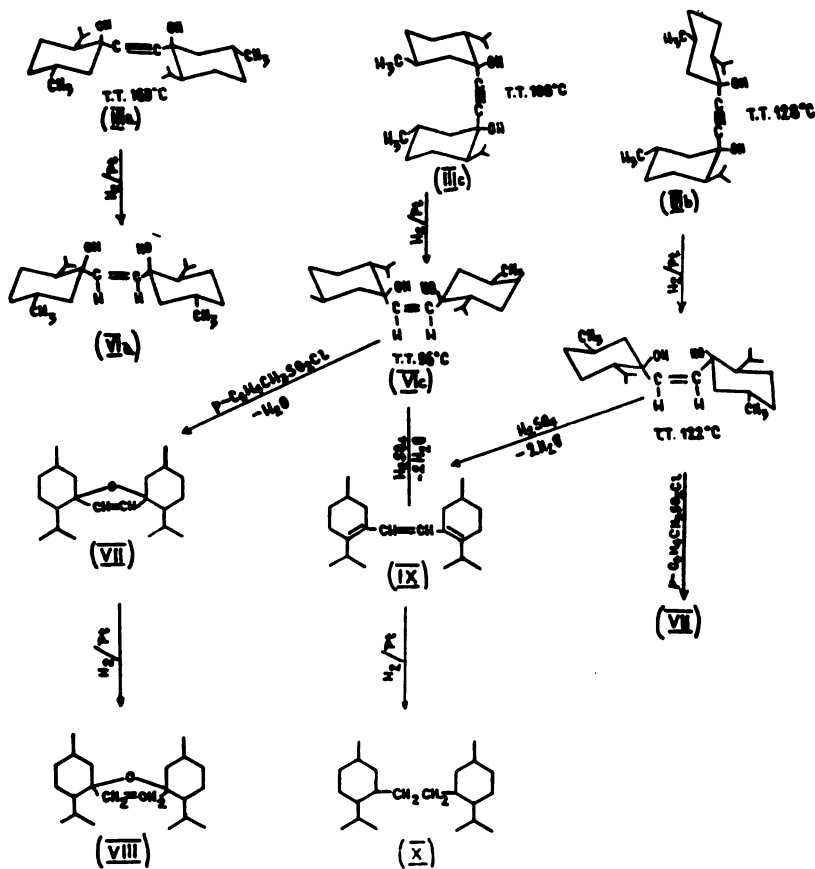
tary analysis and infra-red spectrum corresponded to the olefinic glycol (VIb)*. The isomer of m. p. 108°C was hydrogenated more slowly so that the time required for the selective hydrogenation of this acetylenic bond was two times longer, in this case the other isomer of sym. bis(3--hydroxy-p-menthyl)-ethylene (VIc) (crystalline substance, m. p. 96°) was obtained, its structure was also determined by elementary analysis and infra-red spectrum. The third isomer, m. p. 169°C could not be hydrogenated to the corresponding olefinic glycol (VIa).

---

* This and the other isomer of sym. bis(3-hydroxy-p-menthyl) - ethylene were assumed to possess *cis* configuration since it is known that the catalytic hydrogenation of acetylenes yields only *cis* olefins.

Hydrogenation of ditertiary acetylenic glycols has so far been little investigated[18] so that the above results do not offer a reliable criterion for the determination of the configuration of isolated isomeric acetylenic glycols (III), but some conclusions about their configurations might be drawn on the basis of their different behaviour in the course of hydrogenation.

The isomer of m. p. 169°C which cannot be hydrogenated is likely to have both hydroxyls axially oriented (configuration IIIa); the model of isomer IIIa shows that its acetylenic triple bond is under the greatest steric hindrance, and the approach of hydrogen from the active catalyst surface is rendered difficult. On the other hand, the models suggest that the most stable conformation of this molecule is the one in which the two axial hydroxyl groups are "parallel".

Any rotation about the —C—C $\equiv$ C—C system augments the steric hindrance and therefore there is no conformation which would be, from the stereochemical point of view, more favourable for hydrogenation. Moreover, the high melting point of this isomer (with respect to the other two) also indicates the presence of a system in which free rotation is rendered difficult.

It has already been said that this isomer is the most strongly adsorbed by silica gel and this phenomenon is not consistent with theory since isomers with axial polar groups (hydroxyls in this case) are known to be less strongly held by the absorbent[9]. However, the "abnormal" chromatographic behaviour of this isomer can be easily explained by the fact that its predominent conformation is the one with "parallel" hydroxyl groups in which the orientation of hydroxyls is very favourable for bonding with moleculs of the adsorbent and hence, this isomer is most strongly adsorbed.

The configurations of isomers melting at 108°C and 128°C could not be determined purely on the basis of their behaviour during hydrogenation; therefore, we attemped the dehydration of their olefinic analogues by means of sulfuric acid and p-toluenesulfonyl as shown in the given scheme (p. 55.)

The isomer of sym. bis(3-hydroxy-p-menthyl)-ethylene (VIc) melting at 96°C could not be dehydrated by means of sulfuric acid after Dupant[20], besides some resinous products the starting substance was always isolated. The dehydration of this isomer by means of p-toluenesulfonyl chloride in pyridine solution yielded the oxide compound VII which was not isolated but further hydrogenated in ethanol solution in the presence of platinum as catalyst to bis(-p-menthyl)—α, α'—tetrahydrofuran (VIII).

The structure of the new compound was determined by elementary analysis and infra-red spectrum (adsorption characteristic for cyclic five-membered ethers at 1096 cm^{-1}) .

The other isomer of m. p. 122°C (VIb) behaved quite differently: it could be dehydrated by means of p-toluenesulfonyl chloride and dehydration with 40% sulfuric acid gave the conjugated triene IX.

The latter compound was not isolated but was further hydrogenated in ethanolic solution in the presence of platinum as catalyst to symmetrical p-dimenthyl-ethane (X). The structure of this hydrocarbon unknown until now, was also determined by elementary analysis and the infra-red spectrum.

On the basis of these results and also from the models of these two isomers it may be concluded that the isomer of m. p. 96°C which is dehydrated to cyclic ethers by means of p-toluenesulfonyl chloride has both hydroxyl groups equatorially oriented (VIc) since this configuration, on account of the proximity of hydroxyl groups, is very favourable for the formation of the cyclic ethers VII. On the other hand, this reaction is also favoured by equatorial hydroxyls as equatorial alcohols are not easily dehydrated to ethylenic derivatives.

The isomer of m. p. 122°C is assumed to possess the third configuration with one axial and one equatorial hydroxyl (VIb) which agrees with the experimental data. From Dreiding's model of this isomer it may be seen that the distance between the hydroxyl groups is greater, so that the formation of furan derivative by dehydration is not to be expected, moreover the axial orientation of one hydroxyl group favours the formation of conjugated triene IX. On the basis of all the results obtained in the hydrogenation of isomeric bis(3-hydroxy-p-menthyl)-acetylenes (III) and in the dehydration of isomeric sym. bis(-hydroxy-p-menthyl)-acetylene (VI), the isolated isomers of bis(3-hydroxy-p-menthyl)-acetylene (III) were assumed to possess the following configurations:

isomer of m.p. 169°C has both hydroxyl groups axially oriented (IIIa);

isomer of m.p. 128°C has one axial and one equatorial hydroxyl group (IIIb); and

isomer of m.p. 108°C has both hydroxyl groups in the equatorial position*.

Finally the following conclusions were drown about the sterecchemical course of the second phase of menthone ethynylation in which 3-ethynyl-p-menthyl (II) is added to menthone. The weight ratio of isomers bis(3-hydroxy-p-menthyl)-acetylenes (IIIa, IIIb and IIIc) obtained in the reaction of (-)-menthone and 3-ethynyl-p-menthol, and the fact that the approximate composition of isomeric 3-ethynyl-p-menthols used in this reaction was 9 : 1 (in favour of the isomer with equatorial hydroxyls) indicate that this reaction might be assumed to proceed as follows:

---

* IR-spectra were used for the determination of the configuration of the acetylenic glycol III. It has been established that the spectra of isomeric glycols differ only in the 4000—3000 cm^{-1} region (see experimental). However, since the maxima of the hydroxyl group itn this spectral region originate from the vibration of the bond between oxygen and hydrogen, these data are not reliable for the determination of the orientation of hydroxyl groups. Infra-red spectroscopy of ditertiary acetylenic glycols has so far been studied only by W. Otting.[15]. Unfortunately, he did not use pure isomeric glycols so that his results could not be used.

a) The addition of the complex acetylide anion A to the carbonyl group of (-)-menthone takes place equally from both the equatorial and axial side so that a mixture of isomers IIIb and IIIc is obtained.

b) the equatorial addition of the acetylide anion B takes place predominantly, giving the isomer with IIIa configuration
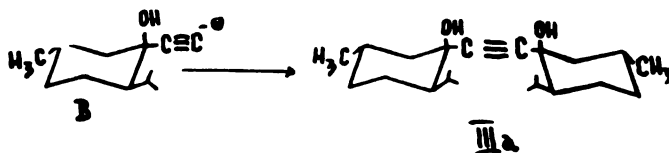
Further investigations in this field will involve the ethynylation of carbomenthone and pulegone.

EXPERIMENTAL

Melting points were determined in an open capillary tube and are not corrected. Infra-red spectra were recorded on a Perkin-Elmer spectrophotometer, Infracord Model-137. The spectra of solids were taken by means of the potassium bromide technique and those of liquids in carbon tetrachloride solution.

For column chromatography A. G. Merck silica gel was used. Thin-layer chromatography was carried out with A. G. Merck "Kieselgel G." as adosrbent; chromatoplates were developed with a mixture of cyclohenaxane and ethylacetate (8 : 2), and detection was performed with 20% solution of $SbCl_5$ in carbon tetrachloride. In some cases iodine vapor was used. Refractive indexes were determined with an ABBe refractometer (Carl Zeiss-Jena).

Isolated oily products were purified by means of short-path distillation, in high vacuo, using standard tubes.

Ethynylation of (-)-menthone

This reaction was carried out by the method of S. Chodorff and M. Dunkel[4]. Menthone, b. p. 99—100°C/18 mm Hg, was used; its purity was chacked by thin-layer chromatography.

Granulated potassium hydroxide (140.3 g; 2.5 moles), dried toluene (299.4 g 3.25 moles) and redistilled n-butanol (37.1 g; 0.5 mole) were placed in a four-necked 1.1 round-bottomed flask, fitted with a mercury-sealed mechanical stirrer, reflux condenser and an inlet tube for acetylene. The flask was dipped in an oil-bath, and the reaction mixture was left to reflux for half an hour. The oil-bath was then removed, and the stirred reaction mixture allowed to cool to room temperature; then, it was

further cooled to —10°C by dipping the flask into an ice-salt bath. FAfter the addition of N,N-domethylamide (36.6 g; 0.5 mole) purified, dry acetylene was passed into the reaction mixture and simultaneously menthone (154.3 g; 1 mole) was added via a separatory funnel at such a rate that the addition was completed in one hour. Acetylene was passed into the reaction mixture for an additional 15 minutes, and then cold water (500 ml) was carefully added to the reaction mixture. The organic layer was separated and treated with carbon dioxide. If necessary, precipitated calcium carbonate was filtered off, and the filtrate was dried over anhydrous magnesium sulphate. The solvent was removed by distillation under reduced pressure and the residue was fractionated with a Widmar column *in vacuo* (10 mm Hg); the following fractions were obtained:

fraction I, b.p. 91—96°C	13.9 g
fraction II, b.p. 97—102°C	6.6 g
fraction III, b.p. 105—107°C	123.0 g
residue (in the flask)	10.2 g

On the basis of physical constants it was established that fraction I consisted of unreacted (—)-menthone ($n_D^{20°} = 1.4503$; IR-spectrum: $v_{max} = 1710$ and 1450 cm^{-1}). Fraction II was not homogeneous and contained in addition to carbinol II a small amount of unreacted ketone. Fraction III, b.p. 105—107°C/10 mm Hg, was pure 3-ethynyl-p-menthol (II). The yield was 68.2% calculated to (—)-menthone); $n_D^{20°} = 1.4726$ (lit. $n_D^{20°} = 1.4718$); IR-spectrum: $v_{max} = 3350$ (—OH group) and 3280 cm^{-1} (—C ≡ C— group).

The purity of 3-ethynyl-p-menthol (II) was checked by thin-layer chromatography. The chromatogram contained two zones of proximate R_f-values indicating the presence of two isomeric carbinols, IIa and IIb. Quantitative chromatographic separation of isomers was not effected on account of the small difference in their polarities.

The residual brown-colored oil (10.2 g) was left overnight in the refrigerator (it became more viscous) and then tritrated with petroleum-ether. The separated white crystals were filtered off and recrystallized from n-hexane yielding bis(3-hydroxy--p-menthyl)-acetylene (III) (7.0 g; 4.2%); m.p. 104—105°C (lit. 103—104°C); IR-spectrum: $v_{max} = 3380$ cm^{-1} (—OH group). By thin-layer chromatography this product was proved to be a mixture of isomers (IIIa, IIIb, IIIc).

Ethynylation of (-)-menthone was repeated several times, the reaction being carried out at various temperatures (from —10° to +110°C). The weight ratio of the reaction products is given in Table 2.

Synthesis of γ-lactone of (3-hydroxy-p-menthyl)-propionic acid (V)

Preparation of ethyl magnesium bromide. Magnesium turnings (12.5 g, 0.52 gram atom), anhydrous ether (50 ml) and some ml of 1 : 1 ethereal solution of freshly distilled ethyl bromide were placed in a three-necked 500 ml round-bottomed flask fitted with a mercury sealed stirrer, reflux condenser (with calcium chloride tube), and separatory funnel. After the beginning of the reaction, ethyl bromide (54.5 g; 0.5 mole) dissolved in anhydrous ether was added from the funnel to the stirred reaction mixture at such a rate that the boiling of ether was kept constant. After the addition of ethyl bromide, the stirring was continued for a further one hour at room temperature.

Carboxylation of 3-ethynyl-p-menthol[12]. Ethereal solution of ethyl magnesium bromide was heated to remove the excess of ether and simultaneously anhydrous benzine (100 ml; dried over sodium) was added from the separatory funnel. The reaction mixture was then cooled to —10°C and 3-ethynyl-p-menthol (45.1 g; 0.25 mole) was added slowly so that the addition took one hour and a half. After the addition was complete, the icebath was replaced by an oil-bath, and the reaction mixture refluxed till the end of the reaction. On cooling, the content of the flask was transferred into a steel autoclave of 1 l. A large excess of carbon dioxide (about 200 g) was added as quickly as possible, the autoclave was closed and shaken for 24 hours at room temperature. The complex obtained was hydrolized cold (0°C)

with a calculated amount of 15% sulphuric acid plus an excess of 20%. When the initial foaming of the reaction mixture had ceased, the aequeous solution was saturated with sodium chloride and extracted with ether. The ethereal solution was treated with sodium bicarbonate solution and the layers were separated; the bicarbonate layer was again extracted with ether in order to remove nonacid products; it was then acidified with 15% sulphuric acid, saturated with sodium chloride and extracted with ether. The ethereal solution was dried with anhydrous sodium sulphate, filtered and ether was removed by distillation. The residual dark oil (31.4 g) was left in the refrigerator for several hours and then was tritrated with petroleum-ether; the deposited white crystals were filtered off and recrystallized from benzene. The yield of (3-hydroxy-p-menthyl)-propionic acid (IV) was 48% (26.9 g); m.p. 174°C; IR- -spectrum $v_{max} = 3380$ (—OH group), 2235 (—C $=$ C—) and 17L5 cm^{-1} (—COOH group).

Analysis:

Calculated for $C_{13}H_{20}O_3$ (224.29)	C 69.61%;	H 8.99%
Found	C 69.50%;	H 8.93%

Preparation of γ-lactone of (3-hydroxy-p-menthyl)-propionic acid (V). To a solution of (3-hydroxy-p-menthyl)-propionic acid (IV) (11.2 g; 0.05 mole) in ethanol (100 ml), Adam's catalyst (PtO_2, 200 mg) was added. The reaction mixture was hydrogenated under atmospheric pressure in the usual way. On absorption of 2 moles of hydrogen (2.24l; hydrogenation took a few minutes) the reaction mixture was filtered, ethanol was removed by distillation and the residual oil extracted with ether. Ethereal solution was dried with anhydrous magnesium sulphate, ether was removed by distillation and the residue distilled in vacuo furnishing γ-lactone (V) (10.3 g; 98%); b.p. 165°C/12 mm Hg; $n_D^{20°} = 1.4799$; IR-spectrum: $v_{max} = 1780$ (—O—CO— group) and 1455 cm^{-1} (cyclohexane ring). Further purification of the spirolactone V was effected by short-path distillation in high vacuum.

Analysis:

Calculated for $C_{13}H_{22}O_2$ (210.31)	C 74.24%;	H 10.54%
Found	C 74.11%;	H 10.53%

According to thin-layer chromatography the spirolactone V was not homogeneous but consisted of two isomers (the lower zone on the chromatogram was more intense).

Synthesis of bis(3-hydroxy-p-menthyl)-acetylene (III)
according to Inhoffen and Weisermel[16]

Preparation of lithium methyl[21]. Metallic lithium (4.3 g; 0.62 gram atom; previously pealed and cut in about 200 pieces) and absolute ether (60 ml) were placed in a three-necked roundbottomed flask (350 ml) fitted with a mercury sealed mechanical stirrer, reflux condenser (protected from moisture with a calcium chloride tube) and a separatory funnel. A solution of freshly distilled methyl iodide (43.0 g; 0.31 mole) was placed in the separatory funnel and 40 drops of this solution were added in order to start the reaction. (If no reaction occurs, the reaction mixture is slightly warmed for some minutes). The addition of ethereal methyl iodide solution was continued at such a rate that the ether was kept boiling. After 30—40 minutes the addition was complete and the reaction mixture was stirred at room temperature for one hour. Then it was diluted with ether and left aside for some minutes; the deposited lithium iodide formed in the reaction was filtered off as quickly as possible, and the dark violet ethereal filtrate containing lithium methyl (0.31 mole) was kept in a dark and cold place. Before use, the amount of reactive lithium in lithium methyl solution was determined titrimetrically.

Condensation of lithium derivative of 3-ethynyl-p-menthol with (-)-menthone. A solution of 3-ethynyl-p-menthol (22.6 g; 0.125 mole) in absolute ether (50 ml) was placed in a four-necked roundbottomed flask (1000 ml) fitted with a mechanical stirrer, reflux condenser (protected from moisture), separatory funnel and gas inlet tube. Dry nitrogen was passed into the stirred reaction mixture which was allowed to cool to—10°C (ice-bath) and then ethereal solution of lithium methyl (0.31 mole) was added from the separatory funnel at such a rate that its addition took 30 minutes.

Then the ice-bath was replaced by a water-bath and the reaction mixture was refluxed for 40 minutes. Without interrupting the heating of the reaction mixture a solution of (-)-menthone (19.3 g; 0.125 mole) in absolute ether (50 ml) was added slowly in the course of 30 minutes, and the reaction mixture heated for an additional three hours. The water-bath was then replaced by an ice-bath and a calculated amount of saturated ammonium chloride solution was added. The content of the flask was transferred to a separatory funnel, the layers were separated and the organic layer washed with water until neutral to lithmus. After drying with anhydrous magnesium sulphate, the ethereal solution was filtered; ether was removed by distillation under reduced pressure and the residue was fractionated in vacuo yielding unchanged menthone (3.9 g; 20%) and 3-ethynyl-p-menthol (4.1 g; 18.1°,). The nondistillable residue (31.2 g) was kept for several hours in the refrigerator and then was tritrated with petroleum-ether furnishing white crystals which were filtered off and recrystallized from n-hexane. The yield of bis(3-hydroxy-p-menthyl)-acetylene (III) was 56.2%, (23.4 g); m.p. 105—106°C; IR spectrum: $v_{max} = 3380$ cm $^{-1}$ (—OH group).

This product showed no melting point depression in admixture with bis(3--hydroxy-p-menthyl)-acetylene, synthesized by direct ethynylation of (-)-menthone; its IR-spectrum was identical with the spectrum of glycol III, synthesized from acetylene and (-)-menthone.

Chromatographic separation of isomeric bis(3-hydroxy-p-menthyl)-acetylenes

A mixture of stereoisomeric acetylenic glycols (IIIa, IIIb, IIIc) (1g), m.p. 104—105°C, was dissolved in cyclohexane (10 ml) and chromatographed on a column (height 80 cm; diameter = 1.5 cm) of silica gel (A. G. Merck). The elution was effected first with pure cyclohexane and then with a mixture of cyclohexane and ethyl acetate whereby the amount of ethyl acetate in the mixture was gradually incresed. Fractions of 5 ml were collected. After the elution of two less polar isomers, the third isomer was eluted with pure ethyl acetate. The results of chromatographic separation are given in Table 2.

TABLE 2

Fractions	Eluent	Volume of eluent in ml	Weight in g	M. P.	Isomer
1—18	Cyclohexane	90	—	—	—
19—36	Cyclohexane + 2% ethyl acetate	90	0.41	128°	IIIb
37—44	— " —	40	—	—	—
45—54	Cyclohexane + 5% ethyl acetate	100	0.43	108°	IIIc
54—60	— " —	35	—	—	—
61 — etc	Ethyl acetate	—	0.09	169°	IIIa

After separation, the isomeric acetylenic glycols (IIIa, IIIb, IIIc) had following constants:

a) Isomer IIIa: m.p. 169°C; IR-spectrum: $v_{max} = 3220$ cm $^{-1}$ (—OH group).
Analysis:
Calculated for $C_{22}H_{38}O_2$ (334.52)   C 78.98%; H 11.45%
Found   C 79.01%; H 11.18%
b) Isomer IIIb: m.p. 128-C; IR-spectrum: $v_{max} = 3570$ and 3400 cm$_{-1}$ (—OH group)
Analysis:
Calculated for $C_{22}H_{38}O_2$ (334.52)   C 78.98%; H 11.45%
Found   C 78.74%; H 11.71%
c) Isomer IIIc: m.p. 108°C; IR-spectrum: $v_{max} = 3350$ cm $^{-1}$ (—OH group)
Calculated for $C_{22}H_{38}O_2$ (334.52)   C 78.98%; H 11.45%
Found   C 78.94%; H 11.36%
Each isolated isomer showed depression when the melting point was determined in admixture with either of the other two.

Hydrogenation of bis(3-hydroxy-p-menthyl)-acetylene

a) *Isomer of m.p.* 128°C (IIIb). To a solution of acetylenic glycol IIIb (335 mg; 0.001 mole) in ethanol (30 ml) Adam's catalyst was added (PtO$_2$; 30 mg) and the reaction mixture was hydrogenated under atmospheric pressure. After the absorption of a calculated amount of hydrogen (22.41; 0.001 mole) hydrogenation was interrupted, the catalyst was filtered off and ethanol was removed under reduced pressure. The residual oil was taken up in ether, the ethereal solution dried with magnesium sulphate, filtered and ether removed in vacuo. The colorless oil obtained crystallized on standing in a refrigerator. Recrystallization from n-hexane yielded sym. bis(3--hydroxy-p-menthyl)-ethylene (VIb) (250 mg), m. p. 122°C. IR spectrum: $v_{max} = 3380$ and 3220 cm^{-1} (—OH group).

Analysis:

Calculated for C$_{22}$H$_{40}$O$_2$ (336.54)	C 78.51%; H 11.98%
Found	C 78.80%; H 12.28%

b) *Isomer of m.p.* 180°C (IIIc). Selective reduction of this isomer was caried out as described for IIIb. By using 335 mg (0.001 mole) of acetylenic glycol IIIc and 30 mg of Adam's catalyst we isolated 260 mg of sym. bis(3-hydroxy-p-mentyl)-ethylene (VIc), m.p. 96°C. The isolation was effected in the usual way. IR spectrum $v_{max} = 3220$ cm^{-1} (—OH group).

Analysis:

Calculated for C$_{22}$H$_{40}$O$_2$	C 78.51%; H 11.98%
Found	C 78.38%; H 11.79%

c) *Isomer of m.p.* 169°C (IIIa). The hydrogenation of this isomer was carried out as described for IIIb and IIIc. However, no hydrogenation took place and the starting acetylenic glycol IIIc was isolated.

Dehydration of sym. bis (3-hydroxy-p-menthyl)-ethylene (VI) by means of sulphuric acid [20]

a) *Isomer of* m.p. 122°C (VIb). In a round-bottomed flask (25 ml) fitted with a reflux condenser thylenic glycol VIb (220 mg) and 40% sulphuric acid (5 ml) were placed. The flask was heated at 120°C in an oil-bath for 4 hours. Then the reaction mixture was cooled to —10°C, neutralized with saturated sodium bicarbonate solution, transferred to a separatory funnel and extracted with ether. The ethereal solution was washed with water until neutral to lithmus, dried with magnesium sulphate, filtered, and ether removed by distillation. The residual oil (unsaturated hydrocarbon IX) was taken up in ethanol (30 ml), the solution was transferred to a long-necked flask (100 ml) and after addition of Adam's catalyst (30 mg) it was hydrogenated under atmospheric pressure. When the absorption of hydrogen ceased, the reaction mixture was filtered and worked up in the usual way. The oil obtained was chromatographed on a column of silica gel, whereby the cyclohexane fraction furnished sym. p-dimenthyl ethane (X) (160 mg). This hydrocarbon was purified by distillation in high vacuum, b.p. 150°/1 mm Hg. IR-spectrum: $v_{max} = 1455$ cm^{-1} (cyclohexane ring; no bands characteristic for vibrations of hydroxyl group and single C—O bond were observed).

Analysis:

Calculated for C$_{22}$H$_{42}$ (306.56)	C 86.19%; H 13.81%
Found	C 86.22%; H 12.36%

b) *Isomer of* m.p. 96°C (VIc). This isomer could not be dehydrated under the experimental conditions given above. Attempts to effect its dehydration by means of sulphuric acid of a higher concentration (up to 80%) were also unsuccessful (product became resinous).

*Dehydration of sym. bis(3-hydroxy-p-menthyl)-ethylene (VI) by
means of p-toluenesulphonyl chloride*

a) *Isomer of* m.p. 86°C (VIc). p-Toluenesulphonyl chloride (0.2 g) was added
to a solution of isomer VIc (200 mg) in pyridine, placed in a round-bottomed flask
of 25 ml. The flask was closed and left to stand for 24 hours at room temperature.
Then it was connected with a reflux condenser and the reaction mixture was heated
in an oil-bath at 110—120°C for 15 minutes. On cooling, the content of the flask
was poured into a calculated amount of ice-cold 3% hydrochloric acid and extracted
with ether. The ethereal layer was successively washed with 3% hydrochloric acid
(three times), saturated sodium bicarbonate solution (until neutral reaction) and water;
then it was dried with anhydrous magnesium sulphate, filtered and ether removed
by distillation. The residual oil (VII) was taken up in ethanol (30 ml), Adam's catalyst
(30 mg) was added and the mixture was hydrogenated under atmospheric pressure
in the usual way. When the absorption of hydrogen ceased, the catalyst was filtered
off, and the solution worked up in the usual way furnishing bis(3-p-menthyl)-α,α'-
-tetrahydrofuran (VIII), (140 mg); b.p. about 160°C/1 mm Hg; IR-spectrum:
$v_{max} = 1096$ cm^{-1} (characteristic band for five-membered cyclic ethers).

Analysis:

Calculated for $C_{22}H_{40}O$ (320.54)   C 82.43%; H 12.58%

Found   C 82.44%; H 12.16%

b) *Isomer of* m.p. 122°C (VIb). Dehydration of this isomer by means of p-tolue-
nesulphonyl chloride in pyridine solution always yielded the starting olefinic glycol
VIb.

ACKNOWLEDGEMENT

REFERENCES

1. Rupe, H. and A. Gassman. "Aldehyde aus Acetylen-carbinolen. 1. Methyl-4-
   -isopropyl-cyclohexyliden-3-acetaldehyd" — *Helvetica Chimica Acta* (Basel)
   12: 193—205, 1929.

2. Rupe, H. and A. Gassman. "Die Umlagerung von Acetylen-carbinolen. Über
   (d) Isomenthan und (l) Menthan" — *Helvetica Chimica Acta* (Basel) 17:
   283—285, 1934.

3. Papa, D., F. J. Viliani and H. F. Ginsberg. "A New Class of Hypnotic: Unsa-
   turated Carbinols" — *Archives of Biochemistry and Biophysics* 33: 482—483,
   1951.

4. Chodroff, S. and M. Dunkel. "Acetylenic Alcohols" — *U. S. Patent* No 2, 919, 281

5. Kawaga, M. "Rearrangement of Cyclic Ethynylcarbinols. III" — *Chemical and
   Farmaceutical Bulletin* (Tokyo) 9: 391—403, 1961, cited in: *Chemical Abstracts*
   55: 24808—34810.

6. Mićović, V. M., S. Mladenović and M. Stefanović. "Reakcija tropinona s aceti-
   lenom (Reaction of Tropinone with Acetylene) — *Glasnik Hemijskog Društva*
   (Beograd) 28: 285—290, 1963.

7. Gverdynteli, M. I. and T. Sh. Mikadze. "K voprosu o mekhanizme reaktsii Favorskogo" (On the Mechanism of the Favorsky Reaction) — *Doklady Akademii Nauk SSSR* (Moskva) 89: 861—864, 1953.

8. Babajan, A., B. Akopjan and R. Gjuli-Kovčjan. "Die Darstellung der Acetylen--glykole" — *Journal Chimie General* 9: 1631—1632, (cited in: *Chemisches Zentralblatt* 1: 695, 1940).

9. Barton, D. H. R. "The Conformation of the Steroid Nucleus" — *Experientia* (Basel) 6: 316—320, 1950.

10. Nazarov, I. N., A. B. Kamernitskii and A. A. Akhrem. "Prosteishie analogi kortikosteroidov. I. Stereokhemie tsiangidrinogo i atsetilenogo sinteza. Konfiguratsii l-tsiano-2-etinil-2-metiltsiklokhesanov-l" (Simple Analogs of Corticosteroids. I. Stereochemistry of Cyanhydrin and the Tethynylation Reaction Configuration of l-cyano-1-ethynyl-2-methyl-cyclohexanol-1) — *Zhurnal Obshchei Khimii* (Moskva) 28: 1458—1468, 1958.

11. Bautev, M. J., A. A. Akhiem, A. D. Matveeva, A. B. Kamrnitskii and I. N. Nazarov. "Opticheskoe issledovanie konformatsii nekatorikh gem. zameshen'-nikh tsiklogeksanov" (Optical Investigation of the Configurations of Some Chemical Mixtures of Cyclohexans) — *Doklady Akademii Nauk SSSR* (Moskva) 120: 779—786, 1958.

12. Haynes, L. J., and E. R. H. Jenes. "Researches on Acetylenic Compounds. V. α, b-Acetylenic Hydroxy-Acid" — *Journal of the Chemical Society* 1: 503—506, 1946.

13. Totsin, Zh. I. "O atsetilenmagnievykh soedeniakh. Novyi obshii sposob polu-cheniia apirtov s atsetilenskogo sviaeiu" (On Acetylene-magnesium Compounds. A New General Method for the Preparation of Alcohols with Acetylenic Bond) — *Zhurnal russkogo fiziko-khimicheskogo obshchestva* (Moskva) 34: 100—107, 1902.

14. Wetiz, J. H. and F. A. Miller. "The Infra-Red Spectra of a Number of Isomeric Normal Acetylenic Compounds" — *Journal of the American Chemical Society* (Easton) 71: 3441—3444, 1949.

15. Otting, W. Über Kumulene VIı: Die Ultrarot Spectren einiger Kumulene und Acetylenglykole" — *Chemische Berichte* (Weinheim) 87: 611—624, 1954.

16. Inhoffen, H. and K. Weissermel. "Studien in der Vitamin D-Reihe II. Partial-synthese des iso-Tachysterin-methyläthers" — *Chemische Berichte* (Weinheim) 87: 187—193, 1954.

17. Reppe, W. "Äthynylierung" — *Annalen der Chemie* (Darmstadt) 1—224, 1955.

18. Zalkind, S. and J. M. Gverdtsiteli. "The Addition of Hydrogen to Acetylenic Compounds XXXI. Catalytic Hydrogenation of Acetylene γ-Glycols Contai-ning Cyclopentyl Radicals" — *Journal of General Chemistry of the USSR* 9: 855—862, 1939; cited in: *Chemical Abstracts* 34: 387, 1940.

19. Lindlar, H. "Ein neuer Katalysator für selektive Hydrierung" — *Helvetica Chimica Acta* (Basel) 35: 446—450, 1952.

20. Dupont, M. G. "Recherches sur les γ-glycols acetyleniques et sur les cetohydro-furynes qui en derivent" — *Annales de chimie et de physique* (Paris) 30: 485—588, 1913.

21. Gilman, H., E. A. Zoellner and W. M. Selby. "The Yields of Some Organo-lithium Compounds by the Improved Procedure" — *Journal of the American Chemical Society* (Easton) 55: 1252—1258, 1933.

BULLETIN
OF THE CHEMICAL
SOCIETY
Belgrade

(Glasnik Hemijskog društva — Beograd)

Vol. 30, No. 4 - 6, 1965

Editor:

ĐORĐE M. DIMITRIJEVIĆ

CONTENTS

INVESTIGATION OF THE SHORT-WAVE END OF THE SOLAR SPECTRUM BY MEANS OF ARTIFICIAL SATELITES AND ROCKETS*

by

C. L. MANDEL'SHTAM, B.N. VASIL'EV, IU.K. VORON'KO, I.P.TINDO
A. N. SHURYGIN, and E. N. FETISOV

P. N. Lebedev Institute of Physics of the USSR Academy of Sciences

O. Kont's statement that man will never, under any conditions discover the chemical composition of the heavenly bodies is well known. A few years later, Kirchoff established the presence of sodium, calcium and other elements in the atmosphere of the sun. Since then, over a hundred years ago, spectroscopy has given not only data on the composition but also basic information on the structure and state of the atmosphere of the sun, stars and other heavenly bodies. On the other hand, spectroscopy owes its theoretical and experimental development in the main to astrophysicists. During the last decade completely new perspectives have opened up for this collaboration between spectorscopists and astrophysicists. This is because the spectral region accessible to study from the earth is limited by a narrow "window" in the absorption of the atmosphere, from 3000 Å to about 13 µ.

Early in the nineteen-forties the development of radio-astronomy began, using another "window", extending from centimeter wavelengths up to some tens of meters. Many important results were already obtained by this method. The possibility of transporting apparatus outside the earth's atmosphere by means of artificial satellites and rockets has made the whole short-wave region of the spectrum, below 3000 Å, available for study. This region contains extremely important and manifold information on the heavenly bodies. Although its study is essentially only just beginning, many results of fundamental importance have already been obtained.

This communication briefly presents the results of investigations of the short-wave "end" of the spectrum of the sun carried out in the last few years at the P. N. Lebedev Institute of Physics of the Soviet Academy of Sciences. This short-wave radiation is due to the solar corona and extends in wavelength down to a few angstroms.

---

* Communicated at the XIth Colloquium Spectroscopicum Internationale B elgrade, 1963.

It has been studied theoretically by Shkolovskii[1], Elwert[2], de Jager[3], and Kazachevskaia and Ivanov-Kholodnyi[4], and experimentally by Friedman and co-workers[5] and Paunds[6].

In our tests the radiation receivers were photon counters with windows of beryllium foil and thin mica sheet, cutting off the long-wave end of the spectrum at about 10 Å.

A block diagram of a counting channel is shown in Fig. 1. Ionization of the gas in the counter by photons gives rise to electrical impulses. These are amplified, shaped and counted by semiconducterized electronic system, and then encoded and transmitted by a telemetric system to the earth, where they are recorded on a strip recorder.[7]
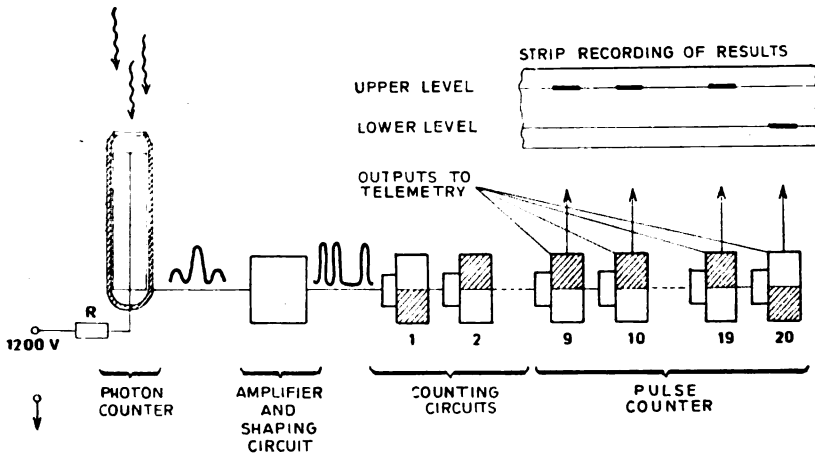
Fig. 1 Block diagram of a measuring channel

Figure 2 shows the impulse counting rate registered by the above setup during the ascent of a vertically launched geophysical rocket to a height of about 105 km[8]. The counter was mounted on the outside of the equipment container, which after the powered part of the trajectory was released from the rocket, oriented itself towards the sun, and remained so oriented for the remaining ascending and descending parts of the trajectory. Figure 2 also shows the readings of a control counter rotated at angle of 15° to the direction of the sun. As may be seen from the graph, a rise in X-radiation, began to be registered at a height of about 92 km above the earth's surface. The zenith angle of the sun was about 90°. Knowing the absorption of the air for wavelengths within the range detected by the counter it is possible to calculate the energy distribution curve
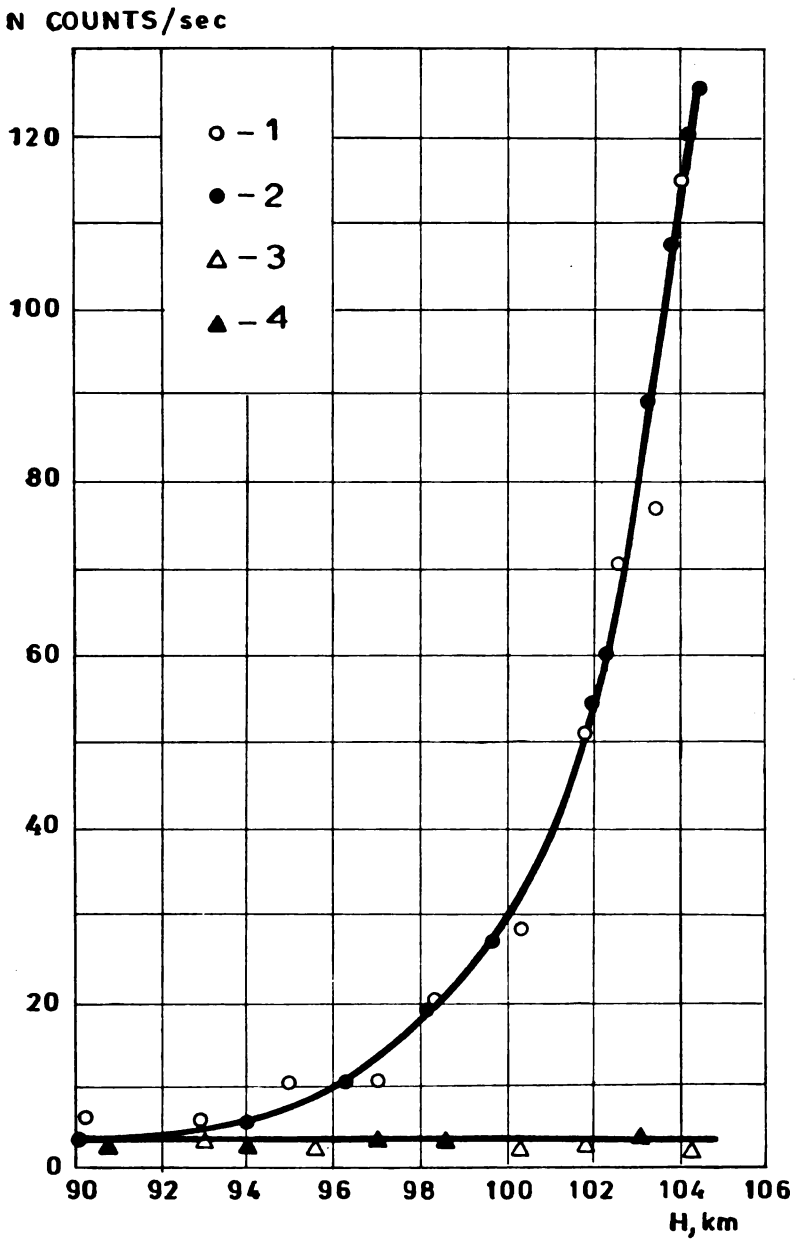
Fig. 2 Count rate as a function of altitude. 1, 2 — readings of the test counter during ascent and descent and descent, respectively. 3,4 — same, for the control counter
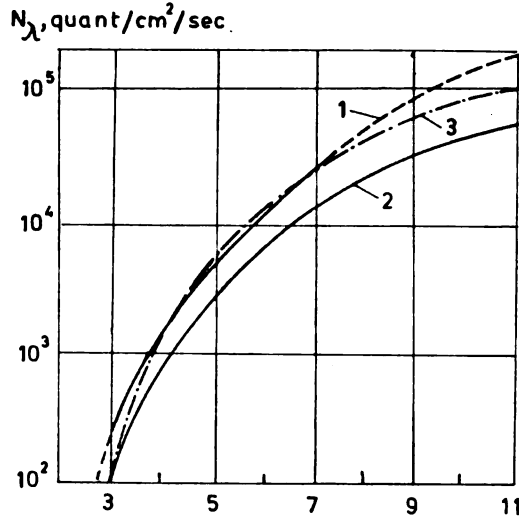
Fig. 3. Energy distribution for the short-wave "end" of the solar spectrum.
1 — Morning launching, 2 — Evening launching, 3 — Theoretical curve for
$T = 4.5 \times 10^6 \, °K$

for this region of the sun's spectrum. This is shown in Fig. 3. The
corresponding curve for another rocket launched the same day is
also shown. The difference between the curves is within the limits
of error to which the spectral sensitivities of the counters were known.
Both curves refer to a quiet sun, and show rapid fall in intensity for
wavelengths shorter than 10 Å: the radiation flux in this region is
$7.3 - 3.2 \times 10^{-4}$ ergs/cm²/sec.

To obtain information about the radiation flux in this region
of the spectrum over a longer time interval, apparatuses were mounted
on the second and third sputniks, each of which stayed in orbit about
24 hrs[9]. The second sputnik carried six blocks of counters with
their axes oriented in six mutually perpendicular directions. In order
to obtain continuous information on the solar radiation, the sputnik
also carried a memory device. Every three minutes this device read
off and recorded the state of the trigger cells of the counting device,
to which all six blocks of detectors were fed. Just before the end of
the 24 hr flight, on a command from the earth, all the information
stored by the memory device was transmitted telemetrically to the
earth and recorded. The results are shown in Fig. 4. The horizontal
lines under the time scale indicate when the satellite was in the shadow
of the earth. The peaks are due to the slow rotation of the satellite,
causing the sun to move in and out of the visual field of the counters.
The non-zero counts when the ship was entering and leaving the
shadow of the earth are noteworthy. It was found upon analysis that
these regions correspond geographically to the entrance of the sate-
lite into the zone of "branches" of the outer radiation belt of the
earth; the counts are due to fast electrons (see Fig. 5).
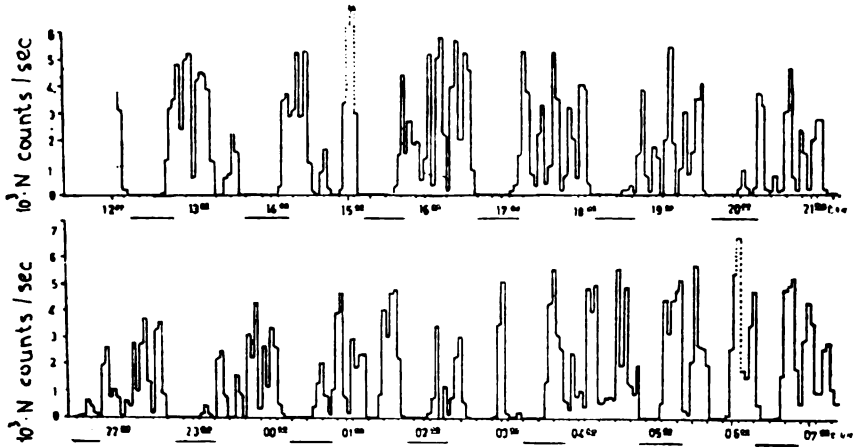
Fig. 4. Measurements made using the second artificial satellite. Moscow time
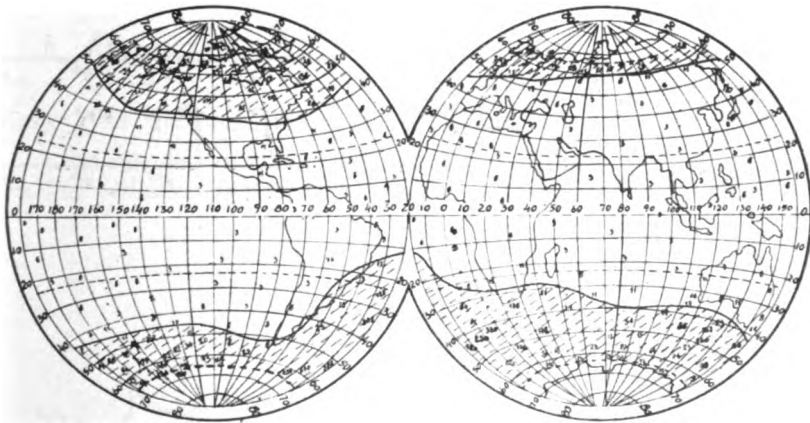
Fig. 5. Zone of increased corpuscular radiation. The numbers are counter pulses per second

As may be seen from Fig. 4, the overall level of X-radiation from the sun remained fairly constant during the 24 hrs at $7-8 \times 10^{-4}$ ergs/cm²/sec. It seems that during a number of solar flares which occurred during the flight of the satellite, the radiation flux showed a sharp rise, causing overloading of the photon counters and the counting system, and hence not seen on the graph.

On the third spaceship two photon counters connected in parallel were mounted on the self-orienting solar batteries, so that they were always pointing towards the sun. A second pair of counters were controls and registered only particles, while a third pair was mounted on the body of the ship. The results of measurement are shown in Fig. 6. As may be seen from the figure, the overall level of X-radiation also remained fairly constant over the 24 hrs, and was $2-3 \times 10^{-4}$ ergs/cm^2/sec. The counts of the control counters above background also correspond geographically to areas of increased corpuscular radiation.

In order to determine which zones of the solar corona are responsible for the generation X-rays, measurements were carried out during a total eclipse of the sun (15 February 1962), when the transition zone between the chromosphere and the corona and also the inner part of the corona are blocked of by the moon. The counters
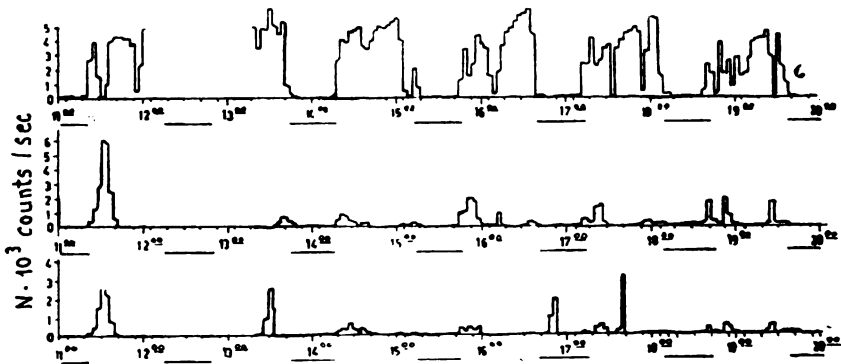
Fig. 6a
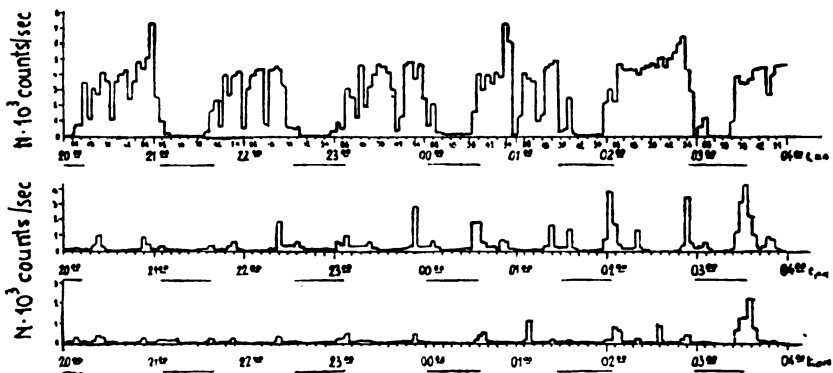
Fig. 6b

Measurements made with the third artificial satellite. Moscow time

were mounted outside the equipment container of a rocket. The launching time and trajectory of the rocket were chosen so that the peak of the trajectory (about 96 km) lay approximately on the axis of the shadow cone. The flux of radiation below 10 Å was about s × 10^{-5} erg/cm²/sec[10]. If it is taken that the radiation flux is proportional to the exposed area of the corona, this corresponds to a flux of 4 × 10^{-4} erg/cm²/sec for a completely exposed corona, which agrees well with the measurements given above. Hence radiation shorter than 10 Å is generated throughout extensive regions of the corona.

To elucidate the mechanism of origin of soft X-rays in the solar corona, the spectral distribution and flux of bremsstrahlung and recombination radiation due to protons and helium ions, and of the emission line, bremsstrahlung and recombination radiation of the "heavy ions" most abundant in the corona, were calculated for the region shorter than 10 Å for several temperature values[11]. The ion concentration was calculated assuming equilibrium between ionization and photorecombination. The cross sections for the corresponding processes were found using the expressions of Elwert and Ivanov-Kholodnyi, taking into account recombination to excited levels.[12]

For the ratio of the concentrations of ions in the $(i+1)$th and i-th states we get

$$\frac{N_{i+1}}{N_i} = 10^8 \frac{kT}{\lambda_i^2} e^{-\lambda_i/kT}$$

where λ_i is the ionization potential in electron volts.

To calculate the intensity of emission line, free-bound, and free-free radiation the following corresponding equations were used:

$$I_e = \Sigma\Sigma N_e N_i h \nu < \sigma v >$$

$$I_{fg} = \Sigma \Sigma N_e N_i Z_i^4 \frac{K}{T^{3/2}} g_I e^{-h/kT}$$

$$I_{ff} = \Sigma\Sigma N_e N_i Z_i^4 \frac{K}{T^{1/2}} \frac{K}{2v_i} g_{II} e^{-h\nu/kT}$$

For the excitation cross section averaged over a Maxwellian velocity distribution $< \sigma v >$ an approximation was used [13]. The calculations were carried out on a computer.

The results of calculation for the spectral distribution of energy and the integral radiation flux are shown in Fig. 7 and Table 1, respectively. It may be seen that the basic contribution is made by recombination radiation of the heavy ions. The transitions at the limits of the series of the corresponding ions which come within the spectral region of interest here are of relatively low intensity.

TABLE 1

Flux of soft X-rays shorter than 10 Å radiated by the solar corona, in $erg/cm^2/sec.$ at a distance of T. a. u. outside the earth's atmosphere

Element	Form of radiation	T in millions of degrees					
		1.5	2	2.5	3	3.5	4
"Heavy" ions: N, O, Ne, Mg, S, Si, Ca, Fe	Emission line	$5.9.10^{-8}$	$1.2.10^{-6}$	$7.7.10^{-6}$	3.10^{-5}	$8.4.10^{-5}$	$1.8.10^{-4}$
	Bremsstrahlung	$1.9.10^{-8}$	$2.6.10^{-7}$	$1.4.10^{-6}$	$3.8.10^{-6}$	$9.1.10^{-6}$	$1.6.10^{-5}$
	Recombination	$3.6.10^{-6}$	$3.9.10^{-5}$	$1.5.10^{-4}$	$3.4.10^{-4}$	$5.7.10^{-4}$	$8.3.10^{-4}$
He III	Bremsstrahlung	$3.6.10^{-7}$	$4.5.10^{-6}$	$2.2.10^{-5}$	$6.2.10^{-5}$	$1.3.10^{-4}$	$2.4.10^{-4}$
	Recombination	$4.5.10^{-7}$	$3.9.10^{-6}$	$1.4.10^{-5}$	$3.2.10^{-5}$	$5.8.10^{-5}$	$8.9.10^{-6}$
H II	Bremsstrahlung	$4.4.10^{-7}$	$5.7.10^{-6}$	$2.7.10^{-5}$	$7.7.10^{-5}$	$1.7.10^{-4}$	$3.0.10^{-4}$
	Recombination	$1.0.10^{-7}$	$9.7.10^{-7}$	$3.6.10^{-6}$	$6.6.10^{-6}$	$1.6.10^{-5}$	$2.5.10^{-5}$
Total radiation		$5.0.10^{-6}$	$5.5.10^{-5}$	$2.3.10^{-4}$	$5.5.10^{-4}$	$1.05.10^{-3}$	$1.7.10^{-3}$
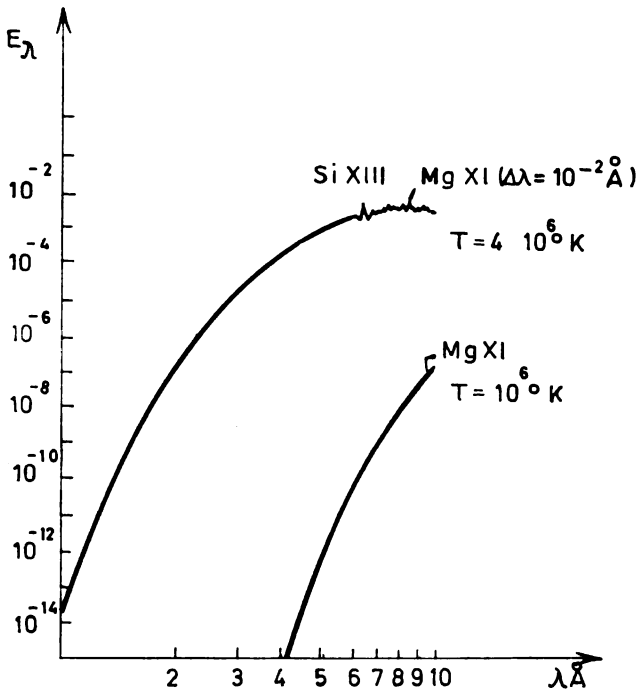
Fig. 7. Theoretical energy distribution for the region below 10 Å.
The vertical lines denote intense lines of ions

Hence the spectral distribution in the range below 10 Å is determined by the term $e^{-h\nu/kT}$. Referring again to Fig. 3, it may be seen that the experimental energy distribution can be well described by this expression (curve 3). Similarly, this function also describes well the experimental distribution obtained in the test of 21 February 1961 during a solar eclipse. Hence it is possible to determine the temperature of radiating zones of the corona at the time of measurement from the experimental curves. Assuming an exponential dependence of energy on ν also for measurements made using sputniks, then from the data given by two counters with somewhat different spectral sensitivities it is possible to evaluate the temperature of the radiating zones. The data is summarized in Table 2.

TABLE 2

Summary of the experimental data

Date	21 Aug 1959	19—20 Aug 1960	1—2 Oct 1960	15 Feb 1961
Flux of radiation below 10 Å (erg/cm²/sec)	7.2 $3.2 \cdot 10^{-4}$	7—$8 \cdot 10^{-4}$	2—$3 \cdot 10^{-4}$	$4 \cdot 10^{-4}$
Radiation temperature (°K)	$4.5 \cdot 10^{6}$	$3 \cdot 10^{6}$	$2 \cdot 10^{6}$	$1 \cdot 5 \cdot 10^{6}$
Intensity of Fe XIV 5303 Å	71	91 88	51 47	65

The temperature values determined in this way come out much higher than the value of $1-1.5 \times 10^6$ degrees obtained by measurement of the radio-frequency radiation of the corona and other methods. Similarly, the measured absolute radiation flux is two orders of magnitude higher than that calculated for a temperature 1.5×10^6 degrees. This, along with other astrophysical data, is evidence of inhomogeneity of the corona — the presence in it of "condensations", i.e. zones with a particle density higher than the rest of the corona, and at a higher temperature, these zones making the main contribution to the measured X-radiation. The experimental and calculated radiation fluxes agree well if it is taken that the condensations have a particle concentration about an order of magnitude higher than the rest of the corona and a volume of a few hunderdths of the whole corona.

From Table 2 it may be seen that there is some correlation between the radiation flux and the intensity of the green Fe XIV line at 5303 Å, for which systematic measurements are being made at corona observation posts. The excitation (ionization) potential of this line is 355 e.v. and it has an intensity maximum at a temperature of $1-1.5 \times 10^6$ °K, i.e. it is radiated from somewhat cooler regions of the corona.

All the above results refer to a quiet sun in a period of average solar activity. It will definitely be of interest to repeat these experiments during the coming "Quiet Sun Year". Then it will be possible to get data on the extreme short-wave radiation of the sun and the zones of its generation in the corona during a period of minimum solar activity. It is also important that such measurements be carried out during solar flares.

Translated by: *Paul Pignon*

REFERENCES

1. Shklovskii, I. S. — *Uspekhi fizicheskikh nauk* 30 : 63, 1946.
   — *Izvestiia Krymskoi Astrofizicheskoi observatorii* 4 : 80, 1949.
2. Elwert, G. Z. — *Naturforschung* 9a : 637, 1954.
   Elwert, G. J. — *Geophysics Research* 66 : 391, 1961.
3. Jager, C. de. — *Annales de Geophysique* 11 : 1, 1955.
4. *Kazachevskaia*, T. V., and G. S. Ivanov-Kholodnyi — *Astronomicheskii Zhurnal* 36 : 102, 1959.
5. *Friedman*, H. — *Space Research* 1 : 695, 1960; 2 : 1021, 1961.
   Kreplin, R. W., T. A. Chubb, and H. Friedman. — *Journal of Geophysical Research* 67 : 2231, 1962.
6. Paunds, K. A. — *Monthly Notices of the Royal Astronomical Society* 123(4), 1962.
7. Vasil'ev, B. N., A. I. Shurygin, I. P. Tindo, and IU. K. Voron'ko — *Iskusstvennye sputniki Zemli* 15 : 85, 1963.
8. Mandel'shtam, S. L., I. P. Tindo, IU. K. Voron'ko, B. N. Vasil'ev, and A. I· Shurygin. — *Iskusstvennye sputniki Zemli* 10: 12, 1961.
9. Mandel'shtam, S. L., I. P. Tindo, IU. K. Voron'ko, and B. N. Vasil'ev. — *Iskusstvennye sputniki Zemli* 11: 3, 1961.
10. Mandel'shtam, S. L., IU. K. Voron'ko, I. P. Tindo, A. I. Shurygin, and B. N. Vasil'ev. — *Doklady Akademii nauk* 142: 77, 1962.
11. Fetisov, E. N. — *Astronomicheskii zhurnal* (in press).
12. Ivanov-Kholodnyi, G. S., G. M. Nikol'skii, and R. A. Gulichev. — *Astronomicheskii zhurnal* 37: 799, 1960.
    Ivanov-Kholodnyi, G. S., and G. M. Nikol'skii. — *Astronomicheskii zhurnal* 38: 828, 1961.
13. Vainshtein, L. A. — *Optika i spectroskopiia* 11: 301, 1961.

SATURATED VAPOR PRESSURE OF NEON AND ARGON

by

JOVANKA M. ŽIVOJINOV

In this work the author used the equation of state of saturated vapor of monatomic fluids, in which there are two basic magnitudes of the thermal state, the pressure p and the boiling temperature at the given pressure, $T°K$. The author obtained this equation in work[1] using her earlier works[2] and [3], which are based on statistical and quantum mechanics, and the equation of state for an ideal gas.

The above mentioned equation is expressed by

$$ln\frac{p_c}{p} = a\left(\frac{T_c}{T} - 1\right) \tag{1}$$

where p is the critical pressure and T_c is the critical temperature of the monatomic fluid, while a is the constant value for each chemical element, which the author found in work[1] to be

$$a = \frac{s}{RT_c} \tag{2}$$

where s denotes the sublimation heat of the given fluid at $0°K$, and R is the universal gas constant.

The purpose of the present work was to apply eq. (1) to two monatomic fluids, neon (Ne) and argon (Ar). The triple point of neon is $T_c = 24.5°K$, the critical point $T_c = 44.74°K$[4], and the sublimation heat at $0°K$ is $s = 446$ cal g atom[5]. It is seen from Table 1 that, for neon, experimental data for pressures and corresponding boiling temperatures is known for the whole temperature range from triple to critical. This is why constant a in eq. (1) was determined for each pressure and temperature (from Table 1) using this experimental data. Hence, from eq. (1),

$$a = \frac{ln\dfrac{p_c}{p}}{\dfrac{T_c}{T} - 1} \tag{3}$$

TABLE 1

Vapour pressure of neon

$a = 5.05577$

T [°K]	p [mm Hg]	$\ln \dfrac{p_c}{p}$	$\dfrac{T_c}{T}$	$a = \dfrac{\ln \dfrac{p_c}{p}}{\dfrac{T_c}{T} - 1}$	δa %
24.65 t. p.	325	4.14914	1.81501	5.08363	— 0.6
25.06	373	4.01164	1.78532	5.10832	— 1.4
26.50	605.2	3.52767	1.68830	5.12517	— 1.4
27.48	816.2	3.22856	1.62809	5.14026	— 1.6
31.39	2264.8	2.20799	1.42529	5.19166	— 2.6
32.91	3171.5	1.87126	1.35947	5.20568	— 2.9
36.34	6057.2	1.22422	1.23115	5.29620	— 4.8
39.56	10042	0.71870	1.13094	5.48873	— 8.6
43.90	18472	0.10920	1.01913	5.70697	—12.9
44.74	20603.6				

TABLE 2

Vapour pressure of argon
$a = 6.27943$

$T [°K]$	$p [atm]$	$in\frac{p_c}{p}$	$\frac{T_c}{T}$	$a = \dfrac{in\frac{p_c}{p}}{\frac{T_c}{T}-1}$	$\delta a \, °/_0$
83.97 t. p.	0.6739	4.26577	1.79493	5.36625	+ 15.3
90	1.321	3.59273	1.67467	5.32520	+ 15.2
100	3.23	2.69864	1.50720	5.32066	+ 15.3
120	11.98	1.38788	1.25600	5.42140	+ 13.7
130	19.99	0.87588	1.15938	5.49539	-- 12.5
140	31.3	0.42750	1.07657	5.58303	·· 11.1
150	46.8	0.02523	1.00480	5.25714	16.3
150.72 c. p.	47.996				

2*

Digitized by Google

Therefore, for the lowest temperature, $T = 24.65°K$:

$$a = 5.08363 \tag{4}$$

From eq. (2):

$$a = 5.05577 \tag{5}$$

Comparing this value and the one obtained from eq. (3), we see that the difference is very small, i.e., $\delta a = -0.6\%$. To check the other values for constant a in eq. (2) for neon, eq. (3) was used in an analogous way for a whole series of temperatures in the saturated vapor range of this fluid. The thus obtained values from the experimental data in Table 1 are given at the end of the Table. Finally, for each case we also found the differences between these values and those obtained from eq. (2). As is seen from the table, the greatest difference is for the temperature which is closest to the critical, i.e., $\delta a = 12.9\%$.

The other fluid is argon. Its triple point is at $T_{tr} = 83.83°K$ and the critical at $T_c = 150.72°K$. The sublimation heat at $O°K$ is $s = 1880$ cal/g atom[5]. For this fluid we also know the experimental data for the pressures and corresponding boiling temperatures for the whole temperature range from triple to critical. They are shown in Table 2[4]. For example, from eq. (3) for the lowest temperature, $T = 83.97°K$,

$$a = 5.36625 \tag{6}$$

and from eq. (2):

$$a = 6.27943 \tag{7}$$

Here, $\delta a = +15.3\%$, i.e., considerably greater than in the case of neon. In an analogous way, we determined values for constant a from the experimental data in Table 2 for the whole range of temperature up to the critical. This data is given at the end of Table 2. We also show the difference between these values and those given under (7). In this case too the greatest difference is that for the temperature closest to the critical, i.e., $\delta a = +16.3\%$.

All the results obtained here show that it can be considered that the value for the constant in eq (1) is expressed by eq. (2). The author ascribes the differences mostly to the liquid phase, and she considers that except for those physical properties mentioned in the work[2] some of the others should be introduced in statistical mechanics.

REFERENCES

1. Živojinov, J. "Jednačina stanja jednoatomnih elemenata" (Equation of State of Monatomic Elements) — *Radovi Zavoda za fiziku Elektrotehničkog fakulteta* (Beograd) 4(7): 57—60, 1964.

2. Živojinov, J. "Određivanje broja atoma u gram-atomu zasićene pare na osnovu kvantno-statističkog razmatranja" (Determination of the Number of Atoms per Gram-Atom of Saturated Vapor on the Basis of Statistical and Quantum Mechanics) — *Radovi Zavoda za Fiziku Elektrotehničkog fakulteta* (Beograd) 2: 1—17, 1962.

3. Živojinov, J. "Statističko-kvantno tumačenje uslova ravnoteže između tečne i parne faze na temperaturi ključanja jednoatomnih elemenata" (Explanation of the Equilibrium Conditions between Liquid and Vapor Phase at the Boiling Temperature of Monatomic Elements Based on Statistical Mechanics) — *Glasnik hemijskog društva* (Beograd) 27(5—6): 1—14, 1962.

4. Landolt-Börnstein. *Zahlenwerte und Funktionen aus Physik-Chemie-Astronomie-Geophysik und Technik* — Berlin: Geophysik und Technik, 1960.

5. Gurney, W. *Introduction to Statistical Mechanics* — New York, 1949.

DETERMINATION OF THE DIFFERENCES BETWEEN THE GROUND LEVELS OF ENERGIES IN VAPOR AND LIQUID STATE OF MONATOMIC ELEMENTS

by

JOVANKA M. ŽIVOJINOV, LJILJANA N. VASILJEVIĆ and NADEŽDA Ž. BOŽIN

Using the relations obtained by J. Živojinov in her earlier works[1],[2], we wished to determine the difference between the ground levels of the energies of the vapor and the liquid atoms of monatomic elements at the boiling temperature $T°K$ in the range from triple to critical temperature.

The author[2] obtained the following relation between the molar (or specific) volumes of vapor V'' and liquid V' at some temperature T:

$$\frac{V'' \cdot e^{-\frac{\eta}{RT}}}{V'} = \text{const} \qquad (1)$$

where η is the sublimation heat per vapor atom at $0°K$ and k is Boltzmann's constant. Strictly this relation would only hold for an "ideal monatomic fluid", i.e., a fluid having the physical properties described[1]. The purpose of the present work was to apply this formula to real monatomic fluids, so as to see whether the relations obtained for an "ideal fluid" apply to real fluids. Since for them at a given boiling temperature there is experimental data for the densities of vapor ρ'' and liquid ρ'[3], and not for their specific volumes, and since it is known that these magnitudes are related, expression[1] may be written in the following form:

$$\frac{\rho' \cdot e^{-\frac{\eta}{RT}}}{\rho''} = C \qquad (2)$$

Since in addition to this the literature gives data for the sublimation heat per g-atom[4] and since it is assumed[1] that

$$\eta = \frac{s}{N} \qquad (3)$$

where N is Avogadro's number, expression (2) takes the form

$$\frac{\rho' \cdot e^{-\frac{s}{RT}}}{\rho''} = C \qquad (4)$$

where R is the universal gas constant. In order to show that this expression obtained on the basis of Statistical and Quantum Mechanics can also be used for real fluids and that s is only the sublimation heat, it will be used here first to determine the sublimation heat of krypton (Kr). Since two unknowns, s and T, figure in relation (4), it will be

TABLE 1

Latent heat of sublimation of krypton at $0°K$ (3)

$$s = 2540 \; \frac{cal}{g\text{-}atom} \quad T_2 = 144{,}05°K \quad \rho_2' = 2{,}2202 \; \frac{g}{cm^3} \quad \rho_2'' = 0{,}03739 \; \frac{g}{cm^3}$$

$T_1 \; °K$	$\rho_1' \frac{g}{cm^3}$	$\rho_1'' \frac{g}{cm_3}$	$ln\left(\frac{\rho_2' \rho_1''}{\rho_2'' \rho_1'}\right)$	$s \frac{cal}{g\text{-}atom}$ Eq. 8	$\Delta s \frac{cal}{g\text{-}atom}$	$\delta s \%$
153.35	2.1363	0.05774	0.4731	2232.2	+ 307.8	+ 12.1
163.70	2.0350	0.09004	0.9659	2302.5	+ 237.5	+ 9.3
170.94	1.9574	0.12014	1.2932	2352.3	+ 187.7	+ 7.4
180.84	1.8338	0.17576	1.7389	2445.8	+ 94.2	+ 3.7
188.40	1.7255	0.23501	2.0903	2540.8	− 0.8	− 0.03
193.61	1.6379	0.2903	2.3537	2631.0	− 91.0	− 3.6
199.65	1.5161	0.3774	2.6933	2767.3	− 227.3	− 8.9

first used for the following two temperatures: $T_1 = 153.35°K$ and $T_2 = 144.05°K$, for which corresponding experimental data for density is shown in Table 1. For temperature T_1 from (4):

$$\frac{\rho_1' \cdot e^{-\frac{s}{RT_1}}}{\rho_1''} = C \qquad (5)$$

and for T_2:

$$\frac{\rho_2' \cdot e^{-\frac{s}{RT_2}}}{\rho_2''} = C \tag{6}$$

From these two equations we obtained the following relation for determining the sublimation heat

$$s = \frac{RT_1 T_2}{T_1 - T_2} \, ln \frac{\rho_1'' \rho_2'}{\rho_1' \rho_2''} \tag{7}$$

If we substitute all the corresponding experimental data from Table 1 in it, we obtain

$$s = 2232 \cdot 2 \, \frac{cal}{g\text{-}atom} \tag{8}.$$

TABLE 2

Latent heat of sublimation of krypton at 0^0K

$$T_2 = 153.35 \; {}^0K \qquad \rho_2' = 2.1363 \, \frac{g}{cm^3} \qquad \rho'' = 0.05774 \, \frac{g}{cm^3} \tag{3}$$

T^0K	$ln\left(\frac{\rho_2' \, \rho_1''}{\rho_2'' \, \rho_1'}\right)$	$s \, \frac{cal}{g\text{-}atom}$ Eq. 7	$\Delta s \, \frac{cal}{g\text{-}atom}$	$\delta s \%$
163.70	0.4929	2374.7	165.3	6.5
170.94	0.8202	2428.0	+ 112.0	4.4
180.84	1.2658	2536.5	+ 3.5	— 0.13
188.40	1.6172	2647.9	— 107.9	— 4.2
193.61	1.8806	2754.9	— 214.9	— 8.4
199.65	2.2203	2916.4	— 376.4	— 14.8

It is reported in the literature[4] that $s = 2540$ cal/g atom. There-
fore, the value reached in eq. (8) contains an absolute error $\Delta s = = +307.8$ cal/g atom, or a relative error $\delta s = +12.1\%$. In a completely
analogous way, the sublimation heat of krypton was determined for
six other temperatures and the temperature T. The experimental
data for the densities at these temperatures and the theoretical values

TABLE 3

Latent heat of sublimation of krypton at 0^0K

$$T_2 = 163.70\ ^0K \quad \rho_2' = 2.0350\ \frac{g}{cm^3} \quad \rho_2'' = 0.09004\ \frac{g}{cm^3} \qquad (3)$$

$T_1\ ^0K$	$ln\left(\dfrac{\rho_2'\ \rho_1''}{\rho_2''\ \rho_1'}\right)$	$s\ \dfrac{cal}{g\text{-}atom}$ Eq. (7)	$\Delta s\ \dfrac{cal}{g\text{-}atom}$	$\delta s\ \%$
170.94	0.3273	2512.8	+ 27.2	+ 11
180.84	0.7730	2652.0	— 112.0	— 4.4
188.40	1.1243	2788.6	— 248.6	— 9.8
193.61	1.3877	2920.9	— 380.9	— 15.0
199.65	1.7274	3119.4	— 579.4	— 22.8

TABLE 4

Latent heat of sublimation of krypton at 0^0K

$$T_2 = 170.94\ ^0K \quad \rho_2' = 1.9544\ \frac{g}{cm^3} \quad \rho_2'' = 0.12014\ \frac{g}{cm^3} \qquad (3)$$

$T_1\ ^0K$	$ln\left(\dfrac{\rho_2'\ \rho_1''}{\rho_1''\ \rho_2'}\right)$	$s\ \dfrac{cal}{g\text{-}atom}$ Eq. (7)	$\Delta s\ \dfrac{cal}{g\text{-}atom}$	$\delta s\ \%$
180.84	0.4457	2764.5	— 224.5	— 8.8
188.40	0.7970	2920.1	— 380.1	— 15.0
193.61	1.0604	3075.1	— 535.1	— 21.1
199.65	1.4001	3306.0	— 766.0	— 30.1

TABLE 5

Latent heat of sublimation of krypton at 0⁰K

$$T_1 = 180.84\,^0K \qquad \rho_2' = 1.8338\ \frac{g}{cm^3} \qquad \rho_2'' = 0.17576\ \frac{g}{cm^3} \qquad (3)$$

$T_1\ ^0K$	$ln\left(\dfrac{\rho_2'\,\rho_1''}{\rho_2''\,\rho_1'}\right)$	$s\ \dfrac{cal}{g\text{-}atom}$ Eq. (7)	$\Delta s\ \dfrac{cal}{g\text{-}atom}$	$\delta s\ \%$
188.40	0.3513	3144.8	— 604.8	— 23.8
193.61	0.6147	3347.8	— 807.8	— 31.8
199.65	0.9544	3638.9	—1098.9	— 43.3

TABLE 6

Latent heat of sublimation of krypton at 0⁰K

$$T_2 = 188.40\,^0K \qquad \rho_2' = 1.7255\ \frac{g}{cm^3} \qquad \rho_2'' = 0.23501\ \frac{g}{cm^3} \qquad (3)$$

$T_1\ ^0K$	$ln\left(\dfrac{\rho_2'\,\rho_1''}{\rho_2''\,\rho_1'}\right)$	$s\ \dfrac{cal}{g\text{-}atom}$ Eq. (7)	$\Delta s\ \dfrac{cal}{g\text{-}atom}$	$\delta s\ \%$
193.61	0.2634	3663.1	— 1123.1	— 44.2
199.65	0.6030	4004.8	— 1464.8	— 57.7

for the sublimation heat *s* from eq.(7) are given in Table 1. As can be seen, by combining the values for temperature T_2 and a temperature higher than T_1, we obtain such values for *s* that the errors first decrease with increasing temperature and then increase, remaining always below that mentioned above. In Table 2 are given values for *s* obtained from (7) by combining the temperature $T_2 = 153.35°K$ and the other six higher temperatures. The results again show that the errors first decrease with increasing temperature and then increase. The greatest error is with the highest temperature, i.e,. $\delta s = -14.8\%$. Tables 3,4,5 and 6 contain data obtained in an analogous way, and they show that the errors are now greater than before and that *s* is never lower than the values reported in the literature (except in Table 3 for $T_1 = 170.94°K$).

In the rest of this work we shall use the theoretical results obtained by J. Živojinov in her work[2]. She found that

$$\frac{\rho' \cdot e^{-\frac{s}{RT}}}{\rho''} = \frac{3}{e^{-\frac{s}{RT_c}}} \qquad (9)$$

where T_c is the critical temperature of some monatomic element. From this expression it follows that the sublimation heat is

$$s = \frac{RT_c T \ln \frac{\rho'}{3\rho''}}{T_c - T} . \qquad (10)$$

This relation also holds for an "ideal fluid". Besides, as is seen, it is more convenient because it can be used to determine the sublimation heat for any temperature T. Now we will show what results this newer expression gives if it is used for krypton. Its critical temperature is $T_c = 209.41°K$, so for $T = 144.05°K$ and according to the data for densities from Table 7

$$s = 2736.6 \frac{cal}{g\text{-}atom} \qquad (11)$$

Hence, $\Delta s = -196.6$ cal/g atom and $\delta s = -7.7\%$. Completely analogously the sublimation heat of krypton was determined for some other temperatures. The results are shown in Table 7. It can be seen that with increasing temperature the errors first increase and then decrease.

TABLE 7

Latent heat of sublimation of krypton at 0°K

$T°K$	ρ' (3) $\frac{g}{cm^3}$	ρ'' (3) $\frac{g}{cm^3}$	$\ln \frac{\rho'}{3\rho''}$	$s \frac{cal}{g\text{-}atom}$ Eq. (7)	$\Delta s \frac{cal}{g\text{-}atom}$	$\delta s \%$
144.05	2.2202	0.03739	2.985	2736.6	— 196.6	— 7.7
153.35	2.1363	0.05774	2.512	2858.3	— 318.3	— 12.5
163.70	2.0350	0.09004	2.019	3007.7	— 467.7	— 18.4
170.94	1.9574	0.12014	1.692	3127.4	— 587.4	— 23.1
180.84	1.8338	0.17576	1.246	3280.7	— 740.7	— 29.2
188.40	1.7255	0.23501	0.895	3338.4	— 798.4	— 31.4
193.61	1.6379	0.2903	0.631	3216.3	— 676.3	— 26.6
199.65	1.5161	0.3774	0.292	2484.6	+ 55.3	+ 2.2

Argon is the next monatomic element for which expression (10) will be used. Its triple point is at $T_t = 83.83°K$ and the critical at $T_c = 150.75°K$[3]. The lowest temperature for which experimental data[3] for densities was obtained is $T = 92.01°K$. According to the data for the densities in Table 8, the sublimation heat from eq. (10) is

$$s = 1897 \cdot 8 \frac{cal}{g\text{-}atom} \qquad (12).$$

TABLE 8

Latent heat of sublimation of argon at 0°K

$T°K$	(3) $\rho' \frac{g}{cm^3}$	(3) $\rho'' \frac{g}{cm^3}$	$ln \frac{\rho'}{3\rho''}$	$s \frac{cal}{g\text{-}atom}$ Eq. (10)	$\Delta s \frac{cal}{g\text{-}atom}$	$\delta s\%$
92.01	1.37396	0.00801	4.046	1897.8	— 17.8	— 0.9
97.77	1.32482	0.01457	3.411	1884.9	— 4.9	— 0.3
111.93	1.22414	0.03723	2.394	2067.0	— 187.0	— 9.9
122.40	1.13851	0.06785	1.721	2225.0	— 345.0	— 18.3
132.96	1.03456	0.12552	1.010	2260.4	— 380.4	— 20.2
137.65	0.97385	0.15994	0.707	2224.6	— 344.6	— 18.3
141.62	0.91499	0.19432	0.450	2090.2	— 210.2	— 11.2

The literature reports that $s = 1880$ cal/g atom, according to which $\Delta s = -17.8$ cal/g atom and $\delta s = -0.9°_0$. Other data for temperatures nearly up to the critical is given in Table 8. This again shows that with increasing temperature the errors first increase and then decrease, and, besides, all the values obtained for the sublimation heat are higher than those cited in the literature.

The third element is neon. Its triple point is at $T_t = 24.57°K$ and critical at $T_c = 44.41°K$. Expression (10) will be used for a whole series of temperatures in the above mentioned temperature range, because for them experimental data for densities exists (as shown in Table 9). Thus, for example, for $T = 25.24°K$ the sublimation heat is

$$s = 504 \cdot 9 \frac{cal}{g\text{-}atom}. \qquad (13)$$

TABLE 9

Latent heat of sublimation of neon at 0°K

$T\,^{\circ}K$	(3) $\rho'\ \dfrac{g}{cm^3}$	(3) $\rho''\ \dfrac{g}{cm^3}$	$ln\ \dfrac{\rho'}{3\,\rho''}$	$s\ \dfrac{cal}{g\text{-}atom}$ Eq. (10)	$s\ \dfrac{cal}{g\text{-}atom}$	$\delta\,s\%$
25.24	1.23824	0.00534	4.347	504.9	— 58.9	— 13.2
26.22	1.22215	0.00711	4.048	514.7	— 68.7	— 15.4
27.22	1.20421	0.00939	3.755	524.5	— 78.5	— 17.6
30.20	1.14960	0.02013	2.946	652.3	— 106.3	— 23.8
33.16	1.08832	0.03831	2.248	584.5	— 138.5	— 31.0
36.12	1.01750	0.06742	1.615	620.7	— 174.7	— 39.1
37.90	0.96728	0.09310	1.242	637.9	— 191.9	— 43.0
39.15	0.92803	0.11592	0.981	644.1	— 198.1	— 44.1
41.135	0.85421	0.16563	0.541	599.4	— 153.4	— 34.4

The data reported in the literature[4] for this value is 446 cal/g atom, and therefore $\Delta s = -58.9$ cal/g atom and $\delta s = -13.2\%$. The sublimation heat data obtained for the other temperatures is given in the above Table. It is seen that with increasing temperature the errors increase, and the value for the sublimation heat is always higher than that reported in the literature.

Expression (10) will now be applied to xenon. Its triple point is at $T_t = 161.26°K$ and the critical at $T_c = 289.76°K$. The lowest temperature for which experimental data exists for density[3] is $T = 206.36°K$. According to the data for the densities from Table (10), using expression (10),

$$s = 3913 \cdot 6 - \frac{cal}{g\text{-}atom}. \tag{14}$$

The literature[4] cites the value $s = 3850$ cal/g atom, so $\Delta s = -93.6$ cal/g atom and $\delta s = -2.4\%$. For the other temperatures nearly up to the critical, the results are shown in Table 10. It is seen that the theoretical values are mainly higher than those cited in the literature.

TABLE 10

Latent heat of sublimation of xenon at 0°K

$T °K$	(3) $\rho' \dfrac{g}{cm^3}$	(3) $\rho'' \dfrac{g}{cm^3}$	$ln \dfrac{\rho'}{3\rho''}$	$s \dfrac{cal}{g\text{-}atom}$ Eq. (10)	$\Delta s \dfrac{cal}{g\text{-}atom}$	$\delta s °\!\!/_0$
206.36	2.763	0.059	2.748	3913.6	— 93.6	— 2.4
213.16	2.699	0.079	2.432	3895.3	— 75.3	— 2.0
213.86	2.694	0.078	2.443	3962.0	— 142.0	— 3.7
230.26	2.605	0.103	2.132	4748.9	— 928.9	— 24.3
233.86	2.506	0.139	1.793	4317.5	— 497.5	— 13.0
242.86	2.411	0.180	1.496	4458.8	— 638.8	— 16.7
247.91	2.297	0.235	1.181	4026.7	— 206.7	— 5.4
253.16	4.292	0.238	1.166	4642.1	— 822.1	— 21.5
263.16	2.169	0.313	0.837	4766.2	— 946.2	— 24.8
268.16	2.074	0.363	0.644	4601.8	— 781.8	— 20.5
273.16	1.987	0.421	0.453	4290.5	— 470.5	— 12.3
278.16	1.879	0.501	0.223	3077.8	· 742.1	- 19.4

In conclusion it may be said that all the fluids dealt with have a relatively low triple point. The triple point of the "ideal fluid" is assumed to be at O°K. Nevertheless, the results show that relations established for "ideal fluids" on the basis of statistical and quantum mechanics[1,2] can also be used for real fluids. The differences show that some other physical properties should be ascribed to the "ideal fluid" so that it would be still closer to the behavior of the real fluids.

Institute of Physics
University of Beograd

REFERENCES

1. Živojinov, J. "Određivanje broja atoma u gram atomu zasićene pare na osnovu kvantno-statističkog razmatranja" (Determination of the Number of Atoms in a Gram Atom of Saturated Vapor on the Basis of Quantum-Statistical Considerations). — *Radovi Zavoda za fiziku, Elektrotehnički fakultet* (Beograd) II(3): 3—17, 1962.

2. Živojin, J. "Statističko-kvantno tumačenje uslova ravnoteže između tečne i parne faze jednoatomnih elemenata" (Statistical-Quantum Consideration of the Conditions of Equilibrium between the Liquid and Vapor Phase of Monatomic Elements) — *Glasnik hemijskog društva* (Beograd) 27(5—6): 241—252, 1962.

3. Landolt-Börnstein. *Zahlenwerte und Funktionen aus Physik-Chemie-Astronomie* — Berlin: Geophysik und Technik, 1960.

4. Gurnay. *Introduction to Statistical Mechanics* — New York, 1949.

POLAROGRAPHIC DETERMINATION OF LEAD IN CADMIUM

by

SRETEN N. MLADENOVIĆ

In hydrochloric acid solutions lead and cadmium give well defined polarographic waves at dropping mercury electrode.

The half-wave potentials of the reduction of lead and cadmium ions differ one from another to an extent which makes possible their quantitative determination. An example is the determination of lead and cadmium in cathodic and cast zinc, where the content of lead is usually ten times greater than that of cadmium. The cadmium wave appears after the zinc wave. The polarographic determination of lead in cathodic and cast cadmium with a lead content smaller than 1×10^4 times the cadmium content is also carried out in an electrolyte containing hydrochloric acid. In this case the waves of lead and cadmium are not distinctly separate and therefore the limiting current of lead ion reduction cannot be precisely determined. In samples with a lower lead content the waves of lead and cadmium are superposed (overlapped) and the quantitative determination of lead in cadmium is not possible.

To replace this method, Vdovenko and Spivakovskaia[1] have recommended a colorimetric method for determining lead by means of dithizone. In this method lead is quantitatively precipitated with strontium sulphate as collector, after which lead sulphate and strontium sulphate are dissolved in an alkaline ammonia solution of EDTA. After the dissolution, lead is determined with dithizone. However, it was observed that strontium sulphate withdraws a small amount of cadmium as well. This interfering cadmium is removed by repeated dissolution of lead and strontium sulphate in concentrated nitric acid. Thus, the dissolution of lead and cadmium sulphate is rather difficult.

The new polarographic method employs some of the principles of the above colorimetric method for the determination of lead with dithizone. Lead is first precipitated with strontium sulphate in the form of lead sulphate, as in the colorimetric method, and then it is dissolved in ammonia solution of EDTA. The further course of the

3
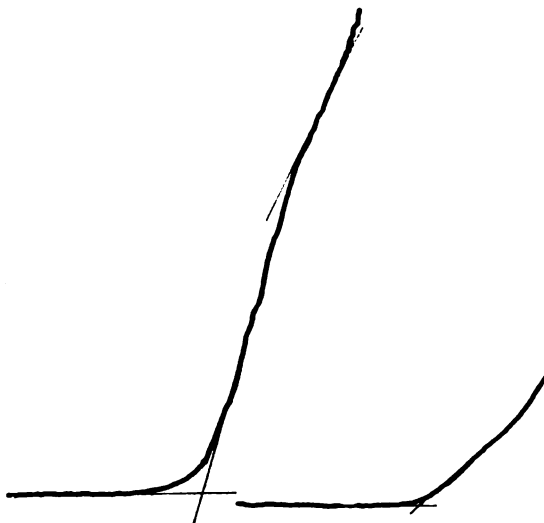
Fig. 1

polarographic method differes from the colorimetric method in that the solution of lead and strontium sulphate is acidified and the lead is then determined polarographically.

Only by such procedure is the polarographic wave of lead sharply and distinctly separated from the cadmium wave. The appearance of the cadmium wave near the lead wave on a polarogram indicates that strontium sulphate has taken up a certain amount of cadmium (Fig. 2).
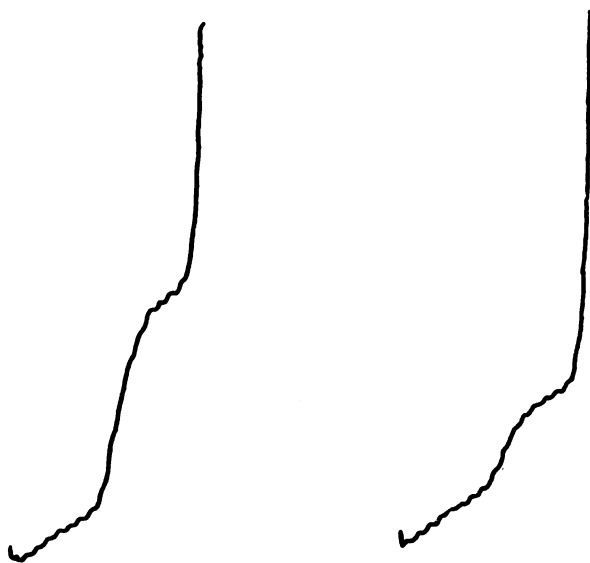
Fig. 2.

The accuracy of the method was checked with samples containing known amounts of lead and cadmium in proportions corresponding to those usually encountered in cathodic and cast cadmium. The determination of lead in cadmium in the presence of different amounts of a standard lead solution gave the same result for lead content regardless of the amount of lead added (Table1).

TABLE 1

Taken: 1 g of cadmium — Height of the polarographic wave of lead in Cd: 8 mm

Added amount of lead in mg	Height of the polarographic wave with added lead, in mm	Lead content %
0.05	19	0.0036
0.10	31	0.0035
0.15	42	0.0035
0.20	54	0.0035

The polarographic determination of lead in cadmium was carried out in the following way:

One gram of cadmium was dissolved in 25 ml of nitric acid (1 : 5) and the solution was evaporated until dry. The residue was dissolved in 100 ml of water, and to the stirred solution first 5 ml of 25% sodium sulphate solution and then 1 ml of 15% strontium sulphate solution were added. The precipitation of strontium sulphate was improved by scratching the precipitate with a glass rod. After one hour the precipitate was filtered off (blue marked filter paper was used). The flask in which the precipitate was obtained was washed several times with small amounts of water, and the same water was used for washing the precipitate. The flask was put beneath the filter, the filter paper was punctured, and the precipitate was transferred to the flask by means of 10—15 ml of warm water. Then, 20 ml of hot alkaline ammonia EDTA solution was poured over the filter paper (0.05 N EDTA and conc. ammonium hydroxide 4: 1) and the latter was again washed with water. The filtrate was stirred and heated until the dissolution of the precipitate was complete. The cold solution was then transferred to a 50 ml volumetric flask and, after addition of 1 ml of 0.5% gelatin solution and 10 ml of conc. nitric acid, the flask was filled with water to the mark. The solution was then polarographed.

This procedure for the polarographic determination of lead in cadmium is more convenient and gives more accurate results than the known methods published so far.

School of Technology
Institute of Physical Chemistry
and Electrochemistry
Beograd

REFERENCES

[1] Vdovenko M. E., and I. S. Spivakovskaia. "Primenie trilona B pri opredelenii mikrokolichestv svinca v metallicheskom kadmii" (The Application of Trillon B in the Determination of Micro Amounts of Lead in Metallic Cadmium) — *Zavodskaia Laboratoriia* (Moskva) 27: 963—964, 1961

3*

COULOMETRIC DETERMINATION OF COPPER*

by

SRETEN N. MLADENOVIĆ and GOJKO DUNKIĆ

The indirect coulometric titration of copper developed by Tutundžić and Mladenović[1] was carried out in electrolytes containing a definite amount of sulphuric acid. When the amount of sulphuric acid used was too small, copper could not be determined precisely, since the titration end-point was attained before the quantitative separation of copper at the cathode was achieved. Another disadvantage of this coulometric copper determination is that the minimal required amount of sulphuric acid in the electrolyte depends on the amount of copper to be determined.

In the modified procedure for coulometric copper determination, the quantitative copper separation is independent of the acid content in the electrolyte. Thus, it is possible to achieve a quantitative separation of copper at the cathode from either acid or neutral solutions.

In acid and alkaline copper sulphate solutions the following reactions take place at the electrodes:

at the cathode

$$Cu^{2+} + 2e \longrightarrow Cu \quad . \quad . \quad . \quad e_0 = 0.34V$$
$$2H^+ + 2e \longrightarrow H_2 \quad . \quad . \quad . \quad e_0 = 0.00V$$

At the anode:

$$2 H_2O - 4e \longrightarrow 4 H^+ + O_2 \quad . \quad . \quad e_0 = 1.23V$$
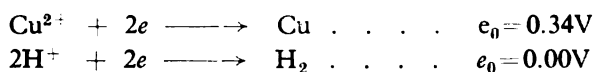
With respect to the size of the electrochemical potential of the above electrode reactions, it can be assumed that copper separates at the cathode before hydrogen. From concentrated copper sulphate solutions, copper separates before hydrogen, but, from dilute solutions, copper and hydrogen separate simultaneously. In both cases the acidity of the solution increases with evolution of oxygen at the anode. The amount of acid generated in the solution is equivalent to the amount of deposited copper. When the separation of copper is finished, the amount of acid in the electrolyte is not further augmented, since only water is further decomposed and the solution is thus merely made more concentrated. After separation of the copper, the acid in the electrolyte is titrated coulometrically.

The current strength, that is, the current density can affect the accuracy of the copper determination only when vigorous gas evolution at ·high current density causes losses on account of sprinkling Table 1).

<div align="center">TABLE 1</div>

Electrolyte for copper separation:
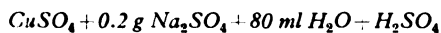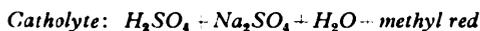
$CuSO_4 + 0.2\ g\ Na_2SO_4 + 80\ ml\ H_2O + H_2SO_4$

Coulometric titration of the acid:

Catholyte: $H_2SO_4 + Na_2SO_4 + H_2O$ -- *methyl red*

Anolyte: $KCl + H_2O$

Experiment No.	Copper separation		Titration of the acid		Copper		Error %
	Current strength	Time in min.	Current strength	Time in sec.	Taken mg	Found mg	
1.	0.2	30	30.0	999	3.98	3.97	— 0.07
2.	0.2	30	30.0	995	3.97	3.94	— 0.80
3.	0.2	30	30.0	1001	3.97	3.99	0.52
4.	0.2	30	30.0	1204	5.96	5.99	0.67
5.	0.2	30	30.0	1203	5.96	4.98	0.41
6.	0.5	45	30.0	589	1.975	1.780	—10.0
7.	0.5	45	30.0	587	1.975	1.751	—11,3
8.	0.5	45	30.0	598	1.975	1.898	— 4.00
9.	0.5	45	30.0	592	1.975	1.817	— 8.00
10.	0.5	45	30.0	584	1.975	1.712	—13.3

The negative error may be ascribed to the sprinkling of the electrolyte and to the incomplete separation of copper at high current density.

In the determination of copper amounts from 2 to 10 mg, the error was limited to +1.7% (Table 2).

The accuracy of the copper determination is not affected by the amount of sulphuric acid present in the aqueous copper sulphate solution. When the electrolytic bridge between the anolyte and the catholyte is enriched with hydrogen ions, the error is positive (Table 3). In experimets 5, 6 and 7 (Table 3) the errors are greater than elsewhere on account of diffusion and migration of hydrogen ions from anolyte to catholyte through the electrolytic bridge.

Sodium sulphate, which is employed as the conducting salt in the electrolyte, has no effect on the determination of copper — provided that the titration is not carried out at high current density and the sodium sulphate contains no impurities which could react at the electrodes during electrolysis.

The longer the process of copper separation at high current density is, the better and more quantitatively the copper is deposited

TABLE 2

Electrolyte for copper separation:
$CuSO_4 + 0.2\ g\ Na_2SO_4 + 80\ ml\ H_2O + H_2SO_4$
Coulometric titration of the acid:
Catholyte: $H_2SO_4 + Na_2SO_4 + H_2O +$ *methyl red*
Anolyte: $KCl + H_2O$

Experiment No.	Copper separation		Titration of the acid		Copper		Error %
	Current strength	Time in min.	Current strength	Time in sec.	Taken mg	Found mg	
1.	0.2	30	30.0	813	1.990	1.980	—1.20
2.	0.2	30	30.0	812	1.990	1.988	—1.50
3.	0.2	30	30.0	809	1.990	1.960	—1.65
4.	0.2	30	30.0	995	3.970	3.938	—0.80
5.	0.2	30	30.0	1001	3.970	3.990	0.52
6.	0.2	30	30.0	999	3.970	3.997	0.07
7.	0.2	30	30.0	1204	5.96	5.99	0.67
8.	0.2	30	30.0	1206	5.95	6.02	1.04
9.	0.2	30	30.0	1203	5.96	5.98	0.41
10.	0.2	30	30.0	1405	7.94	7.99	0.51
11.	0.2	30	30.0	1403	7.94	7.96	0.25
12.	0.2	30	30.0	1407	7.94	8.00	0.82
13.	0.2	30	30.0	1605	9.93	9.98	0.45
14.	0.2	30	30.0	1604	9.93	9.97	0.35
15.	0.2	30	30.0	1603	9.93	9.96	0.31

TABLE 3

Electrolyte for copper separation:
$CuSO_4 + 0.2\ g\ Na_2SO_4 + 80\ ml\ H_2O + H_2SO_4$
Coulometric titration of the acid:
Catholyte: $H_2SO_4 + Na_2SO_4 + H_2O +$ *methyl red*
Anolyte: $KCl + H_2O$

Experiment No.	0.1 n H_2SO_4 ml	Copper separation		Titration of the acid		Copper		Error %
		Current strength	Time in min.	Current strength	Time in sec.	Taken mg	Found mg	
1.	0.00	0.2	30	30.0	404	3.95	3.99	1.00
2.	0.00	0.2	30	30.0	398	3.95	3.92	—0.62
3.	1.00	0.2	30	30.0	703	3.95	3.93	—0.17
4.	1.00	0.2	30	30.0	704	3.95	3.98	1.00
5.	2.00	0.2	30	30.0	1010	3.95	4.00	1.25
6.	2.00	0.2	30	30.0	1012	3.96	4.02	1.75
7.	4.00	0.2	30	30.0	1620	3.95	4.04	2.50
8.	4.00	0.2	30	30.0	1610	3.95	3.96	0.10

on the electrode and the error in the determination is diminished (Table 4).

TABLE 4

Electrolyte for copper determination:
$CuSO_4 + 0.2 g Na_2SO_4 + 80 ml H_2O + H_2SO_4$
Coulometric titration of the acid:
Catholyte: $H_2SO_4 + Na_2SO_4 + H_2O + methyl\ red$
Anolyte: $KCl + H_2O$

Experiment No.	Copper separation		Titration of the acid		Copper		Error %
	Current strength	Time in min.	Current strength	Time in sec.	Taken mg	Found mg	
1.	0.5	45	40.0	592	1.975	1.816	— 8.0
2.	0.5	45	40.0	574	1.975	1.580	— 20.0
3.	0.5	45	40.0	555	1.975	1.330	— 32.7
4.	0.5	45	40.0	576	1.975	1.605	— 18.7
5.	0.5	60	50.0	477	1.975	1.877	— 5.0
6.	0.5	60	50.0	476	1.975	1.871	— 5.3
7.	0.5	120	40.0	601	1.975	1.935	— 2.00
8.	0.5	120	40.0	606	1.975	2.00	1.33

In all the experiments in which smaller amounts of copper were found, the titrated solution was evaporated to dryness and the copper was detected my means of potassium ferrocyanide.

The indirect coulometric titration was carried out in 100 ml glass vessels. The cathode was a perforated platinum cylinder of 30 mm diameter and 50 mm height, containing holes of 1 mm diameter at distances of 1 mm. The anode was a perforated platinum cylinder of 11 mm diameter. Other accessories were the same as used in the usual coulometric titrations.

On the basis of our experiments, it may be concluded that, in indirect coulometric copper determination, the best results for copper are obtained at a current strength of 0.2 A, with or without the addition of 1 ml of 0.1 N sulphuric acid.

Institute of Physical Chemistry
and Electrochemistry
School of Technology
Beograde

REFERENCES

1. Tutundžić, P. S., and S. Mladenović. "Indirekte coulometrische Titration von Kathionen und Anionen" — *Analytica Chimica Acta*, in press.

INHIBITED DECARBOXYLATION OF OXALACETIC ACID IN THE PRESENCE OF DEOXYCHOLIC ACID IN ABSOLUTE ETHANOL

by

MILUTIN STEFANOVIĆ and STANISLAVA N. LIPOVAC

Oxalacetic acid (OAA) is known to decarboxylate in aqueous solution to form pyruvic acid (PA) with a decrease of absorbance at 260 m μ[1]. In organic solvents, however, such as absolute ethanol, after a fast initial decrease of absorbance at 260 m μ, which is interpreted as a ketonization of the enol-form of the acid[2,3], OAA shows a slow change of absorbance with time at the same wave length[4].

The fast and the slow spectral changes observed in the OAA solution can be accounted for by changes in the concentration of the absorptiometrically active enol-form of OAA:

$$\left(a \; \frac{enol}{260 \; m\mu} = 8.72 \cdot 10^3 \; cm^{-1} \; M^{-1} \; 1\right)^{(4)} \left(Eq. 1—4\right).$$

$$Enol — OAA \; \underset{}{\overset{}{\rightleftharpoons}} \; Keto — OAA \; \overset{k}{\rightarrow} \; Enol — PA + CO_2$$

$$[En] \qquad\qquad [Ke] \qquad\qquad\qquad \updownarrow \; K_2$$

$$Keto — Pa \tag{1}$$
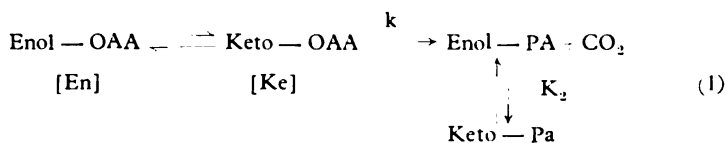
$$\frac{d \, CO_2}{dt} = k \, x \, [Ke] \tag{2}$$

$$K_1 = \frac{[Ke]}{[En]} \tag{3}$$

$$\frac{d \, CO_2}{dt} = k \, x \, K_1 \, x[En] \tag{4}$$

Where **k** is the overall rate constant of decarboxylation of the keto-form of OAA, and K_1 and K_2 are the apparent keto-enol equilibrium constants of OAA and PA, respectively.
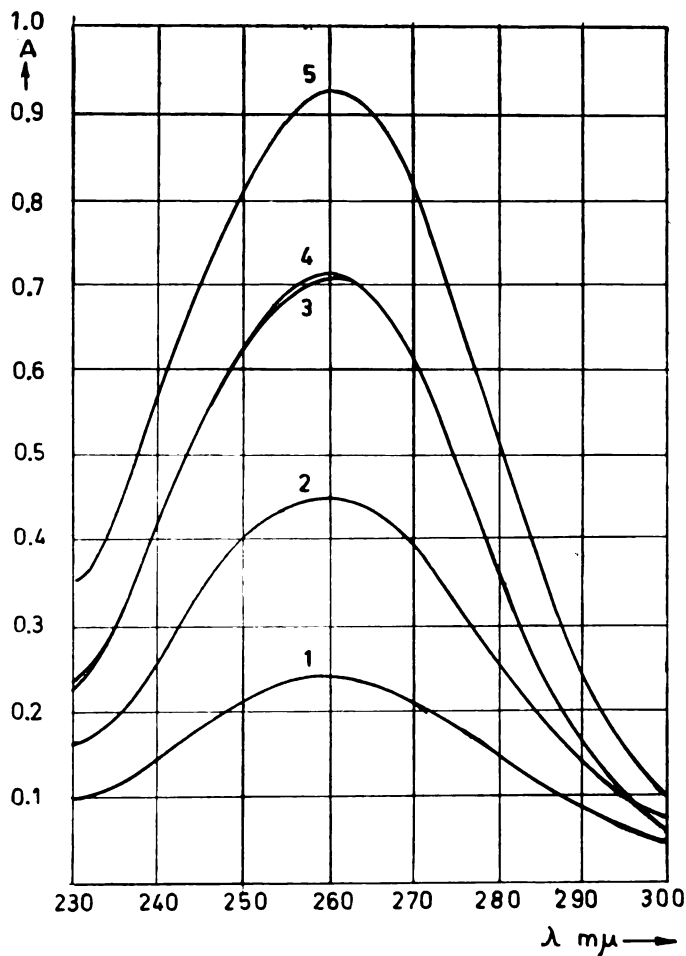
Fig. 1.

Absorption spectra of ethanol solutions of OAA in the presence of deoxycholic acid ($\alpha_D^{25°} = 53.90°$ in ethanol, m. p. 170—172°C) concentrations of OAA and concentrations of deoxycholic acid

(1)	$4 \times 10^{-5}\ M$	$16 \times 10^{-5}\ M$
(2)	$8 \times 10^{-5}\ M$	$32 \times 10^{-5}\ M$
(3)	$12 \times 10^{-5}\ M$	$48 \times 10^{-5}\ M$
(4)	$12 \times 10^{-5}\ M$	0.0
(5)	$16 \times 10^{-5}\ M$	$64 \times 10^{-5}\ M$

Spectra were recorded using a Bausch and Lomb Spectronic 505 spectrophotometer in cuvettes of 1 cm light path at room temperature within 2—4 minutes after preparation of the solutions.

Spectrophotometric measurements of OAA in absolute ethanol in the presence of deoxycholic acid in the molar ratio of 1 : 4 show that the general shape of the absorption spectrum of OAA remains unchanged with its characteristic maximum at 260 mμ. (Fig. 1). The apparent absorptivity of such solutions, 2—4 minutes after their preparation, is the same in the presence and in the absence of deoxycholic acid, that is, a_p 260 mμ $= 5.66$ x 10^3 cm^{-1} M^{-1} 1. However, the slow change of the absorbance at 260 mμ, which reflects the change of the concentration of the enol-form of OAA (Eq. 4) due to decomposition of the keto-form of OAA[5,6], is different depending upon the concentration of deoxycholic acid in the ethanol solution. The relative rate of the absorbance changes of OAA is lower in the presence of deoxycholic acid and has a minimum value when the molar ratio of deoxycholic and oxalacetic acid lies between 2 and 4 (Fig. 2).
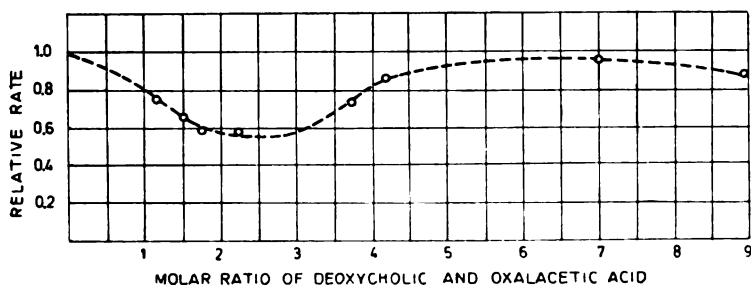
Fig. 2.

Relative rate of absorbance change calculated as a ratio of the initial slopes of the first order plots of log $A_t^{260\ mμ}$ $-f(t)$ and log $A'^{260\ mμ}_t = f(t)$ in the absence and in the presence of deoxycholic acid in the respective molar ratios. Each cuvette (1 cm light path) initially contained $7 \times 10^{-5} M$ of OAA. Measurements were made at $25° \pm 0.1°$ C using a Unicam SP. 500 spectrophotometer with a constant temperature cell holder.

The decrease of the absorbance change with time at 260 mμ upon the addition of deoxycholic acid in the optimal concentration can be accounted for by (*i*) slower ketonization of the enol-form of OAA, or by (*ii*) slower decarboxylation of the keto-form of OAA. If deoxycholic acid would slow down enol-keto interconversion of OAA in such a manner that this process becomes a rate determining step, the apparent absorptivity (a_p) of OAA would change immediately in the presence of deoxycholic acid. Therefore, the explanation cited above under (*ii*) — that is, decreasing rate of decarboxylation of OAA in the presence of deoxycholic acid (molar ratio 2—4) — seems to be the more pertinent.

The mode of possible decarboxylation inhibition of OAA in absolute ethanol by menas of deoxycholic acid is not yet clear. However, the existence of inclusion compounds in the solutions was proposed[7], and therefore it might be assumed that the possible orientation of deoxycholic acid molecules around OAA could probably lower the

rate of decomposition, increasing the free energy of activation of the active species of OAA in decarboxylation. Further, the appearance of the helical complex of macromolecular dimensions of sodium deoxycholate in aqueous solution buffered with glycilglycine[8] and similar phenomena that we have observed in the concentrated ethanol solution of deoxycholic acid after heating may support our assumption that some inclusion in the solution could stabilize decomposition of the moiety included. Our preliminary experiments show that OAA as "guest" and deoxycholic acid as "host" can form a crystalline inclusion compound in the molar ratio of about 1 : 4.

School of Science
Institute of Chemistry
and Physical Chemistry
Beograd

REFERENCES

1. Kosicki, G. W., and S. N. Lipovac. — *Canadian Journal of Chemistry* 42: 403, 1964.

2. Banks, B. — *Journal of the Chemical Society* 63, 1962.

3. Gruber, W., Peliciderer, G., and Wieland, T. — *Biochemische Zeitschrift* 328: 245, 1956.

4. Kosicki, G. W., and S. N. Lipovac, in: XI *Colloquium Spectroscopicum Internationale, Belgrade* — 1963.

5. *Steinberger*, R., and F. H. Westheimer. — *Journal of the American Chemical Society* 71: 4158, 1949; *ibid.* 73: 429, 1951.

6. Pedersen, K. J. — *Acta Chemica Scandinavica* 6: 285, 1952.

7. Cramer, F. *Einschlussverbindungen* — Berlin: Springer-Verlag, 1954., p. 86.

8. Rich, A., and D. Blow. — *Nature* 182: 423, 1958.

SPECTROPHOTOMETRIC DETERMINATION OF VITAMIN K₃ (MENADIONE) IN MENADIONE-SODIUM BISULPHITE PREPARATIONS

by

VILIM J. VAJGAND and FILIP S. UVODIĆ

Vitamin K_3 (menadione, menaphthone) is the most active compound of the vitamin K group. Its structure is 2-methyl$-1,4$-naphthoquinone
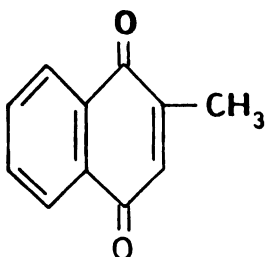
It is a light-yellow crystal substance, insoluble in water, partially soluble in alcohol and easily soluble in oils. Its melting point is from $105-107°C$.

Recently the bisulphite derivative of menadione has been more frequently used in therapy:
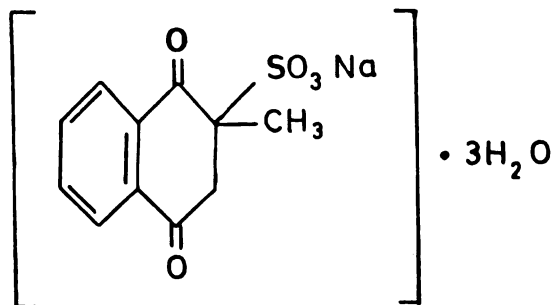
Distinct from menadione, it is insoluble in alcohol and easily soluble in water.

Besides other methods (cerimetric and polarographic), a great number of colorimetric procedures for the determination of menadione have been published. We shall only mention those most frequently used:

1. Determination with 2,4-dinitrophenylhydrazine in ammoniacal solutions[1];

2. Determination with ethyl ester of cyanacetic acid in ammoniacal solutions[2];

3. Determination with hydrochloric acid and zinc chloride in alcoholic solutions[3].

Vitamin K_3 cannot be directly determined from $K_3.NaHSO_3$. Menadione is first precipitated with the addition of sodium hydroxide, extracted with some organic solvent which is evaporated, the residue dissolved in a suitable solvent, and finally determined[4]. This procedure is time-consuming, it requires a large quantity of substance for investigation (more than 50 mg), and during the operation there may be losses which cause lower results compared with the theoretical ones. This prompted us to develop a direct polarographic method for the determination of bisulphite forms of menadione[5] which is fast and accurate and therefore allows the determination of 2—8 mg aliquots.

Proceeding with the study of this problem, we developed a new spectrophotometric method by which it is possible to determine with sufficient accuracy 0.03 to 0.05 mg of vitamin K_3 and even smaller amounts.

EXPERIMENTAL PROCEDURE

USP standard menadione and a sample of 98.5% declared purity "Merck" menadione (for biological purposes) were used. The purities of both samples were checked by the standard method[4], the titration being performed in an inert atmosphere[6]. Sodium bisulphite was checked iodometrically for content of SO_2. The solutions for spectrophotometric determination were prepared with absolute alcohol and Britton-Robinson buffers, which were checked on a "Radiometer PHM 22r" pH-meter. All spectra were recorded on a UNICAM SP-500 spectrophotometer with checked quartz cells and a light path 1000 cm long.

As far as we know, no description of a spectrophotometric method for direct determination of menadione in its bisulphite compounds has been published so far. This work is an attempt to develop a suitable method of determining the bisulphite form of vitamin K_3 using pure menadione as the primary standard.

In order to follow the spectrophotometric behavior of vitamin K_3 (soluble in ethanol) and $K_3.NaHSO_3$ (water soluble only), we used 20% alcohol solutions as the solvent.

We had noticed that the absorptivity* of vitamin $K_3.NaHSO_3$ changes with the pH of the solution, so we used buffer mixtures with Britton-Robinson buffer solutions. We studied the behavior of vitamin $K_3.NaHSO_3$ in 20% alcohol solutions of Britton-Robinson buffers at different pH (Fig. 1), and noticed that at pH below 6 there are two maxima, at 231 mµ and 265 m µ, which are characteristic for $K_3.NaHSO_3$
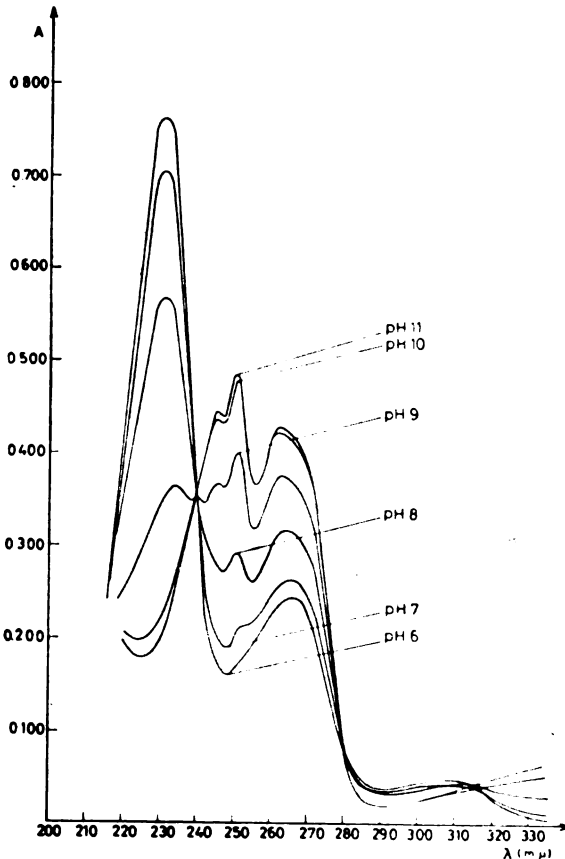
Fig. 1

In solutions with a pH above 6, two new maxima appear, at 251 mµ and 245 m µ, characteristic for pure vitamin K_3. Finally, at pH values above 9 there are only the last two maxima, while the maxima of vitamin $K_3.NaHSO_3$ disappear, which proves the presence of menadione only. In Britton-Robinson buffer of pH 7, vitamin $K_3.NaHSO_3$ gives maxima which indicate the presence of both menadione and its bisulphite form, so we chose this pH of the solution.

---

* (older expression) — $E_{1\ cm}^{1\%}$ — specific extinction coeficient

To express the results of vitamin K_3.NaHSO$_3$ with a calibration curve, we studied the behavior of vitamin K_3 in the presence of gradually increasing amounts of sodium bisulphite. We made 20% alcohol solutions of menadione in Britton-Robinson buffer of ph 7, concentration 2.10^{-5} M/l, with the addition of increasing amounts of sodium bisulphite in concentrations varying from 1.10^{-5} to 4.10^{-4} M/l, or $0.5 - 20$ times the concentration of vitamin K_3. Figure 2 shows htat the maximum at 251 mμ disappears only with a twelve-fold excess of sodium bisulphite.
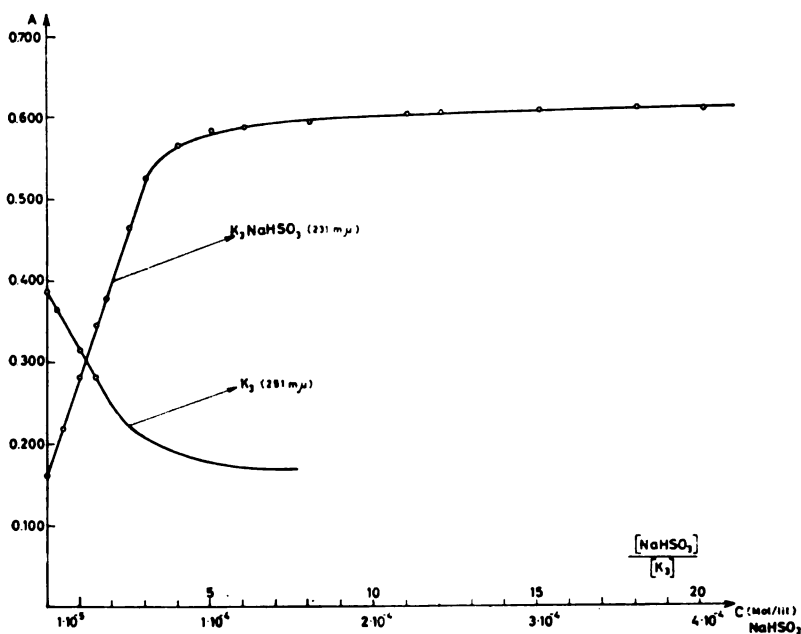
Fig. 2

Figure 3 shows the decreasing height of the maximum of menadione at 251 mμ and the increasing height of the maximum of its bisulphite form at 231 mμ with the addition of sodium bisulphite.

The solutions for the calibration curve were prepared by weighing equal amounts of the reference standard menadione dissolved in absolute alcohol, the concentration of which varied from 2.10^{-6} to 2.10^{-5} M/l. Sodium bisulphite was added so that its concentration in all solutions was 15 times that of the menadione. Finally the solutions were made up to the mark with the buffer. The amount of alcohol in the final standard solutions was always 20%.

The test samples were prepared in the same way.

Curve (g) $2 \cdot 10^{-5}M/1$ menadione
Curve (f) $2 \cdot 10^{-5}M/1$ menadione + $1 \cdot 10^{-5}M$ NaHSO$_3$
Curve (e) $2 \cdot 10^{-5}M/1$ menadione + $2 \cdot 10^{-5}M$ NaHSO$_3$
Curve (d) $2 \cdot 10^{-5}M/1$ menadione + $3 \cdot 10^{-5}M$ NaHSO$_3$
Curve (c) $2 \cdot 10^{-5}M/1$ menadione + $4 \cdot 10^{-5}M$ NaHSO$_3$
Curve (b) $2 \cdot 10^{-5}M/1$ menadione + $6 \cdot 10^{-5}M$ NaHSO$_3$
Curve (a) $2 \cdot 10^{-5}M/1$ menadione + $24 \cdot 10^{-5}M$ NaHSO$_3$
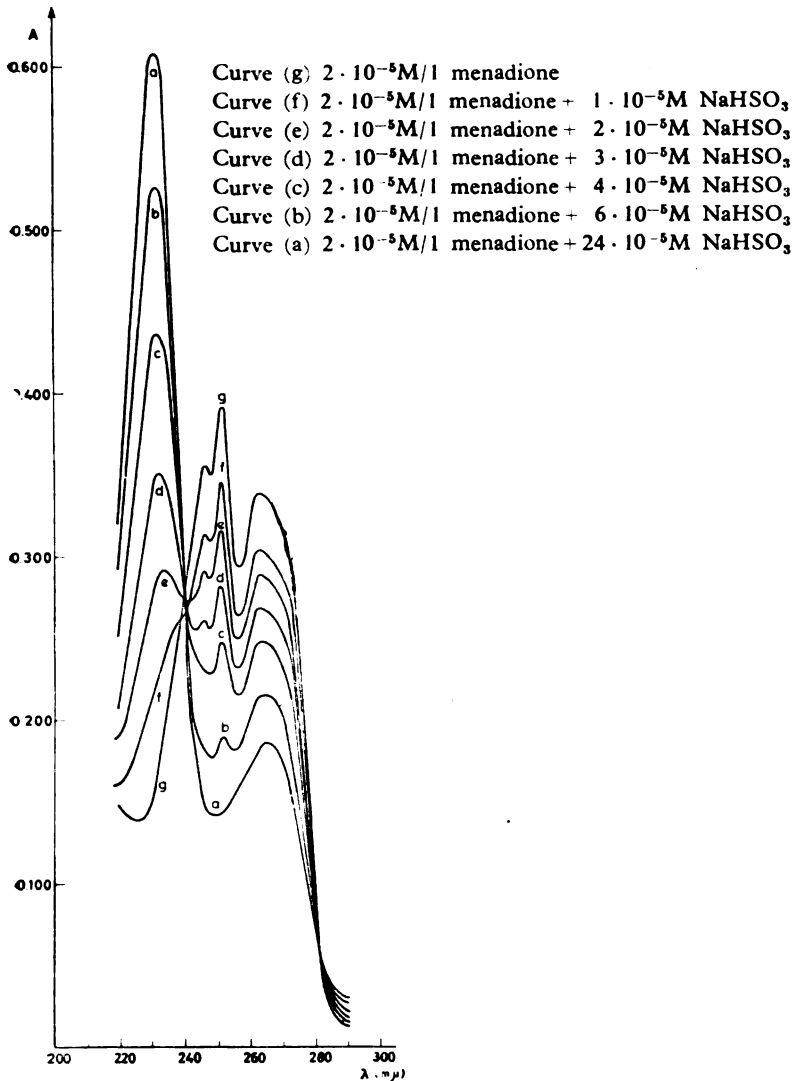
Fig. 3

The amount of K_3 in K_3.NaHSO$_3$ samples was first determined spectrophotometrically. The results are shown in Table 1 together with the results obtained by the USP method.

The content of vitamin K_3 in injection solutions claiming to contain 10 mg of vitamin K_3.NaHSO$_3$/ml was determined. The results are given in table 2 together with those obtained by the USP method.

4

TABLE 1

DETERMINATION OF THE CONTENTS OF MENADIONE IN SAMPLES
OF RAW MATERIALS OF MENADIONE-SODIUM BISULFITE

Sample	Spectrophotometric method				USP method			
	Taken mg $K_3 \cdot NaHSO_3$ in aliquot	Found mg K_3	% K_3 in $K_3 \cdot NaHSO_3$	Mean	Taken mg $K_3 \cdot NaHSO_3$	Found mg K_3	% K_3 in $K_3 \cdot NaHSO_3$	Mean
1	0.0274	0.0145	52.9		300.0	151.2	50.4	
	0.0392	0.0205	52.3	52.9	300.0	154.7	51.6	50.7
	0.0529	0.0283	53.5		300.0	150.3	50.1	
2	0.0274	0.0146	53.3		300.0	153.0	51.0	
	0.0392	0.0208	53.1	53.4	300.0	155.0	51.7	51.2
	0.0529	0.0284	53.7		300.0	153.3	51.0	
3	0.0274	0.0144	52.6		300.0	150.5	50.2	
	0.0392	0.0205	52.3	52.8	300.0	151.1	50.4	50.6
	0.0529	0.0283	53.5		300.0	153.4	51.1	

TABLE 2
DETERMINATION OF CONTENTS OF MENADIONE IN MENADIONE -SODIUM BISULFITE INJECTIONS

Injections contain 10 mg of Menadione-Sodium Bisulfite/ml

Sample	Spectrophotometric method					USP method				
	Taken mg $K_3 \cdot NaHSO_3$ in aliquot	Found mg K_3	% K_3 in $K_3 \cdot NaHSO_3$	mg K_3/ml	Mean	Taken mg $K_3 \cdot NaHSO_3$	Found mg K_3	% K_3 in $K_3 \cdot NaHSO_3$	mg K_3/ml	Mean
1	0.0274	0.0142	51.8	5.18	5.13	50.0	35.3	50.6	5.06	5.06
	0.0392	0.0200	51.1	5.10			25.3	50.6	5.06	
	0.0529	0.0271	51.2	5.13		50.0				
2	0.0274	0.0141	51.5	5.15	5.14	50.0	27.3	54.6	5.46	5.31
	0.0392	0.0200	51.0	5.10			25.8	51.6	5.16	
	0.0529	0.0274	51.8	5.18		50.0				
3	0.0274	0.0146	53.3	5.33	5.35	50.0	26.5	53.0	5.30	5.35
	0.0392	0.0209	53.3	5.33			27.0	54.0	5.40	
	0.0529	0.0285	53.9	5.39		50.0				

4*

The content of vitamin K_3 in coated tablets claiming to contain 10 mg of vitamin $K_3.NaHSO_3$ per tablet was also determined. The results have not been compared, because USP-XVI does not give a method for the determination of $K_3.NaHSO_3$ in coated tablets. The results are shown in Table 3.

TABLE 3

DETERMINATION OF CONTENTS OF MENADIONE IN MENADIONE
-SODIUM BISULFITE COATED TABLETS

Coated Tablets contain 10 mg Menadion-Sodium Bisulfite

SPECTROPHOTOMETRIC METHOD					
Sample	Taken mg $K_3 \cdot NaHSO_3$ in aliquot	Found mg K_3	$\% K_3$ in $K_3 \cdot NaHSO_3$	mg K_3 per tablet	Mean
1	0.0274	0.0140	51.1	5.11	5.13
	0.0392	0.0200	51.0	5.10	
	0.0529	0.0274	51.8	5.18	
2	0.0274	0.0145	52.9	5.29	5.32
	0.0392	0.0208	53.1	5.31	
	0.0529	0.0283	53.6	5.36	
3	0.0274	0.0140	51.1	5.11	5.10
	0.0392	0.0199	50.8	5.08	
	0.0529	0.0271	51.2	5.12	

Comparison of the results obtained by this method with those obtained polarographically[5] shows good agreement. However, as expected, slightly lower results were almost always obtained by the official method[4], because the large number of operations cause losses. This points out the advantage of the newly-developed polarographic and spectrophotometric methods, which allow direct determination of vitamin K_3 in the preparations.

Received July 14, 1965.

REFERENCES

1. *The National Formulary*. XI edition — Washington: American Pharmaceutical Association, 1960, 201—202.
2. Kofler, M. "Fluorimetrische und colorimetrische Bestimmung von 2-Methyl-1, 4-naphthochinon" — *Helvetica Chimica Acta* (Basel) 28: 702—713, 1945.
3. Bandelin, J. F., and E. R. Pankratz. "The Colorimetric Determination of Menadione" — *Drug Standards* (Washington) 27: 36—39, 1959.
4. *The United States Pharmacopeia*, 16th rev. — Easton, Pa: Mack Publishing Company, 1960, p. 402.
5. Vajgand, V., and F. Uvodić. "Polarographic Determination of Vitamin K_3 (Menadione) in Menadione-Sodium Bisulphite Preparations" — *Glasnik hemijskog društva* (Beograd) To be published.
6. *British Pharmacopeia* — London: Direction of the General Medical Council, 1963, pp. 467—470.

DYNAMIC ADSORPTION AND DESORPTION OF VAPORS OF ORGANIC SOLVENTS ON ACTIVATED CHARCOAL AND SILICA GEL. I

by

SLOBODAN K. KONČAR-ĐURĐEVIĆ and IVANKA P. PETKOVIĆ

As far as we know and as confirmed by other authors[1], there is insufficient data in the literature on the rate of the dynamic adsorption of vapors on solid granular adsorbents. E. Wicke[2] investigated the rate of adsorption and desorption of gases on porous materials — studying the effect of porosity and local temperatures on it, and giving an empirical formula for desorption curves as a function of characteristic flow rate constants, layer thickness and length of time.

J. Elston Ahlberg[3] investigated the dynamic adsorption of water vapor in a gaseous medium which does not condense on granular silica gel, and he found that it depends on the temperature, the partial vapor pressure, the gas flow rate, the quantity of vapor already adsorbed, the grain size of the adsorbent and the thickness of the layer adsorbed. S. Crespi[4] studied the dynamic adsorption and desorption of water vapor in air on silica gel, pying special attention to the effect of the air flow rate, humidity distribution, gel position and dynamic desorption. The purpose of the present work was to investigate the adosrption and desorption rates of vapors of different concentrations from an indifferent gaseous carrier of constant flow rate. We also wished to investigate the effect of temperature on the phenomenon studied, expecting the result of two concurrent effects of opposite tendencies: the effect of changed diffusion rate and changed adsorption capability.

Of the above factors influencing the adsorption rate — and obviously also the desorption rate — we investigated in more detail the effect of the nature of some adsorbents (silica gel and activated charcoal), adsorptives (benzene, alcohol, tri-chlor-ethylene), concentrations and temperatures, with constant layer thickenss of the adsorbent, grain size and flow rate.

EXPERIMENTAL PROCEDURE

The apparatus used (Fig. 1) consists of a compressor (1) which conducts air into a reservoir (2) in order to damp pressure oscillations. From it the air is led through tube T and by taps 12 and 12′ the desired
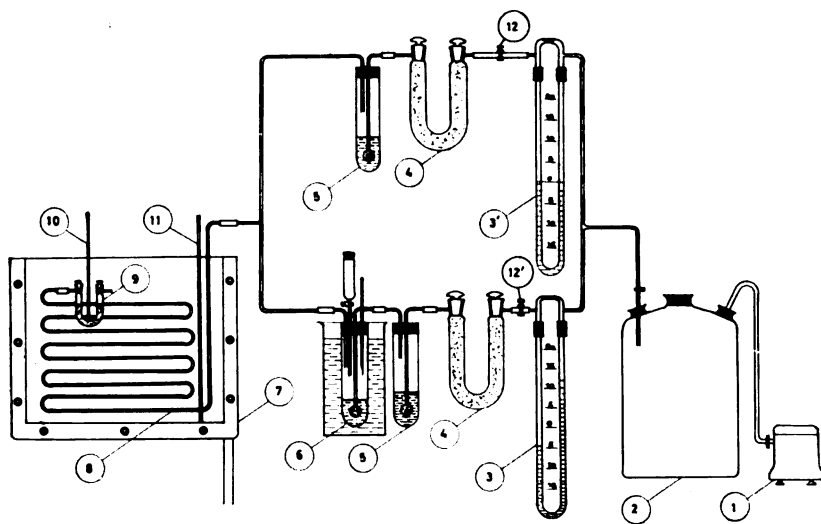
Fig. 1

1. Centrifugal compressor
2. Gas tank
3& 3) Manometers
4) U-tube with CaCl$_2$
5) Wash bottle with conc. H$_2$SO$_4$

6) Adsorbate vessel
7) Thermostat
8) Glass tube spiral
9) U-tube with the adsorbent
10) Thermometer

11) Stirrer

volume is let into tube system I or II. After passing through manometers 3 and 3' for flow-rate determination, the air passes through waterless CaCl$_2$ (4) and conc. H$_2$SO$_4$ (5) to dry. In tube I there is a thermostat with a vessel (6) containing a liquid organic solvent through which dry air passes, becoming saturated with its vapors. The saturated air from tube I mixes with the pure dry air from tube II. It enters the thermostat containing water and, passing through the long tube system (8), it gets to the temperature of the thermostat and then enters into the U-tube (9) containing the adsorbent. The temperature of the thermostat is measured with a thermometer (10) in the immediate vicinity of the vessel containing the adsorbent.

The ratio at which air saturated with vapor was mixed with pure air depended on what partial vapor pressure in the mixture adsorbed was to be obtained. From our investigations, we concluded that, because of good dispersion, the air which passes through the solvent contained in vessel (6) is almost saturated with vapors of the solvent. We also found that the air flow rate has no considerable effect on air saturation. Therefore we considered that the air coming out from the vessel (6) was vapor saturated, i.e., for a given temperature it had a partial pressure which corresponded to the vapor pressure of the solvent. The desired lower concentrations of solvent vapors were obtained by adding pure dry air to the vapor saturated air coming out of tube I. In determining the amounts of pure and saturated

air, we had to take account not only of the resulting partial vapor pressure, but also of the total amount of gaseous mixture obtained. Since the work was done at a constant flow rate, we had to adjust the definite volume of air so that it would be constant, so that the condition of equal flow rate would be fulfilled throughout the different experiments. In this calculation we did not take into account the increase of volume because of the presence of the solvent vapors, since even if wrok was done most carefully the mixture flow rate would change, because at the beginning of adsorption the vapors are almost quantitatively adsorbed, while at the end, almost unadsorbed, they leave the adsorption vessel without any change in the mixture volume. This difference is much more pronounced at higher vapor concentrations.

Granular activated charcoal of unknown origin and silica gel prepared in our own laboratory (5) were used as the adsorbents. Before use the adsorbents were sifted and the fraction $-4+5$ mesh to DIN 1171 was kept. Therefore, the grain size varied from $1.2-1.5$ mm.

Before adsorption we always degassed the adsorbent with dry air to a constant weight: activated charcoal at 120°C and silica gel at 250°C, for 2.30 and 4 hours, respectively. Portions of $3-4$ grams of adsorbent were always used.

The solvents were: benzene-C_6H_6, alcohol-C_2H_5OH and trichlor-ethylene-$CHCl:CCl_2$. They were first predistilled and the fraction boiling at 87.2°C was taken. As is seen, we used pure hydrocarbon, alcohol and unsaturated substituted hydrocarbon. Polar and nonpolar adsorptives were used.

Desorption was tested immediately after adsorption and it was carried out by passing dry air, always at the same flow rate of about 0.394 l/min, through the adsorbent, which was in the U-tube, in the thermostat at the same temperature at which adsorption was performed.

During adsorption and desorption the change in the weight of the adsorbent was measured every fifteen minutes. Only at the beginning of adsorption the change was determined every five minutes for the first three points of the adsorption rate curve.

RESULTS

Adsorption of benzene on silica gel at 25°C

The adsorption rate was measured for four cases in which the partial pressure of benzene vapor in the mixture changed while the flow rate remained constant. The results are shown in Graph. 1.

Curve I represents the adsorption rate at the partial pressure of benzene vapor $p_1 = 95$ mm Hg. In this case and in all the following adsorptions the flow rate was about 0.366 l/min. For curve II, $p_2 = 64.71$ mm Hg; for curve III$_{bis}$, $p_3 = 40.87$ mm Hg; for curve IV, $p_4 = 22.39$ mm Hg. Corresponding desorption curves are shown in Graph. 2.
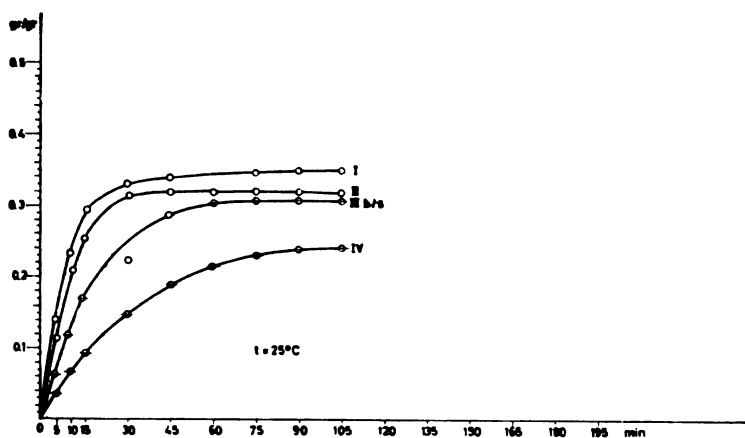
Graph 1.

Adsorption of benzene on silica gel at 25°
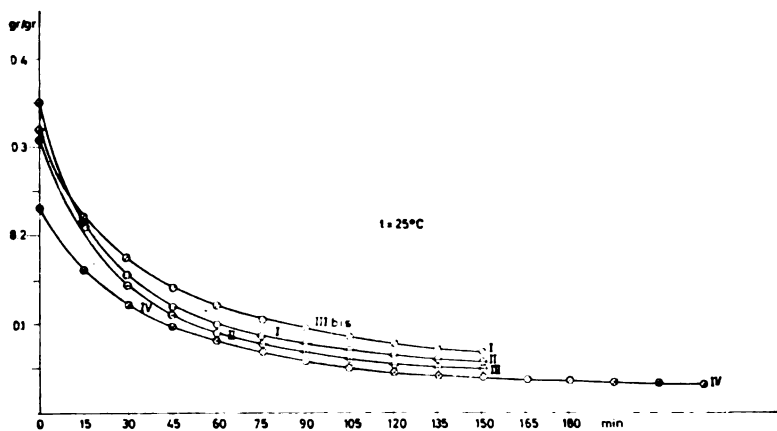
Graph 2.

Desorption of benzene from silica gel at 25°

Adsorption and desorption of tri-chlor-ethylene on silica gel at 25°C.

Graph 3 shows the adsorption rate of tri-chlor-ethylene vapor on silica gel.

For curve I, $p_1 = 73$ mm Hg; for curve II, $p_2 = 49.78$ mm Hg; for curve III, $p_3 = 30.9$ mm Hg; for curve IV, $p_4 = 17.16$ mm Hg. The corresponding partial pressures of tri-chlor-ethylene in the mixture for curves VI and VIII were $p_6 = 8.73$ mm Hg and $p_8 = 3.95$ mm Hg.
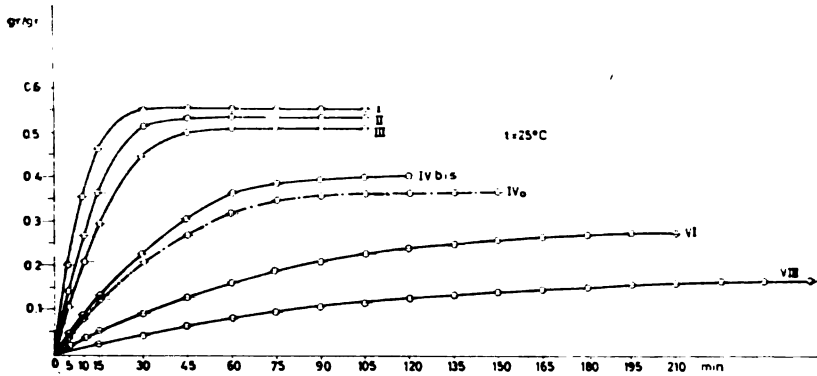
Graph 3
Adsorption of tri-chlor-ethylene on silica gel at 25°
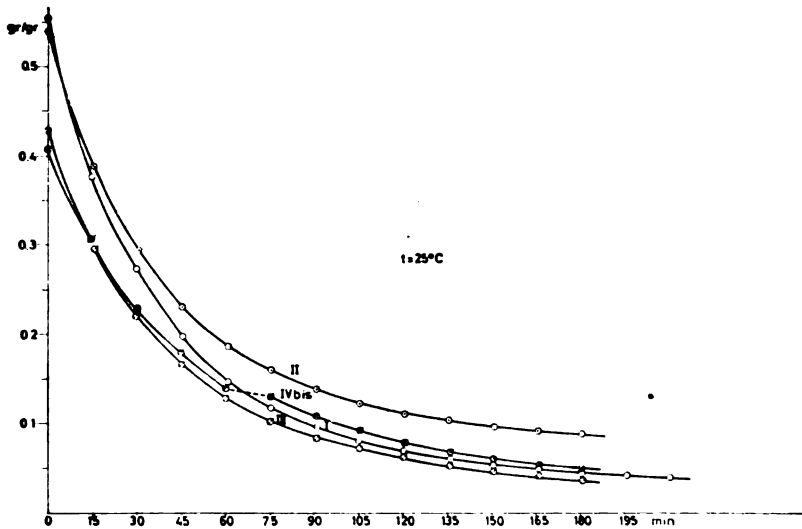
Graph 4
Desorption of tri-chlor-ethylene from silica gel at 25°

This graph also shows the change in the adsorption power with the age of the silica gel. Curves IV_{bis} and IV_0 were recorded under absolutely the same conditions, except that curve IV_0 was recorded four months after curve IV_{bis}. As is seen, adsorption power decreases with the age of the silica gel[6]. Desorption is shown in Graph 4.

It is interesting to examine the fourth case of tri-chlor-ethylene desorption on silica gel: after recording a few points, between 60 and 75 min, in putting the U-tube with silica gel in its usual place in the apparatus, we accidently placed the input of the U-tube where
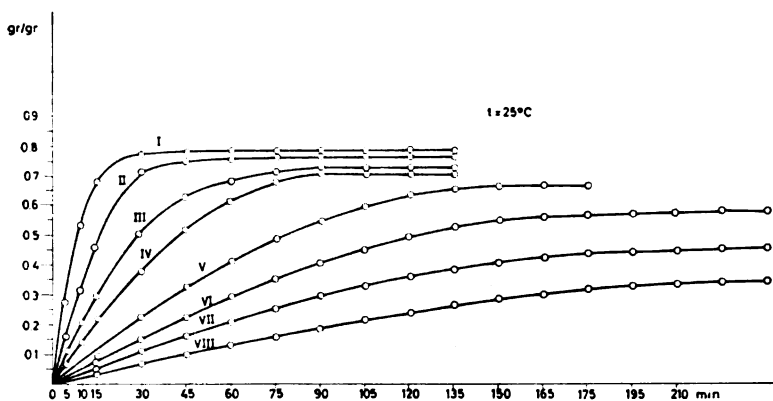
Graph 5

Adsorption of tri-chlor-ethylene on active carbon at 25°
(I : p · 73 mm Hg, II : p 50 mm Hg, III : p = 31.29 mm Hg, IV : p =
= 16.02 mm Hg, V : p = 11.54 mm Hg, VI : p = 7.8 mm Hg, VII : p =
= 6.61 mm Hg, VIII : p = 3.60 mm Hg).
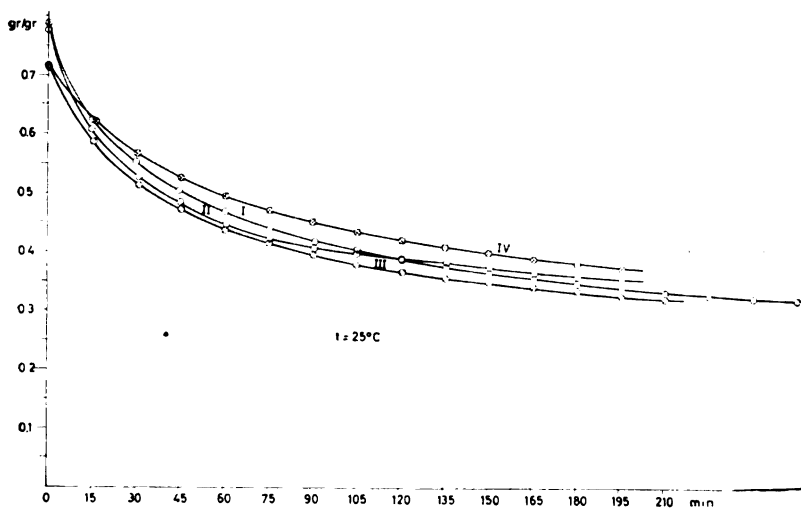
Graph 6

Desorption of tri-chlor-ethylene from active carbon at 25°

the output should have been. This exchange caused a jag in the conti-
nuity of the curve, which shows that the gradient of adsorptive con-
centration in the adsorbent influences the shape of the desorption curve.

*Adsorption and desorption of tri-chlor-ethylene on activated charcoal
at 25°C.*

The shapes of the curves are the same as in the preceding ad-
sorptions, except for the activated charcoal, which shows higher
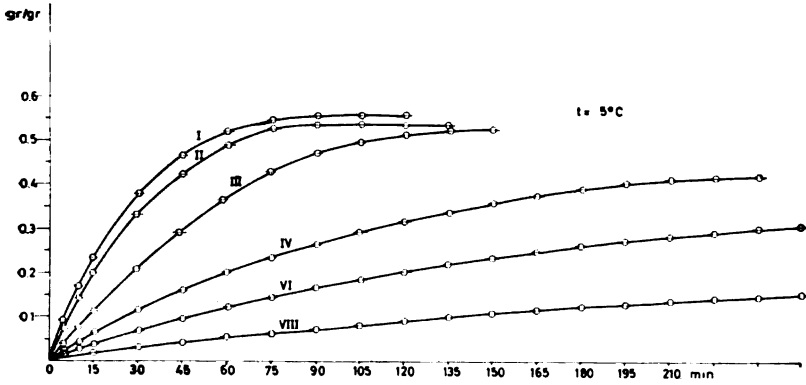
Graph 7

Adsorption of tri-chlor-ethylene on silica gel at 5°

(I : p = 24.8 mm Hg, II : p = 18.02 mm Hg, III' : p = 9.72 mm Hg, IV : p = = 5.95 mm Hg, VI : p = 3.56 mm Hg, VIII : = 1.24 mm Hg)
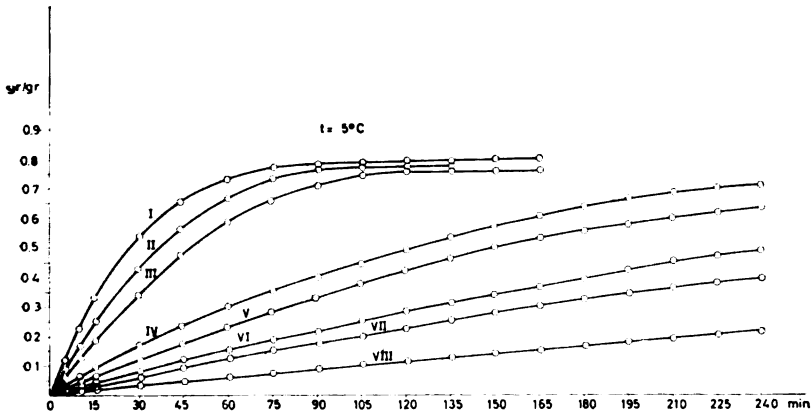
Graph 8

Adsorption of tri-chlor-ethylene on active carbon at 5°

(I : p = 24 mm Hg, II : p = 18.92 mm Hg, III : p = 11.20 mm Hg, IV : p = 5.73 mm Hg, V : p = 3.58 mm Hg, VI : p = 3.27 mm Hg, VII : p = 2.20 mm Hg, VIII : p = 1.20 mm Hg)

adsorption power for tri-chlor-ethylene than silica gel. From these graphs, as well as from the preceding ones, it is seen that the first isothermal adsorption rates have a sharp rise. With lower and lower partial pressures and concentrations, the establishment of equilibrium is slower and slower, and the rise of adsorption isotherms more gradual, i.e., the parabolic shape gradually disappears.

We next investigated dynamic adsorption at 5°C.

Adsorption and desorption of tri-chlor-ethylene vapor on silica gel and activated charcoal at 5°C.

It is known that with lower and lower vapor concentrations in the mixture the adsorption rate curves lose their parabolic shape and gradually become linear shape. We were interested in whether this linearity can be obtained. This meant that it was necessary to get into the range of very low partial vapor pressures, i.e. concentrations. In the case of silica gel we obtained an approximate linearity for $p = 1.24$ mm Hg, while activated charcoal gave an almost complete linearity at $p = 1.20$ mm Hg.

Comparing Graphs 7 and 8 with the corresponding Graphs 3 and 5 at 25°C, it can be seen that the shape of the adsorption isotherms is in fact the same, except that the adsorbed quantity is smaller at the beginning of adsorption and larger at the end. Because of this, the slope of these adsorption isotherms is smaller than of those at 25°C. At a lower temperature the vapor pressure is also smaller, therefore, in the beginning, the adsorption is smaller because a smaller quantity of vapor contacts the adsorbent per unit time.

At the time of recording the adsorption isotherms we also measured desorption for every other case (II, IV, VI and VIII) at 5°C. The desorption curves are shown in Graphs 9 and 10.
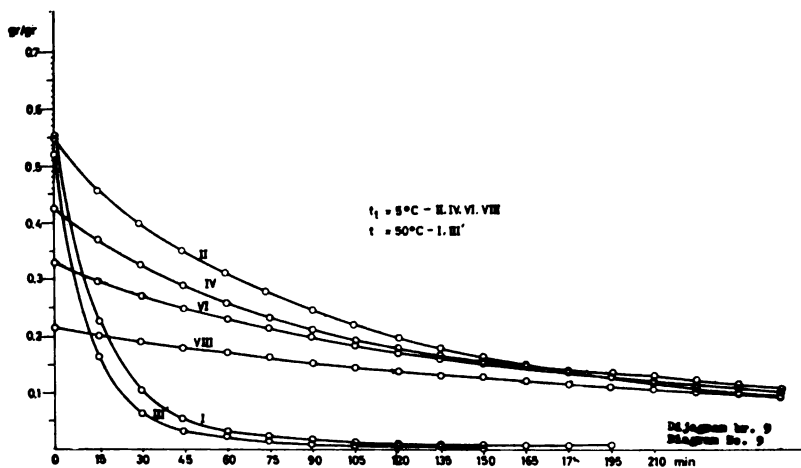
Graph 9
Desorption of tri-chlor-ethylene from silica gel at 5°

From these graphs it can be seen that the quantity desorbed is still smaller and desorption is slower at 5°C than at 25°C. In addition, the curves show a very sharp decrease of desorption power by a considerable value of the adsorptive concentration in the adsorbent. The time required for adsorption and desorption at 5°C is longer than that required at 25°C. The difference is greater the smaller the concentration.

Graph 10 shows a change in the desorption power for curves I and III, for which desorption was carried out at 50°C, which is not the same temperature at which adsorption was carried out. We see that with such an increase of temperature not only does desorption last a shorter time, but it is also more complete, almost quantitatively.

If we observe the durations of the adsorption and desorption processes, we see that desorption always lasts longer. E. Wicke[7] also reports that the difference between the adsorption and desorption
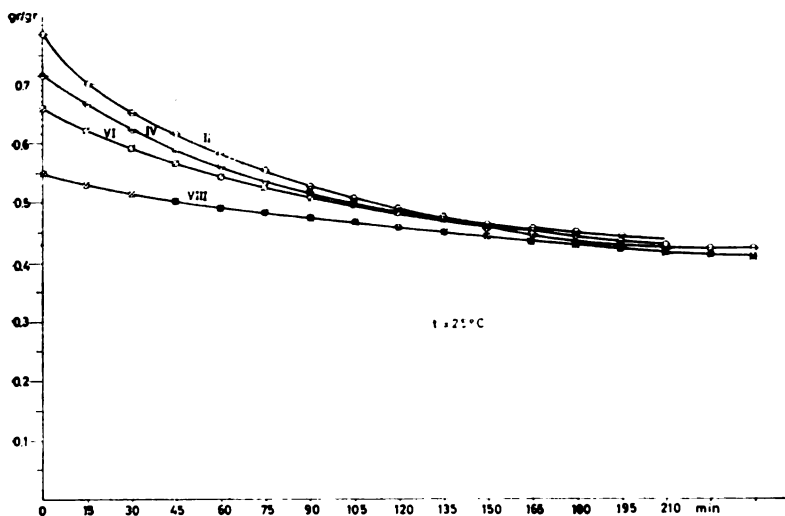
Graph 10.

Desorption of tri-chlor-ethylene from active carbon at 5°

rates is particularly great in dynamic processes, which is of special importance in the technical application of adsorption. It is a law that desorption is faster in the beginning if the previously adsorbed quantity of vapor was larger. The remaining quantity of undesorbed vapors does not seem to depend on the quantity of vapors previously adsorbed, and in a visible time, at a given temperature, the desorption rate tends to a certain common extreme value.

Faculty of Technology
Institute of Chemical Engineering
Beograd

REFERENCES

1. Crespi, S. "Contribution expérimentale a l'étude de l'adsorption et de la désorption dynamique de la vapeur d'eau par le gel silica" (Suite et fin).

2. Wicke, E. "Empirische und theoretische Untersuchungen der Sorptiongeschwindigkeit von Gasen an porösen Stoffen II" —*Kolloid-Zeitschrift* 86: 295—313, 1939.

3. Ahlberg, J. E. "Rates of Water Vapor Adsorption from Air by Silica Gel" — *Industrial and Engineering Chemistry* (Washington) 31: 988—992, 1939.

4. Crespi, S. "Contribution expérimentale a l'étude de l'adsorption et de la désorption dynamique de la vapeur d'eau par le gel de silica". — *Chaleur et Industrie* (Paris) (284): 53—58, 1949.

5. Krczil, F. "Herstellung von Kieselsäuregel" — *Kolloid-Zeitschrift* 77: 146—152, 1936.

6. Gyani, B. P. "Adsorption of Alcohol on Silica Gel" — *Journal of the Indian Chemical Society* (Calcutta) 27(11): 577—585, 1950.

7. Wicke, E. "Empirische und theoretische Untersuchungen der Sorptiongeschwindigkeit von Gasen an porösen Stoffen II" — *Kolloid-Zeitschrift* 86: 295—313, 1939.

8. Weyde, E. und E. Wicke. "Die Destalt der Sorptionsflaschen bei der Ad- und Desorption unter verschiedenen Bedingungen — *Kolloid-Zeitschrift* 90: 156—171, 1940.

9. Wicke, E. "Untersuchungen über Ad- und Desorptionsvorgange in körnigen, durchströmten Adsorberschichten" —*Kolloid-Zeitschrift* 93: 129—157, 1940.

ELECTRON MICROSCOPIC INVESTIGATION OF THE POROUS STRUCTURE OF THE VANADIUM CATALYST FOR THE OXIDATION OF SULFUR DIOXIDE*

by

DRAGOMIR KARAULIĆ, ŽARKO JOVANOVIĆ and ANA TERLECKI

INTRODUCTION

Many elements and their compounds have been investigated as catalysts for the oxidation of sulfur dioxide (alloys of silver, gold, platinum, molybdenum, natural clay with large contents of oxides of iron, nickel, cobalt, bromine, copper, their mixtures in various combinations, etc.), and only two of them, platinum and vanadium oxide, are industrially important[1,8,9]. The catalytic activity of platinum is much more pronounced, but its exceptional sensitivity to undesirable chemical action and its high price are considered, serious disadvantages.

In the sulfuric acid industry catalytic masses based on vanadium pentoxide are mostly used.

The activity of the vanadium catalyst during its use in sulfur dioxide oxidation is gradually decreased by the chemical and physical changes occurring on the surface. The nature of the chemical changes has not been completely investigated, because the action mechanism of the components has not been explained in detail. The schematic division of the components into active mass (V_2O_5), carrier (SiO_2) and promoters (alkaline metals) underwent considerable changes during detailed investigations of the action of variously combined masses under different conditions[3]. According to Boreskov[1], very active sulfovanadates of the metals used as promoters distributed over the surface of silicon dioxide are assumed to be formed on the surface of the catalyst. The composition of these sulfovanadates and the equilibrium conditions of mixtures of polyvanadates, sulfates and pyrosulfates at various temperatures and partial pressures of sulfur trioxide have not been accurately investigated. The aggregation state of different sulfovanadates has not been reliably determined either, since at the process temperature they could exist in the form of liquid solution or of a solid stabilized on silicon dioxide.

---

* Presented at the 34th International Congress of Industrial Chemistry, September 1963, Belgrade.

Besides the chemical conversions which lead to increased activity, the temperature and different components of the reacting gaseous mixture cause degradation of the active modifications and formation of different less active compounds. It is difficult to check and confirm the above assumption, because of the complex composition and structure of the catalyst and the complicated mechanism of the catalytic reactions which have not been fully investigated and for which there are explanations which do not support the assumption about the formation of the above mentioned inactive compounds.

The physical changes are manifold: during the action of the catalyst changes occur in the total active surface, the number, dimensions and statistical distribution of pores on the surface. Changes in the internal structure of the catalyst cause changes in the adsorption properties, hence in the activity as well.

More detailed knowledge of the structure of the vanadium catalyst during use is of great importance not only for practice, but also for elucidating the mechanism of the catalytic reaction taking place on the surface. Indirect methods of investigating the physical structure by adsorption isotherms, changes in the total porosity or by reontge-nographic investigations give a general picture of the mean values for the size, pore distribution and crystal structure of the catalyst. These results are insufficient to elucidate the properties of complex catalytic system which can represent materials with rather poorly developed or completely damaged structure. For more detailed investigation of the change of structure, we used uhe electron microscope method which allows direct investigation of the degree of dispersion and the porous structure by means of visual observations and photo-registration of magnitudes up to 20 Å.

EXPERIMENTAL PROCEDURE

The reproduced surfaces were observed on an ELMI-D.2 Carl Zeiss Jena electron microscope with a maximum possible direct enlargement of 30.000 x and a resolving power up to 20 Å. The samples were prepared by the modified method of two-phase polystyrene--carbon replicas, which proved to be suitable for manifold successive investigations of the same sample surfaces of a mass used in different time periods. This method allowed accurate recording of the surface relief without structure damage.

A vanadium catalyst used in an industrial plant was investigated, i.e., samples of the new mass, samples used in the laboratory reactor for the oxidation of sulfur dioxide for 48 hours and for 30 days, and samples used in an industrial plant for 5 years.

Parallel with the change in the catalyst porous structure, we investigated the change of activity in the reactor constructed in our laboratory, in which the reproduced working conditions are the same as the first stage of a power reactor.

RESULTS AND DISCUSSION

The porous structure of the new mass not used in the reactor is shown in Fig. 1.
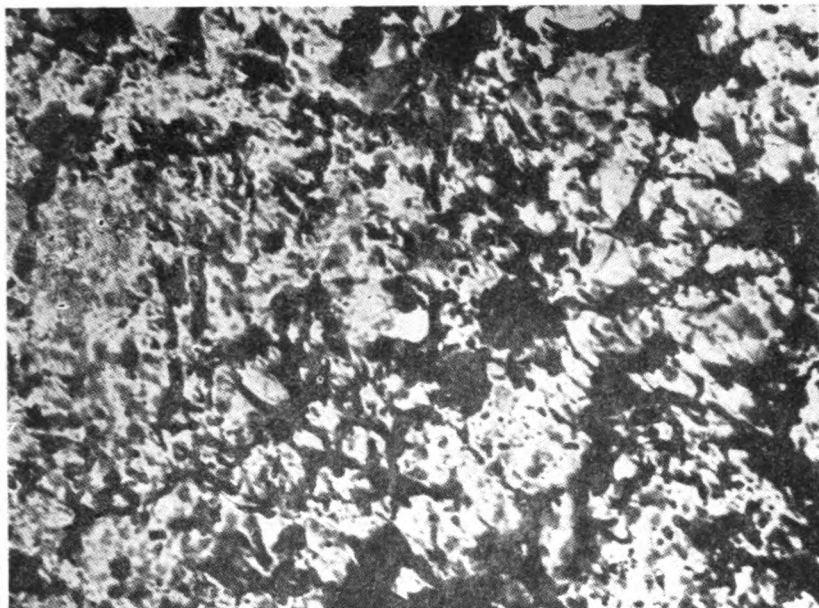
Fig. 1 — The surface of the new catalyst mass. Total enlargement 48,000 × .

Figure 1 shows the developed relief with pore holes of various dimensions. The diameters vary from several tens to several thousands of Å. The pore distribution, indicated with black dots (fields), is not uniform; in some places there are transitions between the macro pores and also in the arrangement of micro pores in them. The pore size varies from 50 Å to 1×10^{-4} cm. On the mass activated by converting a gasous mixture containing about 1% sulfur dioxide for 8 hours, no changes were observed in the porous structure. The pore distribution was about the same as that of the new mass. The slight deviations are within the limits of error proceeding from the reproduction of the investigated material.

Considerable changes were observed on the surface relief of the catalyst used in the laboratory reactor for 48 hours. A detail of the sample surface is shown in Fig. 2. Compared with the new mass the total number of pores is considerably smaller because of the disappearance of micro pores. The other significant change is the appearance of tiny crystals up to 1×10^{-5} cm. Further observations of the catalyst sample which was used for a longer time showed a growth of the crystals formed in the beginning of the process. Their development is relatively fast. In a short time the crystals cover a considerable part of the surface, thus causing a fundamental change in its relief.

5

Fig. 2 — The catalyst surface after being used for 48 hours. Total enlargement 24,000 × .
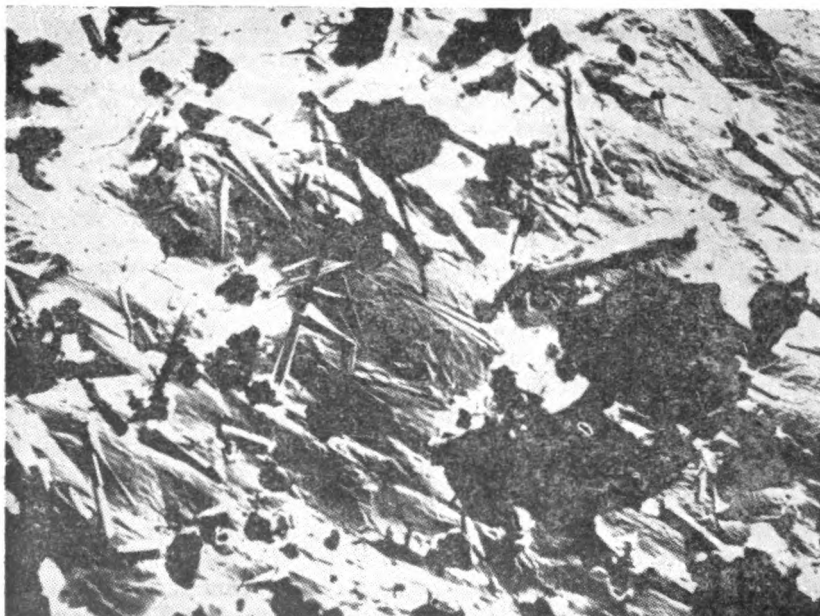
Fig. 3 — The catalyst surface after being used for 30 days. Total enlargemen 26,000 × .

Figure 3 shows the surface of the catalyst used for 30 days. The crystals formed are clearly visible. Their number has not essentially changed, but their dimensions have become considerably larger. The mean size of the crystals is about 5×10^{-4} cm. The porous structure of this sample is obviously damaged. Pores of large dimensions are visible, since some parts of the surface are undamaged. Further investigations of the samples showed changes in the already mentioned way.

Fig. 4 — The catalyst surface used in industry for a period of 5 years. Total enlargement 18,000 ×.

Figure 4 shows the catalyst surface after being used in industry for a period of 5 years. It shows that after long use the porosity of the relief is reduced and the number of crystals increased.

The figures show that the original structure of the new catalyst has completely changed; the developed surface relief has been transformed into an unformed mass. The greater part, about 23% of the surface, is covered by crystals whose size, in some cases, is 1×10^{-3} cm.

Data on the statistical distribution of pores[5,6] obtained from the electron microscope photos is shown in Fig. 5. Pore diameters expressed in Å are plotted on the abscissa and the number of pores of the corresponding diameters expressed in percentages are plotted on the ordinate. The four curves represnt the four catalyst samples: the absolutely new mass, the masses used for 48 hours and for 30 days in the laboratory reactor and the mass used for 5 years in industry.

5*
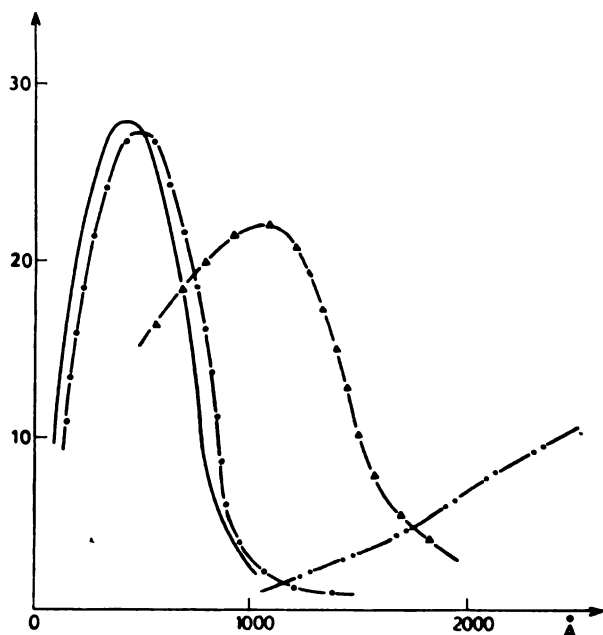
Fig. 5 — Statistical distribution of pores over the surface of the catalysts used
for different time periods.

——————— new catalyst
— . — . — . activated catalyst
— ▲ — ▲ — catalyst used for 30 days
— .. — .. — catalyst used for 5 years.

The curves for the statistical distribution of pores indicate hete-
rogeneous porous structure of the vanadium catalyst. The smallest
visible pores on the surface have diameters of about 30 Å, which
should not be considered the lower limit of pore size, because of the
limited possibilities of the microscope used for the measurements.

The pore diameters of the new mass were:

from	30— 100 Å	9%
"	100 — 1000 Å	81%
above	1000 Å	10%

The decrease in the number of pores with small diameters
during work is sharp. The mass used for 48 hours did not have pores
with diameters smaller than 100 Å. The diameter of the smallest
pores on the mass used for 30 days was more than 1000 Å. The shift of
the curve maximum towards larger pore diameters indicates a relative
increase in the contribution of macro pores and disappearance of
micro pores with use.

Figure 6 shows the increase of crystals formed on the same samples and their numbers expressed in percentages. The size of the crystals in cm is plotted on the abscissa and the number of crystals of the corresponding sizes expressed in percentages is plotted on the ordinate.
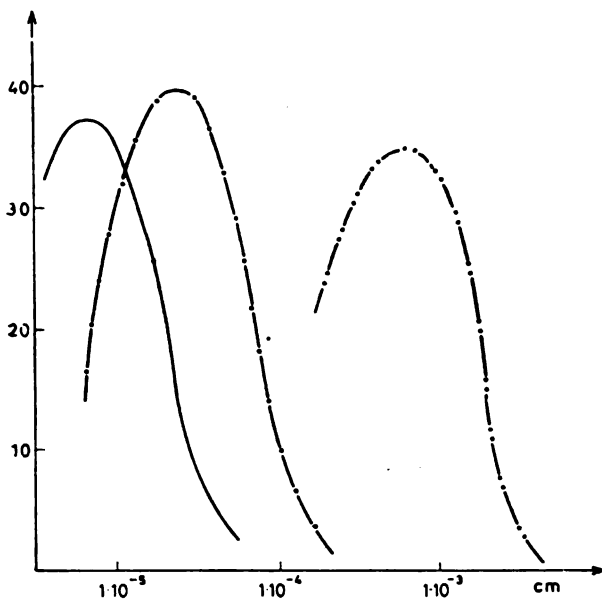
Fig. 6 — Dispersion of crystals on the catalyst surface

———————— catalyst used for 48 hours
— . — . — . catalyst used for 30 days
— .. — .. — catalyst used for 5 years

The shift of the curves towards the higher values of the abscissa shows a permanent increase in the number of crystals during the use of the catalyst. The proportionally small differences in the maxima of the curves indicate that there is mainly an increase of crystal size — not the formation of new ones. Besides, the negligible changes in the shape of the curves indicate that the crystal growth is uniform.

Figure 7 shows the conversion values obtained on the same masses at temperatures of 400−500°C.

The conversion value was determined under identical conditions in the laboratory reactor. Comparison of the curves for the new mass, the mass used 30 days in the laboratory reactor and the mass used for 5 years in the plant showed that catalyst transformations established by electron-microscope investigations were accompanied by a corresponding change of activity. Further extensive investigations will show the effect of each catalyst transformation on the total activity and the relation of physical and chemical influences which determine the duration of a catalytic mass in use.
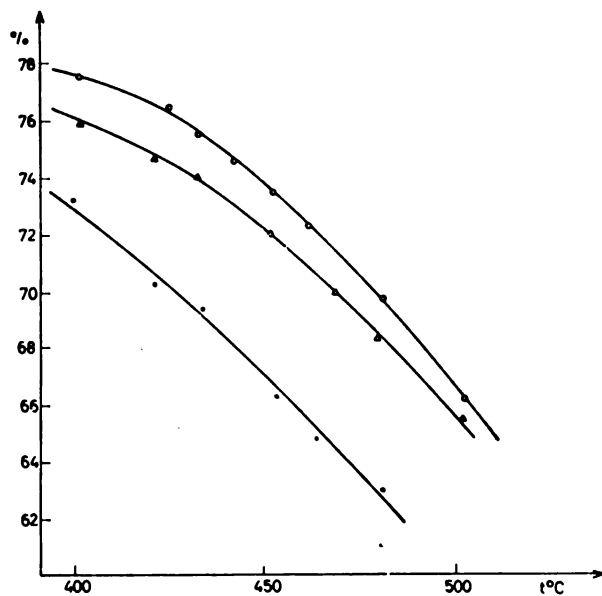
Fig. 7 — Change in conversion with change in the working temperature on catalysts used for different periods of time.

— ○ — ○ — new catalyst
—▲ —▲ —▲ catalyst used 30 days
— ● — ● — catalyst used 5 years

The subject of further needed investigations will be the structural properties of the crystals formed, their chemical composition, characteristics of the crystal lattice and influence on the energy properties of the catalyst surface. This will represent a considerable contribution to the understanding of the mechanism of action of vanadium catalysts in the oxidation of sulfur dioxide.

Institute for Chemical, Technological and Metallurgical Research, Belgrade.

REFERENCES

1. Boreskov, G. K. *Kataliz v proizvodstve sernoi kisloty* (Catalysis in the Production of Sulfuric Acid) — Moskva: Goskhimizdat, 1954.

2. Colette, F. and L. Scheepers. "L'oxydation catalitique de l'anhydride vanadique" — *Chemie et industrie* (Paris) 63(3): 246—251, 1950.

3. Frazer, J. N., and W. Y. Kirkpatrick. "A New Mechanism for the Action of the Vanadium Pentoxide — Silicoalkali Pyrosulphate Catalyst for the Oxidation of Sulphur Dioxide" — *Journal of the American Chemical Society* (Easton, Pa)62(7): 1659—1664, 1940.

4. Holmes, N. H., and L. A. Elder. "Vanadium Compounds as Catalysts for the Oxidation of Sulphur Dioxide" — *Industrial and Engineering Chemistry* (Easton, Pa.) 22(5): 471—476, 1930.

5. Kiselev, A. V. "Osnovnye strukturnye tipy adsorbentov i ikh vliianie na adsorbtsionnye svoistva" (Basic Structural Types of Adsorbents and their Effect on Adsorption Properties) — *Zhurnal fizicheskoi khimii* (Moskva) 23(4): 452—458, 1949.

6. Roginskii, S. Z. "O primenenii elektronnoi mikroskopii k issledovaniiu statisticheskikh osobenostei aktivnykh tverdykh tel" (On the Application of Electron Microscopy in the Investigation of Statistical Properties of Active Solid Bodies) — *Problemy kinetiki i kataliza* (Moskva) 7: 72—77, 1949.

7. Scott, W. W., and E. B. Layfield. "Characteristics of Vanadium Catalyst and a New Catalyst for Sulphuric Acid" — *Industrial and Engineering Chemistry* (Easton, Pa) 23(6): 617—621, 1931.

8. Ullman, P. "Schwefelsäure — Kontaktverfahren" — *Enzyklopädie der technischen Chemie* (Berlin) 9: 317, 1932.

9. Waeser, B. *Die Schwefelsäurefabrikation* — Brunswick: Frieder, Wieweg-Sohn, 1961.

BULLETIN
OF THE CHEMICAL
SOCIETY
Belgrade

Editor:
ĐORĐE M. DIMITRIJEVIĆ

C O N T E N T S

STRUCTURAL ANALYSIS OF ORGANIC COMPOUNDS BY CHROMATOGRAPHY

by

Ž. PROCHÁZKA

In the last two decades we are witnesses of a tremendous evolution of chemistry. This evolution is not primarily a consequence of some new chemical theory, but mainly of the introduction of new methods of analysis of organic compounds, among which paper chromatography and thin layer chromatography, although very simple, modest and cheap, play a very important role. These methods have been used mainly for analytical and micropreparative purposes. However, it is possible to use chromatographic methods for structure analysis of organic compounds too. In this respect, detection reactions have been mainly utilized, i.e., classical color reactions on paper chromatograms or chromatostrips. It is evident that the application of a reagent to a separated mixture on a chromatogram is far more specific and, in general, adventageous than its application to an unseparated mixture, where highly selective reagents are required.

However, chromatography offers another approach to the study of structure of organic compounds, i.e. the analysis of R_F-values. Martin[1] and later on Bate-Smith and Westall[2] have demonstrated that a function of R_F, the so-called R_M function:

$$R_M = \log (1/R_F - 1) \qquad (1)$$

is very useful in structure studies, because it possesses superpositional and linear properties. In this respect it is similar to some other physico-chemical functions, for example molecular weight, molecular refraction etc. These functions can be calculated by summing atomic weights, atomic refractions, etc. The R_M value of a compound can be calculated in a similar manner from partial R_M values for atoms or functional groups, according to the equation

$$R_M^{..} = m\, \Delta\, R_{M(A)}^{..} + n\, \Delta\, R_{M(B)}^{.} + \ldots + K \qquad (2)$$

where m is the number of functional groups or atoms of kind A, $\Delta\, R_{M(A)}^{.}$ the $R_M^{..}$ value for the given functional group or atom, n the number of functional groups of kind B etc. K is a constant (see below).

The most simple and common functional group in organic molecules is the methylene group (or the C-atom). When determining the

ΔR_M value, i.e. the group constant of this group, it is best to choose homologous series of compounds, as for example dicarboxylic acids, to chromatograph several of them in the given system, and measure their R_F values. These are then transformed according to equation 1 (or using a table or graph constructed by means of this equation) to $R_M^{\cdot}$ values, and the difference in R_M (ΔR_M) of several homologous pairs is then calculated by substraction. An example in Table 1 illustrates the procedure.

TABLE 1

Calculation of the CH_2-group constant

Acid	Number of CH_2 groups	R_F	R_M	$R_{M(CH_2)\,n} - R_{M(CH_2)\,n-1}$ $\Delta R_{M(CH_2)}$
Succinic	2	0.31	+ 0.347	− 0.312
Glutaric	3	0.48	+ 0.035	− 0.269
Adipic	4	0.63	−0.234	−0.290
Pimelic	5	0.77	−0.524	
			Average value	− 0.290

Chromatographic system: butyl acetate-water, paper Whatman No. 4 equilibrated with water vapor[3].

The same method is used for the determination of $R_M^{\cdot\cdot}$ for the carboxyl group. From the R_M of a carboxylic acid the $R_M^{\cdot}$ of the decarboxylated compound is subtracted, as represented in Table 2.

TABLE 2

Calculation of the group constant for the phenolic hydroxyl group

Compound	R_F	R_M	$R_{M(I-OH)} - R_{M(I)}$ $\Delta R_{M(OH)}$
D,L-5-hydroxytryptophan	0.14	+ 0.79	+ 0.262
D,L-tryptophan	0.23	+ 0.528	
5-hydroxy-3-indolyl-acetic acid	0.19	+ 0.63	+ 0.283
3-indolylacetic acid	0.31	+ 0.347	

I = indole nucleus. — Chromatographic system: methyl acetate-isopropanol — 25% ammonia (45:35:20) adsorbent silica gel G (Stahl), chromatography chamber saturated with the mobile phase[4].

The value of the constant K in equation 2 depends on the ratio of phases on the paper and can easily be calculated by subtracting all the ΔR_M values from the R_M of the studied compound. For example, if the R_M of adipic acid is measured in a given system, and from it double the ΔR_M value for the carboxyl group and four times the ΔR_M value for the methylene group is subtracted, the constant K is obtained. This constant is called the fundamental or basic constant, or sometimes also the paper constant[5]. It depends mainly on the ratio of phases on the paper. The method of measuring and calculating K suggests a paradoxical idea, viz. that a "substance" deprived of all groups, atoms and structural features has an R_M value equal to K. Of course, this is in full accord
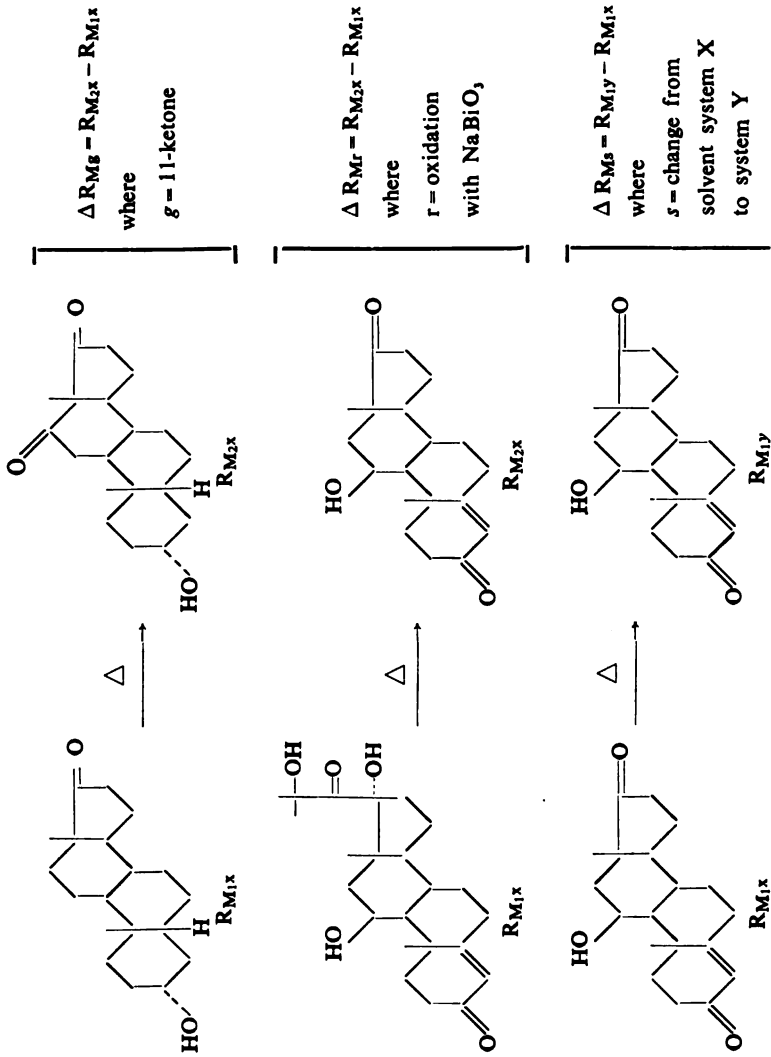
Fig. 1. Examples of the calculation of three types of ΔR_M in the steroid field.

with the real meaning of the constant, because it is a property of the paper and the system and not of any "substance".

Before giving practical examples of the use of chromatography for structural analysis, it should be mentioned that equation 2, which is a mathematical expression of Martin's theory of the additivity of the R_M-function, has often been declared to be invalid, but at last, mainly thanks to the work of Bush[6], it has been proved to be correct, or at least extremely useful. Bush has extended the concept of ΔR_M. He distinguishes three kinds of ΔR_M (increments of R_M): for functional groups or atoms (or isomerism and other structural features), for chemical reactions, and for the change of R_M when the substance is chromatographed in another system (see Fig. 1).

However, even with this improvement or elaboration of the method, equation 2 cannot usually be used for the calculation of R_M values in thin-layer chromatography. The main reason for this failure is illustrated in Fig. 2.
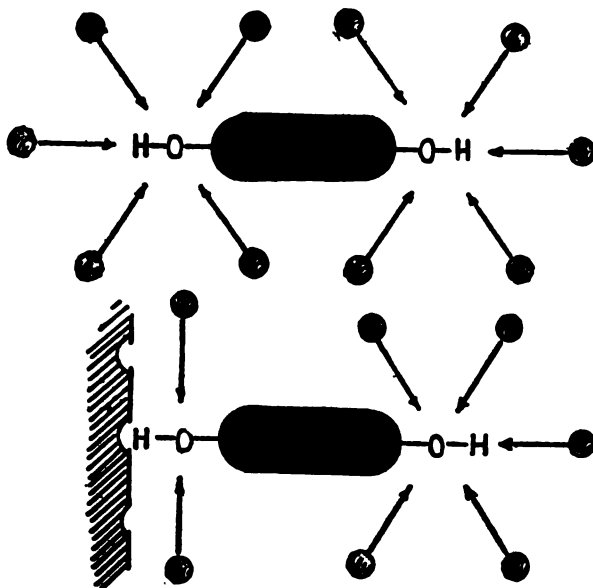
Fig. 2. Schematic representation of the solute-solvent interaction in partition (above) and adsorption chromatography (below).

Martin's theory is an expression of the fact that identical functional groups show the same type of interaction with the solvents, and hence cause the same change of the R_M value if added to or subtracted from a given molecule. Figure 2 represents schematically the fact that absolutely identical functional groups cannot show the same type of interaction with the mobile solvent if the molecule is rigid, and the functional group strongly adsorbed (polar groups!). An adsorbed group is sterically hindered by the adsorbent and is less accessible for the solvent

molecules than the other groups which are not adsorbed. However, Brenner *et al.*[7] found that Martin's law is obeyed in the case of homologues, i.e., ΔR_M^- for the methylene group, which is practically not adsorbed by the usual adsorbents of polar character, is really a constant, even in adsorbtion chromatography. Of course, its value is very small in comparison with other functional groups.

Before going on to practical examples of the use of the equation 2, it must be emphasized that accurate measurement of R_M values is essential for the use of this method. It is evident that constant R_M and ΔR_M values can only be obtained if measured under well-defined standardized conditions.

Example 1

The most instructive example of the use of paper chromatography for structural analysis is the method devised by Reichl[8]. It consists in choosing a pair of solvents whose composition is very similar, almost identical, and differring only by a component which reacts selectively with only one type of functional group in the molecule. Howe[9], for example, used the following two systems:

a) isopropanol-dilute aqueous ammonia solution;

b) isopropanol-dilute aqueous sulphur dioxide solution.

All functional groups except acidic or basic groups will be unaffected, in both systems and hence the ΔR_M values for methylene, hydroxyl, oxyde, etc, will be identical in both systems. On the other hand, different ΔR_M values will be found for the carboxyl or the amino group. The value for the carboxyl group will be much lower for the acidic system than for the ammonia system. Using model substances, ΔR_{Ms} for one carboxyl group, i.e. the difference in the R_M value of a monocarboxylic acid for the acid system and the basic system, can be readily determined, and knowing this, also the number of carboxyl groups in any substance. If ΔR_{Ms} for an unknown substance in the two systems is equal to the value determined with the model substances, the unknown substance is a monocarboxylic acid. If it is twice or three times higher, then the substance is a dicarboxylic or tricarboxylic acid respectively. In this connection it is important to note that chromatography permits the determination of the number of carboxyl groups even in an impure sample, on a submicro scale. No other physico-chemical method can do this.

Example 2

Macek[10] used the same principle for the determination of the number of α-diol groupings in the steroid molecule. The two systems were:

a) formamide-impregnated paper and chloroform as the mobile phase;

b) paper impregnated with formamide containing a small amount of boric acid and chloroform as the mobile phase. Steroids without α-diol groups had identical R_F values in both systems, whilst those them had smaller R_F values and hence different R_M values in the system containing boric acid. This behavior is ascribed to complexing of α-diols with boric acid. If the increment of R_M, i.e. ΔR_{Ms}, was 0.3 — 0.4, it was caused by one α-diol grouping, if it was 0.8 — 1.2, by two α-diol groupings.

Example 3

Macek has shown[11] also that assignement of a reserpoid to the normal or iso-series can easily be made by studying its chromatographic behavior. In chromatography of alkaloids of the reserpine (normal) series on paper impregnated with formamide, as compared to paper impregnated with formamide containing additional ammonium formate, the R_M values decrease by 0.71 — 0.86. In the iso-series, on the other hand, this decrease is only about half as large and the ΔR_{Ms} values range from 0.38 to 0.48. Chromatography of an alkaloid of an unknown configuration in both systems always established the configuration on the third carbon atom unequivocally (see I and II), even when an authentic sample was not at hand or in a mixture.
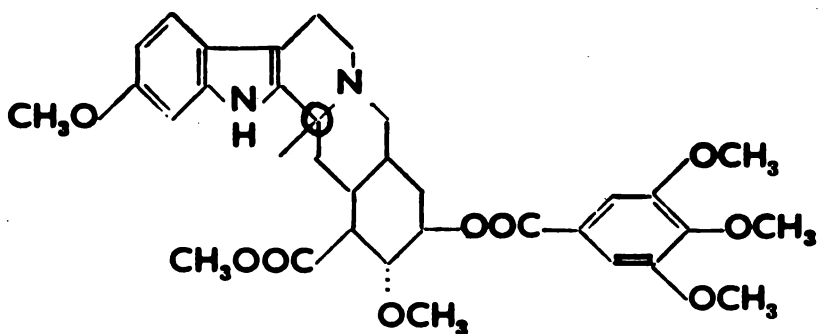
reserpine
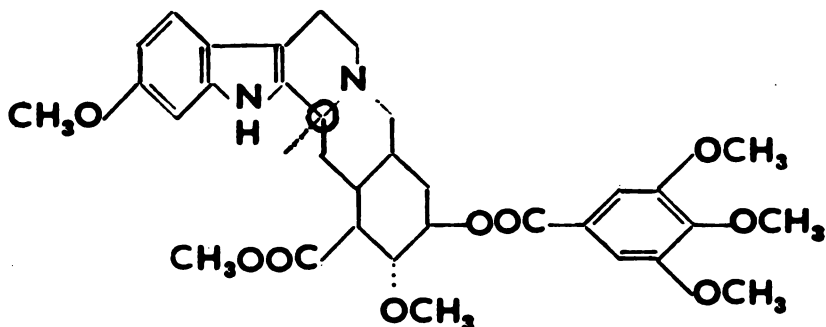
*iso*reserpine

In a similar manner the measurement of $\triangle R_{Mr}$ can be utilized for structural analysis. The R_M change of a substance is measured in a single system before and after carrying out a reaction with it. For example, the difference of R_M between a known substance containing one hydroxyl group in its molecule and its acetate is determined in a suitable system. Then the R_M difference of the analyzed unknown substance and its acetate is determined in the same system, and the result (i.e. $\triangle R_{Mr}$ for acetylation) is divided by the $\triangle R_{Mr}$ found for mono-acetylation, as determined with the model. The value obtained, usually close to a whole number, represents directly the number of free, acetylable hydroxyl groups in the substance. This method is equivalent in principle to the classical method of determination of acetylable hydroxyl groups, when the substance and its acetate are submitted to elementary analysis and from the difference in composition the number of acetyl groups derived. The advantage of paper chromatography is that it permits acetylation with not entirely pure substances and on a microgram scale. According to Edwards[12], for example, formulation can be carried out directly on the paper, by exposing the paper with the spotted substance, or by exposing a two-dimensional chromatogram after the first run, to formic acid vapors.

In this connection it will be useful to mention briefly some reactions that can be carried out directly on the paper:

Hydrogenation of unsaturated fatty acids[13] in the presence of colloidal palladium. The fatty acid is spotted first on the start, then a colloidal solution of palladium is spotted over the original spot, and the still wet spot is exposed to hydrogen in a hermetically sealed chamber.

In a similar manner acetonidation can be carried out[14]. The substance on the paper is wetted with a solution of perchloric acid and after drying exposed to acetone

vapors at 29 °C for a suitable time. If the R_M value of the substance is changed after this treatment, it can be inferred that the formation of an acetonide (isopropylidene dioxy derivative) has taken place, and hence that a diol grouping was present in the molecule.

Some reductions too can be carried out directly on the paper. For example, dehydroascorbic acid can be reduced by exposing the chromatogram to hydrogen sulphide. Methylation can be carried out on paper with diazomethane, hydrolysis of a glycoside can be carried out by spraying the chromatogram with hydrochloric acid and heating. Oxidation of some easily oxidizable secondary alcohols can be also carried out directly an paper by dropping chromic acid solution on the spotted substance. Saponification with alkalis, permanganate oxidation, oxidation with potassium periodate, maleic anhydride addition, halogenation, etc., can also be carried out directly on the paper. If these operations are followed by chromatography and exact measurement of $\triangle R_{Mf}$ of the reaction product, much more information can be obtained than by only qualitative inspection of the chromatogram. The nature of the change can be fairly accurately demonstrated, and the number of functional groups determined.

Paper chromatography can be very advantageously used for the demonstration of intramolecular hydrogen bonding in organic molecules. If an intramolecular hydrogen bond is present in the molecule, the R_F value will be much higher than expected or calculated.

Example 4

4-hydroxycoumarin can easily be condensed with formaldehyde to give dicoumarin (Fig. 3). In carbon tetrachloride with 2% of acetic acid the R_F value of 4-hydroxycoumarin is 0.2, i.e. $R_M + 0.60$. In Fig. 3 this is represented diagrammati-
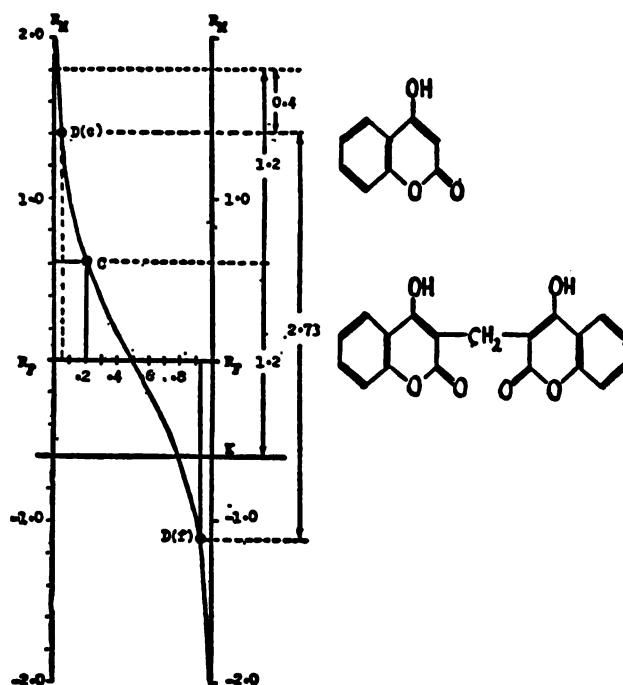
Fig. 3. Calculation of the theoretical R_M and R_F of dicoumarin (lower formula). C — position of 4-hydroxycoumarin on the R_M against R_F plot; D(c) — calculated position, D(f) — found position for dicoumarin on the same plot.

cally. Now, if hydrophilic substituents prevail over lipophilic ones, the substance has an R_M that is higher than the fundamental constant K (see equation 2). If the molecule of such a substance is doubled, its R_M value will be still greater, the difference between R_M and K will be twice as large as in the former case. In our case the difference between R_M for 4-hydroxycoumarin and K is, as can be seen in Fig. 3, $+0.60 - (-0.60) = +1.2$. When 4-hydroxycoumarin is transformed to dicoumarin, we can consider that it is doubled and simultaneously substituted with a methylene group. Thus, in order to calculate the R_M value for dicoumarin we have to double the value $+1.2$ and add the value for the methylene group, which is -0.4 in our system, i.e.: $2 \times 1.2 + (-0.4) = 2.0$. It can be seen from the diagram that the R_F value of dicoumarin should be much lower than that of 4-hydroxycoumarin, i.e. 0.02. However, the measured R_F of dicoumarin was 0.93. It is evident that the substance behaves as if it did not contain so many polar groups, primarily hydroxyls, as it should. The difference between the calculated and found value is 2.73, which corresponds to the disappearance of more than one hydroxyl group ($\triangle R_{M(OH)}$ in this system is approx. 2). This behavior is evidence for intramolecular hydrogen bonding. In fact, the structure of dicoumarin and similar bis-derivatives of 4-hydroxycoumarin is best represented by formula III[15].
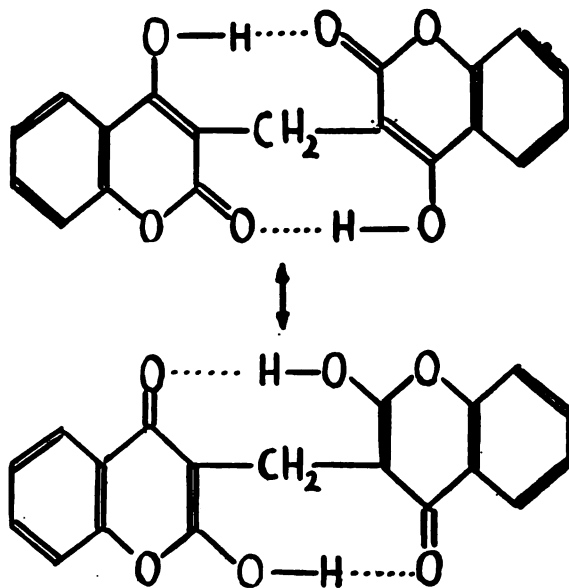
Paper chromatography is especially useful for structure elucidation in the steroid field. In this field Busch[6] has brought the method to a high degree of perfection. He has collected extensive experimental material, i.e. a great number of group constants, with all kinds of $\triangle R_M$ values.

Example 5

In the microbial transformation of steroids a few miligrams of a known steroid in a nutritive medium is transformed by moulds or bacteria and the medium is then extracted with an organic solvent. The extract is analysed by paper chromatograph. In most instances more than one transformation product can be detected on the paper. Measuring R_M values of the products and calculating the differences between them and the R_M value of the starting material gives direct information on the character of the product Table 3 lists approximate $\triangle R_{Mg}$ values in four solvent systems for various substituents[6] and Table 4 $\triangle R_{Mr}$ values for several reactions of substituents ·in the stationary phase containing water and methanol (also ethanol, ethylene glicol, propylene glycol or formamide), the mobile phase being a mixture of benzene-toluene and light petroleum (in various proportions) saturated with the stationary phase[16].

TABLE 3

Approximate ΔR_{Ms} values for various substituents on the steroid molecule[6]

Substituent	Additional feature	Solvent system[a]			
		ligroin 66 toluene 33 methanol 85 water 15	ligroin 66 benzene 33 methanol 80 water 20	ligroin 50 toluene 50 methanol 70 water 30	benzene 100 methanol 50 water 50
3 = O	Δ4	1.35			1.2
3 β—OH	Δ5	1.9			
6 β—OH	Δ⁴, 3 = 0	1.2	1.3	1.1	1.6
11 = O		0.61	0.81	0.72	0.82
11 β—OH		1.0	1.2	1.0	1.0
11 α—OH		1.6	1.8	1.6	1.6
15 α—OH		1.55	1.85	1.6	
20 = O		0.7	0.7	0.6	
20 β—OH		1.5			0.7
C = C		0.03 to 0.6			
—CH₂—		—0.12 to —0.21			
C₁₉—skeleton		—2.7			—.45

(a) The chromatographic paper is equilibrated with the vapours of the lower phase (overnight) and then run with the upper phase.

TABLE 4

Approximate ΔR_{Mr} values for various reactions of substituents [16] *of the steroid molecule* [a]

Reaction		ΔR_{Mr}
—CH₂OH	⟶ —CH₂OAc	— 1.5
R.COCH₂OH	⟶ R.COCH₂OAc	— 0.9
>CH—OH	⟶ >CH—OAc equatorial	— 1.3
	axial	— 1.1
>C—OH	⟶ >C—OAc	— 0.9
>CH—OH	⟶ >C=O equatorial	— 0.8
	axial	— 0.4
20 C=O	⟶ 20β—OH	+ 0.9
	20α—OH	+ 1.06
>C=O	⟶ >CH₂	— 0.7
>C=O	⟶ >C⟨O O⟩	— 0.9
—COOH	⟶ —COOCH₃	— 2 to —3
⟩	⟶ OH / OH	+ 2.4
⟩	⟶ O	+ 0.2
3β—OH, Δ⁵	⟶ 3C=O, Δ⁴	— 0.25
3α—OH, (5β)	⟶ 3C=O, (5β)	— 0.8
3C=O, Δ⁴	⟶ 3α—OH (5β)	+ 0.4

(a) For solvent systems see the text.

It can be seen, for example, that not only is the $\triangle R_{Mg}$ value for the hydroxyl group much higher than that for the keto group, and still higher than the $\triangle R_{Mg}$ for the double bond, but also that the $\triangle R_{Mg}$ values for different types of hydroxyl group differ appreciably. For example, equatorial hydroxyl groups have higher $\triangle R_M$ values than axial ones. Hydroxyls at different positions in the steroid molecule also have characteristic $\triangle R_M$ values. For instance, the $\triangle R_M$ value for the 11β-hydroxy group is the lowest, and can easily be distinguished from the 11α or some other hydroxyl group. Now, if determination of the $\triangle R_{Mg}$ values is combined with determination of $\triangle R_{Mr}$ of the newly formed transformation products, after carrying out simple reactions, as for example acetylation, reduction with hydrides, oxidation with chromic acid, etc., it is possible, in most instances, to propose very good hypothetical formulae (structures) for the transformation products even before a single components is isolated in the pure state. Thin-layer chromatography is not so useful in this respect.

In the field of macromolecular chemistry too, paper chromatography can be very useful. This is illustrated by the following example.

Example 6

By copoymerizing caprolactam with acetanilide for a very short time, a mixture is formed (Fig. 4). Apart from the starting components, it is difficult to identify the spots by simply inspecting the chromatogram. It is evident that the sequence of spots must be regular, the R_F values either increasing or decreasing with the increase of
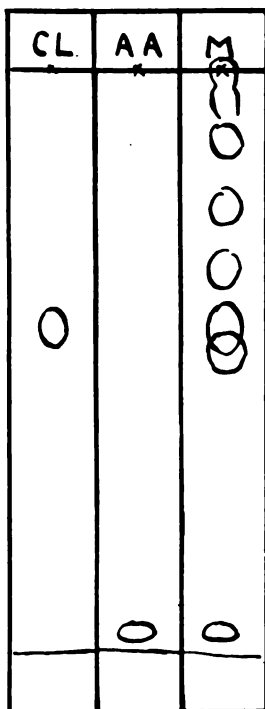
Fig. 4. Paper chromatograms of caprolactam, acetanilide and their reaction mixture in butyl acetate-water.

molecular weight (dimer, trimer, tetramer etc.). However, it is almost impossible to predict without quantitative treatment of the R_F values, whether the dimer will have the lowest or the highest R_F value, the trimer the next to it, etc. It is therefore necessary to calculate, at least approximately, the theoretical R_M (and R_F) values for the

dimer, trimer, tetramer, etc. The $\triangle R_{M(CH_2)}$ value in the system used (carbon tetra-chloride $+ 2\%$ acetic acid) is known (-0.40). R_M for the amide group was calculated from the R_M value of caprolactam, by substracting from it five times the value for the methylene group (see Fig. 4). $\triangle R_M$ for the phenyl group was calculated in a similar manner, by subtracting from R_M for acetanilide the value for the amide group and the value for the CH_2 group (usually equal or similar to that for the methyl group). Knowing the $\triangle R_M$ values for these three groups it is possible to calculate, by simple addition, the R_M values for the oligomers and thus establish the correct sequence. Much more work was necessary (synthesis, isolation of single oligomers by chromatography, and elementary analysis) to establish the same sequence by the classical procedure[17].

It is not the aim of this paper to prove that only paper chromatography should be used for structure studies in organic chemistry. However, this method can be very useful when it complements other physico-chemical methods, as for example infrared, ultraviolet, NMR, mass spectroscopy etc., and quantitative treatment of chromatographic data can supply more evidence and more reliable information on the structure than simple qualitative inspection of the chromatograms, not to mention that the procedure is also much cheaper[18].

Countercurrent distribution techniques and gas-liquid chromatography can be used for the same purpose, but instead of R_M the logarithm of the distribution coefficient or the retention volume or time should be used. However, the work is more time consuming, the apparatus more expensive, and less data is available in the literature. On the other hand, gas-liquid chromatography is more suitable for automation and can be made more accurate.

Institut of Organic Chemistry
and Biochemistry
Academy of Sciences
Prague, Czechoslovakia

REFERENCES

1. Martin, A. J. P. — *Biochemical Society Symposia* (Cambridge, England) 3: 4, 1949.
2. Bate-Smith, E. C. and R. G. Westall. - – *Biochimica et Biophysica Acta* (Amsterdam 4: 427, 1950.
3. Šanda, V., Ž. Procházka and H. Le Moal. — *Collection of Czechoslovak Chemical Communications* (Prague) 24: 420, 1959.
4. Stahl, E. and H. Kaldenwey. — *Zeitschrift für Physiologische Chemie* (Berlin) 323: 182, 1955.
5. Procházka, Ž. *Priručka laboratornich chromatografických metod*, edited by O. Mikeš. — Prague: Státní nakl. techn. literatury, 1961, pp. 33—38.
6. Buch, I. E. *The Chromatography of Steroids*. — London: Pergamon Press, 1961.
7. Brenner, M., A. Niederwieser, G. Pataki and R. Weber. *Dünnschicht Chromatographie*, edited by E. Stahl. — Berlin: Springer Verlag, 1962, pp. 79—137.
8. Reichl, E. R. — *Mikrochimica Acta* (Wien) 955, 1956.
9. Howe, J. R. — *Journal of Chromatography* (Amsterdam) 3: 389, 1960.
10. Macek, K. and Z. Vejdělek. — *Nature* (London) 176. 1173, 1955.
11. Macek, K. — *Experientia* (Basel) 17: 162, 1961.
12. Edwards, R. W. H. — *Journal of Endocrinology* (London) 22, XXVI, 1961. *The Biochemical Journal* (London) 82: 48P, 1962.
13. Kaufmann, H. P. and D. K. Chowdhury. — *Chemische Berichte* (Weinheim) 91: 2117, 1958.
14. Leland, L. S. and T. Foell. — *Journal of Chromatography* (Amsterdam) 3: 381, 1960.
15. Knobloch, E. and Ž. Procházka. — *Chemicke Listy* (Prague) 47: 1285, 1953.
16. Neher, R. *Steroid Chromatography*. — London: Elsevier Publishing Company, 1964.
17. Pavlíčkova, J. Private communication.
18. Procházka, Ž. — *Chemicke Listy* (Prague), 58: 911, 1964.

DETERMINATION OF THE CRITICAL PRESSURE
OF MONOATOMIC ELEMENTS

by

JOVANKA M. ŽIVOJINOV

This paper presents a comparison between the results obtained with the Van der Waals equation of state and those from the equation obtained by the author in an earlier work[1].

From classical thermodynamics it is known that Van der Waals equation gives the following relationship between the critical magnitudes:

$$\frac{p_c V_c}{R T_c} = \frac{3}{8} \tag{1}$$

where p_c is the critical pressure, V_c the critical volume, T_c critical temperature and R the universal gas constant. Hence, the critical pressure is given by

$$p_c = \frac{3}{8} \cdot \frac{R T_c}{V_c} \tag{2}$$

In paper (1) the following relation was obtained for the case of equilibrium between liquid and vapor phase at boiling point for a monoatomic element:

$$\frac{V''}{V'_e \, {}^{s/RT}} = \frac{3}{e^{s/RT_c}} \tag{3}$$

Here V'' is the specific volume of the vapor, V' that of the liquid at the boiling point T (in °K), and s the latent heat of sublimation at 0 °K. Since only two of the basic magnitudes of the thermal state, the volume and the temperature, appear here, we may use the equation of an ideal gas to determine the pressure:

$$pV = RT \tag{4}$$

By substituting V'' from (3) into equation (4) we get the pressure of the saturated vapor:

$$p = \frac{RT}{3r' \dfrac{e^{s/RT}}{e^{s/RT_c}}} \tag{5}$$

TABLE 1

Critical pressure

Element	$P_c \dfrac{K_p}{cm^2}$ Exper. [2]	$\rho_c \dfrac{g}{cm^2}$	$T_c \,°K$	A	$P_c \dfrac{K_p}{cm^2}$ from eq. [2]	$\delta p_c \%$	$P_c \dfrac{K_p}{cm^2}$ from eq. [2]	$\delta p_c \%$
He	2.26	0.0693	5.26	4.003	2.88	—27.5	2.56	—13.4
Ne	26.86	0.4835	44.74	20.183	34.08	—26.9	30.30	—12.8
Ar	47.996	0.53078	150.72	39.944	63.688	—32.6	56.611	—17.9
Kr	54.9	0.909	210.56	83.80	72.63	—33.9	64.	—19.0
Xe	58.22	1.154	289.86	131.30	81.01	—39.7	72.0	—24.2

Since at the critical temperature $T = T_c$ and $V'_c = V''_c$, from this equation we obtain the following relationship for the critical magnitudes:

$$pc = \frac{RT_c}{3 V''_c} \tag{6}$$

The same quantities appear here as in relation (2), except that in the first case the constant is different.

Both expressions are used here to determine the critical magnitudes of the following monoatomic elements: helium (He), neon (Ne), argon (Ar), krypton (Kr) and xenon (Xe).

The experimental data for all the quantities in expressions (2) and (6) are presented in Table I. The table also shows the atomic weights of the given elements and the theoretical values for the critical pressure as given by the two above expressions. The difference between the theoretical and the experimental values are also given. They show that much better values for the critical pressure are obtained with equation (6), derived here, than with equation (3), derived earlier from statistical and quantum mechanical considerations and the equation of state of an ideal gas (4).

REFERENCES

1. Živojinov, J. »Kvantno-statističko tumačenje uslova ravnoteže između tečne i parne faze na temperaturi ključanja jednoatomnih elemenata« (Quantum-statistical Interpretation of the Conditions of Equilibrium between Liquid and Vapor Phase at the Boiling Point of Monoatomic Elements) — *Glasnik hemijskog društva* (Beograd) 27: 5—6, 1—16, 1963.

2. Kaye, G. W. C. and T. H. Laby. *Physical and Chemical Constants and Some Mathematical Functions* — London: Longmans, 1960.

2*

LUMINESCENT PROPERTIES OF MANGANESE AND ZINC CHLORIDE WITH SOME AMINES

by

I. BURIĆ, S. ŠLJIVIĆ and K. VELAŠEVIĆ

The fluorescence of manganese chloride with some organic bodies has been studied by several authors [1, 2, 3, 4]. In work [3] the fluorescence of some amines with manganese chloride was investigated. We investigated $MnCl_2$ complexes with diethyl aniline, 2,6-dimethyl aniline and n-n-dimethyl aniline.

Manganese chloride forms two complexes with diethyl aniline. One molecule of manganese chloride with one molecule of diethyl aniline and two molecules of hydrochloric acid form a complex that gives a reddish-orange fluorescent color with a maximum emission fluorescent spectrum at 6130 Å. The other complex is formed of one molecule of manganous chloride with two molecules of diethyl aniline and one molecule of hydrochloric acid. It gives an intense green fluorescent color with a maximum emission fluorescent spectrum at 5280 Å.
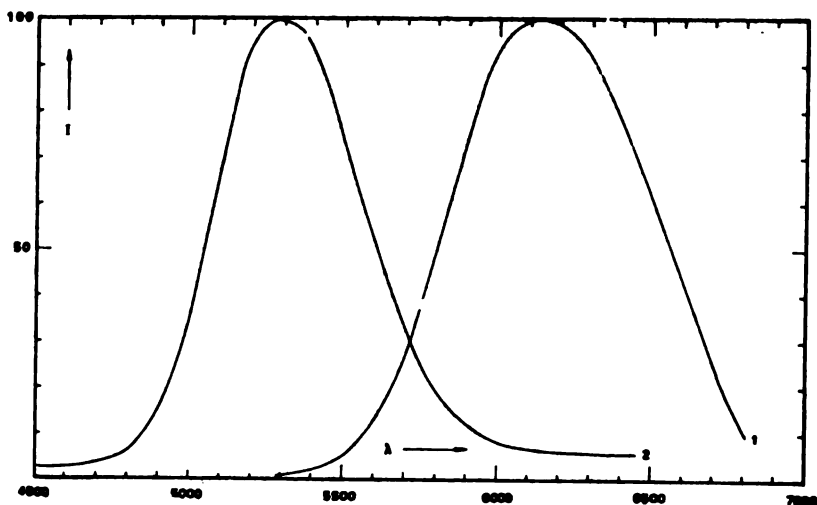
Fig. 1.

Both complexes are stable and they show very intense fluorescence. After long standing no changes in the intensity or spectral distribution of the complexes are observed.

Figure 1 shows the emission fluorescent spectrum at room temperature of both complexes excited with the Hg line of 3650 Å. Curve (1) represents the complex that emits a reddish-orange fluorescent color and curve (2) the one that gives green fluorescence.

Manganese chloride with 2,6-dimethyl aniline and n-n-dimethyl aniline forms complexes which give an intense fluorescent color from red to orange if taken in molecular ratios. The maximum emission fluorescent spectrum of a complex of manganous chloride with 2,6-dimethyl aniline is at 6230 Å, and that of manganous chloride with n-n-dimethyl aniline is at 6130 Å.

The emission fluorescent spectra at a temperature of 20 °C in Wood's light are shown in Fig. 2. Curve (1) represents the complex of manganous chloride with 2,6-dimethyl aniline and curve (2) manganous chloride with n-n-dimethyl aniline.
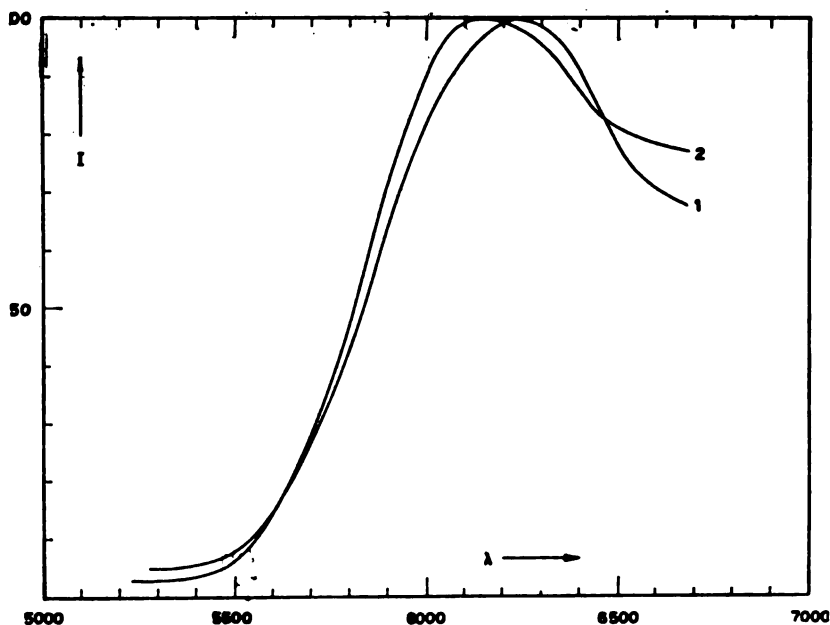
Fig. 2.

It may be seen from the above mentioned works and from the spectra in the present paper that all maxima of the complexes which emit a red fluorescent color lie in the very close boundary region which has a maximum emission fluorescent spectrum of manganese chloride ignited with HCl. On the other hand, the maxima of the emission fluorescent spectrum which emits a green fluorescent color lie in a very narrow spectral region and they very often differ by several angströms.

The mean life-time of the green complexes is $T = 0.46$ *ms* at $t = 20$ °C, while that of the reddish-orange complexes is $T = 0.032$ *ms*.

Zinc chloride with aromatic amines (aniline, diethyl aniline, *n-n*-dimethyl aniline and *o*-toluidine) form bodies which have a very high intensity of fluorescence and differ in intensity of fluorescence and spectral distribution.

With aniline, zinc chloride emits a light greenish-yellow fluorescent color when taken in molecular ratios, heated until it melts and then cooled. The maximum emission fluorescent spectrum lies at 4970 Å. The thus prepared mixture shows intense phosphorescence, the intensity and duration of which depend on the thickness of the layer investigated — they increase with the layer thickness. If the excitation source is taken as 3650 Å instead of 2540 Å, the intensity and duration of phosphorescence considerably increase. In both cases green phosphorescence appears and lasts about 15 seconds. O-toluidine and *n-n*-dimethyl aniline with zinc chloride emit a pale to light blue fluorescent color with the maximum emission fluorescent spectrum for ortho-toluidine at 5070 Å and for *n-n*-dimethyl aniline at 8807 Å.

Ortho-toluidine with zinc chloride gives an intense green phosphorescence of less intensity and duration than in the case of aniline with zinc chloride.
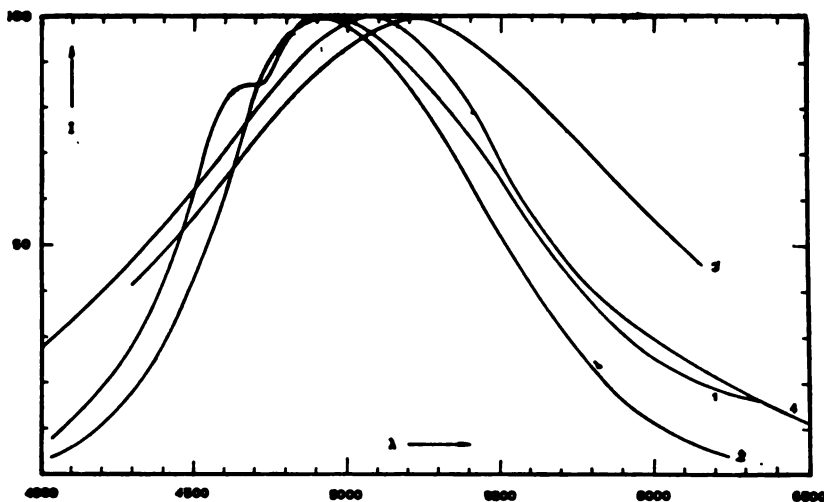
Fig. 3.

Zinc chloride with diethyl aniline emits a yellowish-green fluorescent color with the maximum emission fluorescent spectrum at 5230 Å. In this case phosphorescence was not observed.

Figure 3 shows the emission fluorescent spectra of zinc chloride with: aniline (curve 1), ortho-toluidine (curve 2), *n-n*-dimethyl aniline (curve 3), and diethyl aniline (curve 4) at 20 °C and 3650 Å.

REFERENCES

1. Šljivić, S. — *Comptes rendus de l'Academie de Science Française* (Paris) 245: 2047, 1957.

2. Nikolić, K., Hugnes Payen de la Garauderie and S. Schlivic — *Comptes rendus de l'Academie de Science Française* (Paris) 250 (séance du 20 juin): 4143—4145, 1960.

3. Hugnes Payen de la Garauderie — *Comptes rendus de l'Academie de Science Française* (Paris) 254 (9 avril): 2739—2740, 1962.

4. Velašević, K., S. Šlijvić and I. Burić — *Comptes rendus de l'Academie de Science Française* (Paris) 257 (23 décembre): 4163—4166, 1963.

POLAROGRAPHIC DETERMINATION OF ANTIMONY IN LEAD*

by

SRETEN MLADENOVIĆ

The bromatometric method for the determination of antimony in lead is long and very inconvenient for the determination of small amounts of antimony. The polarographic determination of antimony in lead cannot be performed from the usual supporting electrolytes on account of ready hydrolysis of antimony salts, coprecipitation of antimony and incomplete separation of antimony from lead[1, 2, 3, 4].

It is known that lead gives no polarographic wave in ammoniacal solution of EDTA[5], whereas in such a solution antimony produces well-defined waves. In ammoniacal solution lead forms a very stable complex with complexon III. However, in the same solution antimony forms a less stable complex which is more easily decomposed, i.e. which is more dissociated. Therefore, antimony ions formed by the dissociation are reduced at the dropping mercury electrode in a much greater amount than the ions of lead. The fact that only antimony gives a polarographic wave in ammoniacal solution of EDTA.

We have investigated the linear dependence of the wave height of antimony on the amount of antimony for quantities ranging from 1 to 8 mg of antimony in solutions containing known amounts of lead nitrate or metallic lead.

In the determination of antimony in amounts from 1 to 8 mg we have established a linear dependence of wave height on antimony concentration (Table 1).

In experiments with amounts of antimony smaller than 0.5 mg per 100 ml of solution the dependence of the wave height upon the amount of antimony was not linear.

The results of polarographic determination of antimony in lead alloys containing from 0.45 to 0.9% of antimony were consistent with results obtained volumetrically (Table 2).

TABLE 1

Supporting electrolyte: 0.2 g Pb²⁺ + 30 ml solution (1.6 M NH₄Cl +
+ 6 M NH₄OH + 1% Na₂SO₃ + 3 g gelatin/l) + 1 g complexon III + H₂O to 50 ml.

Experiment	Amount of antimony mg	Wave height, mm
1	1.00	12.0
2	2.00	24.0
3	3.00	36.0
4	4.00	48.0
5	6.00	71.0
6	8.00	96.0

TABLE 2

Lead Coating	Wave height, mm		Antimony added, mg	Antimony content, %	
	Sample	Sample plus antimony		Polarographic	Volumetric
1	18.0	29.0	1.00	0.82	0.83
		40.0	2.00	0.82	
2	17.0	28.0	1.00	0.77	0.77
		39.0	2.00	0.77	
3	23.0	41.0	1.00	0.65	0.65
		59.0	2.00	0.65	
4	28.0	52.0	1.00	0.58	0.57
5	16.0	34.0	1.00	0.45	0.45

An excess of complexon III over the amount stoimetrically required for lead does not affect the polarographic determination of antimony. The determination is not affected by the presence of tin either, since the latter forms stable complexes with complexon III in ammoniacal solution; thus, antimony can be determined in the presence of tin.

On the basis of our experiments the described polarographic method for the determination of antimony can be applied to lead alloys containing not less than 0.25% of antimony.

The determination of antimony in lead alloys should be performed in the following way:

A. Procedure I

Lead alloy (0.500 g) is heated strongly with conc. sulphuric acid (6 ml) to ensure complete dissolution of antimony. A white precipitate indicates that the entire antimony is dissolved. To the cooled reaction mixture containing a white precipitate of lead sulphate, water (about 15 ml) is added carefully along the flask windows sides. After cooling,

the reaction mixture is neutralized and made alkaline with conc. ammonia. To the stirred reaction mixture complexon III (1 g) is then added in order to dissolve the precipitate of lead sulphate. For more rapid dissolution the reaction mixture can be heated as well. The cooled solution is then transferred to a 50 ml volumetric flask and made up to the mark with distilled water. This solution must have an alkaline reaction. Two 20 ml aliquots of this solution are then transferred to two 50 ml volumetric flasks by means of a pipette. To one flask a fixed amount of standard antimony solution is added. (Standard antimony solution is obtained by dissolving metallic antimony in conc. sulphuric acid. The standard solution usually contains 1 mg of Sb per ml.) Then supporting electrolyte (15 ml) is added to each of the two volumetric flasks. The supporting electrolyte is prepared in the following way: to 250 ml of warm electrolyte consisting of 100 ml of conc. ammonia and 27 g of ammonium chloride, 2.5 g of anhydrous sodium sulphite is added carefully. The solution is then heated to boiling and with constant stirring 0.75 g of gelatin and 5 mg of complexon III are added.

After the addition of the supporting electrolyte, both volumetric flasks are filled up to the mark with boiling water. After shaking the solution is polarographed determined. The half-wave potential of antimony in this solution is about — 1.0 V.

B. *Procedure II*

Lead antimony alloy (0.5 g) is treated as described in Procedure I and the reaction mixture obtained neutralized with potassium hydroxide and then gelatin (0.15 g) is added. After the dissolution of gelatin, complexon III (2 g) is added and the reaction mixture is stirred until the dissolution of the precipitate is complete. The solution is then quantitatively transferred to a 50 ml volumetric flask and made up to the mark with boiling distilled water. Two aliquots of 20 ml each are pipetted to two flasks and 1 ml of saturated sodium sulphite solution is added to each aliquot. Before polarographic determination 0.50 ml of antimony solution (1 mg Sb/1 ml) is added to one flask and 0.50 ml of acid solution (10 ml of conc. H_2SO_4 + 90 ml of HCl) to the other.

The advantages of Procedure II are a smaller amount of complexon III and slightly greater rapidity.

It is worth mentioning that antimony is very rapidly and precisely determined from lead nitrate solution to which antimony is added. However, from solutions obtained by dissolving lead containing antimony alloy in nitric acid the values obtained for antimony are always smaller than the exact values.

School of Technology
Department of Physical Chemistry
and Electrochemistry

REFERENCES

1. Zotta, M. "Polarographic Analysis of Refined Lead" — *Gazz. Chim. Ital.*, 78: 143, 1948.
   Milner, G. W. C. *The Principles and Applications of Polarography and other Electro-analytical Processes* — London: Longmans, Green and Co., 1957. p. 384.

2. Cozzi, D. "Die polarographische Bestimmung der Unreinheiten an Fe, Cu, Cd, Zn, Sb und Sn im gelänterten Blei" — *Analytica Chimica Acta* (Amsterdam) 4: 204—210, 1950.

3. Kraus, R. and J. V. A. Novak. "Polarographische Bestimmung des Antimons in Hartblei" — *Die Chemie* (Weinheim) 56: 302—303, 1943.

4. Hourigan, H. F. and J. W. Robinson. "Polarographic Determination of Antimony in Lead-Antimony Alloys" — *Analytica Chimica Acta* (Amsterdam) 10: 281—291, 1954.

5. Prshibik, R. *Kompleksony v khimicheskom analize* — Moskva: Izdatel'stvo inostranoi literatury, 1960.

DYNAMIC ADSORPTION OF ORGANIC VAPORS ON BLOCKED ADSORBENTS

by

S. KONČAR-ĐURĐEVIĆ and IVANKA PETKOVIĆ

There are many works dealing with dynamic adsorption of vapors on adsorbents[1, 2, 3, 4, 5, 6]. We have also dealt with this problem, studying the adsorption rate of organic vapors from mixtures with dry air through a well-defined layer of adsorbent. The regularities we found are graphically presented in an earlier paper[4].

In the present work we used the same method as before with the exception that instead of a pure adsorbent we used adsorbents on which certain quantities of acidic, basic, or neutral dyes had been adsorbed from liquid solutions. Such adsorbents, assuming that the corresponding adsorption centers are covered by a certain quantity of adsorbed dye, are called "blocked adsorbents". The number of covered, blocked active adsorption centers depends on the quantity of dye adsorbed. On the blocked dry adsorbents secondary adsorption of vapors from the gaseous phase was performed and dynamic adsorption up to the equilibrium state was studied.

The final purpose of our studies with blocked adsorbents was to discover the nature of the active sites, the structure of the adsorbent and the nature of the adsorption bond: whether it is capillary condensation or surface adsorption.

METHOD

Adsorption was performed in the following way: first, the organic dye was adsorbed from a liquid solution and then after drying, the adsorbent was used for adsorbing organic vapors in a mixture with air.

In order to draw definite conclusions it was necessary to fix the adsorbed dye to a certain site in the adsorbent so that in the secondary adsorption of organic vapors the adsorbed molecules would not change places or react with it[1]. This condition was considered to be fulfilled if the dye was insoluble in the solvent whose vapor was used for secondary adsorption. This is why we chose methylene blue, in which case we performed primary adsorption from aqueous solutions. Benzene, toluene and xylene (mixture of O-, m- and p-xylene), in which methylene blue does not dissolve, were used as organic vapors. Activated charcoal and silica gel were used as adsorbents.

Activated charcoal was used because it, more or less, equally adsorbs acid, basic and neutral organic molecules.

The dye was adsorbed by static adsorption, the concentration of the solution being measured colorimetrically before and after adsorption, for determining the amount adsorbed. The concentrations of the starting solutions were: 0.003%, 0.03%, 0.1%, 0.2% and 0.5% of methylene blue. The starting weight of the pure dry adsorbent was about 3 grams.

After adsorption from the solution the adsorbent was filtered and dried at 85 °C to constant weight. Drying was done at 85 °C because of the possible instability of methylene blue molecules at high temperatures. After drying the adsorbent was poured in the vertical branch of a U-tube. This was necessary so that the gaseous mixture would flow uniformly through the granular layer of the adsorbent.

We used dry air saturated with vapors of the organic solvents. The flow rate of dry air was always the same, 2.30 l/min. That of the gaseous mixture was higher since this air got saturated with vapors of the solvent through which it passed and came out as a mixture at 20 °C.

The solvent was kept in a thermostat by which the temperature of the liquid and vapor was kept constant. Because of the good dispersion of the gaseous in the liquid phase and its subsequent passage through glass wool soaked with the solvent (it was above the liquid at the inlet of the mixture draw-off tube) the air could be considered saturated with the vapors.

The gaseous mixture was passed through the measured U-tube with the adsorbent. The U-tube was kept in a water thermostat at 25 °C. This precaution was necessary so as to prevent vapor condensation on the adsorbent.

The weight increase of the U-tube was determined on an analytical balance every 5 minutes during the first 15 minutes and then every 15 minutes until equilibrium was established.

It should be pointed out that subsequent migration of molecules when such samples are left for 24 hours without adsorption may cause subsequent adsorption. However, this happens in such small quantities that in our measurements the difference my be neglected.

The results are briefly presented below.

EXPERIMENTAL

Activated charcoal, (Special for Gas Absorption, BDH), grain size 1.5 to 2 mm was used. A starting amount of three grams of charcoal, after degassing to a constant weight at 120 °C, was put into various concentration (0.003%, 0.03%, 0.1%, 0.2%, 0.5%) aqueous solutions of methylene blue.

The solutions were made by diluting the initial (0.5%) solution to the above concentrations.

After adsorption from the solution at room temperature, which lasted from 5 to 12 days, with occasional shaking, the solution was measured with Lange's colorimeter to determine the amount of color dye adsorbed.

After static adsorption of the dye, the charcoal was filtered and dried at 85°C to constant weight. One of the vertical branches of a small U-tube was filled with this charcoal and a 2.30 l/min current of air saturated with vapors of benzene, toluene, and xylene at 20°C. was passed through it.
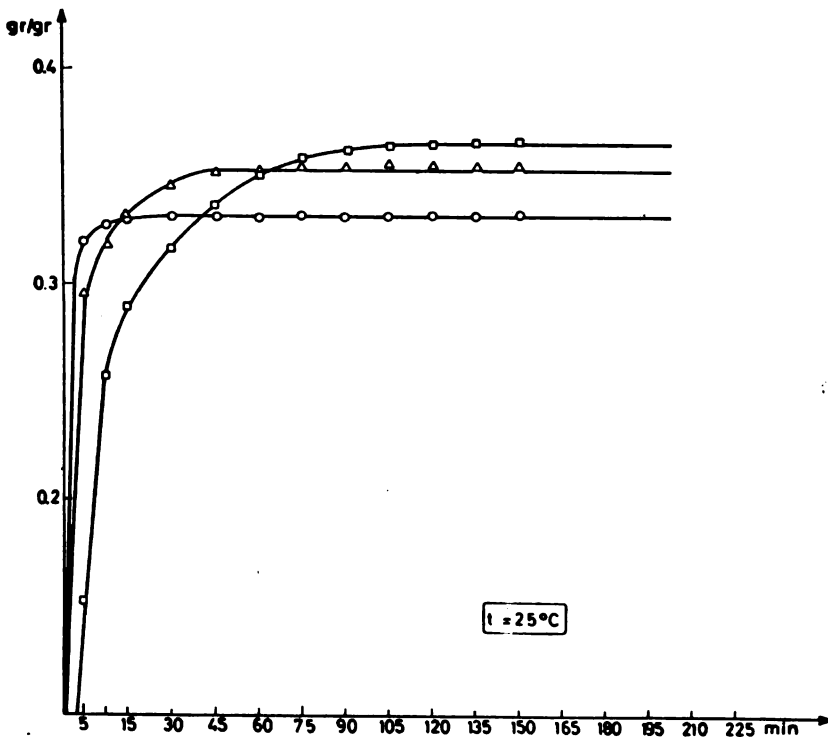
Fig. 1

Dynamic adsorption of benzene, toluene and xylene vapor on
unblocked carbon.

O — Benzene 0.332 g/g
△ — Toluene 0.355 g/g
□ — Xylene   0.366 g/g

The vapor adsorption rate was determined directly by weighing the U-tube on an analytical balance every 5 minutes for 15 minutes, and then every 15 minutes until constant weight. The air was first dried by passage through conc. H_2SO_4 and then through a U-tube filled with calcium chloride.

The results are represented by the following adsorption rate curves.

Figure 1 shows the increase in weight of the adsorbent on adsorption of benzene, toluene, and xylene vapors on non-blocked activated charcoal.

The figure shows that xylene is adsorbed most, next toluene and least benzene. It also shows that the radius of curvature of the adsorption rate curves decreases in the same order. It should be borne in mind that the molar concentrations of the vapor in air increases from xylene through benzene, because of the different vapor pressures at the test temperature.

Figure 2 shows the dynamic adsorption rate of benzene vapor on activated charcoal blocked with different amounts of adsorbed methylene blue.

The figure shows that the quantity of benzene adsorbed increases slightly for a very small amount of adsorbed dye (0.0010 g/g), and then gradually decreases with further increase of the amount of dye.
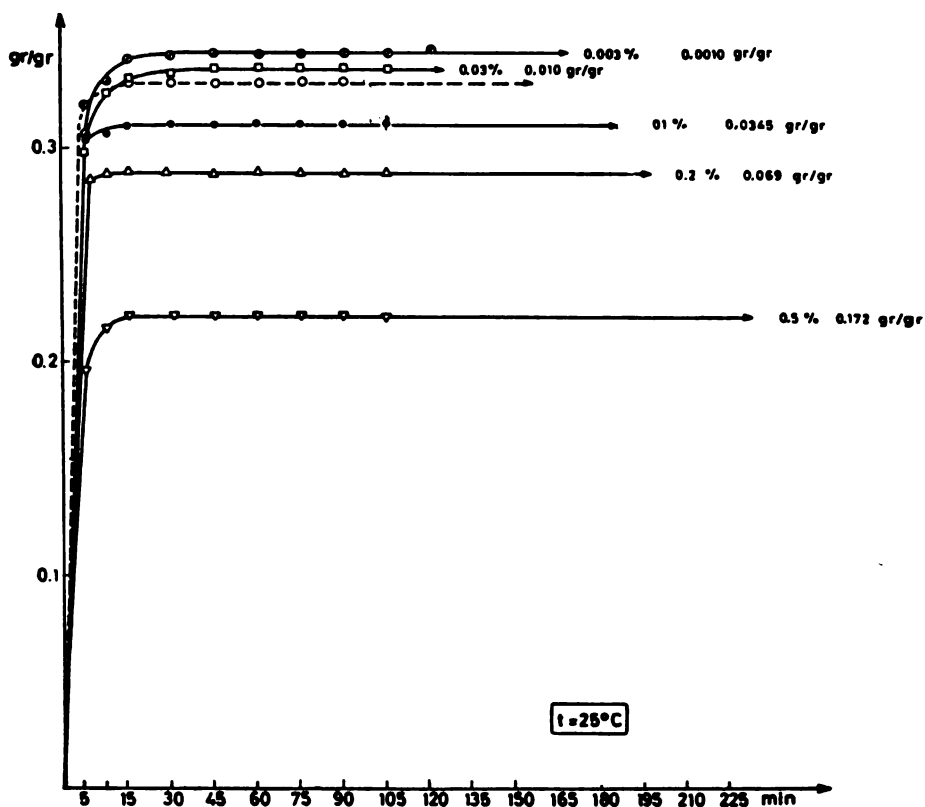
Fig. 2

Dynamic adsorption of benzene vapor on unblocked carbon and carbon blocked
with different concentrations of methylene blue

Figure 3 shows the dynamic adsorption of toluene vapor on activated charcoal
blocked with methylene blue. It is seen that the amount of adsorbed vapor decreases
with increasing degree of blocking.
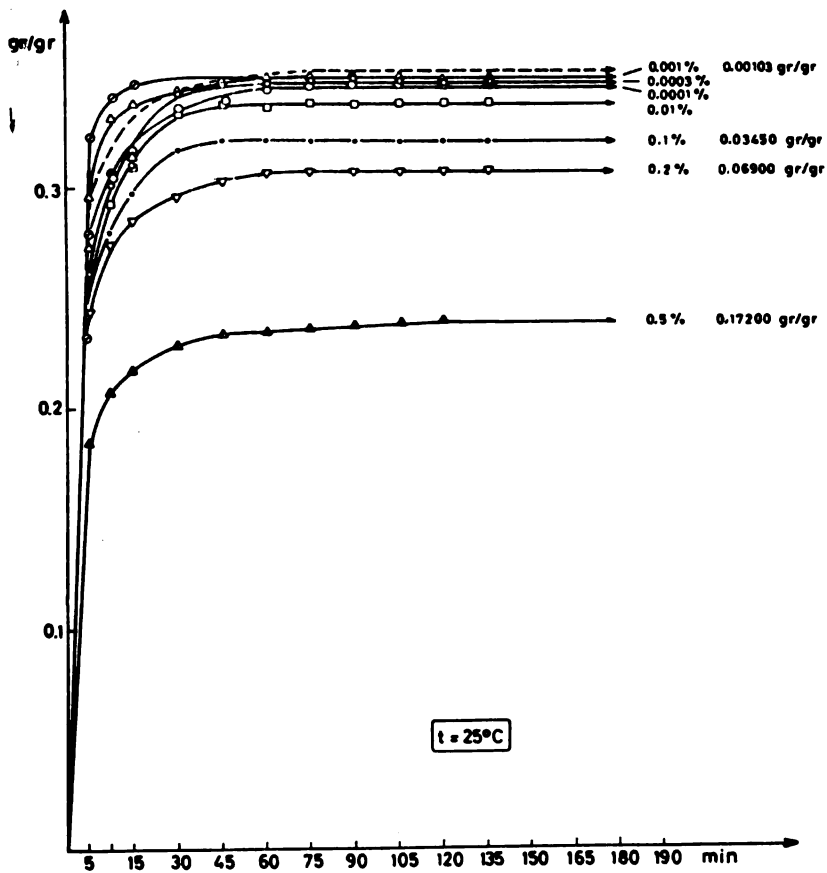
Fig. 3

Dynamic adsorption of toluene vapor on unblocked carbon and carbons blocked
with different concentrations of methylene blue.

3
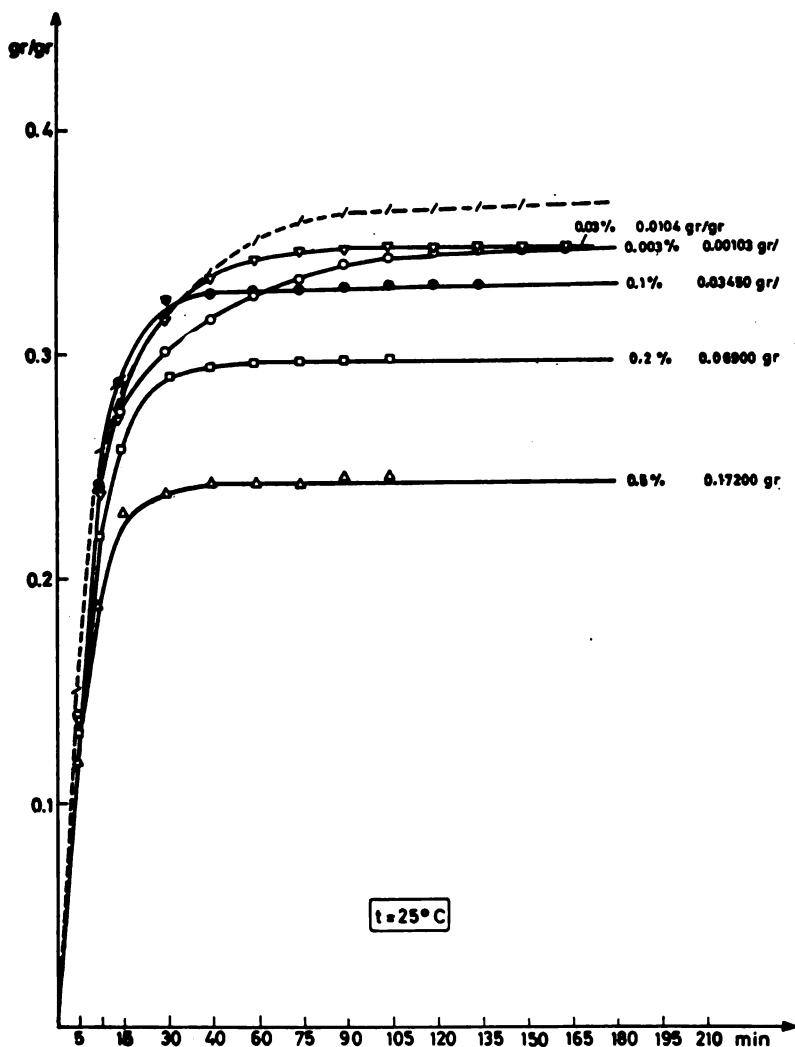
Fig. 4

Dynamic adsorption of xylene vapor on unblocked carbon and carbons blocked with different concentrations of methylene blue.

Figure 4 shows the adsorption of xylene vapor on activated charcoal, blocked with the same concentrations of methylene blue as in the case of benzene. As in the case of toluene, the adsorption of vapor decreases with increasing degree of blocking.
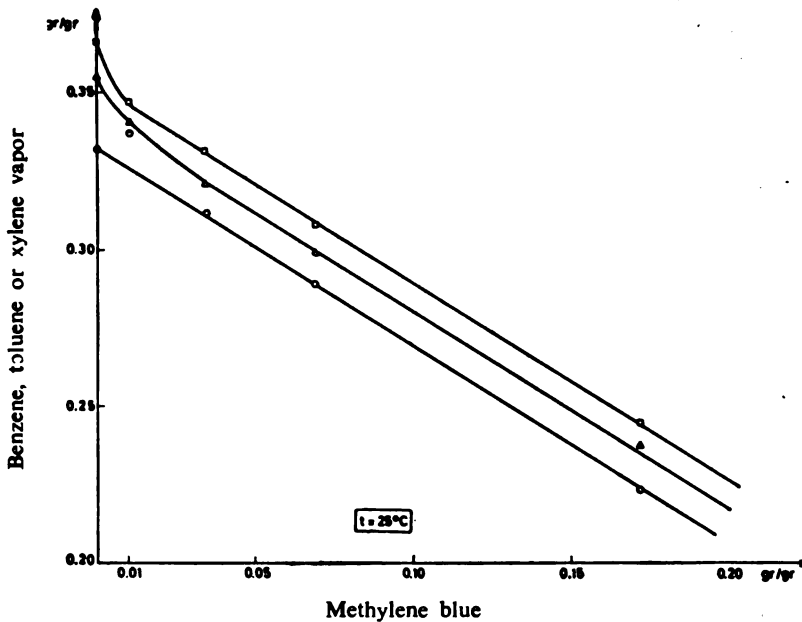
Fig. 5

Dynamic adsorption of solvent vapor on active carbon blocked with different concentrations of methylene blue.

○ — Benzene
△ — Toluene
□ — Xylene

Figure 5 shows the ratio of adsorbed vapors (g/g) to adsorbed methylene blue, also per gram of adsorbent (g/g). It is seen that there is an almost linear relationship between the two quantities. There is a certain deviation in the case of benzene (at a methylene blue concentration of 0.03%) and in the case of toluene and xylene (for unblocked adsorbent), but of a different nature.

3*
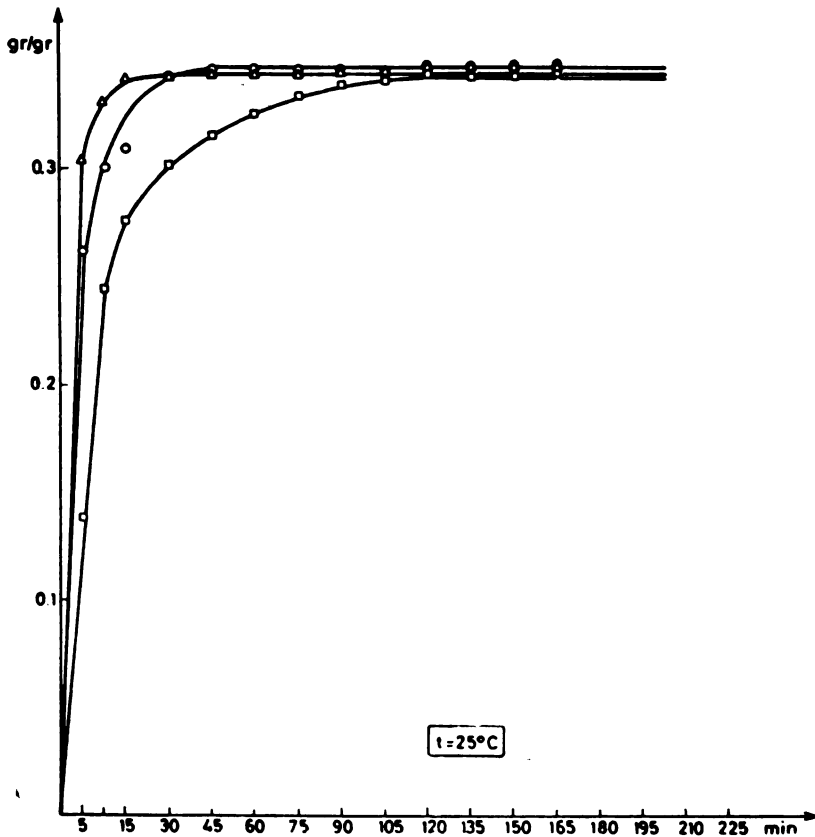
Fig. 6

Dynamic adsorption of benzene, toluene and xylene vapor on carbon blocked
with 0.0010 g of methylene blue.

△ — Benzene 0.348 g/g
○ — Toluene 0.348 g/g
□ — Xylene 0.346 g/g

The following figures show the adsorption curves for benzene, toluene and
xylene vapors on charcoal blocked with the same quantities of methylene blue:
0.0010 g (Fig. 6); 0.0103 g (Fig. 7); 0.0345 g (Fig. 8); 0.0690 g (Fig. 9); 0.1720 g
(Fig. 10).
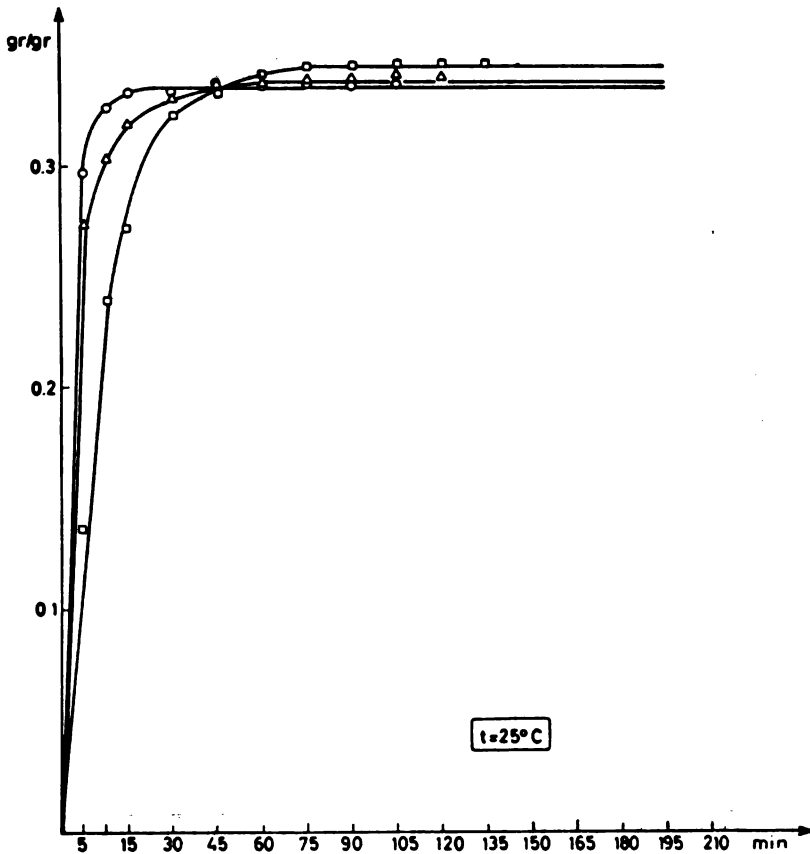
Fig. 7

Dynamic adsorption of benzene, toluene and xylene vapor on carbon blocked with 0.010 g methylene blue.

O — Benzene 0.337 g/g
△ — Toluene 0.341 g/g
□ — Xylene 0.347 g/g

It is seen that in this case the relative quantity of vapor adsorbed does not change: xylene is always adsorbed most, the toluene and then benzene, independent of the quantity of methylene blue.
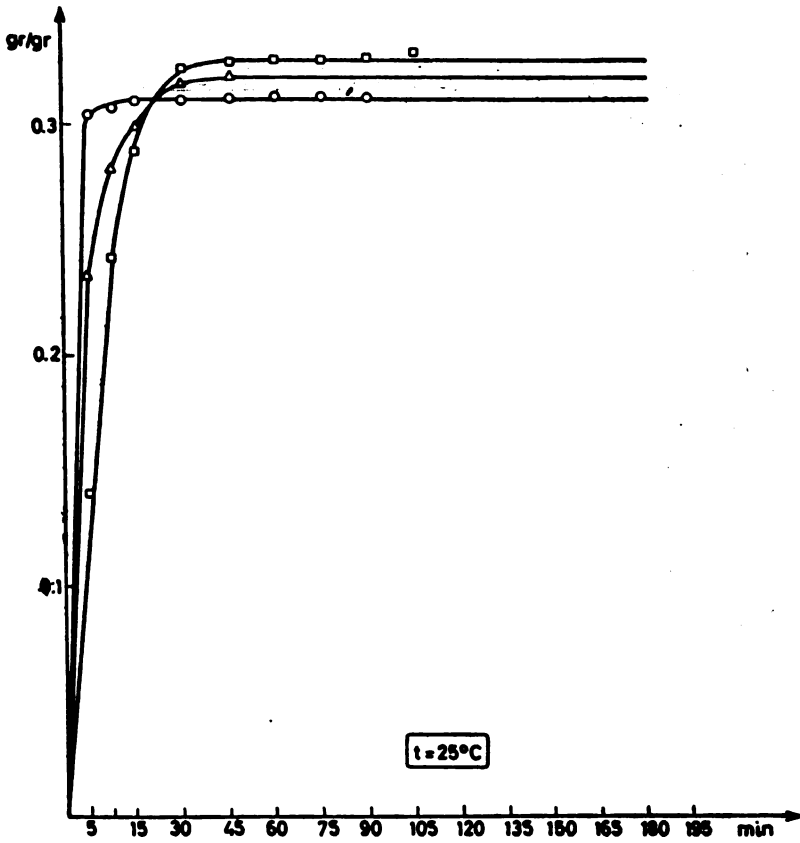
Fig. 8

Dynamic adsorption of benzene, toluene and xylene vapor on carbon
blocked with 0.0345 g of methylene blue.

O — Benzene 0.312 g/g
△ — Toluene 0.321 g/g
□ — Xylene 0.329 g/g
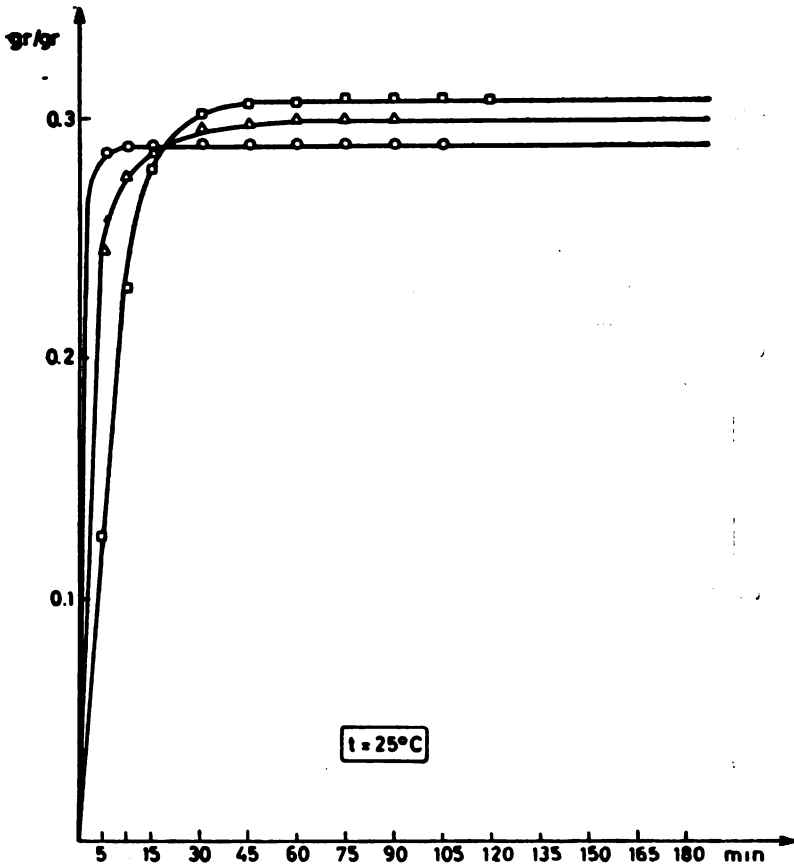
Fig. 9

Dynamic adsorption of benzene, toluene and xylene vapor on carbon
blocked with 0.0690 g of methylene blue.

⊙ — Benzene 0.289 g/g
△ — Toluene 0.299 g/g
□ — Xylene 0.308 g/g
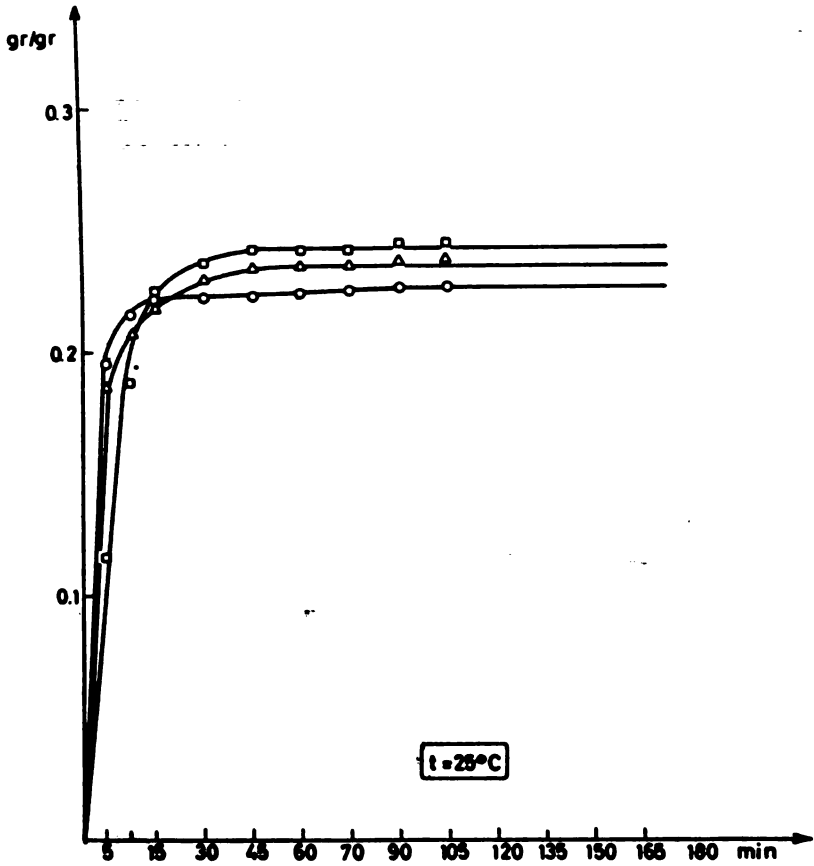
Fig. 10

Dynamic adsorption of benzene, toluene and xylene vapor on carbon blocked with 0.172 g of methylene blue.

△ — Benzene 0.227 g/g
⊙ — Toluene 0.238 g/g
□ — Xylene 0.245 g/g

Faculty of Technology
Institute of Chemical Engineering
Beograd

REFERENCES

1. Hassler, J.W. and W.E.Mc Minn. "The Nature of Active Carbon' *Industrial and Engineering Chemistry* (Washington) 37: 645—649, 1945.

2. Timofeev, D.P. and N.l.Alekseeva. "Kinetika adsorptsii pri narastano hchei i kontsentratsii gaza v potoke" (Kinetics of Adsorption with Increasing Concentration of Gas in Current) — *Zhurnal prikladnoi khimii* (Moskva) 36(9); 1919—1928, 1963.

3. Masamune, S. and J.M. Smith. "Adsorption Rate Studies — Significance of Pore Diffusion" — *American Institute of Chemical Engineers* (New York) 10(2): 246—252, 1964.

4. Končar-Ðurđević, S. and I. Petković. — Glasnik hemijskog društva (In press).

5. Crespi, S. "Contribution expérimentale à l'etude de l'adsorption et de la desorption dynamique de la vapeur d'eau par le gel de silice" — *Chaleur et industrie.* (Paris) 284: 53—58, 1949.

6. Taylor, R.K. "Water Adsorption Measurements of Silica Gel" — *Industrial and Engineering Chemistry* (Washington) 37: 649—653, 1945.

THE INFLUENCE OF AGEING ON SOME RHEOLOGIC CHARACTERISTICS OF STARCH GELS

by

LJUBOMIR ĐAKOVIĆ and PETAR P. DOKIĆ

After an aqueous suspension of starch is heated at about 95 °C and then cooled, a starch paste, i.e., a gel is formed in which solvated macromolecules of the starch constituents — amylose and amylopectin — are structured so as to form a relatively stable molecular lattice in which there may be a considerable quantity of solvate-bound and mechanically trapped water.

After some time changes occur in the structure of the gel — dissociation of the water, subsequent association of molecular fragments and aggregation and coarsening of the initial spatial molecular lattice. These changes are considered to be particularly pronounced in amylose, causing its crystallization and gradually increasing crystallinity of the system, and hence the corresponding changes in the whole system. This process in starch gels, mainly caused by changes occurring in amylose, is called aging or retrogradation.

There is no need to emphasize the practical importance of observing or preventing retrogradation in starch paste, because it is clear that it is in fact an essential process upon which depend the usefulness and storage life of products containing starch in *clusterized* form.

According to Holc[1] retrogradation of amylose proceeds in three phases:

1) Spiral macromolecules of amylose get straightened out, absorbing the corresponding amount of energy;

2) Open chains, i.e., amylose molecular segments get mutually oriented after losing the solvate envelope;

3) Hydrogen bridges are formed between the neighboring -OH groups so that several molecules aggregate thus forming a crystal structure.

Methods by which the process of retrogradation can be observed quantitatively are important in preventing starch gel aging; in this respect we have the following possibilities[2]: 1. Roentgenography; 2. Observation of changes in the resistance of amylose to enzymatic breakdown; 3. Viscosimetry; 4. Observation of the changes in turbidity or transparency; 5. Chromatographic methods, 6. Infrared spectrophotometer, ultraviolet absorption and electron microscopy; 7. Determi-

nation of amylose in solution; 8. Determination of iodine absorption by amperometric or potentiometric titration.

Rheological methods can also be used to observe the changes induced by retrogradation in starch gels — e.g. observation of visco-elastic properties of the crumb of bread after a certain time. It is also interesting that H. J. Kornel[3] has shown that the coefficient of thi-xotropy depends on the starch concentration in the starch gel, the volume ratio of amylose to amylopectin, the temperature of measurement and the aging time. Wheaten starch gels are markedly thixotropic at 25 °C, while amylopectin gels are only negligibly thixotropic. The thi-xotropy of starch gels is much less at 60 °C, while amylopectin behaves almost like a Newtonian fluid. According to Kornel the coefficient of thixotropy increases if the gels are left to age for 16 hours.

Adopting Holo's standpoint on the development of retrogradation, as cited before, the above changes occurring in amylose must also influence the rheological behavior of the system. The present investigations were performed to discover what rheologic changes take place in starch gels in a given concentration range, in dependence on the aging time and the rheological conditions of measurement (shearing rate).

RESULTS

Corn starch, produced by a Zrenjanin factory, and distilled water were used.
A Reotest PV rotational viscosimeter with coaxial cylinders was used for the measurements. The rate of rotation of the inner cylinder could be adjusted from 5/18 to 243 rpm. which with the given dimensions of the outer and inner cylinders gives a shearing rate of from 0.2 to $1.3 \ 10^3 \ sec^{-1}$. The shearing stresses which can be measured with this instrument range from 120 to $3.10^4 \ dgn/cm^2$.

Starch pastes were prepared by heating a dispersion of starch in distilled water in a closed vessel, constantly stirring with a propeller mixer for 45 minutes. The fluid was heated to 95°C in the first 30 min, i.e. the heating rate was about 2°C/min. This temperature was maintained for another 15 minutes. The procedure for preparation was determined on the basis of viscographic curves obtained with Braben-der's viscograph.

The concentrations of the pastes were adjusted to lie within the measuring range of the instrument. They were calculated by weight of dry starch and amounted to 4%, 8% and 12%.

After the pastes had been prepared measurements were first made frequently' and later at 24-hour intervals. Therefore, we can give the results of measurements for two groups of time intervals:

a) about 40 minutes from the completion of paste preparation;

b) after from 1 to 10 days.

In both cases the gels were prepared separately and kept at the same temperature, 9°C, so as to accelerate aging and prevent the spoiling of samples (if kept at room temperature). Measurements on the rotational viscosimeter were made after adjusting the temperature to 17±0.05°C for all samples.

Measurement of the shearing stress τ (dyn/cm^2) at different shearing rates D(sec^{-1}) have shown that the shearing stress increases with shearing rate so that the apparent viscosity ηa:

$$\eta_a = \frac{\tau}{D} \ [p]$$

considerably decreases with increasing shearing rate. This decrease is more pronounced the more concentrated the gel, as is seen in Fig. 1, where values ln η_a are plotted against D.
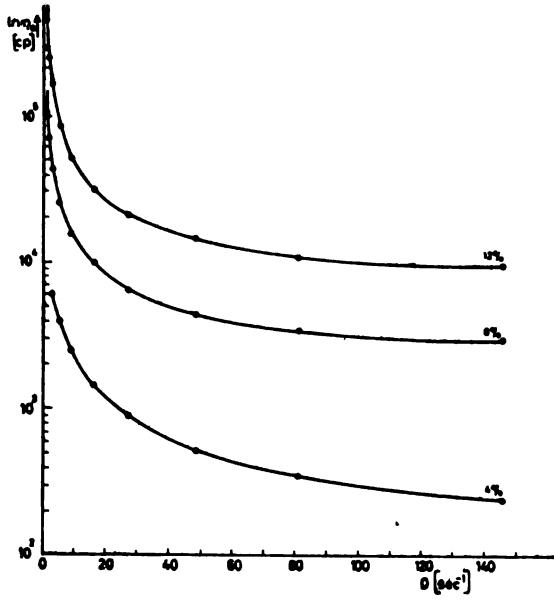
Fig. 1

Curves of ln η_a: rate of shear D (sec^{-1}), for different concentrations of starch gel.
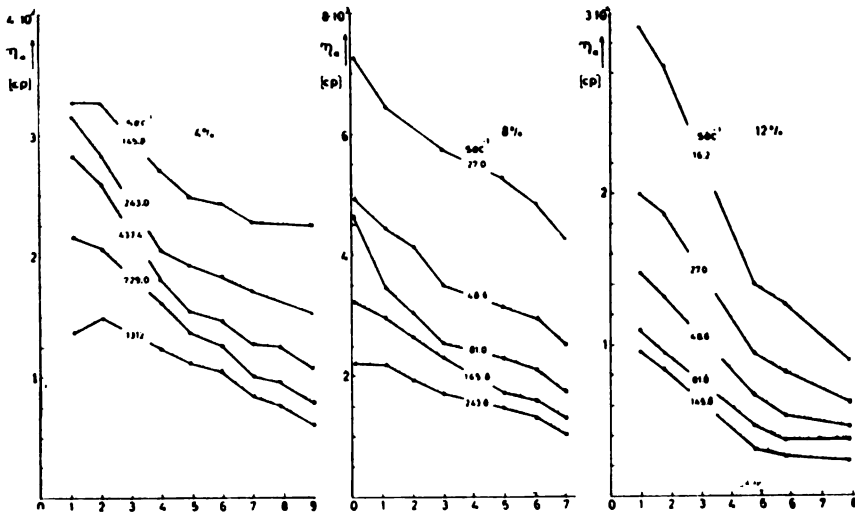
Fig. 2

Apparent viscosity η_a (cp) against time of ageing (days), measured at different rates of shear (sec^{-1}) for different concentrations of starch gel.

The dependence of viscosity on time differs depending on whether it was measured at short or long intervals. In the case of frequent measurements, immediately after gel preparation, the viscosity first increases and then decreases, while in the case of long interval measurements the results show a constant decrease of viscosity with time, irrespective of the shearing rate at which the apparent viscosity was measured.

The changes of apparent viscosity with time in gels of different concentrations are easily seen in the apparent viscosity — time graphs, in which the curves represent η_a as a function of time at various shearing rates (Fig. 2).
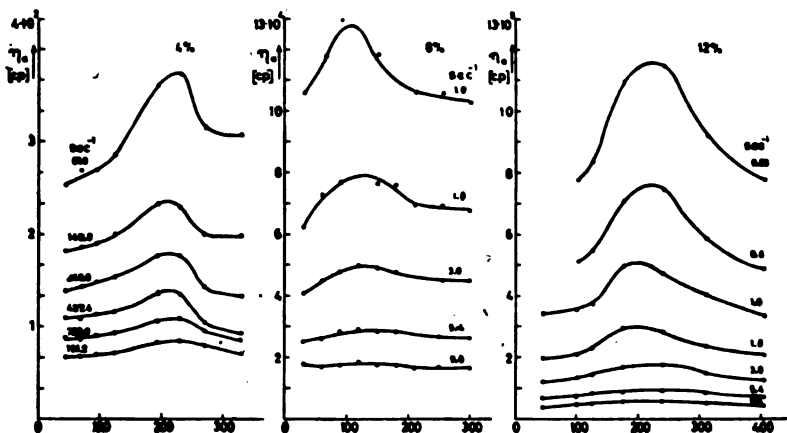
Fig. 3

Apparent viscosity in (cp) against time of ageing in minutes measured at different rates of shear (sec⁻¹), for the given concentrations of the starch in %

The measurements of apparent viscosity at shorter time intervals, i.e. immediately after the preparation and cooling of the gels, show that the shearing rate at which the apparent viscosity is measured is also of certain importance: the height of the viscosity maximum depends on the shearing rate. The smaller the shearing rate the higher the maximum (Fig. 3).

DISCUSSION

The fact that the apparent viscosity changes with the aging time is of considerable importance because these changes result from the internal changes produced by aging (e.g. dissociation of the bound water, aggregation, change in shape and configuration of macromolecules, orientation, etc.).

The results point to the possibility of observing the aging process using a coaxial cylinders viscosimeter, and to the fact that rheological methods allow observation of aging even at concentrations of 4—12%, at which starch gels do not have much mechanical rigidity but are more or less thixotropic and not elastic.

The viscosity of a structured system with linear macromolecules, under constant measuring conditions, strongly depends on their size and configuration, i.e. asymmetry. Changes in asymmetry, regardless

of their cause, cause changes in viscosity. Thus, increase in viscosity of the system may result from increased asymmetry of macromolecules due to the unwinding of amylose molecules, increase of solvation, increased structuralization of the system, etc. Decrease in viscosity is due to the orientation of asymmetric molecules, dissociation of solvate-bound water and aggregation of lengthwise oriented linear macromolecules.

Change in viscosity under different measuring conditions, in our case at varying shearing rates D (secp^{-1}) (Figs. 1 and 3), indicates the presence of asymmetric macromolecules. The viscosity of a system with asymmetric molecules is lower the higher the shearing rate, or at a constant shearing rate the viscosity is higher the more asymmetric the particles.

The variation of viscosity with time at constant shearing rate (Fig. 3) leads to the conclusion that the asymmetry of linear particles in the system changes. We shall not go into the reasons for these changes (solvation, dissociation, linkage, orientation or aggregation). Hence the appearance of a maximum at various shearing rates (Fig. 3) could be considerd of change in the asummetry of amylose molecules. If only changes in amylopectin, were in question, this "rate" effect would not exist.

The results have also shown that the measuring conditions also play a certain role, particularly the shearing rate. In our case, changes of apparent viscosity with time are more pronounced at lower shearing rates. This is so because at low shearing rates the effect of particle asymmetry on the viscosity is grater.

Faculty of Technology
Institute for Chemistry
Novi Sad

REFERENCES

1. Holló, J., J. Szejtli and G.S. Gantner. "Der Mechanismus der Retrogradation von Amylose" — *Die Stärke* (Stuttgart) 12(4): 106—108, 1960.

2. Holló, J., J. Szejtli and G.S. Gantner. "Untersuchung der Retrogradation von Amylose" — *Die Stärke* (Stuttgart) 12(3): 73-77, 1960.

3. Cornell, H.J. "The Effect of Amylopectin on the Properties of Starch Gels" — *Die Stärke* (Stuttgart) 15(2): 43—50, 1963.

THE EFFECT OF SOLVENTS ON THE PROPERTIES OF POLYSTERENE OBTAINED BY STEREOSPECIFIC POLYMERIZATION*

by

PAULA S. PUTANOV, BORISLAVA D. VUČUROVIĆ
and SPOMENKA D. PETROVIĆ

The use of catalysts with a stereospecific effect in polymerization processes has become very important in the past 10 years from both the theoretical and the piactical point of view. Owing to the exceptional activity of Ziegler's catalysts, it has become possible to synthesize polymers which, in crystallizing capability and mechanical properties, may be compared with the so far unequalled natural polymers. The great variety of petrochemical raw materials and the improved technology of processes have made possible the synthesis of new types of polymers and copolymers of exceptional physical, chemical and mechanical properties. It may be expected that this progress will continue with further improvement of Ziegler's catalysts and the discovery of new possibilities of their use.

The great practical importance of stereospecific polymerization has led to intense study of its mechanisms. So far several hypotheses have been published of the process of stereospecific polymerization — action of free radicals, ion exchange, formation of intermediary active complexes, or a heterogeneous mechanism. These hypotheses have been experimentally confirmed within limited ranges of experimental conditions and for specific types of monomers. However, a general theory of stereospecific catalysis which would give a unique explanation of all the effects investigated and practically used so far has not yet been developed [1, 2, 3, 4].

At this level of knowledge of the mechanism of stereospecific polymerization the effect and role of solvents in polymerization cannot be interpreted or envisaged with absolute certainty. Some general theoretical hypotheses based on the influence of solvent association in cases in which the reactants are activated may be made if the polarity, the dielectric constant, and other properties of the solvent are known.

Experimental expeiience has also shown that the rate of ion po y-merization depends on the polaiity of the medium. The polymerization

---

* Reported at the XIth Symposium of the Serbian Chemical Society in Beograd, January 1965.

4

rate and the molecular weight of the polymers increase with increasing polarity of the medium. In the polymerization of styrene dissolved in benzene, carbon tetrachloride and similar solvents, polymers of smaller molecular weight are obtained. The dependence of the molecular weight of polystyrene on the property of the solvent is very high, which is ascribed to the different activity of the macroradicals in different solvents.[3] Experiments have also shown that, in anion polymerization of dienes in the presence of metal alkyls, the properties of the solvent also exert considerable influence on the order of monomer incorporation in the macroanion and, therefore, on the structure of the polymers.

Changing the polarity of the *R-Me* bond by using solvents of different polarities, one can regulate the order of monomer incorporation, i.e., the degree of stereoregularity of the increasing chain. The last monomer in the chain is the ion pair itself and that is why the monomer coming between these ions is influenced by them. In case the solvent can form solvates of a complex with one or two members of the ion pair, the properties of the solvent naturally influence the macromolecular structure in anion polymerization.[4]

The effect of the solvent on the course of stereospecific polymerization and on the properties of the polymers obtained has not only theoretical but also a specific practical significance as well. The availability and the price of the solvent, the conditions for its application and regeneration, its toxic effect, volatility and other physical and chemical properties may have a considerable influence on the industrial realization of the process.

EXPERIMENTAL

The present work is a study of the results of polymerization of styrene in benzene, toluene and xylene as solvents.

Styrene was polymerized in a glass apparatus consisting of a three-necked flask with a thermometer, a dropping-funnel and a reflux condenser, was used. A glycerine bath was used for heating and a magnetic mixer for mixing.

The experiment was carried out in a sealed transparent plastic chamber containing an absolutely inert atmosphere. The chamber has openings for gas inlet and outlet and the inert atmosphere is established in it by alternately introducing and evacuating gas with a vacuum pump. The gas was nitrogen purified of oxygen and moisture.

Polymerization of styrene was performed with a conventional Ziegler catalyst composed of titanium tetrachloride and triethyl-aluminum in a 1:2 molar ratio. Fresh redistilled styrene was added through the dropping-funnel of the three-necked flask containing a Ziegler catalyst synthesized just before. The styrene was added at 70—78°C, stirring constantly with the magnetic mixer. Polymerization lasted altogether five hours.

The effect of the different solvents under identical polymerization conditions was investigated by comparing the molecular weight, specific weight, softening temperature, consistency, color and yield of the polymers. The molecular weight of the polystyrene was determined by the viscosimetric method at 30°C. The specific weight was measured with a picnometer at room temperature to $\pm 1.10^{-4}$ assuming that measurements on an analytical balance were made with approximately the same accuracy. The softening temperature was determined by the capillary method. At a heating rate of 1—2°C per minute we determined the temperature at which the polymer column becomes completely molten. The yield was determined by weighing the polystyrene on a balance to an accuracy of $\pm 1.10^{-2}$.

RESULTS AND DISCUSSION

All results for the above properties of polystyrene are shown in Table 1.

TABLE 1

Polystyrene properties as a function of the type of solvent

Test No.	Solvent	Yield g.	Yield conv. %	Spec. wt g/cm³	Sof.en. temper.	Molec. wt.	Consist- ency	Appea- rance
1	benzene	21.1	79.0	1.0222	115.5	$6.17 \cdot 10^5$	hard	pale yellow
2	,.	19.7	78.8	0.9560	109.5	$6.25 \cdot 10^5$	softer	yellow
3	xylene	19.5	78.0	0.9637	59.5	$4.00 \cdot 10^5$	,,	pale yellow
4	toluene	16.3	65.2	0.9672	66.3	$2.50 \cdot 10^5$	,,	,, ,,
5	benzene	17.2	70.0	0.9462	109.0	$2.74 \cdot 10^5$	hard	,, ,,
6	xylene	21.5	86.0	0.9488	68.0	$0.83 \cdot 10^5$	softer	yellow
7	toluene	13.7	52.8	0.9611	58.0	$1.00 \cdot 10^5$	,,	,,
8	benzene	18.0	72.0	1.0780	145.3	$6.73 \cdot 10^5$	hard	pale yellow

Properties of polystyrene as a function of the type of solvent

In the case of polymerization in benzene, the molecular weights of most of the polymers were slightly higher than those obtained by polymerization in xylene and toluene.

Polymers obtained in benzene in most cases also have slightly higher specific weights (1.0780 in experiment 8 ans 1.0222 in experiment 1) than those obtained by polymerization in xylene or toluene (0.9637 in experiment 3 and 0.9672 in experiment 4).

Polymers obtained by polymerization in xylene and toluene have considerably lower softening temperatures (59.5°C in experiment 3 and 66.3°C in experiment 4) than those obtained in benzene (145.0°C in experiment 8, 115.5°C in experiment 1 and 109.0°C in experiments 2 and 5).

With regard to consistency it may be concluded that polymerization in benzene yields hard polystyrene while in xylene and toluene it yields softer polystyrene.

As for the appearance, the type of solvent does not influence the color of the polystyrene.

Comparison of the polystyrene yields shows that the lowest yield is obtained if toluene is used as the solvent.

Institute for Chemical,
Technological and Metallurgical Research
Beograd

4•

REFERENCES

1. Dawns, F. and Ph. Teyssié. "Mécanismes de polymérisation stéréospécifique par les metaux de transition" — *The Journal of Chemical Physics* (Lancaster) 60(7): 2376—2392, 1963.

2. Natta, G. and J. Pasquon. "The Kinetics of the Stereospecific Polymerization of α—Olefins" — *Advances in Catalysis* (New York) 11(1): 2—65, 1959.

3. Geilord, N. and G. Mark. *Lineinye i stereoreguliarnye polimery* (Linear and Stereoregular Polymers) — Moskva: Izdatel'stvo inostrannoi literatury, 1962.

4. Losev, I. and E. Trostanskaia. *Khimiia sinteticheskykh polimerov* (The Chemistry of Synthetic Polymers) — Moskva: Izdatel'stvo "Khimiia", 1964.

5. Natta, G. "Stereospecific Polymerizations and Catalysis" — *Gazzetta chimica italiana* (Rome) 89(1): 89—126, 1959.

6. Rokhov, Iu., D. Kherd and R. L'uis. *Khimiia metalloorganicheskikh soedinenii* (The Chemistry of Metal-organic compounds). — Moskva: Izdatel'stvo inostrannoi literatury, 1863.

7. Strepikheev, A. and V. Derevitskaia. *Osnovy khimii visokomolekuliarnykh soedinenii* (Principles of the Chemistry of High-Molecular Compounds). — Moskva): Gosydarstvenno nauchno-tekhnicheskoe izdatel'stvo khimicheskoi literatury, 1961.

SOLUBILITY OF ALEKSINAC OIL-SHALE KEROGEN
I — EFFECT OF SOME SOLVENTS BOILING BELOW 100°C*

by

DRAGOMIR VITOROVIĆ and MIRJANA M. ŠABAN

The weak solubility of kerogen in organic solvents is seen in the definition of bituminous oil shales itself. The solubility of kerogen has been an interesting problem and in past years researchers have investigated the action of a large number of solvents on different kinds of oil shales.

This problem has been approached for the purpose of: 1) separating native kerogen or at least some unchanged part of it which would be suitable for structure study, from the mineral matter of the oil shale, in which case the chemical nature of the organic substance could be determined from the nature of the solvent and its effect, or 2) finding out suitable conditions for dissolving the largest possible quantity of the organic substance irrespective of the chemical change involved. This is interesting from the viewpoint of industrial processing of oil shale.

Investigations of bituminous oil shales of different origin by a large number of researchers[1—17] have shown that kerogen dissolves rather weakly in organic solvents at a moderate temperature. In most cases less than 10% and most often less than 3% of the organic substance dissolves. In the above works a great number of solvents of different chemical nature, polarity, boiling point and other characteristics were used. Only some solvents such as pyridine[7] and tetralin[9] dissolved any quantity of kerogen. The extractions were most often carried out with a Soxhlet apparatus. The authors point out that the extraction yield is a function of extraction time,[4,8,9] solvent temperature,[8,9] oil-shale's richness,[8] the kerogen's constitution and the polarity of the solvent,[9,10] and the oil-shale particle size.[8] Some authors determined the nature of kerogen by extraction experiments. The chemical action of solvents, in case they are not chemically inert, is not particularly discussed in these papers; the slightly higher yield in the extraction of some oil shales with solvents such as pyridine, aniline, acetic acid, and cycloxanol [3,7,11,3] may be ascribed to the chemical action of these solvents with pronounced basic or acidic properties.

The weak solubility of kerogen in simple solvents confirms the fact deduced from investigations of other physical and chemical properties that the organic component of oil shale si of a macromolecular

---

* Part of this work was reported at the 34th Intern. Congress on Industrial Chemistry in Beograd, Sept., 1963.

nature. At high temperature and pressure macromolecules depolymerize into fragments of smaller molecular weight which dissolve more easily. Thus for exmple 90% of kerogen of Estonian oil shale can be dissolved in ether and benzene if the shale is first heated at 175°C.[18] Pyrolitic decomposition also explains the exceptionally good solubility of kerogen in solvents with a high boiling point such as tetralin, phenanthrene, etc.[9]. This solubility at high temperature and pressure, so-called thermal dissolution, during which the kerogen changes, is interesting from the industrial point of view. However, since our aim was the isolation of unchanged kerogen we did not use the thermal dissolution methods.

In the present work we investigated the Yugoslav Aleksinac oil shale. One of the properties of the organic component of this shale which has not been investigated so far is its solubility. We considered that knowledge of the behavior of kerogen with various solvents would contribute to the knowledge of the nature of this material. The behavior with solvents of various nature is one of the physical properties that has been used in recent times to explain the structure of organic molecules. At the same time, isolation of pure kerogen or some of its fractions would allow easier and more reliable use of many physical and chemical methods for the study of its structure.

Therefore, we undertook a systematic investigation of the solubility of Aleksinac oil-shale kerogen, first of all to isolate unchanged kerogen or some parts of it.

In choosing the solvent we took into account factors which might affect the kerogen solubility: polarity of the solvent, hydrogen bonding capacity, chemical action of the solvent, etc. The choice was made in the following way:

1) Since kerogen changes of high temperature we used solvents boiling below 100°C for the first experiments so as to avoid pyrolysis;

2) We chose solvents of different polarities and different hydrogen bonding capacity;

3) It is well-known that the combined action of two or more solvents in mixture may be more efficient than the single solvents, and this phenomenon is very often used in practice. Therefore, we also made preliminary investigations of the action of several azeotropic mixtures.

In the first experiments we used the following solvents: petroleum ether, cyclohexane, carbon disulfide, carbon tetrachloride, chloroform, benzene, diethyl ether, acetone, methylene chloride, methly alcohol, ethyl alcohol, ethyl acetate, methyl ethyl ketone, dioxane and diethyl amine. We also used three azeotropic mixtures boiling below 100°C: ethyl alcohol-methyl ethyl ketone, dioxane-cyclohexane and diethyl amine-acetone.

Dioxane has the highest boiling point, 101°C. Some of the solvents are nonpolar: carbon tetrachloride, carbon disulfide, benzene and cyclohexane, then chloroform, methylene chloride, dioxane and diethyl ether, up to polar solvents like ethyl alcohol, methyl alcohol, ethyl acetate, acetone, methyl ethyl ketone and diethyl amine.

According to Ewell's classification,[19,21] the list includes solvents from the second group, those whose molecules contain both an active hydrogen atom and negatively charged atoms with a free electron pair (ethyl alcohol, methyl alcohol, diethyl amine), solvents from the third group, with negatively charged atoms but without an active hydrogen atom (dioxane, acetone, methyl ethyl ketone and ethyl acetate), solvents from the fourth group with active hydrogen atoms but without negatively charged atoms (chloroform and methylene chloride), and solvents from the fifth group which do not form a hydrogen bond (carbon disulfide, carbon tetrachloride, cyclohexane and petroleum ether).

The following four solvents have not previously been used for dissolving the organic component of oil shale: dioxane, ethyl acetate, methyl ethyl ketone and diethyl amine. Neither have the azeotropic mixtures used here.

EXPERIMENTAL

Aleksinac bituminous oil shale was ground in a ball-mill (—100 mesh, 0.149 mm, Tyler).

The content of organic matter determined by the method of Jovanović and Vitorović[22] was 19.14%.

Parallel experiments were also run with raw shale and enriched shale obtained by treating Aleksinac oil shale with hydrochloric acid (1:1) thus removing the carbonates. This was done because we thought the solubility of the kerogen might be better if carbonates were not present. By enrichment we obtained a sample with 32.5% organic matter.

Extractions was performed in a Soxhlet's apparatus. 40—50 g portions of the oil shale were weighed out. Since the amount of the kerogen dissolved depends on the extraction time, all the extractions lasted 100 hours.

The solvents were purified and redistilled if they were not pro analysi. After extraction, most of the solvent was removed by distillation at normal pressure and the rest in vacuum. To determine the reproducibility of the results, experiments with some solvents were repeated.

The solubility of the kerogen of both the raw and enriched shales in different solvents, expressed in wt % of the initial quantity of kerogen, is shown in Table 1. The solvents are listed in order of increasing hydrogen bonding capacity. The solubility in the azeotropic mixtures is shown in Table 2.

The reaction products were only roughly investigated, in order to determine their basic properties. In most cases they were light-brown to brown doughy substances, or sometimes in the form of a brown powder.

The boiling points of the extracts vary from 65—95°C and in most cases they are not sharply defined.

An elementary microanalysis of all extracts was made. There were often difficulties regarding the reproducibility of the results because of the nonhomogeneity of the material. Since sulphur was qualitatively determined in most products, especially in those from enriched oil shale, and in some nitrogen too, these elements were also quantitatively determined. Nitrogen was determined by Dumas's micromethod and sulphur by Schöniger's method.[23]

It is interesting to note that ignition of most of the extracts left some ash. Table 3 gives data on the C/H, C/N and A/S ratios and the quantity of ash obtained on ignition.

The molecular weight was determined by Rast's method using camphor as the solvent. Of all the solvents tested, camphor proved to be the best for extracts of this shale. For example, carbamide and β-naphthol do not dissolve the extracts at all, and in the case of phenanthrene, which dissolves them, there is no depression. The molecular weight varies mainly between 430 and 500. Reproduction of the results was not always satisfactory.

TABLE 1

Solvent	Boiling point	Dissolved, % of total kerogen			
		From raw shale		From enriched shale	
		Exp. 1	Exp. 2	Exp. 1	Exp. 2
Petroleum-ether	40—70°	0.53	0.65	0.88	0.88
Cyclohexane	81°	1.55	—	2.66	—
Carbon-disulfide	47°	1.62	1.03	2.06	1.75
Carbon-tetrachloride	76°	2.16	—	2.36	—
Benzene	80°	2.32	—	2.89	—
Methylene chloride	40°	1.78	—	2.19	—
Chloroform	61°	2.72	—	3.98	—
Diethyl ether	35°	1.78	—	2.17	—
Ethyl acetate	77°	3.19	—	3.98	—
Methyl ethyl ketone	79°	3.89	—	5.30	—
Acetone	56°	2.76	—	3.29	—
Ethyl alcohol	78°	3.81	3.99	4.69	3.99
Methyl-alcohol	65°	3.15	3.07	4.80	4.96
Dioxane	101°	11.44	10.11	6.72	8.08
Diethylamine	56°	12.02	10.62	13.24	11.71

TABLE 2

Azeotropic mixture	Boiling point	Dissolved, % of total kerogen	
		From raw shale	From enriched shale
Diethilamine (72%) — acetone (28%)	51⁰	12.71	11.71
Ethyl alcohol (40%)— methyl ethyl ketone (60%)	74⁰	4.82	6.46
Dioxane (24,6%) — cyclohexane (75,4%)	79⁰	4.15	4.84

To get at least some idea of the nature of the extracts we recorded the infrared spectrum of several extracts: carbon disulfide, dioxane, ethyl acetate, methyl-ethyl ketone, and ethyl alcohol extracts (Perkin Elmer, Mode 137). The similarity of the spectra and their resemblance to the spectrum of native kerogen is obvious. All the spectra show mainly only the characteristic absorption bands of the carbonyl groups, the aliphatic $(CH_2)_n$ chain, and the C—CH_3 groups.

DISCUSSION

Since solubility depends on intermolecular forces, we have tried to correlate the results both with the factors influencing the intermolecular forces of the solvents and the constants which are a measure of these forces.

Therefore we analyzed the correlation of the solubility of the raw and enriched shale with:

a) the temperature of extraction, i.e. the boiling temperature of the solvent;

b) the polarity of the solvent, i.e. the dipole moment and the dielectric constant;

c) the internal pressure of the solvent, particularly of the nonpolar solvents;

d) the hydrogen bonding capacity of the solvent (Ewells classification);

e) the chemical character of the solvent;

f) the change of the efficiency of the single solvents in azeotropic mixtures.

The following conclusions may be drawn:

a) The solubility of the kerogen does not change regularly with extraction temperature, i.e. with the boiling point of the solvent, as

TABLE 3

S – Raw shale extract   *O – Enriched shale extract*

Solvent	C/H		C/H		C/S		Ash (%)	
	S	O	S	O	S	O	S	O
Petroleum ether	6.73	6.33	59.54	61.70	52.01	3.49	0.47	0.41
Cyclohexane	6.58	6.46	71.06	67.21	—	—	0.00	0.00
Carbon disulfide	6.56	6.44	50.54	54.40	12.85	6.72	0.60	0.00
Carbon tetrachloride	6.61	6.32	71.60	90.37	54.96	10.84	0.34	0.62
Benzene	6.58	6.42	75.47	76.59	109.00	—	0.20	0.00
Methylene chloride	6.75	6.54	43.41	50.41	67.30	—	0.51	0.00
Chloroform	6.66	6.57	54.50	65.21	171.6	14.40	0.00	2.60
Diethyl ether	6.68	6.69	37.81	50.55	34.85	—	0.97	0.00
Ethyl acetate	6.76	6.57	54.03	50.65	59.50	21.50	2.10	4.54
Methyl ethyl ketone	7.02	6.86	39.96	62.13	46.15	13.69	1.01	4.36
Acetone	6.99	6.77	79.14	73.44	18.20	—	1.95	1.72
Ethyl alcohol	6.84	6.44	46.50	42.03	32.60	5.53	6.20	2.34
Methyl alcohol	7.11	6.40	39.41	59.18	25.40	9.40	16.47	15.39
Dioxane	6.43	6.45	34.96	44.98	30.00	—	0.30	0.50
Diethylamine	6.97	6.25	8.46	8.34	20.60	—	0.00	0.66
Enriched shale	7.17		99.40		21.77		70.17	
Kerogen	7.36						12.00	

TABLE 4

Solvent	Dipole moment	Dissolved, % of total kerogen
Hexane	0.08	0.53
Cyclohexane	0	1.55
Carbon tetrachloride	0	2.16
Benzene	0	2.32
Carbon disulfide	0	2.57
Dioxane	0.45	11.47
Diethyl-amine	1.10	12.02
Chloroform	1.15	2.72
Diethyl ether	1.15	1.78
Methylene chloride	1.55	1.78
Methyl alcohol	1.66	3.07
Ethyl alcohol	1.68	3.81
Ethyl acetate	1.81	3.19
Acetone	2.72	2.76
Methyl ethyl ketone	2.75	3.86

is seen in Table 1. Therefore it may be concluded that the solubility does not essentially depend on the boiling point of the solvent if it is below 100°C.

b) In Tables 4 and 5 the solvents are listed in order of increasing dipole moment or dielectric constant[24]. Although the kerogen solubility does not change regularly with these constants it may be concluded that it in general increases with increasing values of the constants. The greatest deviations are in the case of dioxane and diethyl amine.

TABLE 5

Solvent	Dielectric constant	Dissolved, % of total kerogen
Hexane	1.890	0.53
Cyclohexane	2.023	1.55
Dioxane	2.209	11.47
Carbon tetrachloride	2.238	2.16
Benzene	2.284	2.32
Carbon disulfide	2.64	2.57
Diethylamine	3.6	12.02
Diethyl ether	4.355	1.78
Chloroform	4.806	2.72
Ethyl acetate	6.02	3.19
Methylene chloride	9.08	1.78
Methyl ethyl ketone	18.51	3.86
Acetone	20.70	2.76
Ethyl alcohol	24.30	3.81
Methyl alcohol	32.63	3.07

c) The internal pressure of the solvents at their boiling points were calculated from the molecular heat of evaporation $(P_i = L_i/V)$.[25] From these values it may be concluded that there is no completely uniform dependence of kerogen solubility on the solvent internal pressure, although it tends to increase with increasing internal pressure (Table 6).

TABLE 6

Solvent	Internal pressure (at)	Dissolved, % of total kerogen
Carbon tetrachloride	2613	2.16
Hexane	2769	0.53
Ethyl acetate	2772	3.19
Benzene	2915	2.32
Diethyl ether	3241	1.78
Acetone	3481	2.76
Chloroform	3813	2.72
Carbon disulfide	3872	2.57
Methyl-ethyl-ketone	4007	3.89
Ethyl alcohol	5780	3.85
Methyl alcohol	7700	3.15

d) As Table 1 shows, the solubility of kerogen in solvents which cannot bond hydrogen (solvents 1—5) is about 2%. It increases to about 4% for solvents capable of hydrogen bonding owing to the active hydrogen or the negatively charged atom in the molecule. In the mixotropic group dioxane and diethyl amine come before methyl alcohol and ethyl alcohol (dioxane as an ether, and diethyl-amine because of the negatively charged nitrogen which forms a weaker hydrogen bond than that formed by negatively charged oxygen). However, these two solvents dissolve more kerogen than others, probably because of superposition of the effects of hydrogenic and chemical bonding with kerogen, and this is why we separated them and put them after alcohol.

The greater efficiency of the solvents which form hydrogen bonds may be ascribed to the presence both of active hydrogen atoms in the kerogen, e.g. hydrogen of the tertiary carbon atom, and of negatively charged atoms (O,N) in the kerogen molecule.

e) The exceptionally high activity of dioxane and diethyl-amine in dissolving kerogen may be asciibed to the basic properties of these two solvents. The free electron pairs per two atoms of oxygen in dioxane and per one atom of nitrogen in the molecule of diethyl-amine, can bind protons with a bond stronger than the hydrogen bond, because of the high electron density, i.e., an acido-basic reaction may occur between these donor molecules and the acidic parts of kerogen molecules containing electron acceptors.

f) Rough data were obtained on the combined action of the solvents in azeotropic mixtures on efficiency in dissolving kerogen. As seen from Table 2, a mixture of diethyl amine with 28% acetone does not influence the efficiency of diethyl amine. The efficiency of a mixture of 25% doixane and 75% cyclohexane lies between the efficiencies of the pure solvents. Only the mixture of ethyl alcohol (40%) and methyl-ethyl-ketone (60%) has a better action than either solvent separately.

As was expected, the solubility of kerogen from enriched oil shale is, with a few exceptions (in the case of dioxane and the azeotropic mixture of diethyl amine and acetone), always about 1.1—1.5 times better than in case of raw shale.

From Table 1 it is seen that in the reproduction of some extraction experiments the relative error was about 10% except in the case of carbon disulfide where it was slightly greater.

Table 3 shows the C/H, C/N and C/S ratios and the quantity of ash obtained on ignition. As is seen, the extraction product C/H ratio for raw shale vaiies from 6.40 to 7.11 and for enriched shale from 6.25 to 6.86. Since the C/H ratios of enriched shale and kerogen (with 12% ashes) are slightly greater, viz. 7.17 and 7.36 respectively, it is obvious that the extracted fractions of kerogen are richer in hydrogen than the native kerogen, as was expected because of the higher solubility of the kerogen fractions of lower molecular weight. This particularly holds for extracts obtained from enriched shale whose C/H ration is almost always slightly smaller than that of raw shale extracts.

The C/N ratio of the raw shale extracts varies from 34.96 to 79.15 and of the enriched shale extracts from 42.03 to 90.37. The nitrogen content in raw shale extracts varies from 0.98 to 2.12% and in enriched shale extracts from 0.81 to 1.17%. The C/N ratio for enriched shale is considerably greater than that of any extract — 99.40. The nitrogen content enriched shale is only 0.65%. Hence it may be concluded that the dissolved fractions of kerogen are richer in nitrogen than the native kerogen. Likewise, it is seen that extracts of raw shale are richer in nitrogen than extracts of enriched shale. This may be explained assuming that the kerogen contains the basic nitrogen which is dissolved in hydrochloric acid in the enrichment of the shale. The pronounced deviation of the C/N value in extracts obtained with diethyl-amine may be ascribed to incomplete removal of the solvent or its presence due to chemical reaction with kerogen fractions.

The C/S iatio of the extracts of raw and enriched shale essentially differ. The former vary from 18.20—171.60 (sulphur content from

0.74 to 5.98%), and the latter from 3.49 to 21.50 (sulphur content from 3.71—18.50%). The C/S ratio of the enriched shale, in which sulphur is both organic and pyritic, is 21.77. Hence in the extraction of enriched oil shale, and of raw shale with polar solvents or solvents with a pronounced hydrogen bonding capacity, the kerogen fractions isolated are considerably richer in sulphur than kerogen itself.

As is seen from Table 3, the quantity of ash on the whole increases with the polarity of the solvent. An exceptionally large quantity of ash, 15—16%, was obtained from the methyl alcohol extract. A detailed analysis of the ash was not made. However, a considerable quantity of iron was found. It may be assumed that the inorganic components of the extract originate from the kerogen molecules.

From the investigation of the action of different solvents on Aleksinac oil-shale kerogen and the knowledge of some of the properties of the extracted kerogen fractions, it may be deduced that the dissolved fragments, and probably the rest of the kerogen too, consists mainly of $(CH_2)_n$ chains with tertiary carbon in the chain and possibly alicyclic rings too. The extracts also contain oxygen in the -CO-group and some other hetero-atoms (N,S).

The acidic nature of certain parts of kerogen may be asserted from the much higher solubility in basic solvents. The dissolved fragments have a smaller molecular weight than the rest of the kerogen.

Faculty of Science
Institute of Chemistry
Beograd

REFERENCES

1. Dolch, M. — *Oesterreichische Chemiker Zeitung* (Wien) 23:122, 1920.
2. Gavin, M. and J. Aydelette. — *United Sates Department of Interior Bureau of Mines Report of Investigations* (Washington) 2313: 300, 1921.
3. McKee, R. and R. Goodwin. — *Industrial and Engineering Chemistry* (Washington) 15: 343, 1923.
4. Van Tuyl, F. and C. Blackburn. — *Oil and Gas Journal* (Tulsa, Okl.) 24: 188, 1925.
5. Blackburn, C. — *Colorado School of Mines* 19: 9, 1924.
6. Hawley, J. — *Bulletin of the American Association of Petroleum Geologists* (Tulsa, Okl.) 13: 303, 1929.
7. Guthrie, B. — *United States Department of Interior, Bureau of Mines Bulletin* (Washington) 415: 105, 1938.
8. Ferris, B. — *Mines Magazine* (Denver) 38: 19, 28, 1948.
9. Bureau of Mines — *United States Department of Interior, Bureau of Mines Report of Investigations* (Washington) 4652: 59, 1950.
10. Moore, J. and H. Dunning. — *Industrial and Engineering Chemistry* (Washington) 47: 1440, 1955.
11. McKinney, J. — *Journal of the American Chemical Society* (Easton, Pa) 46: 968, 1924.
12. Schneider, W. — *Gesammelte Abhandlungen zur Kenntnis der Kohle* 5: 69, 1920.
13. Kogerman, P. — *Archiv für die Naturkunde Estlands* 10(6): 37, 1931.
14. Gaisser, F. and H. Bader. — *Chemiker-Zeitung mit dem Sonderteil, Die Chemische Praxis und der Beilage, Chemisch-Technische Uebersicht* (Heidelberg) 50: 277, 1926.
15. Holmberg, B. — *Chimie et Industrie* (Paris) 16: 394, 1926.
16. Gil-Av, E., S. Heller and F. Stecker. — *Bulletin of the Research Council of Israel* (Jerusalem) 4: 136, 1954.
17. Dulhunty, J. — *Journal and Proceedings of the Royal Society of New South Wales* (Sydney) 76: 268, 1943.
18. Raudsepp, K. — *Trudy Tallinskogo politekhnichskogo instituta*, Ser. A. 73, 120, 1956.
19. Ewell, R. et al. — *Industrial and Engineering Chemistry* (Washington) 36: 872, 1944.
20. Hecker, E. — *Chimia* (Zürich) 8: 233, 1954.
21. Hermanek, S., V. Schwarz, and Z. Chekan — *Collection of the Czechoslovak Chemical Communications* (Prague) 28: 2031, 1962.
22. Jovanović, S. and D. Vitorović. — *Glasnik hemijskog društva* (Beograd) 17: 347, 1952.
23. Schöniger, W. — *Mikrochimica Acta* (Wien) 123, 1955; 869, 1956.
24. Weissberger, A. et al. "Organic Solvents", in: *Technique of Organic Chemistry*, Vol. VII, 2nd. edition — New York: Interscience Publishers, 1955.
25. Glasstone, S. *Textbook of Physical Chemistry* — New York: D. Van Nostrand Company, Inc., 1954.

BULLETIN
OF THE CHEMICAL
SOCIETY
Belgrade

Editor:
ĐORĐE M. DIMITRIJEVIĆ

CONTENTS

METHODOLOGICAL ASPECTS OF THE STUDY OF COMPLEX CHEMICAL REACTIONS

1. INTERMEDIATES AND UNIT STEPS IN CHEMICAL REACTIONS.

by

ALEKSANDAR R. DESPIĆ

I. INTRODUCTION

In the approach and methods of early works in chemical kinetics devoted to elucidating reaction mechanisms and based on comparisons of "black box" results with postulated models of possible reaction mechanisms, certain shortcomings were inherent, which essentially have not been overcome during further development and are still characteristic of the situation in this field today.

Thus until quite recently no attempt was made to set up a system for the generation of the reaction mechanism models to ensure that all the possible and plausible mechanisms would be available for consideration. The more or less intuitive way of generating possible mechanisms might be adequate if only very simple systems were considered, where the total number of possible reaction routes - combinations of possible unit steps, is analysably small. Ever increasing interest in the chemical behaviour of organic substances and similar complex systems has given this problem a special importance that many authors do not seem to be aware of. The serious objection may be raised that besides the mechanisms which have been proposed, other unimagined mechanisms may exist which may explain the observed fact equally well or better. Chemical kinetics contains numerous examples where new experimental evidence discarded currently accepted mechanisms and indicated new ones. This situation has given all conclusions concerning reaction mechanisms the status of working hypotheses, always waiting for additional evidence for or against them, with an unknown degree of reliability.

Dissatisfaction with this situation need not be purely academic, arising from the question of the true representation of the physical reality of the microcosm. A more important aspect seems to be the limitations it places on the capacity of chemical kinetics to make extrapolations and predictions concerning the effects of any deviations of the conditions and the state of the system from those used in experi-

ments on whose basis a particular mechanism is advanced. It seems that a much more desirable situations in that respect would be that in which all possible mechanisms of an overall chemical process which satisfy a given set of experimental results were known. Further research could then be carried out to make eliminations and reduce the number of possible mechanisms, in the ideal case to one. The essential advantage would be that at any stage in the study of a particular system the degree of uncertainty would be known exactly.

This study attempts to offer a systematic approach to these problems starting from the essential ones of selecting intermediates and generating the unit steps which should be available for speculations concerning reaction mechanisms as a whole.

II. INTERMEDIATES IN CHEMICAL REACTIONS

The complexity of any reaction route is determined essentially by the number of intermediate species which can be formed from or between the stable molecules composing the system. Hence, at the outset of any kinetic investigation one is faced with three basic questions: (a) what are the intermediates?; (b) what combinations of them render kinetically distinct unit steps?; (c) what combinations of unit steps give kinetically distinct reaction routes?

With known reactants, composed of atoms in various valency states, as the basic chemical entities, it is possible to derive systematically a number of intermediate species and reaction products, by the methods of combinatorics, which take no account of the physical reality as known to us through chemical experience. Such an approach, although logically impeccable, in most cases introduces at the start so many species that further combinations of them to make unit steps and reaction mechanisms would be impossible to digest by any means known at present. Hence, although the introduction of chemical experience can be objectionable on the ground of being subjective and limited, it seems that at this stage it cannot be avoided.

There seem to be at least three basic levels of chemical experience to be considered. The first is that which can be gained by experimental investigation of the system concerned. This seems quite satisfactory as far as reaction products are concerned, since, being by definition stable molecular species, they can be chemically analyzed by the available methods. This is in fact the first and essential step in any kinetic investigation (cf. e. g. (1) (2)). However, methods for the detection of unstable intermediate species are so far very scarce, and even if this were not so, there would always be doubts as to their capacity to give unambiguous answers. In other words only positive evidence in favor of the presence of a particular species could be accepted, while negative evidence could always be denied by maintaining that the life-time or the concentration of the species was beyond the limits detectable by the method used.

The use of the third and most general level of chemical experience implies assuming the presence of all the species that are known to appear as parts or combinations of molecules present in the system as reactants or reaction products. Thus in many organic reactions the

methyl-radical is a very probable intermediate while the carbon atom will *never* appear and need not be considered. Here the use of the term "never" can again be questioned but the conclusion is reasonable enough for further developments to be based on it with a high degree of certainty. With that approach it is possible to define for any given system a set of intermediate species representing single atoms or atomic groups which could plausibly be formed by splitting or combining the molecules of reactants among themselves or with electrons from an electrode if an electrode process is considered, and this seems to be most widely used in the kinetics literature. However, this way opens a very broad field for speculation and when more carefully considered many of the selections of intermediates made in the past for discussions of possible reaction mechanisms appear rather arbitrary.

It seems possible to interpolate between those levels a second level of experience based on a thermodynamic argument, which does not appear to have been either fully or properly used so far.

From the thermodynamic point of view each point along a reaction coordinate axis between two successive unit steps in a complex mechanism represents a state of a part of the reacting system, which is characterized by a certain standard enthalpy H^0. In the limiting case all such states preceeding the rate-determining step can be considered to be in equilibrium, so that the rate constant is a complex entity given by

$$k_r = \frac{RT}{Nh} \; K^{+} \prod_{i-1}^{k} K_i \qquad (1)$$

where K^{+} is the pseudo-equilibrium constant between the activated state and the state preceeding it, and the K_i are the equilibrium constants for all the unit steps concerned. Taking logs and differentiating with respect to temperature we get

$$\frac{d\ln k_r}{dT} = \frac{d\ln T}{dT} + \frac{d\ln K^{+}}{dT} + \sum_{i-1}^{k} d\ln K_i \qquad (2)$$

Hence for, e.g., reactions in solution, using known relations, we get

$$\frac{E_a}{RT^2} = \frac{1}{T} + \frac{\Delta H^{+}}{RT^2} + \sum_{i=1}^{k} \frac{\Delta H_i^0}{RT^2} \qquad (3)$$

or,

$$E_a - RT = \Delta H^{+} + \sum_{i=1}^{k} \Delta H_i^0 \qquad (4)$$

where E_a is the empirical Arrhenius activation energy and ΔH_i^0 is the standard enthalpy change for the i-th of the k unit steps. Since

ΔH^{+} is always positive and the $\sum\limits_{i=1}^{l} \Delta H_i^0$ is equal to the standard enthalpy change between the initial state and any state along the reaction coordinate, this cannot be larger than the Arrhenius activation energy minus RT. Since this change can be taken to represent the standard enthalpy of the intermediate state referred to the initial state (whose standard enthalpy is arbitrarily taken as zero), and this must be the sum of the standard enthalpies of the intermediates involved, we can formulate a rule:

— no intermediate species in a chemical reaction can have a standard enthalpy with respect to the initial state larger that the Arrhenius activation energy minus RT, and conversely:

— *a possible intermediate species need not be considered as a potential participant in a reaction mechanism if its standard enthalpy with respect to the initial state of the system is larger than the experimentally determined Arrhenius activation energy minus RT.*

An exception to this rule can be found in some specific systems in which equation (1) has a somewhat different form (e.g. chain reactions with mutual termination), which requires the above statement to be somewhat modified. Also, exceptions are systems containing some intermediates which are more stable than the reactants, i.e. which have a negative standard enthalpy with respect to the initial state. In the latter cases the upper limit of the standard enthalpy of other intermediates is higher by the absolute value of the sum of all these standard enthalpies, for there may exist a unit step in which all these stable and very unstable intermediates take part together. Bearing this in mind, and provided thermodynamic data are available, this rule can obviously help select from all the possible intermediates those which are unlikely to participate in the reaction mechanism. This is of the utmost importance for the generation and use of reaction mechanism models, as will be shown on another occasion.

III. GENERATION OF UNIT STEPS

Any consideration of possible reaction mechanisms implies an exact knowledge of all the unit steps that can be operative in the system. The unit steps are normally generated by making all possible combinations between reactants, reaction products and intermediates and selecting those which can have chemical meaning, i.e. which satisfy the stoichiometry of chemical equations, and the kinetic meaning implied in the following assumptions, which are justified both on theoretical grounds and by chemical experience:

(a) By far the most frequent reactions are monomolecular and dimolecular ones. Even termolecular reactions are very unlikely to be competitive with those of lower order, and those of higher orders are never found. Hence, only combinations of one or two species on the

left side of the chemical equation of any potential unit step need be considered. Because of the condition of microscopic reversibility the same must be true of the right side, i.e. no more than two reaction products of each unit step are likely to be found. Exceptions to this are species which are present in large excess, such as electrons or solvent molecules, since at a metallic surface the former are likely to be found at any point of reaction between molecular species, while on the solution side of the interface or in a condensed homogeneous system the same applies to the latter.

(b) In electrochemical reactions multiple electron exchange reactions are unlikely to occur. Although reasons have been given for such a situation as far as specific systems are concerned (3), this to our knowledge has not been given a general quantitative theoretical justification, but can be taken as reasonable on the basis of electrodical experience.

(c) Only those combinations should be taken into account in which stoichiometry between the two sides of the equation is fulfilled, i.e. in which the resulting right side of the chemical equation contains only stoichiometric amounts of species that are already on the list of reactants, intermediates and reaction products.

In this case the number of combinations of the species to be considered as potential unit steps is considerably less than the number of all possible combinations. With R reactants and reaction products and I intermediates the number of potential chemical unit steps can be obtained by summing $(R + I)$, denoting possible monomolecular reactions, with combinations of each of the species with itself and with each of the other species, representing possible dimolecular unit steps, and then multiplying this by the same number of combinations decreased by 1 for the resulting left side of the chemical unit step. We then get that the total number of combinations to be tested for their capacity to render plausible chemical unit steps is

$$n_c = [2(R+I) + C(R+I, 2) - 1][2(R+I) C(R+I, 2] =$$

$$\cong [2(R+I) + C(R+I, 2)]^2 = \frac{(R+I)^2 \cdot (R+I+3)^2}{4} \qquad (5)$$

To obtain electrochemical unit steps each of the above combinations must be tested with an electron added to the chemical equation. Hence, there will be an equal number, n_e, of such combinations, so that the total number of combinations to be considered in an electrochemical system comes to

$$n = n_c - n_e = [(R+I)(R+I+3)]\left[\frac{(R+I)(R+I+3)}{2} - 1\right] \cong$$

$$= \frac{(R+I)^2 (R+I+3)^2}{2} \qquad (6)$$

Since in these combinations each unit step is counted twice, the left side of one chemical equation being taken as the right side in some other combination, the upper limit to the number of the unit steps

is n/2 while the actual number can be expected to be much smaller because of limitation (c).

In simple systems containing a small number of reactants and intermediates the unit steps that can be generated are reasonably obvious, so that no systematic testing of all the above combinations need be undertaken. Thus, although some 162 combinations are potential unit steps in a system containing 2 reactants and 1 intermediate, such as the electrochemical reaction of hydrogen, only 3 unit steps can actually be operative and these can be conceived without investigating all combinations (cf. (2)). However, any more complex system, such as the example given below, offers such a number of combinations that it can hardly be treated without a formal method. This can be found by the following reasoning:

The stoichiometry of each unit step requires that

$$\sum_{r-1}^{R} a_r \cdot M_r + \sum_{i=1}^{I} \bar{a}_i \bar{M}_i = 0 \tag{7}$$

where M_r and M_i are molecular weights and a_r and a_i the stoichiometric factors of all the reactants and intermediates respectively, the latter having a negative sign if on the right side of the unit step equation.

When electrochemical reaction are considered a similar condition must be satisfied because of the electroneutrality of unit steps, i.e. if z_r and z_i are the charges on the reactant and intermediate molecules respectively, then

$$\sum_{r=1}^{R} a_r z_r + \sum_{i=1}^{I} \bar{a}_i \bar{z}_i - a_e = 0 \tag{8}$$

the last being taken as 1 for electrochemical steps (on account of assumption (b)), and as zero for chemical steps.

Conditions (7) and (8) can be summed to give

$$\sum_{r=1}^{R} a_r (M_r + z_r) + \sum_{i=1}^{I} \bar{a}_i (\bar{M}_i + \bar{z}_i) - a_e = 0 \tag{9}$$

which represents a general equation each unit step must satisfy. Hence, systematic variation a_r, a_i and a_e must be made along the lines described earlier so as to cover all the combinations given by (6), a maximum of two positive and two negative stoichiometric factors being taken at a time, the remainder being taken as zero. Obviously, unit steps will correspond only to those sets of stoichiometric factors

$$P = (a_1, a_2, \ldots a_R, a_1, a_2, \ldots a_I, a_e)$$

which satisfy equation (9). In order to avoid recording the reverse of an already obtained unit step, each set which satisfies (9) should be multiplied by -1 and left out if seen to correspond to any set p already in the list.

The application of this method does not present any mathematical difficulty. However, when more complex systems, with a larger number of intermediates are to be treated, it becomes very tedious and in some cases impossible to work out within any reasonable time. This type of difficulty may be easily overcome by the use of digital computers, whose programming and application is therefore demonstrated on the example given below.

Example

Anodic oxidation of ammonia is taken as an example of a moderately complex reaction. The problem of ammonia as a potential fuel in fuel cells has been treated by several authors but Oswin and Salomon[4] and Spahrbier and Wolf[5] were the first to consider its kinetic aspects and to attempt to forward reaction mechanism in terms of which the kinetic behavior could be explained. They started from the assumption that in aqueous alkaline solutions molecular ammonia rather than the ammonium ion is oxidized. This assumption has been accepted here too, it being maintained that in any case, even if both reactions occur simultaneously, kinetically they represent different problems, and at present only the first is considered.

Since the products of anodic oxidation of ammonia are known to be only water and nitrogen, the overall reaction for this process must be

$$2\,NH_3 + 6\,OH^- = N_2 + 6\,H_2O + 6\,e$$
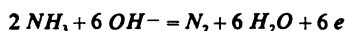
Oswin and Salomon assumed the existence of 3 intermediates only, i.e. of NH_2, NH and N radicals (or surface compounds). Such an assumption considerably simplifies the problem of possible reaction mechanisms, but is difficult to accept a priori without definite proof that no role is played by a number of other species that are otherwise known to exist and some of them to be even quite stable in such systems. These are: H, H^+, H_2, NH_2OH, $(NH_2)_2$, $(NH)_2$ and OH and a variety of other oxidation states of OH and N. Since at this instance no data for the Arrhenius activation energy for this reaction was available, the criterion for the selection of intermediates defined above could not be used. However, since the overall reaction indicates that N and OH^- are not oxidized, all the intermediates containing higher oxidation states of these species, except OH and NH_2OH, were ruled out. Hence in this example it was considered necessary to take 10 intermediates into account.

With the 4 reactants and 10 intermediates equation (9) consists of 5 terms and according to equation (6) a total of 28,084 combinations of a_r, a_i, and a_e must be systematically tested. Equations (7) and (8) applied to this case reduce to the following sets of diophantine equations:

$$17a_1 + 18a_2 + 28a_3 + 18a_4 + 16a_5 + 15a_6 + 14a_7 + a_8 + 2a_{10} +$$

$$+ 17a_{11} + 33a_{12} + 30a_{13} + 32a_{14} + a_e = 0 \tag{10}$$

and

$$a_9 = a_2 + a_e \tag{11}$$

with the reactants and intermediates taken in the following order:

1. NH_3; 2. OH-; 3. N_2; 4. H_2O; 5. NH_2; 6. NH; 7. N; 8. H; 9. H^+; 10. H_2; 11. OH; 12. NH_2OH; 13. $(NH)_2$; 14. $(NH_2)_2$

The coeficients a_i , i = 1 (1) 14 and a_e have to belong to sets:

$$a_i \in \{-2, -1, 0, 1, 2\} \qquad i = 1 (1) 14 \qquad (12)$$

and

$$a_e \in \{0, 1\} \qquad (13)$$

satisfying the following two conditions:

$$\sum_i a_i < 3 \qquad \text{(where the summation is taken over all positive } a_i) \qquad (14)$$

$$\sum_i a_i > -3 \qquad \text{(where the summation is taken over all negative } a_i) \qquad (15)$$

If the sum of all the terms of the left side of equation (10) except the last one is denoted as H, according to the condition given by (14) one has to find all the variations of the coefficients a_i giving H the value either 0 or — 1.

Taking into account conditions (14) and (15) it becomes evident that the function H cannot contain more than four terms different from zero.

The procedure of checking all possible variations of the coefficients a_i within the above system by a simple systematic variation is a time-consuming process requiring a high-speed computer to be accomplished within a reasonable period of time. However, a simplifying algorithm was found here, which reduced computation to one hour of work on the slow type digital computer ZUSSE 22.

This algorithm was done in the following way:

The only possible subsets of coefficients a_i satisfying (14) and (15) are

$$\{-1\}, \{-1, 1\}, \{-2, 2\}, \{1, -2\}, \{2, -1\}$$

A consideration of all the variations of the subsets leads to the conclusion that all the variations for the values of a can be ascribed to one of the following six possible types (T)

T				
1)	$\bar{1}$	1	$\bar{1}$	1
2)	1	1	$\bar{1}$	$\bar{1}$
3)	1	1	$\bar{1}$	$\bar{1}$
4)	0	1	1	2
5)	0	1	$\bar{2}$	1
6)	0	$\bar{2}$	1	1

Taking this as a basis, the computer can be programmed to print out the following table:

$$H \; c \; c \; c \; c \; T$$

where

$$H = \{ 0, 1, -1 \}$$

$$c = \{ 0, 0, 17, 18, 28, 18, 16, 15, 14,$$
$$1, 2, 17, 33, 30, 32 \}$$

and

$$T = \{ 1, 2, 3, 4, 5, 6 \}$$

the values of T being the ordinal numbers of the following table.

TABLE 1
POSSIBLE UNIT STEPS IN THE ANODIC OXIDATION OF AMMONIA INTO NITROGEN AND WATER

1. $NH_3 = NH_2 + N^+ + e$
2. $NH_3 + OH^- = NH_2 + H_2O + e$
3. $NH_3 + OH^- =$
   $= NH_2OH + H + e$
4. $NH_3 + OH =$
   $= NH_2OH + H^+ + e$
5. $NH_3 + NH_2 =$
   $= (NH_2)_2 + H^+ + e$
6. $NH_3 + N = (NH)_2 + H^+ + e$
7. $NH_2 + H_2 = NH_3 + H^+ + e$
8. $(NH_2)_2 + OH -- =$
   $= NH_2 + NH_2OH + e$
9. $NH_2 = NH + H^+ + e$
10. $NH_2 + OH -- = NH + H_2O + e$
11. $NH_2 + OH -- = NH_2OH + e$
12. $NH_2 + H_2O =$
    $= NH_2OH + H^+ + e$
13. $NH_2 + NH =$
    $= (NH)_2 + H^+ + e$
14. $NH + H_2 = NH_2 + H^+ + e$
15. $(NH)_2 + OH =$
    $NH_2OH + N + e$
16. $NH = N + H^+ + e$
17. $NH + OH^- = N + H_2O + e$
18. $NH + N = N_2 + H^+ + e$
19. $N + H_2 = NH + H^+ + e$
20. $H = H^+ + e$
21. $H + OH -- = H_2O + e$
22. $H_2 = H + H^+ + e$
23. $H_2 + OH = H_2O + H^+ + e$
24. $H_2 + OH -- = H + H_2O + e$
25. $H_2O = OH + H^+ + e$
26. $OH -- = OH + e$
27. $NH_3 = NH_2 + H$
28. $NH_3 = NH + H_2$
29. $2 NH_3 = (NH_2)_2 + H_2$
30. $NH_3 + NH_2 = (NH_2)_2 + H$
31. $NH_3 + (NH)_2 =$
    $= (NH_2)_2 + NH$
32. $NH_3 + NH = (NH_2)_2$
33. $NH_3 + NH = 2 NH_2$
34. $NH_3 + NH = (NH)_2 + H_2$
35. $NH_3 + N = NH_2 + NH$
36. $NH_3 + N = (NH)_2 + H$
37. $NH_3 + N_2 = (NH)_2 + NH$
38. $NH_3 + H = NH_2 + H_2$
39. $NH_3 + NH_2OH =$
    $= (NH_2)_2 + H_2O$
40. $NH_3 + OH = NH_2OH + H$
41. $NH_3 + OH = NH_2 + H_2O$
42. $NH_3 + H_2O = NH_2OH + H_2$
43. $(NH_2)_2 = 2 NH_2$
44. $(NH_2)_2 = (NH)_2 + H_2$
45. $(NH_2)_2 + N = (NH)_2 + NH_2$
46. $(NH_2)_2 + N_2 = 2 (NH)_2$
47. $(NH_2)_2 + OH = NH_2OH + NH_2$
48. $NH_2 = NH + H$
49. $NH_2 = N + H_2$
50. $2 NH_2 = (NH_2)_2 + H_2$
51. $NH_2 + NH = (NH)_2 + H$
52. $NH_2 + N = (NH)_2$
53. $NH_2 + N = 2 NH$
54. $NH_2 + N = N_2 + H_2$
55. $NH_2 + N_2 = (NH)_2 + N$
56. $NH_2 + H = NH + H_2$
57. $NH_2 + OH = NH_2OH$
58. $NH_2 + OH = NH + H_2O$
59. $NH_2 + H_2O = NH_2OH + H$
60. $(NH)_2 = 2 NH$
61. $(NH)_2 = N_2 + H_2$
62. $(NH)_2 + OH = NH_2OH + N$
63. $(NH)_2 + H_2O = NH_2OH + NH$
64. $NH = N + H$
65. $2 NH = N_2 + H_2$
66. $NH + N = N_2 + H$
67. $NH + H = N + H_2$
68. $NH + OH = N + H_2O$
69. $NH + H_2O = NH_2OH$
70. $2 N = N_2$
71. $2 H = H_2$
72. $H + OH = H_2O$
73. $H + OH = H^+ + OH --$
74. $H + H_2O = H_2 + OH$
75. $H^+ + OH^- = H_2O --$

H	T		a_e	a_9	a_1	a_2	a_3	a_4	a_5	a_6	a_7	a_8	a_{10}	a_{11}	a_{12}	a_{13}	a_{14}	
1'	1'	17'18	1	1	0	0	0	0	0	0	0	—1	0	0	0	0	0	1. $H^+ + e = H$
—1'	2'	17'18	1	1	1	—1	0	0	0	0	0	0	0	0	0	0	0	
	1'	17'18	1	0	1	0	0	—1	0	0	0	0	0	0	0	0	0	3. $NH_3 + H^+ + e - H_2O$
1'	1'	17'18	1	1	1	0	0	0	0	0	0	0	0	0	0	0	0	
—1'	2'	17'16	1	—1	—1	0	0	0	1	0	0	0	0	0	0	0	0	4. $N^+ = NH_2 + e - NH_3$
—1'	2'	17'16	1	1	1	0	0	0	0	0	0	0	0	0	0	0	0	
0	1'	17'17	0	0	—1	0	0	0	0	0	0	0	1	0	0	0	0	5. $OH = NH_3$
0	2'	17'17	0	0	—2	0	0	0	0	0	0	0	2	0	0	0	0	6. $2OH = 2NH_3$
0	5'	17'33	0	—1	1	0	0	0	0	0	0	0	—1	0	0	0	0	7. $NH_3 - OH$
—1'	1'	18'18	1	—1	—2	1	0	—1	0	0	0	0	2	0	0	0	0	9. $NH_2OH + H^+ + e - 2NH_3$
0'	2'	18'18	0	—1	0	—1	0	1	0	0	0	0	0	0	0	0	0	10. $H^+ + OH - - H_2O$
0	1'	18'17	1	0	0	0	0	1	0	0	0	0	1	0	0	0	0	11. $H_2O = H^+ + OH -$
—1'	2'	18'17	1	—1	0	—1	0	0	0	0	0	0	0	0	0	0	0	12. $OH + e = OH -$
0	4'	28'14	0	0	0	0	1	0	0	—2	0	0	0	0	0	0	0	13. $N_2 = 2N$

Figure 1

Digital computer results for the generation of unit steps in the anodic oxidation of ammonia

(1. NH_3; 2. $OH -$; 3. N_2; 4. H_2O; 5. NH_2^-; 6. NH; 7. N; 8. H; 9. H^+; 10. H_2; 11. OH; 12. NH_2OH; 13. $(NH)_2$; 14. $(NH_2)_2$)

In the programme used in this work not all of the printed lines were usable for converting back into the unit step presentation system of p's described earlier. The lines which, after additional computation of a render either three positive or three negative coefficients are meaningless, since in those cases condition (14) is no longer satisfied. A typical section of the computer results together with their interpretation is shown in Fig. 1.

Further reduction of the number of meaningful unit step equations is due to the fact that some constants in equation (10) have identical values. This introduces what is termed here as a coincidence factor, meaning that, in spite of the fact that the molecular weight stoichiometry is always maintained, some of the obtained chemical equations will not be chemically correct, as e.g. equations (2), (3), (5), (6), (7), (9) in Fig. 1. A complete treatment of this system resulted in 224 chemical equations out of which some had to be rejected because of this incorrectness and some represented the reverse of an already recorded step. The final table consists of 75 unit steps (26 electrochemical and 49 chemical ones) as presented in Table 1.

ACKNOWLEDGEMENT

School of Technology, University
   of Beograd and the Institute for
    Chemistry, Technology and
      Metallurgy — Beograd

REFERENCES

1. Frost, A. A., Pearson, R. G. *Kinetics and Mechanism*, London: John Wiley, 1961
2. Vetter, K. — *Chemie-Ingenieur Technik* **35**: 343, 1963.
3. Conway, B. E., Bockris, J. O'M. — *Electrochimica Acta* **3**: 340, 1961.
4. Oswin, H. G., Salomon, M. *Canadian Journal of Chemistry* **41**: 1686, 1963.
5. Spahrbier, D., Wolf, G. Z. *Naturforschung* **19a**: 614, 1964.

FLUOROMETRIC DETERMINATION OF SOME QUINOLINE COMPOUNDS

by

ILIJA Đ. BURIĆ and KOSTA I. NIKOLIĆ

Some quinoline compounds are very important in medical therapy. Some of these compounds are used as antipyretics, antimalarials, antiseptics and local anaesthetics. Carbon quinolinic acid, which has a carboxyl group in position 4, has isonicotinic acid in the ring, which is known for its tuberculostatic properties. This is why Movrin[1,2] investigated the tuberculostatic activity of derivatives of carbon quinolinic acid -4 with different alcoxy groups in position 6. Esters and hydrazides of these acids have also been investigated. It was found that some compounds may be considered potential tuberculostatic. In view of this importance, we have investigated the possibility of their quantitative and qualitative determination.

Studying a great many quinoline derivatives[3], we have concluded that compounds with an alcoxy group in position 6 and a carboxyl group in position 4 fluoresce strongly if dissolved in water and alcohol. Therefore in determining the quinoline compounds investigated by Movrin we used the fluorometric procedure.

The fluoroscence intensity of the solutions of these compounds and its spectral distribution depends on the pH of the solution. The spectral distribution depends on the absorption spectrum, determined by the acido-basic properties of these compounds. Since the intensity of fluoroscence changes considerably with very small change of pH, and the use of regulator solutions is not advisable because of the presence of substances which may influence the fluoroscence, we performed the determinations in methanol or in a mixture of chloroform and methanol. We determined the hydrazides of 6-ethoxycinchoninic, 6-butoxycinchoninic, 6-propoxycinchoninic, and 2-methyl-6-ethoxycinchoninic, 6-oxycinchoninic acid, and 6-isoamyloxycinchoninic acid and its methyl ester.

EXPERIMENTAL

To measure the intensity of fluoroscence we used a Kipp fluorometer with three selenium photocells, which was fed to a Multiple Mg-4 galvanometer with a sensitivity of about 6×10^{-10} A per mm.

To photograph the fluoroscent spectra we used a Zeiss SPM monochromatos with a Philips AVP-50 photomultiplier. The voltage of the photomultiplier was 1250 V. Excitation was performed with two Philips HPV 125 W mercury lamps.

The solvents were methanol and chloroform, p.a. Methanol was first treated with activated charcoal and twice redistilled. Chloroform was only twice redistilled.

Except for the hydrazide 6-butoxycinchoninic acid, which was dissolved in a mixture of carbon tetrachloride and methanol (1 : 1), the compounds were dissolved in methanol.

The substances determined were synthesized according to the regulations given by M. Movrin[2]. All the compounds synthesized had physical constants which satisfied the conditions prescribed in the regulations for their synthesis.

The concentrations were fluorometrically determined in the following way: The intensity of fluorescence of the solution of highest concentration was taken to be 100, while that of the pure solvent was taken to be zero. The light spot of the galvanometer was set at 100 with the potentiometers on the fluorometer and galvanometer, and at zero by the zeroing device on the galvanometer.

RESULTS AND DISCUSSION

By measuring the fluorescence intensity for different concentrations we obtained calibration curves which are between 0.2 and 30 µg/ml. Figure 1 shows the calibration curve for the hydrazide of 6-propoxy-cinchoninic acid.
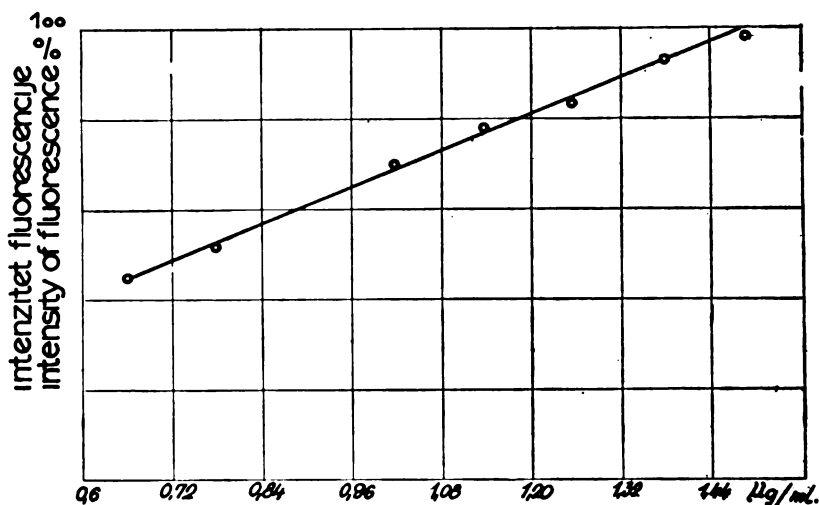
Fig. 1. — Hydraside of 6-propoxycinchoninic acid. Plot of intensity of fluorescence in percent against concentration.

By investigating factors which influence the intensity of fluorescence and affect the accuracy of determination, we have concluded that the presence of the following inorganic salts quenches the fluorescence:

$HgCl_2$ K_2SO_4 $AgNO_3$ CHC_3OOK CH_3COOAg $K_2C_2O_4$ KCl NaCl

LiCl RbCl $LaCl_3$ KBr   KCNS KI

The greatest quenching is caused by the presence of iodide, bromide and thyocyanate ions. If salts which quench fluorescence are present in the solution, they must be removed. For a low concentration of quenching salt, the decrease in the intensity of fluorescence can be calculated from the Stern-Volmer formula:

$$F = F_o \cdot \frac{1}{1 + bc}$$

b = quenching constant
F = fluorescence intensity in the presence of quencher
F_0 = fluorescence intensity without quencher
c = molar concentration of quencher

Determination of the concentration in a yellow solution is not possible because this acts as an optical filter and quenches fluorescence. If colored solutions are used which do not quench fluorescence, it is necessary to obtain a calibration curve under the same conditions. Solutions used for obtaining the calibration curves must have the same color intensity as the test solution. If this is not the case, recorded intensity must be corrected.

Table 1 shows the positions of the maxima of the fluorescent spectra. They differ very little, and in all cases the spectral distribution is about the same, as is seen in Figs. 2 and 3.

TABLE 1

Substance	Amount g/ml	Solvent	Position of the maximum band in the fluorescence spectra 10^3 cm^{-1}
Hydrazide of 6-ethoxycinchoninic acid	10^{-4}	methanol	22
Hydrazide of 6-buthoxycinchoninic acid	10^{-4}	methanol carbon tetrachloride (1 : 1)	22
Hydrazide of 6-propoxycinchoninic acid	10^{-4}	methanol	21.7
Hydrazide of 2-methyl-6-ethoxy-cinchoninic acid	10^{-4}	methanol	21.85
6-Isoamyloxycinchoninic acid	10^{-4}	methanol	22.12
6-oxycinchoninic acid	10^{-4}	methanol	21.9
methylester of 6-isoamyloxy-cinchonininic acid	10^{-4}	methanol	21.87

2*
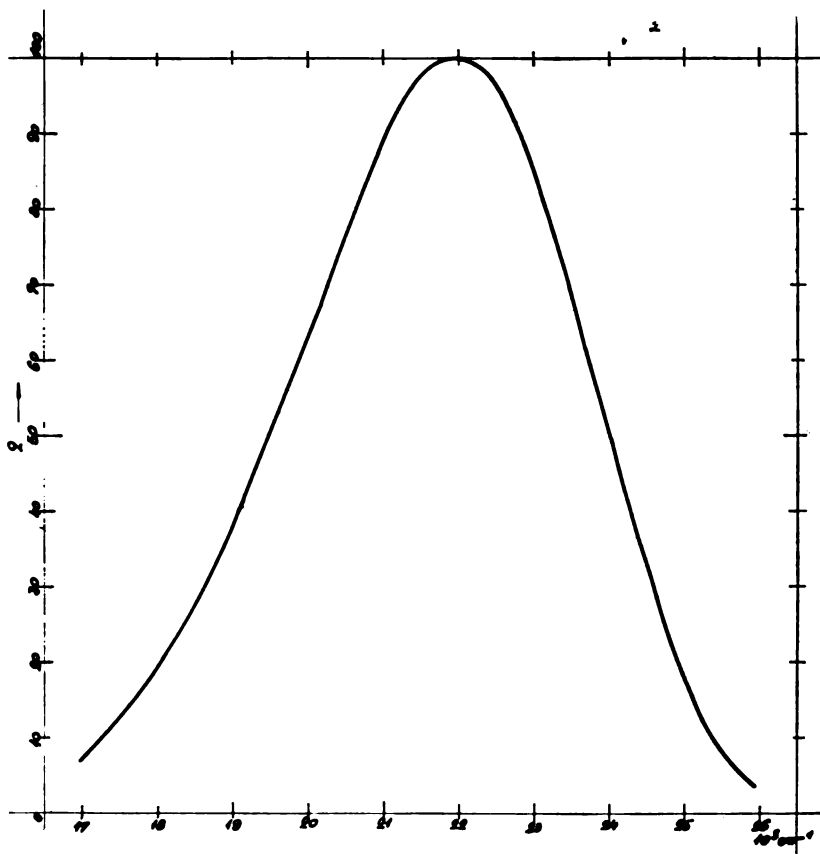
Fig. 2. — Fluorescent spectrum of hydrazide of 6-ethoxycinchoninic acid (10^{-4} g/ml)

This means that the presence of different groups in positions 2, 4 and 6 of the quinoline ring does not have any great effect on the spectral distribution and position of the maximum. Nevertheless, the fluorescence spectra do allow qualitative determination of the substance if used together with other physical constants. This is particularly important in case of small quantities of the substance since the fluorescent spectra can be photographed in the presence of mg/ml quantities.
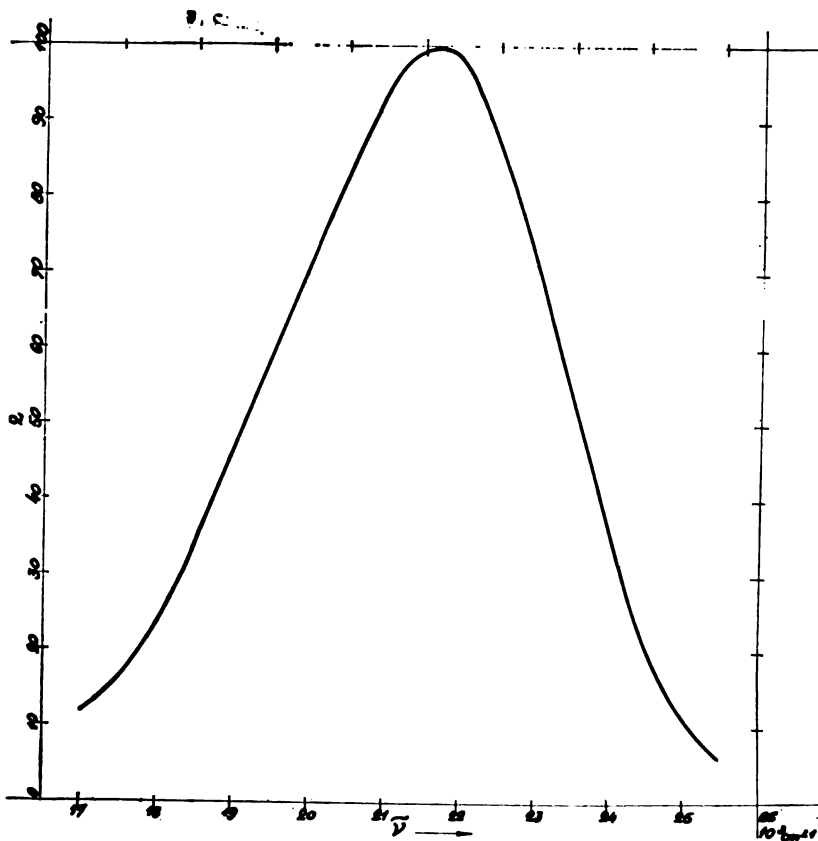
Fig. 3. — Fluorescent spectrum of hydrazide of 6-propoxycinchoninic acid (10^{-4} g/ml).

REFERENCES

1. Movrin, M. *Doctoral Thesis* — Zagreb, 1960.
2. Movrin, M. and D. Barković — *Acta Pharmaceutica Yugoslavia* 7: 119, 1957.
3. Nikolić, K. *Doctoral Thesis* — Beograd, 1959.

POLAROGRAPHIC DETERMINATION OF THALLIUM IN AMMONIACAL SOLUTION OF TRILLON B*

by

SRETEN MLADENOVIĆ

Supporting electrolytes for polarographic determinations do not exhibit much selectivity; two or more ions are often reduced at the same or at very close potentials; in some cases the main component of the solution is reduced before the component to be determined; moreover some supporting electrolytes form very stable complexes with both the component to be determined and one which is not to be determined. However, some supporting electrolytes do not give sparingly soluble compounds with the component which is not being determined and thus the polarographic determination of other substances of the solution is made difficult. In all these and similar cases the polarographic determination of individual components is not possible.

In hydrochloric acid solutions the ions of lead, thallium, tin, cadmium and in some cases those of antimony are reduced at almost the same potential[1].

The ions of thallium, lead[2], copper and tellurium are reduced at approximately the same potentials from ammonium hydroxide and ammonium chloride solution.

The reduction of thallium, bismuth, copper and antimony at a dropping mercury electrode in alkaline hydroxide solution takes place at almost the same potential[1].

The selectivity of some supporting electrolytes for the polarographic determination of some ions can be increased by changing their composition. This is the case with the supporting electrolyte consisting of ammonium hydroxide and ammonium chloride; the addition of complexon III changes its chemical and the polarographic characteristics.

In ammoniacal solution of complexon III lead ions give no precipitate and do not produce a polarographic wave[3]. A great number of other ions behave in the same way (tin, cadmium, nickel, etc.)[4]. However, the ions of thallium, antimony and tellurium are reduced at the dopping mercury electrode.

From Figs. 1a, b, c, it may be seen that the half-wave potentials of thallium, tellurium and antimony are as follows:

$$e_{1/2} \sim 0.65 \text{ V} \quad \text{for thallium}$$
$$e_{1/2} \sim 0.95 \text{ V} \quad \text{for tellurium}$$
$$e_{1/2} \sim 1.10 \text{ V} \quad \text{for antimony}$$

---

* Communicated at XI Meeting of Serbian Chemical Society, January, 1965.
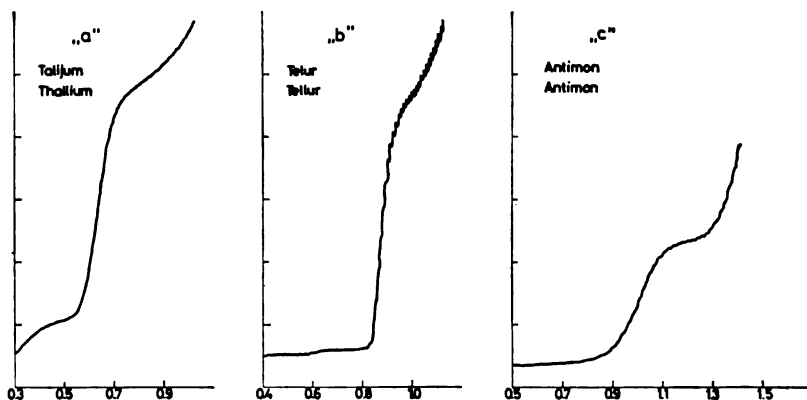
Fig. 1.

The half-wave potentials of tellurium and antimony are not sufficiently distinct and therefore tellurium cannot be determined in the presence of antimony, and vice versa. On the other hand, it is evident that simultaneous determination of thallium and tellurium, and thallium and antimony can be performed.

In Table I the polarographic wave height for various amounts of thallium is shown.

TABLE 1.

Supporting electrolyte: 0.2 g Pb^{2+} + 30 ml solution (1.6M NH_4Cl + 6M NH_4OH + + 1% Na_2SO_3 + 3 g gelatin) + 1 g trillon B + water up to 50 ml

Experiment No.	Amount of thallium in mg	Height in mm
1	0.50	14,0
2	1.0	28.0
3	1.5	42.0
4	2.0	57.0
5	2.5	71.0
6	3.0	84.5
7	3.5	98.5
8	4.0	113.0

The height of the wave increases linearly with the amount of thallium; this linear dependance is not affected by the presence of lead, cadmium and tin and it may be concluded that thallium can be determined polarographically from ammoniacal solution of complexon III in the presence of lead, cadmium and tin.

In the polarographic determination of thallium and antimony from ammonical solution of complexon III, clearly distinct polarographic waves are obtained and their heights are strictly proportional to the concentrations of thallium and antimony (Table II)

The polarographic waves obtained for equal amounts of antimony and thallium in the same supporting electrolyte are not the same height — the antimony wave is several times higher.

The presence of cadmium does not interfere with the simultaneous determination of thallium and antimony. This finding is of practical importance for the determination of thallium and antimony in cadmium solutions. The method used so far for the colorimetric determination of thallium and antimony by means of methyl-violet[5] can be applied only in case thallium and antimony are separated from one another, since both elements react with methyl-violet.

TABLE II

Supporting electrolyte : 0.2 g Pb²⁺ + 30 ml solution (1.6 M NH₄Cl + 6M NH₄OH + + 1% Na₂SO₃ + 3 g gelatin) + 1 g trillon B + H₂O up to 50 ml.

Experimet No.	Amount in mg		Wave height in mm	
	Antimony	Thallium	Antimony	Thallium
1	1.5	7.0	30.0	21.0
2	2.0	6.0	40.0	18.0
3	2.5	5.0	50.0	14.0
4	3.0	4.0	60.0	12.0
5	3.5	3.0	71.0	9.0
6	4.0	2.0	80.0	6.0

The polarographic waves of thallium and tellurium obtained in amoniacal solution of complexon III in the presence of lead are clearly separated and their heights are proportional to the amounts of thallium and tellurium present in the solution (Table III).

TABLE III

Supporting electrolyte : 0.2 g Pb²⁺ + 30 ml solution (6M NH₄Cl + 6M NH₄OH + + 1% Na₂SO₃ + 3 g gelatin) + 1 g trillon B + H₂O up to 50 ml.

Experiment No.	Amount (mg) of		Wave height in mm	
	Tellurium	Thallium	Tellurium	Thallium
1	1.0	7.0	30.0	17.5
2	1.5	6.0	45.0	15.0
3	2.0	5.0	59.5	12.5
4	2.5	4.0	75.0	10.0
5	3.0	3.0	90.0	7.5
6	3.5	2.0	105.0	5.0

From Table III it may be concluded that in simultaneous determination of equal amounts of tellurium and thallium, the tellurium wave is about twelve times higher than the thallium wave.

The results given in Table III show that simultaneous polarographic determination of thallium and tellurium is possible even in the presence of a large amount of lead; the results are not affected by the presence of cadmium either.

The polarographic determinations in ammoniacal solution of complexon III show that thallium and antimony, and thallium and tellurium can be simultaneously determined in solutions containing large amounts of lead. In addition, the polarographic determination of thallium, tellurium and antimony in ammoniacal solution of trillon B is not affected by the presence of cadmium and tin.

School of Technology,
Department of Physical Chemistry
    and Electrochemistry
        Beograd

REFERENCES

1. Kriukova, T. A., S. I. Siniakova, and T. V. Aref'eva. *Poliarograficheskii analiz* (Polarographic Analysis) — Mosiva: Gosudarstvennoe nauchno-tekhnicheskoe izdatel'stvo khimicheskoi literatury, 1959.

2. Mladenović, S. "Polarografsko određivanje bakra pored olova" (Polarographic Determination of Copper besides Lead) — *Glasnik hemijskog društva* (Beograd). In press.

3. Mladenović, S. "Polarographische Bestimmung von Antimon in Blei" — *Glasnik Hemijskog društva* (Beograd). In press.

4. Pršibil, P. *Kompleksony v khimicheskom analize* (Complexons in Chemical Analysis) — Moskva: Izdatel'stvo inostrannoi literatury, 1960.

5. Lur'e, Iu. Iu. and N. A. Filipova. "*Analiz mineralnogo syriia*" (Analysis of Mineral Raw Materials) *Zavodskaiia laboratoriia* 18 : 30, 1952.

EFFECT OF SOME ADMIXTURES OF THE ACTIVITY OF THE CONTACT MASS IN DIRECT SYNTHESIS OF METHYLCHLOROSILANE

by

S. D. RADOSAVLJEVIĆ, M. D. DRAGOJEVIĆ and D. H. VASOVIĆ

In a series of experiments on direct synthesis of methylclhorosilanes using contact masses prepared by precipitating copper[1] chloride in the presence of ferrosilicon[1], we noticed that impurities in the chemicals from which the copperchloride is obtained can considerabliy affect the yield.

It was found that, on an average, the yields were slightly greater if the contact mass was prepared by precipitating copper (I) chloride from a solution of industrial copper sulphate and industrial sodium chloride in ordinary water than if p.a. chemicals and distilled water were used. We supposed that the reason for this was the addition of some admixtures to the contact mass either by cementation on the ferrosilicon or by coprecipitation with copper chloride.

In order to investigate the effect of admixtures, a detailed chemical analysis was made of the materials used. The semiquantitative spectro-graphic analysis* showed that in the industrial copper sulphate there was about 0.01% of silver, nickel, cobalt and lead, and from 0.001 to less than 0.0001% of calcium, magnesium, manganese, silicon, tin, titanium, iron, chromium, zinc and molybdenum.

The chemical analysis of the industrial sodium chloride (non-refined cooking salt) showed the presence of:

Na_2SO_4	0.82%	$CaSO_4$	0.91%
$MgSO_4$	0.27%	KCl	0.07%
SiO_2	0.017%	Al_2O_3	0.001%
MnO	0.001%	P_2O_5	0.001%
heavy metals	0.001%	Fe_2O_3	0.0005%

---

* This analysis was made by Dr. Vera Šćepanović of the School of Technology, Beograd, to whom the authors are indebted.

The indu'trial ferrosilicon had the following composition:

Si	96.71 —96.12%	Fe	1.48—2.68%
Ca	1.18 — 0.59%	Al	0.37—0.26%
Mg	0.06 — 0.04%	Mn	0.05—0.08%
Cu	0.02 — 0.07%	C	0.04—0.08%
S	0.005— 0.006%	P	0.01—0.03%
Ti	0.05 — 0.07%		

In preparing the contact mass the ferrosilicon used to be immersed for some time in a solution of copper sulphate and sodium chloride so that one of the possibilities for impurities to get onto the contact mass was by cementation of metals whose normal potentials are more positive than that of iron. To check this we made an experiment immersing ground ferrosilicon in a solution of industrial copper sulphate for half an hour, the materials being in the same ratios as in preparing contact masses. After precipitation the impurities in the copper sulphate were determined spectrographically.

This experiment showed that copper sulphate which before treatment with ferrosilicon contained

up to 0.01% of silver, nickel, lead

„ „ 0.001% of calcium, silicon

traces of iron, manganese, titanium and tin,

after treatment with ferrosilicon contained

up to 0.01% of calcium, nickel, silicon, iron and titanium

„ „ 0.005% of lead

„ „ 0.001% of manganese

There was no longer any tin or silver.

It may be concluded that treatment of a solution of industrial copper sulphat with ferrosilicon separates silver on the ferrosilicon and probably trace quantities of lead and tin, so cementation on ferrosilicon is one of the possible ways admixtures get added to the contact mass.

The other possibility is that admixtures get added to crystals of copper chloride during its precipitation, so investigations along these lines were also carried out[2]. To this effect copper (I) chloride was prepared in the usual way, by reduction with sodium sulphite from aqueous solution of copper sulphate and sodium chloride[3], p.a. purity, to which certain quantities of other salts were also added. It was shown that copper chloride crystals carry off ions of some elements, whose presence could be determined by semiquantitative spectrographic analysis. In some tests, in preparing copper (I) chloride, to the precipitation solutions salts of some elements were added whose presence was determined in the industrial copper sulphate, viz., calcium, magnesium, iron, cobalt, nickel, aluminium, chromium, and molybdenum. After washing and drying the copper (I) chloride in the prescribed way, the presence of admixtures was determined by semiquantitative spectro-

graphic analysis. In the above cases copper chloride did not contain nickel, cobalt, iron or aluminum but did contain *calcium, magnesium, chromium and molybdenum*. The quantities of these admixtures depended to some extent on their initial concentration in the solution from which copper chloride was precipitated, as may be seen from the data in Table I.

TABLE 1

Quantity of admixtures in copper (I) chloride, as a function of their concentration in the solution from which copper (I) chloride was precipitated

Initial solution 10 g $CuCl_2 . 2H_2O$ in 40 ml water

Added to the solution		Found in CuCl	
0.05 g $CaCl_2$ (4.5×10^{-4} gramatom Ca)		0.01%	Ca
0.5 g „ (4.5×10^{-3} „ „)		0.01%	„
2.5 g „ (2.25×10^{-2} „ „)	more than	0.1%	„
0.047 g $MgCl_2 . 6H_2O$ (2.3×10^{-4} gramatom Mg)		0.002%	Mg
0.47 „ „ (2.3×10^{-3} „ „)		0.003%	„
2.136 „ „ (1.05×10^{-2} „ „)		0.003%	„
0.129 g $CrCl_3 . 7H_2O$ (4.5×10^{-4} gramatom Cr)		0.001%	Cr
6.46 „ „ (2.3×10^{-2} „ „)		0.01%	„
0.089 g $(NH_4)_2MoO_4$ (4.5×10^{-4} gramatom Mo)		0.01%	Mo
4.456 „ „ „ (2.3×10^{-2} „ „)		0.08%	„

Since the above experiments showed that admixture to the contact mass is possible by coprecipitation with copper (I) chloride and cementation on ferrosilicon, in further tests we investigated their effect on the yield in direct synthesis of methylchlorosilanes. To this end, salts whose presence in the copper (I) chloride had been determined earlier were added to the solutions from which copper chloride was precipitated and used for the preparation of the contact mass*, or admixtures were added by immersing ground ferrosilicon in a solution of salts whose ions could be reduced to metals.

Since in case of calcium salts calcium sulphate would be precipitated first because of the presence of sulphate ions formed by sulphite oxidation, of copper (I) chloride for the contact mass was precipitated by first preparing puie copper (I) chloride without the addition of calcium ions, then dissolving it in concentrated hydrochloric acid [$CuCl + \xrightarrow{HCl} H (CuCl_2)$ or $H_2 (CuCl_3)$], and finally adding calcium chloride to the copper chloride complex solution. Diluting this solution with water causes decomposition of the complex and precipitation of copper chloride.

The results given in Table 2 show characteristic examples for each group of experiments. All the experiments were carried out in a horizontal glass reactor, without mixing, with a constant methylchloride flow rate of about 8 g/h.

TABLE 2

Typical results of direct syntheses of methylchlorosilanes with contact masses with admixtures

Way of adding admixtures to contact mass:	Kind and quantity of admixture in the initial soln.	Quantity of methylchlorosilanes obtained					
		in a period of (hrs)	Quantity g	Mean yield g/hr	in a period of (hrs)	Quantity g	Mean yield g/hr
A. *Contact mass prepared by precipitating cca 30 g CuCl in the presence of 170 g ferrosilicon*							
by precipitating CuCl from 620 ml of soln. containing 120 g CuSO$_4$ 5 H$_2$O and 40 g NaCl in the presence of:	no admixture	21	145	6.9	41^2/$_3$	260	6.25
	5 g CrCl$_3$	21	151.4	7.21	46^1/$_2$	291.5	6.27
	10 g CrCl$_3$	21^1/$_2$	161.2	7.5	44^1/$_2$	294.2	6.61
	19 g CrCl$_3$	19	134.2	7.06	40^1/$_2$	239.4	5.91
	25 g (NH$_4$)$_2$ MoO$_4$	18	111	6.15	42	248	5.93
	,, ,,	22^1/$_2$	172	7.65	39	249	6.37
by precipitating CuCl from a solution of 30 g CuCl in conc. HCl in the presence of:	no admixture	23	145	6.3	39^1/$_2$	231.7	5.87
	5 g CaCl$_2$	25	161.9	6.48	41^1/$_2$	246.4	5.94
	10 g CaCl$_2$	24	178.3	7.43	39	276.6	6.94
	20 g CaCl$_2$	26	214.3	8.24	47^1/$_3$	328.2.	6.89
B. *Contact mass prepared by mixing 35 g CuCl and 170 g ferrosilicon in a porcelain ball mill for 1—2 hrs.*							
by immersion of ferrosilicon for 20 min in 250 ml of water containing:	no admixture	24	171	7.12	46	256.2	5.57
	3.06 g AgNO$_3$	20^1/$_2$	298	4.74	45	181	3.98
	0.7 g AgNO$_3$	— —	—	— —	40	156.6	3.92
	0.24 g AgNO$_3$	21	95	4.5	46^1/$_2$	190.3	4.17
	0.05 g AgNO$_3$*	20^1/$_3$	103.8	5.1	40^1/$_3$	192.8	4.79
by immersion of ferrosilicon for 20 min in 250 ml of water containing:	3.41 g SnCl$_2$·2 H$_2$O	22^1/$_2$	105	4.66	37^1/$_3$	176.3	4.72
	0.2 g SnCl$_2$·2 H$_2$O	20	165	8.25	40	319	7.96
	0.5 g SnCl$_2$·2 H$_2$O	—	—	—	40^1/$_4$	360	8.95
	0,7 g SnCl$_2$·2 H$_2$O	20	185.5	9.27	41	352.5	8.60

* The soln. of AgNO$_3$ was acidified with a few drops of HCl to give colloidal AgCl.

From the results it may be concluded that our initial hypothesis on the effect of even trace quantities of admixtures in the contact mass was correct; their addition can induce changes in the activity of the contact mass for the direct synthesis of methylchlorosilanes. Of the admixtures that can be added in the way and in the quantities described above, calcium chloride* probably, and tin quite markedly increases the yield of direct synthesis. Chromium and molybdenum have no pronounced effect, while silver decreases the yield.

REFERENCES

1. Radosavljević, S. M. Dragojević, and M. Jaćović. — *Glasnik hemijskog društva* (Beograd) 21 : 101—104, 1956.
2. Dragojević, M. *Ph. D. Thesis* — Beograd, 1961.
3. *Inorganic Syntheses*, Vol. II. — New York: McGraw Hill, 1946, p. 1.

---

* The positive effect of calcium chforide was also confirmed in another series of experiments in which it was mixed mechanically in large quantities with ferrosilicon and copper (I) chloride.